Université d'Ottawa • University of Ottawa

MECHANISMS OF NEURONAL INTEGRATION IN ADRENOMEDULLARY SYMPATHETIC PREGANGLIONIC NEURONS

By

Jennifer M. M. Wilson

June 2002

A Thesis submitted to

The Faculty of Graduate and Postdoctoral Studies

University of Ottawa

In partial fulfillment of the requirements for the degree of

Doctor of Philosophy in Neuroscience

ABSTRACT

Sympathetic preganglionic neurons innervating the adrenal medulla (AD-SPN) regulate the release of adrenal catecholamines into the bloodstream. This research was undertaken to investigate the intrinsic properties and synaptic pathways characteristic of AD-SPN in neonatal rat spinal cord slice preparation. The presence of Lucifer Yellow from the patch pipette and Rhodamine-Dextran-Lysine from the adrenal medulla in the same neuron post recording identified AD-SPN. Active intrinsic properties revealed and characterised include: a potassium-mediated transient outward rectification present in 96% of AD-SPN and separable into a short 4-aminopyridine- and a long barium-sensitive component; a potassium-mediated sustained outward rectification revealed in TTx, activated positive to –50mV and blocked with quinine. These conductances contribute to the repolarising phase of the action potential. 89% of AD-SPN possessed potassium-mediated anomalous inward rectification. All AD-SPN displayed a high voltage-activated calcium spike that prolongs the action potential. The addition of internal caesium (140mM) revealed a low threshold spike mediated by T-type calcium channels that serve to facilitate burst firing.

75% of AD-SPN exhibited evidence of electrotonic coupling, indicated by characteristic oscillations in membrane potential and confirmed with dual recordings from electrotonically coupled AD-SPN. Electrotonic coupling promoted synchronous activity. An enhanced afterhyperpolarising potential facilitated transient termination of action potential firing forming bursts of activity. A role for calcium in the regulation of neuronal activity via action on electrotonic coupling was suggested by caffeine (10mM) decreasing, BAPTA-AM (15μM) and calcium free aCSF increasing the junctional conductance. Electrical stimulation of the descending fibres in both the ipsi- and contra-lateral funiculi evoked fast EPSPs in all AD-SPN that were mediated by both NMDA and non-NMDA receptors. A subpopulation of AD-SPN received fast IPSPs mediated by GABA acting via $GABA_A$ receptors. A train of stimuli (4x10Hz) in ipsi- and contra-lateral funiculi also evoked a slow IPSP mediated by noradrenaline acting via α_2-adrenergic receptors to increase a potassium conductance.

The results provide insight into central mechanisms that contribute to the regulation of adrenomedullary catecholamine secretion.

TABLE OF CONTENTS

FIGURES

CHAPTER 1

CHAPTER 2

CHAPTER 3

CHAPTER 4

CHAPTER 5

CHAPTER 6

CHAPTER 7

TABLES

ABBREVIATIONS

aCSF	artificial cerebral spinal fluid
AD-SPN	adrenal medulla projecting sympathetic preganglionic neuron
AMPA	α-amino-3-hydroxy-5-methyl-4-isoxazole-proprionate
D-AP5	D(-)-2-Amino-5-phosphonopentanoic acid
BAPTA-AM	1,2-bis(2-aminophenoxy)ethane-N,N,N',N'-tetra-acetic acid tetrakis (acetoxymethyl ester)
ChAT	choline acetyltransferase
cLF	contralateral funiculus
CNQX	6-Cyano-7-nitroquinoxaline-2,3-dione
EPSP	excitatory postsynaptic potential
iLF	ipsilateral funiculus
GABA	gamma aminobutyric acid
GYKI	1-(4-aminophenyl)-4-methyl-7,8-methylenedioxy-5H-2,3-benzodiazepine
5-HT	5-hydroxytryptamine
IPSP	inhibitory postsynaptic potential
mRNA	messenger ribonucleic acid
NBQX	2,3-Dioxo-6-nitro-1,2,3,4-tetrahydrobenzo(f)quinoxaline-7-sulfonamide
NMDA	N-methyl-D-aspartate
2PDKC	two pore domain potassium channel
PACAP	pituitary adenylate cyclase activating polypeptide
PNMT	phenylethanolamine N-methyltransferase
QX -314	N-(2,6-Dimethylphenylcarbamoylmethyl)triethylammonium chloride
TEA	tetraethylammonium
TOR	transient outward rectification
TTx	tetrodotoxin
SLD	short latency depolarisation
SOR	sustained outward rectification
SPN	sympathetic preganglionic neuron
RT-PCR	reverse transcriptase-polymerase chain reaction

ACKNOWLEDGEMENTS

I wish to extend my sincere appreciation to Dr Leo Renaud for affording me the opportunity to study in Canada under his supervision. I am grateful for his insight as a scientist and kindness and patience as a supervisor. I would particularly like to thank him for sharing his command of "scientific English" during the writing of this thesis. I am indebted to Dr David Spanswick for his willingness to share his expertise both technically with regards to the patch clamp technique and scientifically related to SPNs. I would like to extend my gratitude to colleagues and friends; Elaine Coderre for her excellent technical skills and to Dr Lu-Ning Cui for his willingness to help. I wish to acknowledge the Canadian Commonwealth Scholarship and Fellowship Program and the Canadian Institute of Health Research for their financial support.

I wish to extend my gratitude to the many special people that I have had the good fortune of spending time with while in Ottawa; to Chris Veltheim and Marcia Solomon, your paths bring much light to many; to Karolyn Boyd, Carolyn Waring, and Ian Laquian, your friendship and support has been like that of a family. I wish to dearly thank my parents, Frances and David Wilson for their acceptance and continued support in all areas of my life.

To the freedom that comes

When science and spirit are one

PUBLICATIONS

ABSTRACTS

WILSON, J.M., RENAUD, L.P., SPANSWICK. D. (2001)"A role for calcium in the regulation of electrotonic coupling between adrenomedullary sympathetic preganglionic neurons (AD-SPN)" Soc. Neurosci. Abstr. 31, 47.1

WILSON, J.M., CODERRE, E., SPANSWICK, D., RENAUD, L.P., (2000) "Neonatal adrenomedullary sympathetic preganglionic neurons (SPN) receive a noradrenergic slow inhibitory postsynaptic potential" Soc. Neurosci. Abstr. 30, 536.2

WILSON, J.M., CODERRE, E., SPANSWICK, D., RENAUD, L.P., (2000) "Membrane and synaptic properties of rat sympathetic preganglionic neurons innervating the adrenal medulla" Proceedings of the Royal Physiological Society London, 523P

CLAIM TO ORIGINALITY

This thesis consists of seven chapters and is written in a classical thesis format in accordance with the guidelines for presentation of a doctoral thesis to the Faculty of Graduate Studies and Research at University of Ottawa. The results presented in this thesis consist of an original contribution to knowledge concerning the neurophysiological integrative properties of sympathetic preganglionic neurons that project to the adrenal medulla. Insight is gained into the central neuronal mechanisms by which the control of the release of noradrenaline and adrenaline into the bloodstream may be achieved. Summarised below are the salient features of each chapter, relevant to the furtherance of scientific knowledge.

CHAPTER 1; The introduction provides a comprehensive overview of the current concepts of the sympathetic nervous system with particular emphasis on the regulation of catecholamine secretion. In addition the neurophysiological properties of the sympathetic preganglionic neurons that are the final central integrative center for autonomic outflow to the periphery are described.

CHAPTER 2; The methodology is described by which whole cell patch clamp recordings were obtained from sympathetic preganglionic neurons in a rat spinal cord slice. The criteria utilised to identify sympathetic preganglionic neuron that innervate the adrenal medulla (AD-SPN) are established.

CHAPTER 3; The active and passive membrane properties of AD-SPN are described and characterised in detail. Results indicate the expression of three active potassium conductances (an inward rectifying conductance, a transient and a sustained outward rectifying conductance) and 2 calcium conductances (a low threshold and high threshold calcium spike). A functional role for these conductances is investigated. These conductances are relatively uniformly expressed across this population of neurons.

CHAPTER 4; Electrotonic coupling is evident in 75% of AD-SPN. The features of electrotonic coupling are delineated with single electrode recordings and the properties of an electrotonically coupled network of SPN are investigated utilising dual recordings. A model is proposed to account for variable afterhyperpolarisations that contribute towards the generation of burst firing. The regulation of electrotonic coupling by internal calcium is also explored. I wish to formally acknowledge the collaborative effort of Dr David Spanswick and myself that was required to obtain these dual recordings.

CHAPTER 5; Electrical stimulation of both lateral funiculi are used to explore descending fast synaptic input to AD-SPN. The ensuing fast excitatory and inhibitory synaptic potentials are characterised as to their receptor subtypes. Also evident is a biphasic postsynaptic potential that is induced by action potential firing in a neighbouring electrotonically coupled neuron.

CHAPTER 6; Descending slow inhibitory postsynaptic potentials (IPSPs) in AD-SPN follow electrical stimulation of both lateral funiculi. The slow IPSPs are mediated by noradrenaline acting via α_2-adrenergic receptors and mediated by a potassium

conductance. The interaction between the slow IPSP and electrotonic coupling is examined.

CHAPTER 7; The final chapter discusses the intrinsic and extrinsic properties described above in relation to current knowledge of the function of the sympathetic nervous system relating to the control of catecholamines release from the adrenal medulla. Models to illustrate the integrative properties of AD-SPN are presented.

STATEMENT OF AUTHORSHIP

I certify that the work presented here was generated by myself. The exception lies in the generation of some the data in Chapter 4 pertaining to dual recordings from AD-SPN, obtained in conjunction with Dr David Spanswick. Ms Elaine Coderre taught the retrograde labeling of SPN by injections of dye into the adrenal medulla and kindly re-sectioned the spinal cord slices on the cryostat. Dr Leo Renaud supervised the writing of this thesis.

Agent	Action
4-aminopyridine	Potassium channel blocker
Apamin	Potent small calcium activated potassium channel blocker
D-AP5	Competative NMDA receptor antagonist
Arachidonic acid	Potassium channel blocker, 2 pore domain channels
Barium	Potassium channel blocker
BAPTA-AM	Membrane permeable calcium chelator
Bicuculline	$GABA_A$ receptor antagonist
Cadmium	Non-selective calcium channel blocker
Caesium	Broad spectrum potassium channel blocker
Caffeine	Induces calcium release from intracellular stores
Catechol	Potassium channel blocker
CNQX	Potent AMPA/Kainate receptor antagonist
Cobalt	Non-selective calcium channel blocker
GYKI 52466	Selective AMPA receptor antagonist
Lucifer yellow	Non-toxic intracellular fluorescent dye
Muscarine	Selective M-conductance potassium channel antagonist
NBQX	Potent and selective non-NMDA receptor antagonist
Nickel	Calcium channel blocker
Nimodipine	L-type calcium channel blocker
Nifedipine	L-type calcium channel blocker
Nisoxetine	Potent and selective inhibitor of noradrenaline uptake
ω-conotoxin GVIA	Selective blocker of N-type calcium channels
ω-agatoxin IVA	Selective blocker of P/Q-type calcium channels
ω-conotoxin MVIIC	Wide spectrum blocker of N, P & Q type calcium channels
Phentolamine	Non-selective α -adrenergic receptor antagonist
Prazosin	α_1- and α_{2B} -adrenergic receptor antagonist
Propanolol	β-adrenergic receptor antagonist
Quinine	Potassium channel blocker
QX-314	Blocks voltage-activated sodium channels, calcium and potassium channels

Rhodamine-dextran lysine	Non-toxic retrograde tracing fluorescent dye
Strychnine	Glycine receptor antagonist
Tetrodotoxin (TTx)	Selective inhibitor of sodium channel conductance
Tolbutamide	Inhibitor of ATP sensitive potassium channels
Tetraethylammonium	Potassium channel blocker
Xylamine	Noradrenaline uptake inhibitor
Yohimbine	α-adrenergic receptor antagonist

CHAPTER 1

INTRODUCTION

1.11 Preface

The autonomic nervous system regulates and co-ordinates outflow from the central nervous system to the peripheral organs and vasculature. Langley laid the groundwork of autonomic nervous system function based on the key observations that autonomic regulation could be split into two components that often had opposing effects on the targets innervated and that these effects could be mimicked by the application adrenergic and cholinergic agents. The opposing systems were termed parasympathetic and sympathetic (Langley, 1903, 1921). The parasympathetic nervous system originates in the brainstem and sacral spinal cord while sympathetic outflow is exclusively from the thoracolumber region of the spinal cord. The enteric nervous system has also subsequently been recognised as a subdivision of the autonomic nervous system that is restricted to the gastrointestinal system where it co-ordinates gut motility and secretion. The sympathetic nervous system is organised in a hierarchical manner in that supraspinal centres project to the spinal cord sympathetic preganglionic neurons (SPN) that innervate postganglionic neurons in the ganglia or to the adrenal medulla. The postganglionic neurons innervate all autonomic organs of the viscera. Therefore by the mid 1920's Langley had described all the components of autonomic function and proposed that each pathway could be relatively independently activated.

Subsequent studies led by Cannon, reduced the concept of differentiated autonomic outflow proposed by Langley to a system that was designed for generalised operations in the excitatory or inhibitory direction (Cannon *et al.*, 1929; Janig and

McLachlan, 1992a; Folkow, 2000). Indeed the importance of the autonomic nervous system was undermined by studies that documented the survival of animals whose sympathetic paravertebral chain had been removed (albeit in a protected environment). The generalised peripheral effects of sympatho-adrenomedullary activation coupled with extensive postganglionic network-like arbourisations suggested that the autonomic nervous system was relatively undifferentiated and therefore would be controlled in a synchronised "en masse" manner. As the autonomic nervous system was primarily concerned with the response to stress and was activated in a generalised manner these concepts were embedded in the familiar "flight or fight" dictum that has dominated autonomic thinking since Cannon (Cannon, 1939).

In recent years the "flight or fight" concept of autonomic nervous system function is being redefined by physiological studies which indicate that discrete effectors (subunits of the system) are independently regulated (Janig and McLachlan, 1992a, b; Morrison, 2001). For example, electrical stimuli to the hypothalamus can simultaneously activate cardiac and inhibit renal sympathetic nerve activity (Delius *et al.*, 1972; Okada and Ninomiya, 1983). Furthermore, independent regulation is apparent within a target organ. For example, stimulation of adjacent but separate brain regions can alter the ratio of noradrenaline to adrenaline secretion from the adrenal medulla (Folkow, 1954; Matsui, 1965; Feuerstein and Gutman, 1971; Matsui, 1979; Robinson *et al.*, 1983; Matsui, 1984; Marley and Livett, 1987; Matsui, 1987; Edwards *et al.*, 1996). Given this organisation, mass activation of the sympathetic nervous system, as in the "flight or fight" response, would consist not of a generalised response but rather of simultaneous activation of functionally separate units of the sympathetic nervous system.

For this independent control of peripheral autonomic organs to exist, there must be distinct central anatomical and/or physiological correlates, which could reside at singular or multiple levels of the neuraxis. For example, at the level of the preganglionic neurons specificity may relate to chromaffin cell type. For the differential release of noradrenaline and adrenaline from the adrenal medulla, there would need to be distinct supraspinal pathways that connect specifically to SPN that target one or the other types of chromaffin cells. In this manner function specific pathways could provide the basis for the precise selection and fine modulation of peripheral organs and targets in a highly differentiated autonomic nervous system.

The purpose of the research undertaken here is to probe this concept of a differentiated sympathetic nervous system by identifying a function specific central neuronal pathway, namely that of SPN that specifically project to the adrenal medulla (AD-SPN), and investigating the mechanisms that regulate neuronal excitability in this population of neurons.

1.2 The Autonomic Nervous System - Structure and Organisation

Many areas of the nervous system contribute to the reflex and adaptive control of body homeostasis. The central autonomic nervous system receives input from many diverse locations and modalities. Peripheral visceral information is relayed through the glossopharyngeal and vagus nerves to the nucleus tractus solitarius and the rostral ventrolateral medulla. There are visceral afferents to neurons in the thoracic spinal cord that convey information through ascending spinal projections. Other information is derived via neurons sensitive to blood glucose, osmolality and temperature modalities that are located in the hypothalamus and nucleus tractus solitarius. pH changes of

cerebral spinal fluid can be detected by neurons located in the "chemosensitive zone" of the ventral medulla. Circulating steroids can cross the blood brain barrier to act on specific receptors; others may be detected by the circumventricular organs. Processed sensory input from the association and paralimbic areas of the cerebral cortex may convey information to autonomic regulatory sites lower in the neuroaxis. The integration of such information takes place at many levels of the central autonomic nervous system, i.e. in the telencephalon, hypothalamus, brainstem and spinal cord, in order to permit moment to moment control in the activity of peripheral autonomic organs.

The autonomic output flows to the periphery through the cranial and spinal preganglionic neurons. Each receives input from areas mentioned above, and is recognised as having two functionally opposing components achieved through a diffuse postganglionic network. The vagus nerve constitutes the largest output of the parasympathetic system, innervating the heart, all exocrine glands and smooth muscle of the viscera of the neck, thorax and gastrointestinal tracts, including the pancreas and liver. Other cranial parasympathetic nerves control the salivary and lacrimal glands, the pupil and lens. The sacral parasympathetics innervate the bladder, descending colon, rectum and sexual organs. Sympathetic outflow proceeds through the SPN located in the intermediolateral cell column between C_8 and L_2 of the spinal cord that project to all autonomic organs and smooth muscle of the viscera (see Section 1.21).

Many organs have both parasympathetic and sympathetic innervation that control opposing actions. For example, in the heart sympathetic innervation induces tachycardia while parasympathetic input produces bradycardia. The smooth muscles that control the iris relax and thereby induce pupil dilation when the sympathetic neurons are activated, while parasympathetic activation induces pupil constriction. As a general principle of

operation, the sympathetic nervous system is recognised as being activated to cope with life threatening situations by increasing organ function and substrate availability. The parasympathetic system can balance the effects of sympathetic nervous system activation by inducing a recovery through decreasing energy expenditure and replenishing energy stores (Morrison, 2001). The autonomic nervous system is also responsible for endocrine output, through the release of hormones from the hypothalamus, and for the regulation of somatomotor output, via neural connections with the ventral striatum, central pattern generators and motor neurons in the spinal cord.

Sympathetic Nervous System

1.21 Structure and Organisation

The recognition that many central nervous system areas contribute to sympathetic outflow has given rise to the idea of a hierarchical organisation of the sympathetic nervous system. The hypothalamus, at the upper end of the sympathetic hierarchy, projects to autonomic centres in the brainstem and spinal cord and is involved in coordinating and maintaining cardiovascular, thermal, hormonal and metabolic homeostasis (see section 1.43). The middle component of the hierarchy is occupied by the brainstem autonomic medullary regions, that are often seen as the gateway though which all higher input must pass (see section 1.41). These areas may be involved in the reflex control of autonomic functions. The final central station in the sympathetic nervous system belongs to the SPN. SPN are organised symmetrically within the thoracolumbar spinal cord within four discrete nuclei, and topographically throughout the cord, so that upper thoracic SPN innervate the face and neck, while low thoracic SPN regulate the colon (see section 1.31). SPN axons, for the most part are unmyelinated, exit through the

ventral horns and in the white ramus communicantes to innervate postganglionic sympathetic neurons. Postganglionic sympathetic neurons are located in the paravertebral ganglia, within the sympathetic trunk, and in the prevertebral ganglia in the autonomic plexus. Postganglionic sympathetic neurons utilise noradrenaline as their transmitter (except for the sudomotor postganglionic sympathetic neurons that utilise acetylcholine).

The control of a wide range of peripheral targets from SPN within a single spinal segment can be achieved by 1) preganglionic axons projecting to paravertebral ganglia at the same segmental level with the postganglionic axons then traversing within the sympathetic trunk to the appropriate target and/or 2) preganglionic axons may bypass segmental ganglia to innervate paravertebral ganglia at many spinal levels. SPN axons may bypass the paravertebral ganglia altogether to form the splanchnic nerves, projecting to postganglionic sympathetic neurons in prevertebral ganglia, celiac, inferior or superior mesenteric ganglia or directly to the chromaffin cells in the adrenal medullae. The latter represents a unique anatomical arrangement in the sympathetic nervous system, in that it is the preganglionic axons that directly innervate the target organ, the chromaffin cells.

Circulating catecholamines control the level of sympathetic tone in the peripheral viscera by their action on α- and β-adrenergic receptors. For example, activation of peripheral α-adrenergic receptors induces constriction of blood vessels and contraction of smooth muscle in the viscera (except gastrointestinal smooth muscle, which relaxes) and an increase in hepatic glycogenolysis. Activation of β-adrenergic receptors by circulating catecholamines induces an increase in cardiac rate and force, mediates broncho- and blood vessel dilation by relaxation of smooth muscle. Circulating adrenaline has a higher affinity for β-adrenergic receptors while noradrenaline has a higher affinity for α-adrenergic

receptors. Physiological stimuli can promote a differential release of noradrenaline and adrenaline from the adrenal medulla on a moment to moment basis. Exposure to cold and manipulation of the baroreceptor reflex evokes a predominantly noradrenaline release, while hypoglycemia primarily causes an increase in adrenaline release (Feuerstein and Gutman, 1971; Gagner *et al.*, 1985; Khalil *et al.*, 1986; Vollmer *et al.*, 1992). A combination of the ratio of catecholamines released, along with the tissue distribution of α- and β- adrenergic receptors, will determine the peripheral response to sympathoadrenal activation.

Therefore the ratio of catecholamine release must be precisely controlled and the system be able to respond quickly to promote survival in response to threatening stimuli. In addition the alterations in body homeostasis that accompany acutely threatening stressors are mediated by coordinated activity in the adrenal, cardiovascular and respiratory systems.

1.22 Central regulation of the chromaffin cell

The chromaffin cells of the adrenal medulla are specialised postganglionic neurons in that they are the recipients of preganglionic cholinergic innervation (by way of the anterior greater or lesser splanchnic nerve (Young, 1939; Kesse *et al.*, 1988)), and secrete catecholamines into the bloodstream. Indeed chromaffin cells and postganglionic neurons are embryologically derived from a common precursor (Coupland, 1965). The ratio of adrenaline to noradrenaline release in rats and humans under resting conditions is around 3:1, but this can vary between species. The absence of the secretion of noradrenaline from the adrenal medulla in guinea pig, marmoset, dogfish and snake may

be due to the lack of a cortical layer (Parker *et al.*, 1993), whose function may be the methylation of noradrenaline (Livett and Marley, 1993).

What features regulating chromaffin cell mediated catecholamine secretion might contribute towards differential release of noradrenaline and adrenaline? First there are anatomical and physiological differences between noradrenergic and adrenergic secreting chromaffin cells. Anatomically the noradrenergic chromaffin cells tend to be grouped into small functional units whereas adrenergic cells tend to cluster in large groups (Iijima *et al.*, 1992; Kachi *et al.*, 1993). Physiologically, noradrenergic and adrenergic secreting chromaffin cells synthesise different peptides (enkephalins, vasointestinal peptide, substance P) (Kuramoto *et al.*, 1986), possess distinct membrane receptor profiles (nicotinic, muscarinic, angiotensin II, Substance P) (Tomlinson *et al.*, 1987), utilise different mechanisms for release (Marley and Livett, 1987) and release different combinations of co-transmitters.

Second, local circuitry may be a factor. For example it has been recently reported that chromaffin cells are electrotonically coupled and that intracellular calcium rises may propagate between adjacent cells (Martin *et al.*, 2001). In theory, should gap junctions be differentially distributed amoung adrenaline versus noradrenaline secreting chromaffin cells, amplification and synchronisation of activity could favour differential release of noradrenaline over adrenaline, or vice versa.

Third, the terminal branching pattern of preganglionic fibres may be different. Preganglionic axons innervating chromaffin cells give rise to both boutons de passage and terminal synapses (Coupland, 1965; Tomlinson and Coupland, 1990) and one preganglionic fibre may innervate a noradrenergic or adrenergic chromaffin cell but none have been reported to innervate both types (Parker, 1988; Tomlinson and Coupland,

1990). Approximately 700-800 SPN innervate the adrenal medulla and each SPN must make contact with a couple of thousand chromaffin cells (Parker, 1988). Electron microscopic studies demonstrate that each chromaffin cell receives approximately 5 nerve endings (reflecting both pre- and post-ganglionic input) (Tomlinson and Coupland, 1990). The packaging of chromaffin cells into discrete cell clusters has led to the proposal that neurons within these clusters are activated independently by the splanchnic nerve (Hillarp, 1946; Iijima *et al.*, 1992).

Fourth, innervation of the noradrenergic and adrenergic secreting chromaffin cells by preganglionic input may be distinct. In cat, two populations of AD-SPN have been identified based on the localisation of the calcium binding protein calretinin, with those containing calretinin projecting preferentially to the noradrenergic chromaffin cells (Edwards *et al.*, 1996). In rat, electrophysiologically four populations of splanchnic nerve projecting SPN were identified by their responses to electrical stimulation of the rostral ventrolateral medulla. From this two populations of AD-SPN were delineated as projecting to adrenergic and noradrenergic secreting chromaffin cells by their reponses to glucopenia and baroreceptor activation (Morrison and Reis, 1991; Morrison and Cao, 2000).

1.23 Sympathetic nerve activity

The autonomic peripheral organs are under continual modulation by activity in the sympathetic nerves. The tonic rhythmicity that sympathetic nerve discharge is noted for is bilaterally synchronous and is present in both postganglionic and preganglionic nerves, the latter including the splanchnic nerves containing the preganglionic input to the adrenal medulla (Adrian, 1932; Bronk, 1936). The patterning of activity in pre- and

post- ganglionic axons induces rhythmicity that is correlated with various organ cycles: 1) a cardiac rhythm (2-6Hz) is present in most sympathetic nerves and exhibits coherence to, but is not driven by, the baroreceptor nerve discharge; 2) a respiratory rhythm (0.5Hz) is generally activated during inspiration although coherence fluctuates depending on end organ innervation; 3) a 10Hz rhythm originally identified in splanchnic nerves (Cohen and Gootman, 1970), appears enhanced when sympathetic nerve activity is increased but has no known physiological correlate; 4) other low frequency rhythms (0.3-1.2Hz) have also been identified. Not all sympathetic nerves express all these rhythms equally. Within the splanchnic nerve, the dominant pattern of bursting activity is correlated to the respiratory rhythm with maximum activity in the middle inspiratory phase and minimum in the early expiratory. Furthermore, correlations to the cardiac rhythm were present in both a 1:1 and 3:1 relation (Cohen and Gootman, 1970).

In searching for the origin of sympathetic rhythms, investigations focussed on brainstem and medullary regions since midbrain/midcollicular transection resulted in little reduction of arterial pressure (Dittmar, 1873). Neurons in brainstem areas (rostral and caudal ventrolateral medulla, lateral tegmental area, raphe nuclei, pontine parabrachial and kölliker-fuse complex) display varying degrees of coherence with sympathetic nerve activity. However the fact that internal pacemaker-like activity has not been identified conclusively in any brainstem area has led to the proposal that the rhythmicity of sympathetic nerves arises out of a network of cells (for reviews see Sun, 1995; Malpas, 1998).

The role of the spinal cord in the generation of sympathetic nerve activity has been relatively neglected by researchers until the last decade. Spinal cord transection has differential effects on separate nerves exhibiting sympathetic nerve activity (Taylor and

Schramm, 1987). Sympathetic nerve activity can be induced after spinal cord transection by raising the excitability levels by injections of either inhibitory antagonists or excitatory amino acid agonists (Allen *et al.*, 1993) and is coordinated in cardiac nerves upon activation of the aortic constriction sympathetic reflex (Montano *et al.*, 2000; Montano *et al.*, 2001). Furthermore a 10Hz rhythm can be noted in cardiac nerves upon high frequency stimulation of lateral funiculi or injection of NMDA in spinal cats (Kubota *et al.*, 1995; Ootsuka *et al.*, 1995). These observations piqued interest into the possibility that mechanisms within the spinal cord exist to generate the co-ordinated rhythms observed in sympathetic nerve activity. Further evidence for spinally mediated sympathetic rhythms derives from Gilbey's observations of a high degree of coherence and synchronisation of a low frequency (0.04-1.2Hz) thermoregulatory-rhythm between pairs of postganglionic neurons and nerves, upon activation of the central respiratory drive (Johnson and Gilbey, 1996, 1998; Chang *et al.*, 1999a; Chang *et al.*, 2000a). Therefore it is suggested that multiple oscillators with "free run" frequencies exist that may be entrained by a common input (Gilbey, 2001; Staras *et al.*, 2001). This is reminiscent of the idea of "binding" (Farmer, 1998) where a temporal input pattern across a network may adhere multiple oscillators to synchrony.

Sympathetic Preganglionic Neurons

1.31 Organisation and distribution

SPN are present in the thoracolumbar region of the spinal cord and are located in four discrete symmetrical and bilateral areas, often referred to as nuclei, that give rise to a ladder-like formation (Petras and Cummings, 1972). The majority (~90%) of SPN are found within the confines of the intermediolateral cell column located in the lateral horn.

A small population of SPN are present in the lateral funiculi regions, lateral to the intermediolateral cell column. Medial to the intermediolateral cell column are the less defined regions of the intercalated nucleus (between the intermediolateral cell column and central canal area) and the central autonomic area (surrounding the central canal area), where small, but significant, numbers of SPN are located. The latter two areas give rise to SPNs whose dendrites predominantly project in a mediolateral direction thus giving rise to the "rungs" of the ladder arrangement that typifies SPN organisation.

SPN located in the intermediolateral cell column project their dendrites in the rostrocaudal plane giving rise to the "supports" of the ladder. In addition dendrites are also observed to project extensively in the mediolateral and dorsoventral planes. Within the intermediolateral cell column, SPN aggregate into clusters or nests which can contain from 20 to 100 SPN, and which are between 100 and 300μM distance apart, depending not only on the species but also on the segment studied.

SPN are topographically distributed in a rostrocaudal orientation throughout the cord. SPN whose axons innervate the adrenomedullary chromaffin cells (AD-SPN) are the most widely distributed population located in varying extents between spinal cord levels T_1 to L_1 with 20% present in the segment T_9 and over 60% between T_7-T_{10} segments (Figure 1.1, Strack *et al.*, 1988; Jensen *et al.*, 1992). SPN that innervate the superior cervical ganglion are located in upper thoracic (T_1-T_4) spinal cord segments. SPN innervating the inferior and superior mesenteric ganglion are located in low thoracic (T_{10}-L_2) regions (Strack *et al.*, 1988). Logically, the majority of SPN regulate autonomic functions on the ipsilateral side, except for the control of intestine and pelvic viscera, and strictly speaking the heart (see Cabot, 1990).

Further differentiation of SPN with respect to function (i.e. target of postganglionic innervation) is present within the intermediolateral cell column. In the lumbar cord, SPNs whose primary function is vasoconstriction lie lateral to SPN engaged in visceral activities (Janig and McLachlan, 1987). In the thoracic cord, SPN that project to the adrenal gland are located laterally to those that project to the superior cervical ganglion. SPN which project to the stellate ganglion occupy a space in the intermediolateral cell column between the afore mentioned SPN (Pyner and Coote, 1994b).

1.32Chemical Phenotype

Classically cholinergic, SPN synthesise and release the neurotransmitter acetylcholine onto chromaffin cells and postganglionic neurons. Chromaffin cells possess both nicotinic and muscarinic receptors. When activated by acetylcholine, the former induce calcium influx to trigger catecholamine release, while the latter increase inositol trisphosphate inducing calcium release from internal stores. Muscarinic receptors may not be directly involved in catecholamine release (Livett and Marley, 1993).

A number of preganglionic non-cholinergic molecules also contribute to catecholamine secretion. Substance P is present in splanchnic nerve terminals in the adrenal medulla (Lundberg *et al.*, 1978) from where it is released to act both pre and postsynaptically to inhibit nicotinic receptor-mediated catecholamine secretion and prevent desensitisation (Livett *et al.*, 1979; Boksa and Livett, 1984; Zhou and Livett, 1990a, b). Substance P immunoreactivity is present in SPN cell bodies in the intermediolateral cell column with peaks in immunoreactivity observed at L_1 and also T_4-T_7 and T_{12}-L_2 (Krukoff *et al.*, 1985). In opposition to the modulation induced by

substance P, the proposed mechanism of action for the pituitary adenylate cyclase activating polypeptide (PACAP) involves the enhancement of muscarinic and nicotinic induced catecholamine release (Inoue *et al.*, 2000). The origin of PACAP is likely to be preganglionic as PACAP is present in a subpopulation of SPN somata in the intermediolateral cell column (Beaudet *et al.*, 1998) but not in chromaffin cells (Nielsen *et al.*, 1998) and PACAP / choline acetyltransferase (ChAT) immuno-positive fibres surround chromaffin cells in the adrenal medulla (Holgert *et al.*, 1996). Interestingly these fibres preferentially surround noradrenaline containing chromaffin cells, suggesting a function specific pathway.

The leucine- and methionine- enkephalins are present in SPN somata at thoracic levels T_4-T_7 (Krukoff *et al.*, 1985) and enkephalin/ChAT immunoreactive fibres preferentially surround adrenaline containing chromaffin cells (Holgert *et al.*, 1996). Somatostatin immunoreactivity in SPN in the intermediolateral cell column is evident at spinal levels T_1-T_7 and corticotrophin-releasing factor immunoreactivity is present in upper thoracic and lumbar SPN (Krukoff, 1986). However data is not available on whether these may be contained within SPN that project to the adrenal medulla and hence have a role in modulating catecholamine release. Nitric oxide synthase immunoreactivity is also evident in a subpopulation of adrenomedullary projecting SPN (Blottner and Baumgarten, 1992). Vasoactive intestinal peptide, also present in intermediolateral cell column SPN somata in mid and lower thoracic regions (Krukoff, 1986) and in nerve fibres in the adrenal medulla, can evoke catecholamine release from adrenomedullary chromaffin cells and enhance release mediated by acetylcholine (Anderova *et al.*, 1998). Furthermore colocalisation of vasoactive intestinal peptide and enkephalins in cholinergic nerve fibres has been reported (Keast, 1991). Therefore these co-existing molecules are

likely to add complexity to central control of catecholamine secretion by sympathetic innervation.

Electrophysiolgical Properties of SPN

Considerable diversity in the electrophysiological properties of SPN has been documented in previous investigations, which is perhaps not surprising considering the diversity of peripheral organ innervation. To date no data has been published on the intrinsic properties of SPN from a functionally identifiable population and therefore this section will provide an overview of the state of knowledge concerning the whole population of SPN.

1.33 Passive Properties

Utilising intracellular recordings, *in vivo* resting membrane potentials range from –40 to –80mV (Coote and Westbury, 1979; McLachlan and Hirst, 1980; Dembowsky *et al.*, 1985b, 1986). This wide range is possibly attributable to the fact that SPN receive continuous synaptic input in an intact preparation, thus masking a stable "resting" membrane potential. Therefore lack of synaptic input in the *in vitro* preparation is likely to give a better reflection of resting membrane potential values. These values recorded in slice preparations with intracellular sharp electrodes are –61.3±1.6mV in the adult cat (Yoshimura *et al.*, 1986b) and -66±4 mV in the guinea pig (Inokuchi *et al.*, 1993c). Whole-cell recording techniques give values of -52±1.6mV (Pickering *et al.*, 1991) and –62.6 ±9.8mV (Miyazaki *et al.*, 1996) in the neonatal rat.

Time constants, a measure of electrotonic "compactness", are longer in whole cell recordings from neonatal rat *in vitro* (range 31-360ms (Pickering *et al.*, 1991; Spanswick *et al.*, 1994)) than those from intracellular sharp electrode recordings both *in vivo* (range 4-26ms (McLachlan and Hirst, 1980; Dembowsky *et al.*, 1986)) and *in vitro* (range 7-20ms (Yoshimura *et al.*, 1986b)) from adult cat. Differences may reflect the quality in the seal between cell and electrode with the two techniques. In addition temperature may be a factor; whole cell recordings are obtained at room temperature while intracellular recordings are obtained at higher temperatures.

Equally as heterogeneous are the reported values of steady state input resistance. In the neonatal rat these range from 62 to 254 MΩ (Spanswick and Logan, 1990a, b; Lewis *et al.*, 1993; Spanswick *et al.*, 1994; Sah and McLachlan, 1995; Spanswick *et al.*, 1995; Miyazaki *et al.*, 1996). In adult cat input resistance *in vitro* was calculated as 67 to 71MΩ (Yoshimura *et al.*, 1986b) and *in vivo* as 12 to 50 MΩ (Dembowsky *et al.*, 1986, McLachlan & Hirst, 1980). In the adult guinea pig values from 126 to 141MΩ were obtained (Inokuchi *et al.*, 1993c). In contrast to these values, which were all obtained using the intracellular sharp recording technique, the whole cell recording technique yielded input resistance values of at least an order of magnitude higher. In neonatal rat *in vitro*, calculated values ranged from 380 to 2800 MΩ (Pickering *et al.*, 1991, 1994; Spanswick *et al.*, 1994, 1995; Miyazaki *et al.*, 1996), values that may reflect both temperature differences and the high resistance seal between cell and electrode in whole cell recordings and intracellular recording techniques.

1.34 Active Properties

A) The Action Potential

The action potential recorded in SPN somata may be spontaneous but also can be elicited either by stimulation of the ventral roots (antidromic), ventrolateral funiculi (orthodromic) or by intracellular current injection. Data reveal that two components constitute the action potential; 1) a small amplitude (16-40mV), low threshold component indicative of the action potential of the initial segment of the axon and 2) a high threshold, large amplitude (70-80mV) component constituting the soma-dendritic action potential (Dembowsky *et al.*, 1986; Yoshimura *et al.*, 1986b). The depolarising phase of the action potential is due to the activation of both sodium and calcium conductances (Yoshimura *et al.*, 1986b), blockable with tetrodotoxin (TTx) and cobalt respectively. The action potential in SPN is notable for its long duration (1.7±0.3ms in adult guinea pig *in vitro* (Inokuchi *et al.*, 1993c), 4.85±0.05ms in cat *in vivo* using intracellular electrodes (Dembowsky *et al.*, 1986), 8.8±0.4ms using whole-cell recordings in neonatal rat slices (Pickering *et al.*, 1991)), attributable to a prominent shoulder on the repolarising phase of the action potential. That a calcium conductance prolongs the action potential is demonstrated by the absence of the shoulder in low extracellular calcium conditions and in the presence of cobalt (Yoshimura *et al.*, 1986b; Sah and McLachlan, 1995). The repolarising phase of the action potential involves the activation of the delayed outward rectifying potassium conductance, demonstrated by the sensitivity of the duration to the application of tetramethylammonium (TEA) (Yoshimura *et al.*, 1986b; Miyazaki *et al.*, 1996).

B) The afterhyperpolarising potential

In SPN, the action potential is followed by a prominent afterhyperpolarising potential of variable duration. Values obtained with intracellular recording were 16.6mV and 2.8s in adult cat *in vitro* (Yoshimura *et al.*, 1986a), 14mV and 728ms in guinea pig *in vitro* (Inokuchi *et al.*, 1993c), 9mV and 678 ms in adult cat *in vivo* (Dembowsky *et al.*, 1986). Using intracellular versus whole-cell recordings in neonatal rats, values of 3-13mV and 0.5-4s (Spanswick and Logan, 1990a) and 14-33mV and 0.1-1s (Pickering *et al.*, 1991) were obtained. The variation could be due to differences in temperature or internal dialysis of cellular constituents.

It is postulated that the afterhyperpolarising potential comprises two conductances, a fast and slow component, both of which are facilitated by the outward movement of potassium ions. The fast afterhyperpolarising potential is TEA and internal caesium sensitive, indicative of a voltage-activated potassium channel. The slow afterhyperpolarising potential is sensitive to cobalt and calcium free extracellular solution suggesting mediation by a calcium -activated potassium conductance (Yoshimura *et al.*, 1986a). This latter conductance can be separated into 2 components, a transient (apamin sensitive) and a sustained (ryanodine sensitive) component (Inokuchi *et al.*, 1993b; Miyazaki *et al.*, 1996). The shape and time course of the afterhyperpolarising potential between SPN are highly variable (Yoshimura *et al.*, 1986a), which may be attributable to the amount calcium influx during the action potential, or due to other ionic conductances activated during the hyperpolarising phase. Upon blocking the afterhyperpolarising potential, with e.g. noradrenaline, an afterdepolarising potential is revealed (Dembowsky *et al.*, 1986; Polosa *et al.*, 1988) which may be mediated by a calcium dependent inward sodium conductance (Yoshimura *et al.*, 1987d).

C) Active Conductances

The time the membrane potential takes to reach rest on the break of a hyperpolarising current pulse is longer than that predicated by the time constant of the membrane, suggesting the presence of active conductances. Intracellular recordings *in vitro* (Yoshimura *et al.*, 1987e) and *in vivo* (Dembowsky *et al.*, 1986) in cat, guinea pig (Inokuchi *et al.*, 1993c) and whole-cell recording *in vitro* in neonatal rat (Pickering *et al.*, 1991; Miyazaki *et al.*, 1996) report durations from 0.3s up to 2s. This transient conductance is sensitive to extracellular potassium with a reversal potential around -90mV (Yoshimura *et al.*, 1987e). A fast component of this conductance can be blocked with 2-4mM 4-aminopyridine (Yoshimura *et al.*, 1987e; Pickering *et al.*, 1991) suggesting that it is due, in part, to activation of an A-current. The longer duration component remains to be classified.

A decrease in input resistance in SPN is observed upon injection of large hyperpolarising current pulses from resting membrane potentials. This rectification is time independent and has been reported in cat *in vivo* (Dembowsky *et al.*, 1986) and neonatal rat *in vitro* (Pickering *et al.*, 1991), although not all SPN express this conductance. Interestingly, in guinea pig (Inokuchi *et al.*, 1993c) and cat (Yoshimura *et al.*, 1986b), both time-independent and time-dependent rectification have been observed in SPN where the former is sensitive to barium and the latter to caesium.

In recognising SPN heterogeneity with respect to conductances expressed and in attempting to unravel functional implications, several research groups have sub-categorised SPN by their electrophysiological properties. *In vivo* intracellular recordings at T_3 in the cat suggest 3 types of SPN based on the prominence of the initial segment-somatic depolarising inflexion and shoulder, the presence or absence of an

afterdepolarising potential, resting membrane potential, input resistance and ongoing synaptic activity resulting in action potential firing. Transient rectification was observed in 2 out of the 3 groups while inward rectification was differentially expressed in the same 2 groups (Dembowsky *et al.*, 1986). Data recorded at T_2-T_3 in guinea pig slices (Inokuchi *et al.*, 1993c) led to SPN characterisation by duration of afterhyperpolarising potential and action potential, and by the presence of the transient rectifier. The authors suggest SPN may be subgrouped based on the presence or absence of a time-dependent inward rectifier. Although these studies are aimed at the SPN whose axons project to the stellate ganglion (inferior cervical ganglion) as the major effector of the heart, T_2-T_3 also contains SPN which project to the superior and middle cervical ganglion.

1.35 Morphology of SPN

SPN are morphologically diverse with respect to their somata shape and dendritic arbourisation and it remains to be investigated whether such distinctions are related to specific inputs or functional output. SPN somata display at least four distinctly different shapes; round, fusiform with the long axis rostrocaudally orientated, oval or spindle shaped. SPN somata are large with long axis diameters ranging from 38μm in rabbit (Pilowsky *et al.*, 1992) to 24μm in neonatal (Forehand, 1990; Shen and Dun, 1990) and 25μm in adult rat (Pyner and Coote, 1994b). Short axes vary between 20μm and 10μm. Somata shape does not appear to predict nuclear location (Cabot, 1990). Somata size and shape are similar in adult and neonate rat, although in the adult SPN are more tightly clustered with a predominantly rostrocaudal somatic orientation (Pyner and Coote, 1994b).

SPN axons are unmyelinated and arise from the soma or from proximal dendrites (Rethelyi 1958) from where they course through the ventral horn to exit through the ipsilateral ventral roots (Rubin and Purves, 1980). An axonal location for synaptic input to SPN has been observed in both rat and rabbit (Llewellyn-Smith *et al.*, 1995a) and although little is known about these synapses, their location is suggestive of a strong role in the regulation of sympathetic activity.

Extensive dendritic arbourisations arise from intermediolateral cell column SPN, with up to 8 short dendrites projecting laterally into the white matter and up to 4 long medially projecting dendrites (Shen and Dun, 1990). These dendrites rarely branch but can form a plexus-like network around the central canal area or continue towards the contralateral intermediolateral cell column (Vera *et al.*, 1990). Such a feature is seen in AD-SPN and in superior cervical ganglion-projecting SPN. Interestingly in the adult rat, medial projecting dendritic bundles are more dense than in neonate, are contributed to by adjacent clusters and turn at the central canal area to run in a rostrocaudal direction (Pyner and Coote, 1994a). SPN in the intermediolateral cell column can also send dendrites in the rostrocaudal planes for 1.5-2.5mm in adult cat (Dembowsky *et al.*, 1985a) and for 0.6mm in the neonatal rat (Forehand, 1990), within the intermediolateral cell columns. Such distances cover and allow possible contact with SPN in 1-2 clusters above and below original somata location. Based upon the observation of SPN projecting dendrites only in the rostrocaudal direction, the idea of the intermediolateral cell column being a closed nucleus was previously formulated (Dembowsky *et al.*, 1985a). However recent research utilising more advanced tracing methods have disproved this idea (Vera *et al.*, 1986; Pyner and Coote, 1994b, 1995). Typically SPN display dendrites in two of the three dimensions described. SPN with their somata outside the intermediolateral cell

column can exhibit radial dendrites in three dimensions (Forehand, 1990). Total dendritic length ranges from 872 to 4335μM (Forehand, 1990). As the surface area of the somata is estimated to be less than 15% of total membrane surface (Cabot, 1990), the extent of dendritic arbourisation in SPN could have significant effects on membrane resistance and time constants. It is possible that the majority of incoming synaptic information occurs on the dendrites. Indeed the beaded appearance (Bacon and Smith, 1988; Pyner and Coote, 1994b) and observation of dendritic spines (Bacon and Smith, 1988) suggests that these dendrites are synapse-rich and therefore capable of participating in the integration of incoming synaptic potentials.

1.36 Spinal interneuronal networks involving SPN

SPN receive both visceral and somatic information from the periphery. Some of these inputs participate in reflex arcs while others are subject to modulation from supraspinal structures. SPNs are not innervated monosynaptically by any class of visceral or somatic afferents, however these afferents project to lamina V and lateral lamina VII (see Krenz and Weaver, 1998b). A high degree of convergence of such afferent input onto second order interneurons in the dorsal horn may in itself regulate reflex input to SPN. The development of viral tracers which cross synapses in a retrograde direction has enabled labeling of interneurons that are afferent to SPN projecting to a specific target. Using this methodology in the rat, researchers have reported that interneurons to AD-SPN are located in lamina V and in the intercalated area medial to the intermediolateral cell column (Joshi *et al.*, 1995). Interneurons to superior cervical ganglion projecting SPN are located in the reticular division of lamina V and dorsolateral lamina VII (Cabot *et al.*, 1994) and those innervating SPN that project to the

stellate are found in lamina I, V, VII, and X (Jansen and Loewy, 1997). Therefore the likely circuitry is primary afferent to interneuron in either lamina V or VII to SPN.

The lateral funiculi, as well as being a major highway for brain-spinal connections, also contains three distinct cell groups; the lateral cervical nucleus, the lateral spinal nucleus and a scattered neuronal group within the lateral funiculi. That the lateral funiculi cell group and the lateral spinal nucleus innervate SPN is suggested by their labeling upon injection of the stellate ganglion (Jansen *et al.*, 1995a) and kidney (Schramm, 1993) with retrograde viral tracers. Further studies indicate that labeling is also present after injection into the superior cervical and celiac ganglions, and the adrenal gland (Jansen and Loewy, 1997). The lateral funiculi neurons primarily project to SPN although axon termination sites are noted in the ventral horn and in lamina V, VII and X. The lateral spinal nucleus also projects predominantly to the intermediolateral cell column, with slightly different projection topography. In addition to projecting to lamina V, VII and X, termination sites are also present in the medial part of lamina I and lamina II in the cervical and upper thoracic cord while terminations are far less frequent in the lower thoracic regions. Interestingly, projections from the lateral funiculi neurons are bilateral as are those innervating the upper thoracic region from the lateral spinal nucleus However in the cervical cord, the projections of the latter are only ipsilateral (Jansen and Loewy, 1997). As the two groups of neurons were labeled from viral injections into distinct sympathetic ganglia, it is probable that such neurons are capable of affecting different functional subsystems of sympathetic outflow.

1.4 Central descending projections controlling catecholamine release

Catecholamine release is intimately controlled by central sympathetic reflex circuits involving neuronal networks in the brainstem that project to the spinal cord. As mentioned previously (section 1.12) the nucleus tractus solitarius is a major integrative centre for afferent input from the periphery, and is involved in long loop sympathetic reflexes, but itself does not directly project to the spinal cord (Laskey and Polosa, 1988). The vagal and glossopharyngeal cranial nerves terminating in the nucleus tractus solitarius carry information from the cardiac and arterial baroreceptors as well as peripheral chemoreceptors, detecting changes in blood pressure and chemical composition of blood and cerebrospinal fluid. The predominantly excitatory neurons of the nucleus tractus solitarius project to many autonomic centres including the rostral and caudal ventrolateral medulla, raphe nucleus, A5, periaqueductal gray region and the paraventricular nucleus of the hypothalamus, regions that contain neurons that subsequently project towards the intermediolateral cell column. Furthermore the nucleus tractus solitarius receives and integrates emotional and behavioural states from neurons descending from the neocortex and limbic systems (Spyer, 1990).

Neurons in several brainstem autonomic areas send their axons to the intermediolateral cell column. Neurons projecting specifically to AD-SPN have been located by injection of viral retrograde tracers in the adrenal gland and subsequently phenotypically identified with immunohistochemical techniques. Physiologically, numerous discrete brain areas, when electrically or chemically stimulated, evoke a rise or change in ratio of catecholamine release from the adrenal medulla. These 5 key areas include the paraventricular nucleus of the hypothalamus, the A5 noradrenergic cell group, the ventromedial and rostral ventrolateral medulla and the caudal raphe nucleus (Strack *et*

al., 1989a). These central circuits, their role in autonomic function and effects on catecholamine secretion will be reviewed below.

1.41 The ventral medulla oblongata

Two main groups of neurons project from the ventral medulla oblongata to the spinal cord; a) the rostral ventrolateral medulla and b) medial groups that reside in the ventromedial medulla and the caudal raphe nucleus.

A) The rostral ventrolateral medulla

The rostral ventrolateral medulla is an essential component in the sympathetic regulation of blood pressure (Dittmar, 1873; Guyenet, 1990). Indeed excitation or inhibition of these neurons induces large rises or decreases in blood pressure and sympathetic nerve activity respectively. Topographical organisation of neurons in the rostral ventrolateral medulla with regards to end organ function (McAllen and Dampney, 1990) could be the basis of both differential sympathetic nerve activation (Yardley *et al.*, 1989; Hayes and Weaver, 1990; Beluli and Weaver, 1991) and differential patterning within sympathetic nerves with a common function (i.e. vasoconstrictor activity (Dampney and McAllen, 1988)). However the multiplicity of neuronal projections and phenotypes within the rostral ventrolateral medulla precludes clear topographical boundaries. In addition to the activation of vasoconstrictor sympathetic nerves innervating the blood vessels (Dampney *et al.*, 1985; Willette *et al.*, 1987; McAllen, 1989), a rise in blood pressure evoked by stimulation of the rostral ventrolateral medulla is contributed to by an increase in catecholamine secretion from the adrenal medulla (McAllen, 1986). Interestingly the catecholamine secretion contained nearly twice as

much adrenaline as noradrenaline (McAllen, 1986). The multiplicity of sympathetic effector activation upon rostral ventrolateral stimulation resembles the central mechanisms that co-ordinate the fight or flight response. Indeed a population of neurons has been identified in the rostral ventrolateral medulla that project to more than one functional group of SPN, and therefore are likely to form part of a central command network (Jansen *et al.*, 1995b).

The rostral ventrolateral medulla receives substantial input from the nucleus tractus solitarius, and fibres from the area postrema, parabrachial complex, lateral hypothalamus and paraventricular nucleus and the midbrain periaqueductal gray. In turn approximately two thirds of the neurons located within the rostral ventrolateral medulla are reticulospinal with descending projections to the intermediolateral cell column (see Figure 1.2). Half of these form the C1 neuronal pool that shows immunoreactivity for phenylethanolamine N-methyltransferase (PNMT), the enzyme that catalyses the N-methylation of noradrenaline to adrenaline, substance P and neuropeptide Y. However the phenotype of these C1 neurons has not been resolved as adrenaline has not been found in the spinal cord and PNMT inhibition has little effect on sympathetic responses to rostral ventrolateral medulla stimulation (Connor and Drew, 1987; Sved, 1989). The other half of the neurons in the rostral ventrolateral medulla that project to the spinal cord are believed to be glutamatergic (Guyenet, 1990). Other molecules that may participate in these projections include serotonin, substance P, enkephalins, noradrenaline (indicated by tyrosine hydroxylase), somatostatin and neuropeptide Y (Helke *et al.*, 1986; Charlton and Helke, 1987; Hirsch and Helke, 1988; Sasek and Helke, 1989; Strack *et al.*, 1989a). Neurons projecting from the rostral ventrolateral medulla specifically to AD-SPN have been shown to contain PNMT (51%), substance P (19%) and serotonin (>1%) (Strack *et*

al., 1989a). Such a co-localisation of putative neurotransmitters in nerve terminals could allow for modulation of transmission and indicate chemical coding within function specific pathways.

B) The rostral ventromedial medulla and caudal raphe

Neurons in the rostral ventromedial medulla and caudal raphe also contact AD-SPN. Those from the ventromedial medulla also contain PNMT but less substance P than those in the ventrolateral medulla (Strack *et al.*, 1989a). Colocalisation of serotonin and substance P in axons and nerve terminals in the intermediolateral cell column suggests that the rostral ventromedial medulla is a likely contributor of this innervation to SPN. In contrast to the rostral ventrolateral medulla, activation of the rostral ventromedial medulla induces a decrease in blood pressure (Guyenet, 1990).

Stimulation of neurons in the caudal raphe nucleus can induce both depressor and pressor sympathetic responses, indicative of both inhibitory and excitatory neurons projecting to the spinal cord (Gilbey *et al.*, 1981; Zhou and Gilbey, 1995). The firing patterns of raphe neurons that project to the spinal cord can be correlated with cardiac sympathetic nerve activity and are excited by baroreceptor stimulation, indicating a sympathoinhibitory function (Morrison and Gebber, 1982). In addition, inhibition of the serotonergic raphe neurons eliminated the 10Hz component of sympathetic nerve activity (Orer *et al.*, 1996). Utilising SPNs differential responses to raphe nucleus and to rostral ventrolateral medullary stimulation has enabled segregation of SPN that project their axons through the splanchnic nerve into functional groups (Morrison, 1993). Cell bodies in the raphe nucleus that project to AD-SPN contain serotonin and substance P. In addition, colocalisation of serotonin with substance P, thyrotropin-releasing hormone,

enkephalin or somatostatin is observed in fibres surrounding AD-SPN (Holets and Elde, 1982), suggesting that the raphe nucleus may be the source of this input.

1.42 The pontine catecholaminergic groups

The noradrenergic system, originating from the locus coeruleus region in the dorsolateral pons, is perhaps unrivaled in its divergence of projections throughout the central nervous system. A pivotal role for the locus coeruleus complex in autonomic function is implicated by means of its output to "autonomic" areas (e.g. nucleus tractus solitarius, ventrolateral medulla, dorsolateral pons, intermediolateral cell column, paraventricular nucleus, supraoptic nuclei, thalamic nuclei and superchiasmatic nucleus (see Guyenet, 1991) and input from autonomic centres (ventrolateral and ventromedial medulla). Indeed, due to high catecholamine content, tight aggregation of neurons, and varicose axons innervating the central nervous system in its entirety (Ungerstedt, 1971), the locus coeruleus region has been likened to a central sympathetic ganglion (Jones, 1991).

Caecholaminergic neurons in the brainstem are located in distinct clusters that, due to disparate matching with traditional cytoarchitectural borders, have been labeled alphanumerically from A1-A13 (Dahlstrom, 1965). Subsequently transmitter specific retrograde tracing methods established that noradrenergic neurons in the locus coeruleus nuclei, the subcoeruleus nuclei, the medial and lateral parabrachial and Kölliker-Fuse nuclei, areas that correspond to the A5-A7 cell groups, project to the spinal cord (Bjorklund, 1982; Byrum *et al.*, 1984). The tegmento-spinal pathway in the dorsolateral funiculi is composed of axons from A2, A5 and A7 (Loewy *et al.*, 1986; Byrum and Guyenet, 1987; Clark and Proudfit, 1991). Interestingly, neurons from A5, while

predominantly innervating the intermediolateral cell column (Loewy *et al.*, 1979; Strack *et al.*, 1989b), lightly innervate both dorsal and ventral horns (Clark and Proudfit, 1993), suggesting a role in nociception and motor control as well as modulating autonomic outflow.

Retrograde virus tracing studies indicate that the A5 region specifically innervates AD-SPN (Strack *et al.*, 1989a). In addition, chemical stimulation of the A5 area has been reported to produce both an increase and decrease of sympathetic nerve activity (Huangfu *et al.*, 1992). Both electrical and chemical stimulation of the locus coeruleus proper (A6) evoked a biphasic pressor response contributable to a rise in blood pressure via sympathetic vasoconstriction and a release of catecholamines. Only the release of catecholamines was specifically attributable to locus coeruleus stimulation and noradrenergic containing spinal projecting neurons (Drolet and Gauthier, 1985; Goadsby, 1985).

1.43 The Hypothalamus

Evidence accumulated over the last 75 years recognises the control of catecholamine release by neuronal pathways originating in the hypothalamus (Houssay, 1925). In addition, activation of the hypothalamus induces a wide range of emotional (Hess, 1955; Wasman, 1962; Stoddard *et al.*, 1986b) and sympathetic mediated responses including pupillodilation (Loewy *et al.*, 1973), vasopressor responses (Enoch and Kerr, 1967a, b), and changes in heart rate and blood pressure (Stoddard-Apter *et al.*, 1983). Interestingly secretion of catecholamines is not always concomitant with activation of the cardiovascular system (Stoddard-Apter *et al.*, 1983) suggesting that, as in the rostral

ventrolateral medulla, some neurons may form part of a "central command network" that permits the simultaneous activation of various autonomic end organ targets.

Widespread hypothalamic areas have been implicated in catecholamine release when either electrically or chemically stimulated (Harrison, 1939; Francke *et al.*, 1982; Robinson *et al.*, 1983; Stoddard-Apter *et al.*, 1983; Matsui, 1984; Katafuchi *et al.*, 1986; Stoddard *et al.*, 1986a, b). Of particular note are parvocellular neurons in the paraventricular nucleus that project directly to AD-SPN as revealed by retrograde viral tracing studies (Strack *et al.*, 1989a). Support for innervation by paraventricular hypothalamic neurons of AD-SPN was obtained from studies at the light microscope level utilising a combination of retro- and antero-grade tracers (Ranson *et al.*, 1998; Motawei *et al.*, 1999).

Studies evoking catecholamine release by electrical or chemical stimulation reveal two interesting features of central autonomic function: a) that catecholamine secretion could be bilaterally evoked from stimulation of a single hypothalamic site, indicating that descending hypothalamic fibres could decussate at a spinal level (Harrison, 1939; Francke *et al.*, 1982; Ranson *et al.*, 1998); and b) that the proportion of noradrenaline to adrenaline release was not equal, implying distinct central pathways in the regulation of noradrenaline versus adrenaline secreting chromaffin cells (Folkow, 1954).

The latter raises the question: Are the functions of the hypothalamus chemically coded and could this be a mechanism for differential control of adrenal catecholamine secretion? Certainly the range of sympathetic responses evoked by hypothalamic stimulation (see above and also Yamashita *et al.*, 1987; Kannan *et al.*, 1989; Martin and Haywood, 1992) and the diversity of neuronal phenotype suggest this may be a

possibility. Within the hypothalamus five groups of intermediolateral cell column projecting neurons are distinguishable by their specific locations and distinct phenotypes (Figure 1.2) (Hosoya, 1980; Swanson and Kuypers, 1980; Sawchenko and Swanson, 1982; Schwanzel-Fukuda *et al.*, 1984; Tucker and Saper, 1985; Hosoya *et al.*, 1991; Ranson *et al.*, 1998; Motawei *et al.*, 1999): 1) parvocellular neurons of the dorsal and medial paraventricular nucleus that synthesise arginine-vasopressin, oxytocin and met-enkephalin. Additionally, paraventricular neuronal terminals containing vasopressin surround AD-SPN (Motawei *et al.*, 1999); 2) scattered neurons in the retrochiasmatic area that contain α-melanocyte-stimulating hormone; 3) neurons in the perifornical area that synthesise atrial naturetic peptide; 4) lateral hypothalamic neurons containing α-melanocyte-stimulating hormone and orexin/hypocretin and lesser amounts of substance P and galanin; 5) a small neuronal group in the dorsal hypothalamic area that are immunoreactive for tyrosine hydroxylase and occasionally calcitonin gene related peptide (Cechetto and Saper, 1988). Recent studies have demonstrated the co-expression of cocaine-and-amphetamine-regulated-transcript (CART) and pro-opiomelanocortin messenger ribonucleic acid (mRNA) (for α-Melanocyte stimulating hormone) in neurons located in the retrochiasmatic area and lateral arcuate nucleus of the hypothalamus that project to the thoracic cord (Elias *et al.*, 1998). Since leptin induces activation of *cfos* in these neurons, it is thought that they may be involved in regulating thermogenesis and energy expenditure.

1.44 Cortical influence on autonomic function

That the autonomic nervous system is intimately connected to higher cognitive centres is evident by the sympathetic and/or parasympathetic responses associated with an emotional moment. Indeed these interactions were observed over 125 years ago (Bochefontaine, 1876) but it took until the 1930s and 40s when studies by Hess in awake cats indicated clear coupling between the limbic, hypothalamic and autonomic centres in the spinal cord (see Folkow, 2000 for references). The fight or flight response is commonly believed to be a "reflex". However at least in humans, stimuli that may on one occasion induce a rise in catecholamine secretion may be ignored on other occasions. Alternatively emotional responses are well known to induce visceral responses.

Electrical stimulation of cortical areas has identified various regions that are capable of modulating catecholamine secretion. For example, a selective decrease in adrenaline release occurred upon stimulation of antero-medial and lateral parts of the ventral orbital surface (von Euler, 1958). Injection of retrograde transynaptic viral tracers into the adrenal gland results in labeled neurons in 4 main cortical areas; layers III and V of the infralimbic cortex; the insular cortex, in particular the anterior dysgranular cortex; the posterior piriform cortex; various areas in the ventromedial temporal lobe that include the central, basomedial posterior, basolateral posterior and the lateral amygdaloid nuclei, as well as the lateral entorhinal cortex (Westerhaus and Loewy, 2001). Interestingly the infralimbic cortex, insular and temporal cortical regions are interconnected structures raising the possibility that these areas form networks that determine higher brain functions (i.e. emotion and learning), and are able to modulate sympathetic responses accordingly (Westerhaus and Loewy, 2001). The representation of the adrenal system in the cortical areas appears to be more substantial than the cardiac (stellate) or enteric

(celiac) system, which may suggest that catecholamine secretion is under greater influence by these higher brain regions (Westerhaus and Loewy, 2001).

Chemical synaptic transmission to SPN

Since the early 1950's, chemical transmission has been regarded as the most common form of neuronal communication. Over 50 molecules (amino acids, catecholamines and peptides) have been proposed as neurotransmitter candidates to SPN based on anatomical, immunohistochemical, biochemical and electrophysiological data (Laskey and Polosa, 1988).

1.51 Fast excitatory transmission

L-Glutamate acting at ionotropic n-methyl-d-aspartate (NMDA) and non-NMDA receptors is considered to mediate rapid excitatory neurotransmission in vertebrate central nervous system (Watkins, 2000). In the sympathetic nervous system, L-glutamate is proposed to mediate fast excitatory input to SPN that arises from both segmental and supraspinal inputs (Laskey and Polosa, 1988). Spontaneous fast excitatory postsynaptic potentials (EPSP) in cat *in vivo* (Dembowsky *et al.*, 1985b) and those evoked by electrical stimulation of the rostral ventrolateral medulla (Deuchars *et al.*, 1997) or both lateral funiculi and ipsilateral dorsal horn in rat *in vitro* (Spanswick *et al.*, 1998) can be blocked by glutamatergic antagonists implying a role for L-glutamate in excitatory inputs to SPN. Iontophoretically applied L-glutamate excites SPN *in vivo* (Backman and Henry, 1983a) and in a slice preparation (Yoshimura and Nishi, 1982; Shen *et al.*, 1990; Spanswick and Logan, 1990a; Inokuchi *et al.*, 1992c). Further discussion of the role of glutamatergic inputs to SPN is given in Chapter 5.

1.52 Fast inhibitory transmission

Fast inhibitory postsynaptic potentials (IPSPs) can be evoked in SPN by electrical stimulation of the lateral funiculi in cat (Inokuchi *et al.*, 1992b), the rostral ventrolateral medulla (Deuchars *et al.*, 1997) and dorsal and ventral roots in rat (Dun and Mo, 1989; Spanswick *et al.*, 1994). In addition spontaneous unitary IPSPs are observed in rat (Dun and Mo, 1989; Krupp and Feltz, 1993). These IPSPs are mediated by the amino acids, gamma aminobutyric acid (GABA) and glycine, both of which can inhibit the electrical activity of SPN and may have different roles in regulating the excitability of SPN (Krupp and Feltz, 1993) and sympathetic nerve activity (Clement and McCall, 1995).

A) GABA

In the central nervous system, the majority of inhibitory neurotransmission is mediated via GABA acting at GABA ionotropic receptors. GABA has been implicated in the control of blood pressure and heart rate (Gordon, 1985; Dampney, 1994). For a full description of the electrophysiological data concerning GABA and SPN see Chapter 5.

Little is known about supraspinal GABAergic input to SPN. GABA immunoreactive neurons that are located in the rostral and caudal ventrolateral medulla send their axons towards the intermediolateral cell column (Matsumoto *et al.*, 1994) and electrical stimulation of the rostral ventrolateral medulla evokes a monosynaptic GABAergic IPSP in upper thoracic SPN (Deuchars *et al.*, 1997). GABA input to SPN may also arise from a segmental level as GABA synapses are located on SPN somata after a spinal transection (Llewellyn-Smith *et al.*, 1997a), however, many of these may be a result of sprouting in response to injury. In the intact preparation, spinal GABAergic interneurons are primarily located in laminae I – III (Magoul *et al.*, 1987; Todd and

Sullivan, 1990). Several subpopulations of GABAergic interneurons are suggested by co-localisation studies. GABAergic interneurons that contain the calcium binding protein parvalbumin are present in laminae II and III (Antal *et al.*, 1991), while those co-localising with enkephalin are present in laminae I, II, V and X in the spinal cord (Liu *et al.*, 1992). However several studies argue against SPN receiving a segmental GABAergic input. Firstly, transynaptic retrograde tracers injected into the superior cervical ganglia labeled interneurons, that project to SPN, in lamina IV, V and VII but not in laminae I-III (Cabot *et al.*, 1994). Secondly, a lack of spontaneous GABAergic mediated activity has been observed in transverse slices (Dun and Mo, 1989; Krupp and Feltz, 1993).

B) Glycine

A prominent role for glycine in segmental inhibition of spinal autonomic circuits is suggested by the presence of glycine in somata of interneurons throughout the spinal cord, especially in the ventral and lateral horns. The presence of glycinergic receptors on SPN membrane is indicated by strychnine binding and glycine-like immunoreactive inputs to SPN (Cabot *et al.*, 1992). Furthermore ultrastructural studies observe dense gephyrin (which is associated with the ligand-binding, membrane spanning subunits of the glycine receptor) immunoreactivity in SPN neuropil and proximal dendrites, opposing presynaptic boutons (Cabot *et al.*, 1995).

Electrophysiologically, application of glycine to SPN *in vivo* induces a strychnine-sensitive hyperpolarisation in membrane potential (Backman and Henry, 1983a). In addition dorsal horn evoked fast IPSPs in SPNs are strychnine sensitive and mediated by the opening of a chloride conductance (Dun and Mo, 1989; Inokuchi *et al.*, 1992b; Krupp and Feltz, 1993; Spanswick *et al.*, 1994). These glycinergic interneurons

are activated by L-glutamate acting on NMDA, non-NMDA and metabotropic receptors (Spanswick *et al.*, 1994). Spontaneous glycinergic IPSPs are observed in SPN *in vitro* and analysis of IPSP frequencies suggests at least two separate inputs (Krupp and Feltz, 1993; Krupp *et al.*, 1997). Interestingly one of these patterns exhibits bursting firing characteristics that serve to inhibit membrane activity over a long period of time. These data indicate a powerful inhibitory or shunting role for glycine in regulating segmental excitatory input in SPN. Electrophysiological (Inokuchi *et al.*, 1992b) and electron microscopic data (Cabot *et al.*, 1995) raise the suggestion that GABA and glycine may be co-localised in presynaptic terminals. However, unlike the dorsal horn neurons (Todd *et al.*, 1996), co-release has not been demonstrated.

1.53 Slow synaptic transmission and catecholamines

Excitation of brainstem catecholamine areas induces both pressor (Loewy *et al.*, 1979) and depressor (Coote and Macleod, 1974) cardiovascular responses. That catecholamines may have a role in mediating both sympathoinhibition and sympathoexcitation is suggested by the fact that these effects evoked by electrical stimulation of the A5 region can be blocked by injection of catecholamine neurotoxin 6-hydroxydopamine (Loewy *et al.*, 1979; Neil and Loewy, 1982; Woodruff *et al.*, 1986). Furthermore heart rate and blood pressure can be increased or decreased by injection of noradrenaline into the intermediolateral cell column. Exogenously applied noradrenaline in cat and adrenaline in rat produced both depolarisation and hyperpolarisation of SPN membrane potential (Yoshimura *et al.*, 1987b; Miyazaki *et al.*, 1989). In the rat noradrenaline depolarises SPN (Ma and Dun, 1985). In a subpopulation of cat SPN, a slow IPSP (9-12s) evoked by stimulation of the lateral funiculi is mediated by α_2-adrenergic receptors opening potassium channels (Yoshimura *et al.*, 1987c). Yoshimura

and coworkers (1987) also report that a slow EPSP, of similar time course as the slow IPSP is mediated by noradrenaline acting on α_1-adrenergic receptors (Yoshimura *et al.*, 1987c). Anatomical studies also attest to the fact that catecholamines are involved in chemical neurotransmission to SPN. Dense noradrenergic fiber terminals surround nerve cells in the intermediolateral cell column (Carlsson, 1964) subsequently identified as SPN (Chiba and Masuko, 1986; Milner *et al.*, 1988). The binding of adrenergic agonists and antagonists has been demonstrated on SPN membrane (Cabot *et al.*, 1984; Seybold and Elde, 1984). The role of catecholamines in synaptic transmission to SPN is further detailed in Chapter 6.

1.54 Serotonin

The caudal raphe nucleus contains serotonergic neurons that, upon activation, can both inhibit and excite SPN thus both illiciting depressor and pressor sympathetic responses (Gilbey *et al.*, 1981; Zhou and Gilbey, 1995). Iontophoretically applied serotonin to SPN *in vivo* evoked an excitatory response (Kadzielawa, 1983; McCall, 1983) however inhibition and biphasic responses have also been observed (Backman *et al.*, 1990; Lewis and Coote, 1990b; Gilbey and Stein, 1991). SPN responses to serotonin are likely to be related to their function. Studies in cat lumbar cord indicate that the heterogenous response of SPN to serotonin may relate to skin and muscle vasoconstrictor functions (Gilbey and Stein, 1991). Iontophoretically applied serotonin to both adrenal and non-adrenal projecting SPN produced similar excitation (Backman *et al.*, 1990). *In vitro*, serotonin has been shown to cause a slow depolarisation in SPNs (Coote *et al.*, 1981b; Yoshimura and Nishi, 1982; Kadzielawa, 1983; Pickering *et al.*, 1994). Within the central autonomic system, it is proposed that serotonin mediates sympathoexcitation by activation of 5-hydroxytryptamine (5-HT)-2 receptors involving a potassium

conductance while sympathoinhibition results from activation of 5-HT_{1A} receptors (Yoshimura and Nishi, 1982; McCall and Clement, 1994).

1.55 Colocalisation of peptides and receptor expression in SPN

Colocalisation of putative neurotransmitters in presynaptic terminals to SPN may be common place. Virtually all of the nerve fibres that innervate SPN contain either L-glutamate or GABA (Llewellyn-Smith *et al.*, 1992; Llewellyn-Smith *et al.*, 1995b) and over half the terminals in the intermediolateral cell column contain both Substance P and serotonin (Wessendorf, 1987), many of which may also contain glutamate (Minson, 1991). Surrounding AD-SPN and those that project through the splanchnic nerve are serotonin, met-enkephalin, substance P and somatostatin vasoactive intestinal peptide immuno-positive fibres (Hong and Weaver, 1993). Terminals immunoreactive for angiotensin II, neuropeptide Y, thyrotropin-releasing hormone have been demonstrated to synapse with SPN including AD-SPN (Holets and Elde, 1982; Appel *et al.*, 1986, 1987) although actual transmitter release has yet to be shown. Many other fibres harbouring potential neurotransmitter candidates (i.e. oxytocin, neurotensin) come in close opposition with SPN but synaptic release has not been demonstrated nor has direct contact at the ultrastructural level.

In addition to receptors for glutamate, glycine and GABA, serotonin and catecholamines mentioned above, receptors for oxytocin and vasopressin, angiotensin II, thyroid releasing hormone, metabotropic glutamate receptors, PACAP, and substance P are functional in SPN (Laskey and Polosa, 1988; Lai *et al.*, 1997). However to date, physiological release of the ligands for these receptors has not been demonstrated.

Differential expression of receptors occurs in functional populations of SPN; the majority (70%) of AD-SPN are neurokinin receptor-1 immuno-positive in comparison with SPN that project to superior cervical ganglion (38%) (Llewellyn-Smith *et al.*, 1997b). The majority of AD-SPN that exhibit neurokinin receptor-1 immunoreactivity are also immunoreactive for nitric oxide synthase (Grkovic, 1996). Substance P exerts a direct excitatory (Dun and Mo, 1988; Inokuchi *et al.*, 1993a; Cammack and Logan, 1996) and indirect inhibitory effect on SPN (Dun and Mo, 1988) and on AD-SPN (Backman *et al.*, 1990). Furthermore, substance P injected at T_9-T_{10}, acts via neurokinin receptor-1 to induce catecholamine release from the adrenal gland (Riphagen, 1986). These data implicate that modulation of AD-SPN neuronal activity by substance P may regulate catecholamine secretion from the adrenal medulla.

1.6 Electrotonic transmission

The first conclusive reports of electrotonic coupling came from dual intracellular recordings from the crayfish giant motor synapse (Furshpan and Potter, 1959) and cardiac ganglion of the mantid shrimp (Watanabe, 1958) showing bidirectional current transfer. The electrotonic junction is the specialised site of contact that permits a low resistance pathway and is comprised of gap junction channels that, in mammals, are composed of connexin proteins. Within the central nervous system, electrotonic coupling has been recognised in many neuronal networks where synchrony and speed and often reciprocity are necessary for function (Draguhn *et al.*, 1998; Galarreta and Hestrin, 1999; Mann-Metzer and Yarom, 1999). These include the giant motor synapse of the crayfish, where electrotonic coupling promotes escape behaviour (Furshpan and Potter, 1959), the hippocampus where high frequency oscillations require electrotonic junctions (Draguhn

et al., 1998) that may promote seizure activity (Traub and Wong, 1983) and the thalamocortical network where synchronised activity via electrotonic junctions may contribute to the rhythms observed during sleep and seizures (Landisman *et al.*, 2002).

The last ten years has witnessed a surge of information regarding all aspects of electrotonic coupling; from the cloning and characterisation of channel proteins (Hoh *et al.*, 1991; Dermietzel, 1996; Teubner *et al.*, 2001), structure of the pore (Revel *et al.*, 1992; Hoh *et al.*, 1993), ion flux (Bruzzone *et al.*, 1996; Veenstra, 1996; Nicholson *et al.*, 2000) and discrete modulation (Bolanos and Medina, 1996; Rorig and Sutor, 1996b; Jorgensen *et al.*, 1997; Velazquez *et al.*, 1997) to computer modeling studies indicating the influences of and contributions to network activity (Moortgat *et al.*, 2000; Traub and Bibbig, 2000). In addition, a role has been proposed for dysfunctional, mutated or absence of gap junctions and their connexin proteins in several disease states (Simon and Goodenough, 1998; Carlen *et al.*, 2000; Chang *et al.*, 2000b).

In the spinal cord, it is well established that motor neurons are electrotonically coupled during development in both invertebrates (Bennett, 1977; Sillar and Simmers, 1994) and mammals (Fulton *et al.*, 1980; Walton and Navarrete, 1991) and undergo transient re-coupling upon injury (Chang *et al.*, 2000b). Electrotonic coupling is restricted to specific motor neuronal pools (Walton and Navarrete, 1991; Tresch and Kiehn, 2000) and has also been reported in pre-motor interneuronal networks (Saint-Amant and Drapeau, 2001). Within the adult spinal cord connexins 36, 37 and 43 are present in neurons (Rash *et al.*, 1996; Chang *et al.*, 1999b) however their functional role has yet to be resolved (Kiehn and Tresch, 2002).

Rhythmic activity observed in a subpopulation of neonatal rat SPN (Spanswick and Logan, 1990b; Shen *et al.*, 1994) is due to electrical coupling between neurons

(Logan *et al.*, 1996). Simultaneous recordings have confirmed direct current transfer between 4 pairs out of 23 pairs of SPN (Logan *et al.*, 1996) and 21 out of 200 pairs (Nolan *et al.*, 1999). Rhythmic activity that is due to electrotonic coupling can be observed in adult SPN indicating a role for coupled neuronal networks beyond developmental stages (Leslie *et al*, 2000). However the functional importance and consequences of electrotonic coupling in SPN are yet to be elucidated, an issue this thesis will address.

1.7 Hypothesis and Objectives

Mass activation of the sympathetic adrenal nervous system occurs in the reflex "fight or flight" response that is characterised by extensive release of both noradrenaline and adrenaline from the adrenal medulla into the bloodstream. SPN are the final central site for integration of autonomic sympathetic reflexes and the substrate by which central commands to the adrenal medulla are finally processed, integrated and executed. Hence the neuronal output from SPN to the chromaffin cells determines catecholamine secretion. That this is important can be seen in the effect that variation of stimulus frequency and patterning delivered to their axons can have in noradrenaline versus adrenaline release (Allen *et al.*, 1984; Bloom *et al.*, 1988, 1989; Edwards and Jones, 1993). Recognising the intrinsic membrane and extrinsic synaptic mechanisms regulating excitability of AD-SPN is fundamental to our understanding of how the central nervous system regulates adrenal medulla function and catecholamine secretion. Therefore this research was undertaken with the aim of characterising the intrinsic passive and active conductances specific to AD-SPN and to investigate the chemically mediated amino acid and catecholaminergic synaptic input received by AD-SPN from putatively descending

inputs. In addition the presence of electrotonic coupling in this functionally specific cell group is investigated and its effects on individual neurons explored.

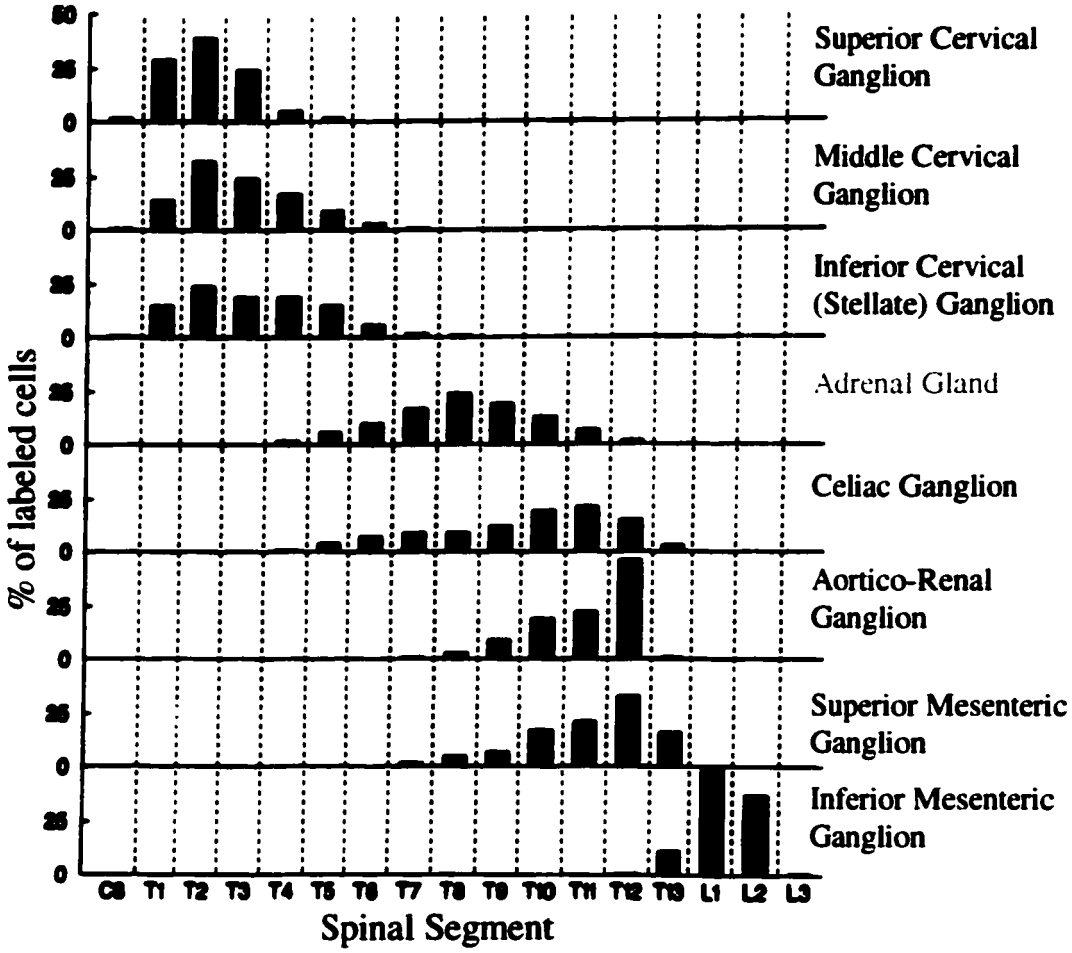

Figure 1.1 Segmental distribution of sympathetic preganlgionic neurons labeled by non-toxic retrogradely transporting dyes injected into major sympathetic ganglia and adrenal gland. Note both the rostrocaudal organisation of SPN inputs to sympathetic ganglia and the location of SPN projecting to the adrenal gland.

(Reproduced from Strack *et al.*, (1988) Brain Research 455, p187-191)

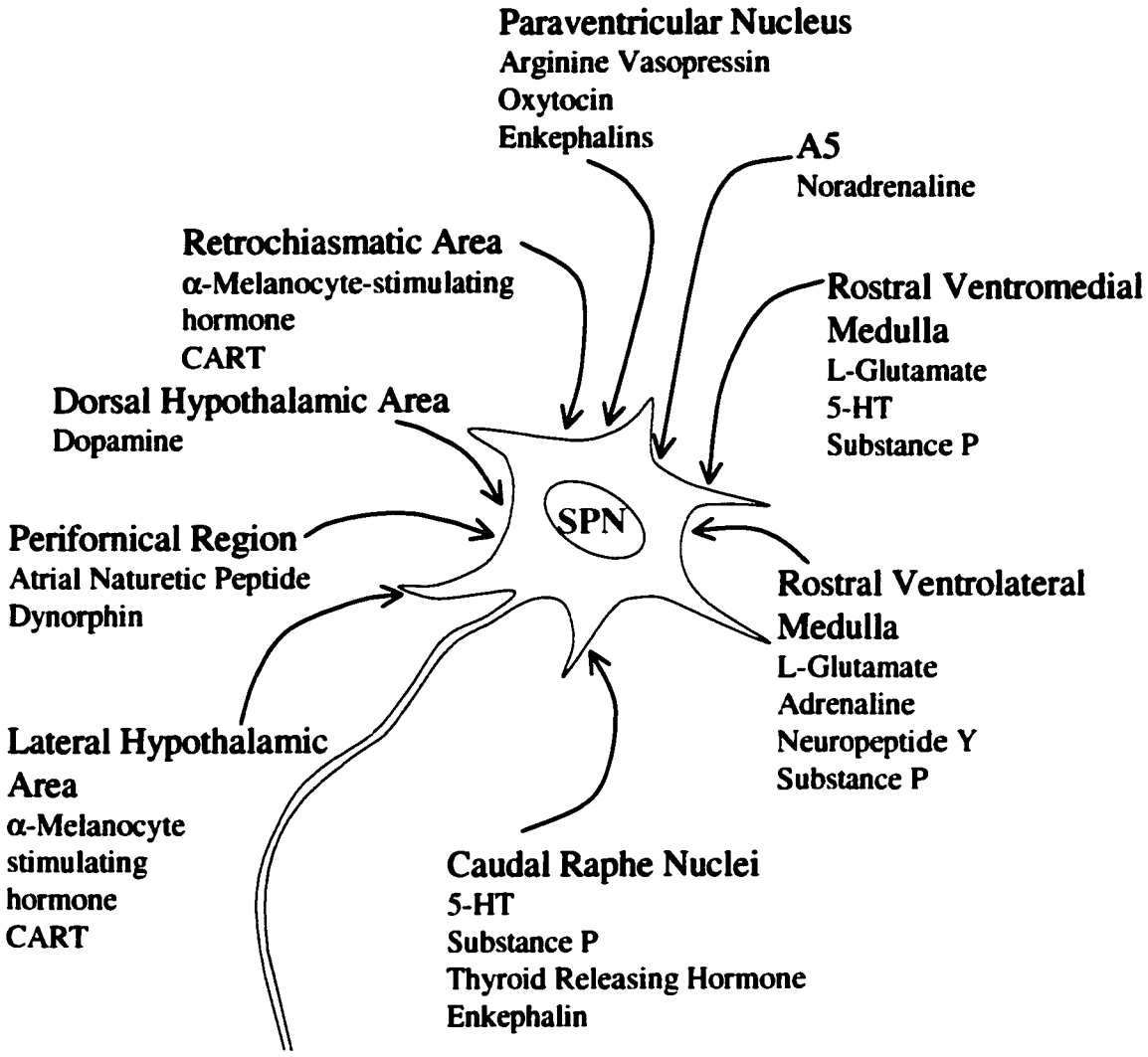

Figure 1.2 – Schematic diagram illustrating the innervation of SPN in the IML by multiple, chemically diverse, fibres arising from brainstem and hypothalamus.

CHAPTER 2

METHODOLOGY

All experiments involved Sprague-Dawley pups that were bred and kept with mother for nursing. They were housed in a controlled environment (temperature; 22 °C, humidity 35%, 12 hour light/dark cycle) and mothers were provided with rat chow and tap water *ad libitum*. Neonatal rats (8-16days) were utilised throughout all experiments due to the relative ease of obtaining live spinal cord slices when compared to adult rats. All protocols were approved by and experiments were performed under the guidelines of the Animal Care Committee of the Ottawa Health Research Institute.

2.1 Pre-labeling of adrenal medulla projecting sympathetic preganglionic neurons

The unique arrangement of preganglionic innervation of the adrenal medullary chromaffin cells can be exploited to permit retrograde labeling of SPN cell bodies in the spinal cord by injection of a non-toxic tracer dye into the adrenal medulla. Neonatal rats were deeply anaesthetised with halothane (4% in O_2) and pedal and tail reflexes were monitored throughout surgical procedures to indicate the level of anaesthesia. The left adrenal gland was exposed and 5-10μl Rhodamine Dextran Lysine (10%, Molecular Probes) injected into the medulla (Figure 2.1). The wound was sutured and animals allowed to recover for 2-8 days. SPN were pre-labeled using methods similar to those previously reported (Viana *et al.*, 1990; Spanswick *et al.*, 1998). Pertinent to this study is the fact that, although the adrenal medulla is relatively slow to develop, by 10 days after birth, splanchnic nerve innervation is functionally mature (Slotkin, 1986; von Dalnok and

Menssen, 1986) and physiological stimuli i.e. hypoglycemia can elicit centrally mediated catecholamine secretion from the adrenal medulla (Slotkin, 1986).

2.2 Slice preparation

Sprague-Dawley rats (9-17days old) were anaesthetised with halothane and a laminectomy performed. A thoracic segment of spinal cord (T_4-T_{12}) was removed and the animal killed by decapitation. Spinal cord slices (400μm thick) were cut using a vibratome (Leica VT1000S) and allowed to equilibrate for 1hour at room temperature in artificial cerebrospinal fluid (aCSF) of the following composition (mM): NaCl, 127; KCl, 1.9; KH_2PO_4, 1.2; $CaCl_2$, 2.4; $MgCl_2$, 1.3; $NaHCO_3$, 26; D-glucose 10; gassed with 95% O_2 , 5% CO_2; pH 7.4, before being transferred to a recording chamber of the submersion type where they were continuously superfused with aCSF. These methods for obtaining whole-cell recordings from rat thoracic spinal cord slices are similar to those extensively utilised in previous studies (Spanswick and Logan, 1990a; Pickering *et al.*, 1991).

A group of experiments required an altered ionic composition of aCSF. In experiments where low external potassium was required, potassium chloride was omitted from the aCSF and potassium phosphate KH_2PO_4 was replaced with equimolar sodium phosphate NaH_2PO_4. For high external potassium, sodium chloride was substituted with 4.4mM potassium chloride, taking the total external potassium concentration to 7.5mM. When nominally calcium free aCSF was required, calcium chloride was omitted and magnesium chloride concentration increased to 5.2mM. A compromised sodium gradient was achieved by substitution with 67mM Tris-sodium chloride, giving a final sodium concentration of 60mM.

2.3 Electrophysiological recordings

Whole-cell recordings avoid the potential of electrode shunting as may occur during sharp microelectrode recordings (Pickering *et al.*, 1991; Pongracz *et al.*, 1991; Staley *et al.*, 1992) and thus were chosen as the recording technique for this study. Run down of channel activity was minimised by the inclusion of adenosine trisphosphate in the patch pipette solution. Indeed no differences in basic membrane properties, calcium or GABA mediated chloride conductances were observed during the course of recordings. SPN possess extensive dendritic arbourisation (Coote, 1988). Therefore whole-cell recordings were obtained in the current-clamp configuration so as to avoid the issue of space clamp. Recordings were obtained from SPN at room temperature (18-21^{0}C) through patch pipettes with resistances of 4.5 –10MΩ filled with the following solution (mM); K-Gluconate, 130; KCl, 10; Mg-ATP 4; EGTA, 1; Hepes, 10; pH 7.4 adjusted with NaOH; mosmol 290-305. Where experiments required internal caesium, caesium chloride (140mM) replaced K-Gluconate and KCl. N-(2,6-Dimethylphenyl carbamoylmethyl)triethylammonium chloride (QX-314) was utilised to block the fast voltage dependent sodium conductance that contributes to the depolarising phase of the action potential in SPN. QX-314 loaded pipettes contained all of the original components plus 4mM QX-314 (Alomone). Lucifer Yellow (5mg/ml, Sigma) or Alexa 594 (70-100μM, Molecular Probes) were included in the patch pipette in order to intracellularly label the recorded neurons. To try to probe electrotonic junction permeability, the smaller Alexa dyes 350 and 480 were occasionally included in the patch pipette. Recordings were obtained with a patch clamp amplifier (Axopatch-1D, Axon Instruments). Although not being a dedicated current-clamp patch amplifier and therefore not ideally suited for

recording fast electrical events, this amplifier is sufficient for the relatively slow events investigated in this study (see Magistretti *et al.*, 1996). Data was acquired with pclamp8 software (Axon Instruments) and stored for offline analysis.

Drugs were made up in stocks in distilled water, except for quinine and arachidonic acid that were dissolved in ethanol, and diluted to the correct concentration in aCSF prior to application. Controls for ethanol were carried out prior to drug application and were without effect. Light exposure was kept to a minimum for light sensitive compounds (i.e. arachidonic acid, nimodipine, nifedipine and carbechol) by covering solutions with tin foil and undertaking experiments in the dark.

2.4 Double labeling of sympathetic preganglionic neurons

In slices from rats in which the adrenal medulla had been injected with rhodamine dextran lysine, cells were recorded on the ipsilateral side using a "blind" approach. Following recording the slices were fixed in 4% paraformaldehyde in phosphate buffer for 8-24hours and subsequently transferred to 25% sucrose in phosphate buffer for 48hours. Slices were frozen and re-sectioned into 25-35μm sections, collected on a glass slide and air-dried. Sections were viewed under a fluorescent microscope (Zeiss Axioskop) with appropriate filters and permanent records were made utilising conventional slide photography.

2.5 Quantification of membrane properties

Resting membrane potential refers to the read-out of the amplifier and was corrected for junction potential offset (10mV) after recording. The input resistance was determined by fitting the portion of the current-voltage curve around steady state

membrane potentials with a straight line. The time constant (tau) was evaluated by fitting the first membrane voltage response to hyperpolarising 20pA current pulses with one or two exponential functions. The amplitude of the action potential was calculated as the difference between peak voltage and threshold generation, and action potential duration was measured at one third peak amplitude. Action potentials were evoked either by antidromic stimulation of the ventral roots in the ventral horn at the exit zone or by a short duration (1ms) high current pulse injected into the SPN. Care was taken to ensure that the current pulse was over before the peak of the action potential was reached. The afterhyperpolarising potential amplitude refers to the maximal negative membrane potential after the action potential and the decay time was calculated as the 90-10% time to decay.

2.6 Indices of strength of electrotonic coupling

The strength of electrotonic coupling was approximated by calculating the coupling coefficient for current transfer and the junctional conductance (Bennett, 1966, 1977). The coupling coefficient is calculated as the ratio of the amplitude of the postsynaptic to presynaptic voltage change and can be represented by the equation;

$$k_{1\text{-}2} = V_1 / V_2$$

By incorporating the steady state input resistances and coupling coefficients into a model in which each neuron is represented by a single compartment joined by a low resistance pathway representing the electrotonic junction, the junctional conductance can be calculated from the equation;

$$Gj_{1\text{-}2} = \frac{R_1 k_1}{((R_1 R_2) - (R_1 k_{1\text{-}2})^2)}$$

where R_1 and R_2 are the input resistances for the pre- and post- synaptic neuron

k_{12} is the coupling coefficient reflecting current transfer from pre- to post-synaptic neuron

For every pair of electrotonically coupled neurons, coupling coefficients and junctional conductances are calculated in both a forward ($k_{1\text{-}2}$ and $Gj_{1\text{-}2}$) and reverse ($k_{2\text{-}1}$ and $Gj_{2\text{-}1}$) direction. The ratios of coupling coefficients, input resistance and junctional conductance are calculated as the ratio of the largest to the smallest value.

2.7 Synaptic responses

Synaptic potentials were evoked by stimulation of the ipsilateral and contralateral funiculi (iLF and cLF respectively) of the spinal cord with concentric bipolar stimulating electrodes with diameters of 25μm. Stimulating intensities ranged from 1 to 13V. To ensure that activation of the lateral funiculi were selective, the stimulating electrodes were maneuvered to areas outside the lateral funiculi. Failure to evoke synaptic potentials from these areas indicated selective activation of fibres in the lateral funiculi and that potentials evoked were not due to current spread through other pathways. For fast synaptic potentials, low frequency stimulation (0.05-0.03Hz) was utilised to ensure consistent postsynaptic potentials. Slow synaptic potentials were evoked by a variety of trains of stimuli, the most common being 4 stimuli at 10Hz (0.008Hz). Other trains tested included 2x10Hz, 2x100Hz, 4x100Hz, all at 0.008Hz. Properties of postsynaptic potentials were defined and calculated thus; rise time refers to the 10-90% time to peak

amplitude, decay time was measured from 90-10% peak amplitude to baseline levels, or by fitting with single exponentials allowing extrapolation of tau values. The latency for all evoked synaptic and electrotonic potentials was calculated from the end of stimuli to onset of response

2.8 Identification of sympathetic preganglionic neurons

Upon whole-cell recording, SPN located in the intermediolateral cell column display a low input resistance, slow firing frequencies and a combination of electrophysiological properties: a shoulder on the repolarising phase of the action potential; a transient outward rectifier; an anomolous inward rectification. However, not all SPN display all these conductances and different combinations can be observed. Interneurons are also present in the intermediolateral cell column and possess distinct properties, with high firing frequencies, high input resistances and lack of the above mentioned conductances. Experiments were performed on SPN that resembled the profile of positively identified AD-SPN (see below).

2.9 Identification of adrenomedullary sympathetic preganglionic neurons

Both transverse and longitudinal slices were prepared to investigate the distribution of AD-SPN in the spinal cord revealed by retrograde labelling with rhodamine dextran lysine. In longitudinal slices, the prelabeled cells were organised in a columnar fashion along the medial edge of the lateral funiculi, ipsilateral to the site of injection (Figure 2.2A), and spanned the thoracic spinal cord between T_3-T_{12} with distinct clusters of labeled cells most prominent around T_7-T_{10}. Occasionally labeled cells were observed in the lateral funiculi. However, no cells were found in the intercalated or

central autonomic areas. This distribution of labeled cells corresponds with previously described locations of AD-SPN (Strack *et al.*, 1988; Jensen *et al.*, 1992; Llewellyn-Smith *et al.*, 1992; Forehand *et al.*, 1994). In the transverse slice labeling was observed in the intermediolateral cell column of the lateral horn, again ipsilateral to the injection site. Rhodamine Dextran Lysine was observed as fluorescence in the cytoplasm and proximal dendrites of the SPN (Figure 2.2Bi-iii). On average 4 or 5 400μm slices with the highest levels of labeling corresponding approximately to spinal segments T_5-T_{10}, were retained for recording purposes.

54 SPN were identified as innervating the adrenal medulla by the presence of double labeling with Lucifer Yellow from the patch pipette (Figure 2.3 Ai, Bi, Ci) and Rhodamine Dextran Lysine from the adrenal medulla (Figure 2.3 Aii, Bii, Cii).

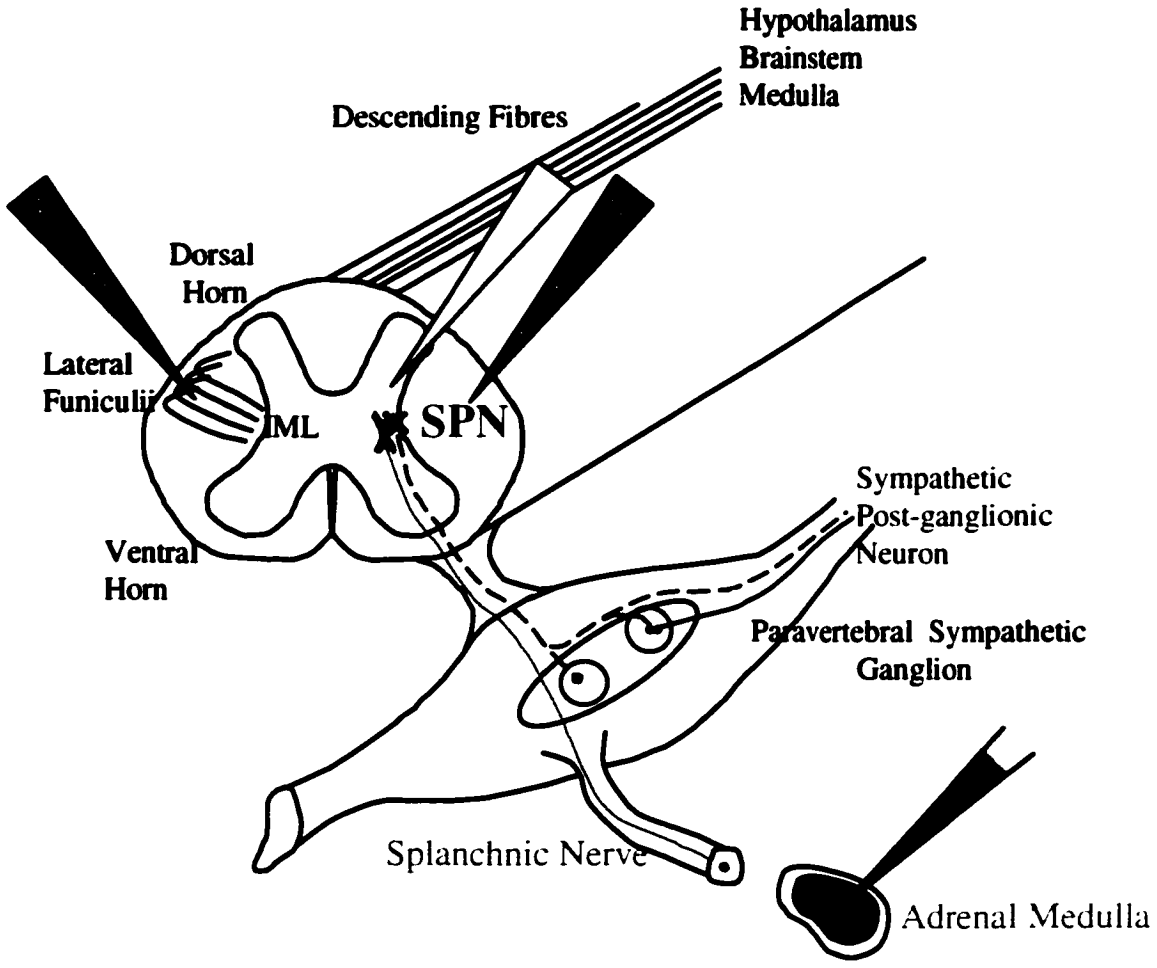

Figure 2.1 A schematic diagram demonstrating the unique features of AD-SPN that enable retrograde labeling from the adrenal medulla. Also indicated are the recording pipette filled with Lucifer Yellow (yellow arrow) and the stimulating electrodes (green arrows) as they are positioned in the transverse slice during recording.

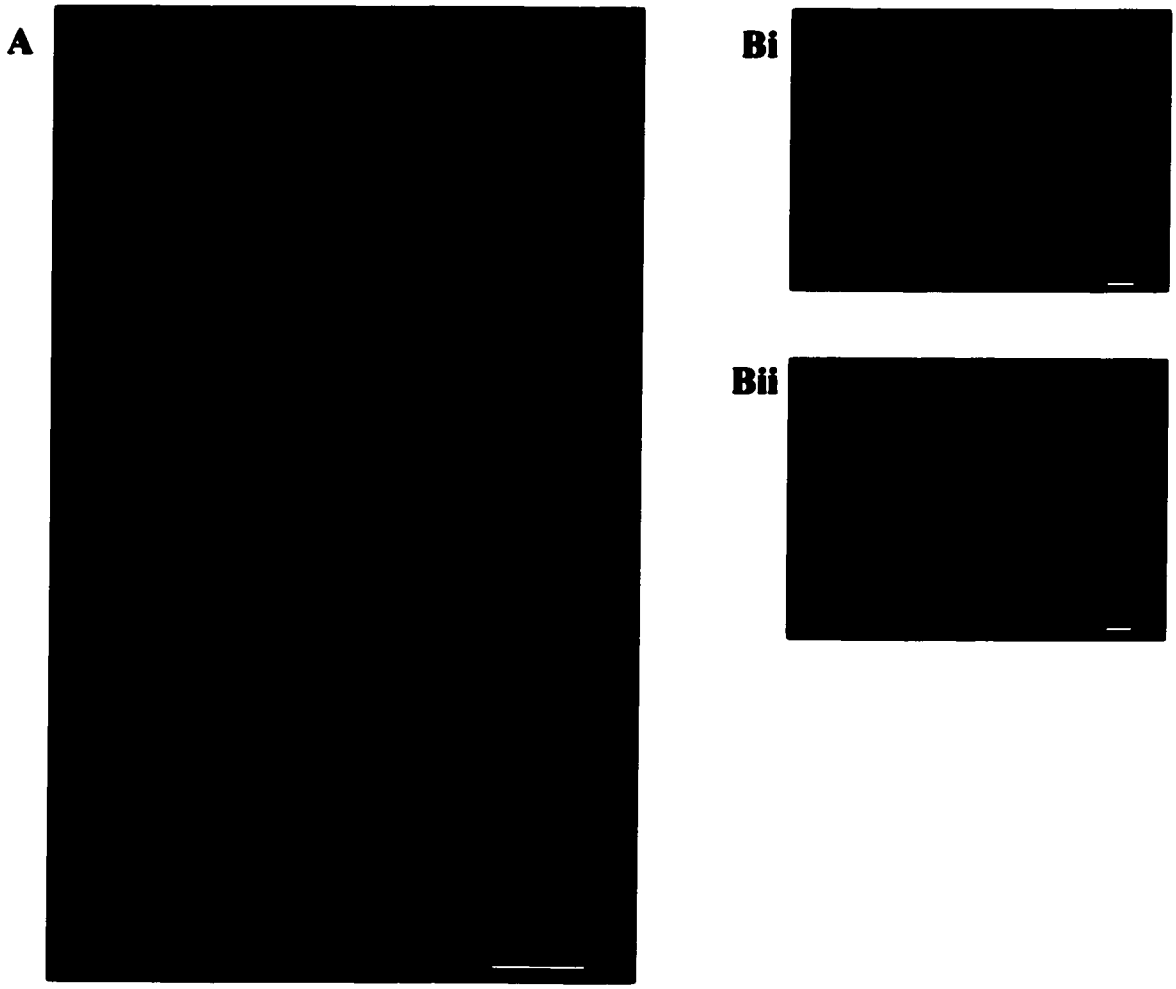

Figure 2.2 Retrograde labels identify SPN that innervate the adrenal medulla. A. Longitudinal section of thoracolumbar spinal cord (35μm) showing the distribution of SPN labeled with the retrograde tracer Rhodamine Dextran Lysine that had been injected into the adrenal medulla. All AD-SPN were observed ipsilateral to the injected gland. Bi,ii, Transverse sections (20μm) of thoracic spinal cord showing SPN labeled with Rhodamine Dextran Lysine after injection into the adrenal medulla. Note labeling of proximal dendrites. Scale bars are 50μm in A and 25μm in B.

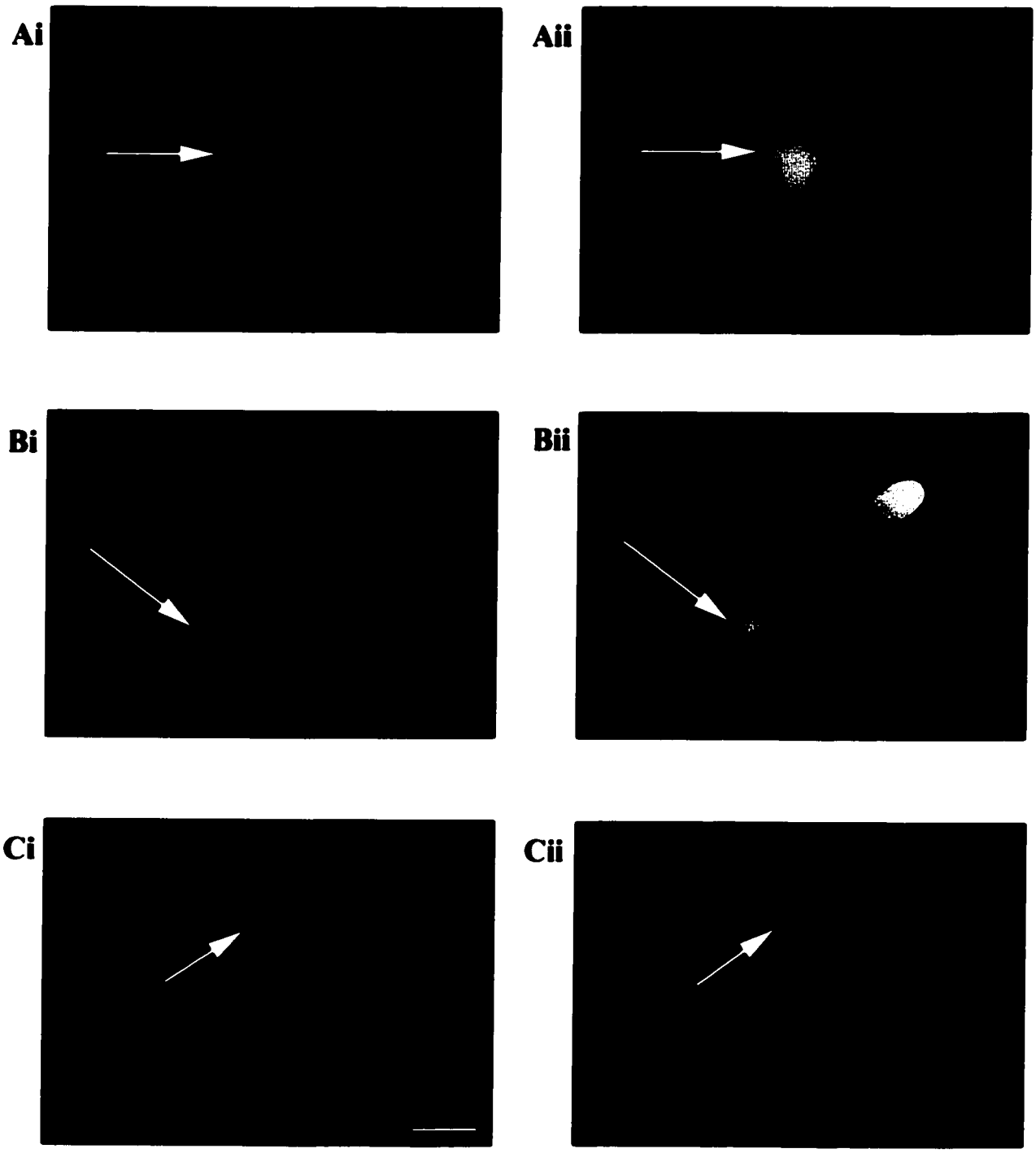

Figure 2.3 Intracellular and retrograde labels confirm recorded SPN innervate the adrenal medulla.

Transverse sections (20-35μm) of thoracic spinal cord showing SPN labelled with Rhodamine Dextran Lysine after injection into the adrenal medulla (Ai, Bi, Ci). The recorded neurons, indicated with arrows, were also filled with Lucifer Yellow from the recording pipette, and therefore identified as innervating the adrenal medulla (Aii, Bii, Cii). Note lack of cross over between filters. Scale bar is 25μm.

CHAPTER 3

INTRINSIC CONDUCTANCES IN ADRENOMEDULLARY SYMPATHETIC PREGANGLIONIC NEURONS

3.1 Introduction

SPN are the major spinal and final integrative site for autonomic reflexes, and are the substrate by which central commands to the adrenal medulla are finally processed, integrated and executed. Therefore characterising the intrinsic properties of these neurons, that endow the neuron with integrative properties and regulate their excitability, is essential for understanding mechanisms by which catecholamine secretion can be regulated.

Potassium selective ion channels are possibly one of the most diverse families of membrane channels, whose specific cellular function is equally as heterogeneous. They are postulated to be important in limiting firing frequency, determining firing patterns and action potential waveform (see Rudy, 1988). Several distinct types of potassium-mediated conductances have been identified in SPN (Polosa *et al.*, 1988; Pickering *et al.*, 1991; Miyazaki *et al.*, 1996), and subgrouping of SPNs has been postulated based upon specific combinations of potassium conductances (Dembowsky *et al.*, 1986; Inokuchi *et al.*, 1993c). However the properties of these conductances and their role in determining firing patterns in a functionally identified population of SPN have not been fully investigated.

Calcium ions subserve diverse functions in neurons, including gene expression, neurite outgrowth, transmitter release, firing patterns, regulation of gap junctions and

intracellular messengers e.g. protein kinases, nitric oxide synthase. Calcium influx can induce regenerative calcium release from internal stores and a central role has been proposed for calcium-dependent forms of synaptic plasticity and calcium-induced neurotoxicity (see Berridge, 1998). Such a wide variety of functions are mediated by an equally diverse range of channels allowing calcium influx to the neurons. Selective calcium entry is achieved by voltage-activated calcium channels. However nonselective ligand-gated channels, the reverse mode of the sodium-calcium exchange pump, and gap junction channels also contribute to raising internal calcium concentrations.

Therefore this chapter aims to identify potassium and calcium conductances specifically in AD-SPN and elucidate their possible functional roles.

3.2 Results

This chapter includes data from 54 SPN that were identified as innervating the adrenal medulla by the presence of double labeling with Lucifer Yellow or Alexa 594 from the patch pipette and Rhodamine Dextran Lysine from the adrenal medulla (see Chapter 2 and Figure 2.3). Also included are data from 130 SPN recorded between T_7 and T_{11}, that express the same conductances as AD-SPN but unidentified as to their target of innervation.

3.21 Passive membrane properties

The basic membrane properties of AD-SPN are summarised in Table 3.1 and corresponding frequency histograms in Figure 3.2. The resting membrane potential of AD-SPN was –62.2± 5.7mV ranging between –40mV and –65mV and showed a normal distribution. The mean neuronal input resistance of 410 ± 241MΩ had a distribution

slightly skewed towards higher resistances. A separate peak suggests the possibility of a subgroup of neurons with a relatively low input resistance. The time-constant of AD-SPN was most accurately estimated by fitting double exponentials to the membrane voltage charging curves induced by injection of small, hyperpolarising rectangular-wave current pulses (10-20pA, 500ms). As suggested by Rall (Rall, 1969), the longest exponential was taken as the time constant (τau). The mean time-constant of AD-SPN was 104 ± 53ms, which distributed normally between 44 and 194ms. A multiplicity of isopotential compartments, indicated by double exponential fits, is in agreement with studies of morphology of SPN revealing large variable shaped somas and extensive mediolateral and rostrocaudal dendritic arborisations (see Coote, 1988).

3.22 Active membrane properties

Active membrane properties of AD-SPN were investigated by examination of the membrane responses to injection of current pulses (-200 to +100pA, 1s duration, 0.01Hz) using potassium-gluconate based internal pipette solutions. The majority of AD-SPN expressed 3 prominent active conductances that could be detected subsequent to injection of hyperpolarising current pulses from resting membrane potentials (Figure 3.3):

1) an instantaneous inward rectification;
2) a transient outward rectification (TOR);
3) a low-threshold calcium conductance revealed following maneuvers to block the transient outward rectification;

and 2 active conductances revealed at membrane potentials positive to resting;

1) a sustained outward rectification (SOR) revealed in the presence of TTx;

2) a high-voltage activated calcium conductance that was observed as a shoulder on the repolarisation phase of the action potential.

3.23 Inward rectification

AD-SPN exhibited a linear current-voltage relationship at steady state membrane potentials between -50 and -80mV. In the majority of AD-SPN (91%), a fall in neuronal input resistance from 410 ± 241MΩ at membrane potentials close to rest to 138 ± 86 MΩ at membrane potentials more negative than –80.7 ±5.5mV (n=36) was observed (Figures 3.3A, 3.4Ai, 3.5Ai, 3.6A). This inward rectification was time-independent and illustrated in the current-voltage relationships by a decrease in the gradient of the slope at negative membrane potentials (Figure 3.3B, 3.4B). To clarify the nature of this conductance, the effects of a range of ion channel blockers and ion substitutions were tested in the presence of TTx (0.5-1μM). Bath application of the non-selective potassium channel blocker barium (100μM) induced a membrane potential depolarisation of approximately 7mV, from holding potentials that ranged between –53 and –56mV. Concomitant was an increase in neuronal input resistance from membrane potentials negative to –80mV from 87 ± 25MΩ to 409 ± 61MΩ (n=6). The instantaneous inward rectification was completely blocked in the presence of barium in all 6 neurons tested (Figure 3.4A). The reversal potential of the barium associated increase in neuronal input resistance was 96 ± 4mV (Figure 3.4B), approximating the reversal potential for potassium ions under these recording conditions (E_K= -96.2mV). In experiments where SPN were caesium-loaded, by replacing potassium with equimolar caesium (140mM) in the pipette solution, the instantaneous inward rectifier was absent (n=32; Figures 3.4B, 3.7A, 3.8B). Similarly,

superfusion of nominally potassium free aCSF reduced the inward rectification (Figure 3.6). Both tolbutamide (10-200μM; n=4) and 4-aminopyridine (2-4mM, n=4) were without effect on this conductance.

3.24 Transient outward rectification (TOR)

The majority (97%) of AD-SPN observed in this study expressed TOR (Figure 3.3A square). This conductance was observed at the offset of the membrane response to hyperpolarising current pulses (-60 to -140pA, 500ms, 0.01-0.1Hz) and manifest as a delayed return to resting or holding potentials ranging between –40 to –55mV (Figures 3.3A, 3.4A, 3.5A, 3.6). At the break of the membrane response to hyperpolarising current pulse injection, this conductance was activated at a mean membrane potential of -62.6 ± 4.8mV (n=36). The mean time constant of decay was 3555 ± 903ms (n=12), which was considerably longer than the time-constant of the membrane (104 ± 53ms) suggesting the presence of an active conductance. The TOR could also be observed in response to depolarising current pulses (80 to 180pA, 2s, 0.08-0.05 Hz) from relatively negative resting or holding potentials (>-70mV), thus manifesting as a delay in reaching threshold for firing (Figure 3.5C).

The TOR could be pharmacologically separated into 2 components. First, a long duration component with a tau of decay of 3272 ± 673ms and amplitude 5.8 ± 1.9mV from holding potentials of –50mV was blocked by barium (2mM, n=4, Figure 3.5A, B). Under the latter conditions, a second component was discerned, with a mean peak amplitude of 8.4 ± 2.3mV from holding potentials of –50mV and tau of decay of 435±133ms (n=3; Figure 3.5B). This component was seen to be reduced by 4-

aminopyridine (2-4mM; n=8). Both components were unaffected by tetraethylammonium chloride (TEA, 100μM to 30mM, n=4), cobalt (100μM to 2mM, n=3), nickel (100μM to 2mM, n=4), cadmium (100μM, n=2) and quinine (100μM, n=5). Both components of the TOR were enhanced upon exposure of the slice to nominally potassium-free aCSF. Under these conditions the membrane potential for activation shifted to more negative potentials. From a holding potential of -55mV the amplitude increased from 8.5 ± 1.4mV to 14.7 ± 3.2mV and tau of decay increased from 523.6 ± 61.1 to 767.5 ± 218.8ms (n=6, Figure 3.6). The membrane potential for activation of this conductance under these recording conditions was –69.7 ± 3.2mV.

In caesium loaded SPN, a conductance was revealed whose profile appeared at the offset of membrane responses to hyperpolarising current pulses as a rebound depolarising shift with a mean peak amplitude of 13.7±3.6mV that decayed with a tau of 527.5 ± 100.9 ms (n=6, Figure 3.7 arrows). The decay value is similar to that of the 4-aminopyridine-sensitive component of the TOR observed with potassium-based intracellular pipette solutions (435±133ms). This rebound depolarising conductance revealed with internal caesium was also apparent upon depolarisation from negative holding potentials between –80 and –100mV (Figure 3.7B), and could be blocked by 4-aminopyridine (2-4mM, n=5; Figure 3.8A). The rebound depolarising conductance was insensitive to: nominally calcium free aCSF (n=11,Figure 3.8Bii); extracellular caesium (2mM, n=2; Figure 3.8Biii) and extracellular barium (<2mM; n=3, data not shown). The insensitivity of the conductance to barium in caesium-loaded SPN, suggests that the slow component of the outward rectifier observed with potassium-based intracellular solutions was blocked by intracellular caesium unlike the 4-aminopyridine sensitive component.

That the rebound depolarisation described here is a potassium conductance insensitive to intracellular caesium was demonstrated as shift in polarity upon superfusion of a nominally potassium free aCSF, again revealing the transient outward rectification rather than the rebound depolarisation (n= 4; Figure 3.7).

3.25 Low threshold calcium spike

A third conductance was a low-threshold calcium spike. Revealed in caesium-loaded neurons after blockade of 4-aminipyridine - and barium-sensitive TORs (Figures 3.8A, 3.9, n=31) this conductance remained stable for the duration of the recording (up to 5hours). This conductance was voltage-dependent and observed at the offset of the response to hyperpolarising current pulse injection (-60 to -140pA, 500ms, 0.01-0.1Hz, Figure 3.9A), or in response to depolarisation from a relatively negative holding potential of around –85 to –100mV (Figures 3.9B). When triggered at the offset of the membrane response to injection of hyperpolarising current pulses and in the presence of internal caesium this conductance was activated at a membrane potential of -77.1±3.9mV, and had a mean peak amplitude of 28.1±7.7mV and a half-time to decay of 441±210ms (n=10). The conductance was initiated as a rapid depolarisation, which could reach threshold for action potential generation (Figure 3.8Aii), with mean peak amplitude of 92.4±13.4mV and duration of 19.7±6.4ms. That this action potential was calcium-dependent was subsequently confirmed by its sensitivity to non-selective calcium channel blockers (see section 3.28).

The proposed selective low-threshold calcium channel blocker nickel completely blocked the low-threshold spike at a concentration of 1-2mM (n=3; Figure 3.9), but was without effect at a concentration of 100μM (n=5). The non-selective potassium channel

blockers barium (2mM, n=2) or TEA (30mM, n=3) were either without effect or enhanced the duration of this low-threshold spike. Superfusion of nominally potassium free aCSF (n=4) or low sodium aCSF (60mM, see Chapter 2.2, n=5) were without effect on the low-threshold spike, as were apamin (100nM, n=3) and 4-aminopyridine (4mM, n=5).

Replacing intracellular potassium with equimolar caesium (140mM) induced a spontaneous burst like pattern of activity in 23 of 31 SPN (Figures 3.10A, 3.11A). From resting membrane potential levels of between –70 and -55mV, a burst of activity was initiated as a rapid depolarising shift that upon reaching threshold for action potential firing triggered 1-15 action potentials before a slow return to baseline membrane potentials. The depolarising shifts lasted 1.5-5 seconds and recurred at a frequency of 0.6 ± 0.2Hz (range 0.1 to 1.5Hz) interspersed with periods of silence (see Figures 3.10, 3.11). In all 3 neurons tested, nickel (2mM) completely and reversibly blocked all spontaneous burst firing patterns (Figure 3.11).

3.26 Sustained outward rectification (SOR)

AD-SPN exhibited a linear current-voltage relationship at steady state membrane potentials between –80mV and –35mV. In the presence of TTx (0.5 to 1μM) and following blockade of calcium components of the action potential with either cadmium (100μM) or nickel (2mM), a SOR in the voltage-current relations was observed at depolarised potentials (n=19 of 19 cells tested). Consecutive incremental depolarising current pulses (10-300pA, 600ms, 0.2Hz) from a holding potential of –50mV revealed a distinct fall in input resistance, from 325 ± 194 to 48 ± 38MΩ at potentials positive to

around –35mV (Figures 3.4, 3.6, 3.7A, 3.8B, 3.9A, 3.12A, 3.13A, 3.14, 3.15). This conductance was sustained over the time-course of the depolarising current pulse injection (600ms) and showed little indication of inactivation at depolarised potentials. The SOR was illustrated in the current-voltage relationships by a decrease in the gradient of the line at depolarised membrane potentials (Figures 3.12B, 3.13B, 3.14C, 3.15Aiii, Biii). Initial injection of depolarising current pulses could evoke a spike (Figure 3.8Bi, 3.14Ai, Bi), which was reduced in nominally calcium free aCSF, revealing a small "notch" preceding activation of the SOR (Figure 3.8Bii, 3.13A, 3.14). The relationship between the amplitude of the notch and the time to peak (or 10-90% rise time) of the current pulse was linear, indicating that this notch was due to capacitive charging of the membrane rather than activation of a conductance (Figure 3.13Bi).

To investigate the ionic mediators of the SOR, AD-SPN were loaded with QX-314 to block sodium conductances. In the presence of TTx (0.5-1μM) and internal QX-314, a shift in the voltage of activation of the SOR from around –35mV to -15±3mV (n=5) was observed (Figure 3.14A,C). Under a compromised sodium gradient $[60mM]_o$ (Figure 3.14B, n=5) minimal changes were noted in the SOR. These data suggest that in AD-SPN QX-314 is acting on potassium conductances, as described in other neurons previously (Nathan *et al.*, 1990, Talbot and Sayer 1996).

Caesium-loading pipettes no changes were noted in the SOR (n=31; Figures 3.7B, 3.8B, 3.14B,C). Thus ionic manipulations and pharmacological experiments were carried out under high caesium conditions. The SOR was insensitive to changes in chloride (140mM internal $CsCl_2$) and calcium (0mM $CaCl_2$ in aCSF, substituted with 5.2mM $MgCl_2$) ion concentration gradients and the calcium channel blockers nickel (2mM, n=7, caesium loaded, Figures 3.9A, 3.14A), cobalt (2mM, n=3 caesium loaded, n=1, Figure

3.13A) and cadmium (100μM, n=7, caesium loaded). As the SOR exhibited a similar time-course and voltage of activation to the M-conductance the effects of muscarine were investigated. SOR was insensitive to extracellular muscarine (40μM, n=2, non caesium loaded). The SOR was also insensitive to the potassium channel blockers 4-aminopyridine (4mM, n=6 caesium loaded, n=11 non caesium loaded, Figures 3.13A, 3.14A), TEA (30mM, n=3, n=9 non caesium loaded, Figure 3.13A) and barium (2mM, n=2 caesium loaded, n=7 non caesium loaded), However, the SOR was completely blocked by the cinchona alkaloid quinine, returning the input resistance to steady state values in 5 of 6 neurons tested (caesium loaded, Figure 3.14B). The potassium channel blocker catechol partly reduced the outward rectification in a concentration-dependent manner (500μM-3mM, n=3) and was particularly effective over the range of membrane potentials between –45 to around –15mV. These effects of catechol were irreversible over the time-course of recording. To identify the nature of the ions mediating this conductance, the effects of changes in extracellular potassium ion concentration were investigated. Reducing extracellular potassium to 0.6mM from 3.1mM (n=4 caesium loaded, n=11 non caesium loaded) was without significant effect on the SOR. However, increasing extracellular potassium concentration from 3.1 to 15mM (n=4) markedly reduced the outward rectification suggesting this conductance was primarily due to a transmembrane potassium flux (Figure 3.12).

Another conductance that may be involved is that mediated by members of the recently cloned two-pore domain potassium channel (2PDKC) family. These channels are proposed to contribute to resting membrane potential and are sensitive to changes in pH and arachidonic acid (Fink *et al.*, 1998; Rajan *et al.*, 2000). Under low extracellular pH

(pH 6.7) the SOR was partly reduced over membrane potentials ranging between –30 to –15mV, although a prominent rectification persisted at membrane potentials less negative than around –15mV (n=4, Figure 3.15A). These effects were reversible on returning the bathing medium to pH 7.4. Bath application of arachidonic acid (100μM) markedly suppressed a component of the SOR in all 4 neurons tested (Figure 3.15B). These effects of arachidonic acid were slow in onset and irreversible over the time-course of the recordings. In addition to these effects on the outward rectification, both arachidonic acid and changes in extracellular pH exerted effects on the resting membrane or holding potential. Bath application of arachidonic acid (100μM) induced a membrane depolarisation of 6.6 ± 2.1mV in 3 of 3 neurons tested. The response was concomitant with an increase in neuronal input resistance in the voltages positive to –25mV from 14.3 ± 2.8 to 82.7 ± 39.2 MΩ, corresponding to 580.2% increase. Similarly, a reduction in extracellular pH from 7.4 to 6.7 induced a membrane potential depolarisation of 8.7 ± 2.1mV (n=4) from resting or holding membrane potentials of –40mV. This response was associated with an increase in neuronal input resistance in the voltage range –40 to –30mV from 144.5 ± 41.8MΩ to 383.3 ± 132.0 MΩ, corresponding to a 265.3% increase. In the absence of TTx, depolarisation of the membrane in the presence of low pH induced action potential firing in previously silent SPN (n=3). This suggests that AD-SPN directly respond to low pH by a partial block of the SOR .

3.27 Effects of ion channel blockers on the action potential

Experiments outlined above identified two outwardly rectifying potassium conductances in AD-SPN: a TOR activated at the offset of the membrane response to

hyperpolarising current pulses; a SOR observed at membrane potentials less negative than around –35mV. A functional role for these conductances in AD-SPN was investigated by applying ion channel blockers to action potentials and associated afterhyperpolarising potentials that were evoked either by antidromic stimulation. In all 6 neurons tested application of 4-aminopyridine, a TOR blocker, slowed the repolarising phase of the action potential increasing the duration, measured at one third peak amplitude, from 3.8±0.5ms under control conditions to 10.6±3.9ms in the presence of 4-aminopyridine. Concomitant with this broadening of the action potential, the afterhyperpolarising potential was significantly reduced. Under control conditions the mean peak amplitude of the afterhyperpolarising potential was 13.1±0.9mV and tau of decay was 151.0±55ms. In the presence of 4-aminopyridine the peak amplitude was reduced to 6.5±1.9mV and tau of decay to 94.6±34.2ms (n=6). As 4-aminopyridine can exert effects on other potassium channel species, we further examined the effects of 4-aminopyridine under conditions whereby other potassium conductances were blocked. In the presence of barium (2mM, n=2) or TEA (30mM, n=2), which block other outward currents expressed in SPN (Miyazaki *et al.*, 1996), the action potential repolarisation was significantly slowed (Figure 3.16A). Under these conditions, the duration of the action potential increased from 3.2±0.4ms in control conditions to 8.0±0.3ms (254.4±39.1%) and 5.6±0.1ms (180.6 ± 22.5%) in the presence of barium and TEA respectively. Subsequent addition of 4-aminopyridine further increased the duration of the action potential by 148.1 ± 8.7% from the control value (100%) in the presence of barium or TEA.

The associated afterhyperpolarising potential was reduced further in the presence of 4-aminopyridine compared to the afterhyperpolarising potential evoked in the presence of TEA alone (n=6). TEA blocks the intermediate afterhyperpolarising potential in SPN (Miyazaki *et al.*, 1996). In the presence of 4-aminopyridine and quinine, application of TEA reduced the peak amplitude from –11.9 ± 0.3mV to 2.8 ± 1.4mV in 3 of 6 SPN tested in this study (Figure 3.16B). Tau values were unable to be measured in these neurons. In the remaining 3 neurons TEA either alone or in the presence of 4-aminopyridine had little effect on the peak amplitude (from –13.1 ± 2.9mV to -12.4 ± 4.6mV) and a variable effect of the tau of decay (from 114.7 ± 22.3ms to 107.3 ± 33.5ms).

The contribution of the SOR to the action potential waveform was investigated by applying quinine. In all 3 neurons tested, quinine slowed the repolarising phase of the action potential, increasing the duration measured at one third peak amplitude from 2.8 ± 0.5ms under control conditions to 4.5 ± 1.1 ms in the presence of quinine (n=3). Isolation of the quinine-sensitive SOR was achieved in the presence of barium and 4-aminopyridine or TEA and 4-aminopyridine. Under these latter conditions, the duration of the action potential increased by 271.4 ± 103.2% in the presence of varying combinations of barium, 4-aminopyridine, TEA and cadmium (n=4). Subsequent addition of quinine increased the duration of the action potential by a further 154.8 ± 25.5% (n=3, Figure 3.16B).

3.28 High threshold calcium spike

The action potential waveform in all AD-SPN was characterised by a distinct shoulder on the repolarisation phase (Figure 3.3 inset). The action potential of AD-SPN had a mean peak amplitude of 78.5 ± 5.6mV and duration of 5.7 ± 6.8ms. Data obtained with high internal caesium (140mM) induced an increase in action potential duration from 5.7±6.8ms to 73.8 ± 29.5 ms (n=10). Addition of TTx (0.5 -1μM) and injection of sustained current pulses (20 to 80pA, 500ms, 0.1-0.1Hz) from holding potentials (-50 to –60mV) evoked a high voltage activated spike with a peak amplitude of 41.9± 8.4mV, and duration of 44.7 ± 15.7 ms (n=8, Figure 3.17). The spike could fire repetitively and remained stable for the duration of the recording (up to 5hours), with no apparent rundown. The addition of nominally calcium free aCSF (substituted with 5.2mM $MgCl_2$) abolished the spike (n= 6 out of 8, Figures 3.8B, 3.14B).

Non-specific divalent cation blockers of calcium channels were bath applied. Cadmium (100μM, n=6) and nickel (2mM, n=4, Figure 3.14A) blocked the high voltage activated spike while cobalt had a variable effect (2mM, n=2 of 4).

The addition of increasing concentrations of barium (0.1–5mM) or TEA (1-30mM) in both potassium-gluconate and caesium based intracellular solutions progressively increased the duration of the action potential in a concentration dependent manner (from control of 3.3±0.3ms to 7.7±1.2ms in 30mM Barium, from control of 3.1±0.4ms to 6.8±1.5ms in 30mM TEA, n=3 each in potassium-gluconate based pipette solution, Figure 3.17A, B). Barium may be acting as the charge carrier, in addition to blocking the potassium channels responsible for repolarising the action potential.

Attempts were made to classify the high voltage activated spike by applying selective calcium channel toxins to the action potential in the presence of internal caesium, external barium and / or external TEA to minimise the contribution of the repolarising potassium conductances. The effects of two L-type calcium channel inhibitors nimodipine and nifedipine (up to 10μM) were investigated. Both were without effect on the duration of the action potential during 10 minutes of drug application (nimodipine n=4, nidefipine n=2, Figure 3.18C). A concentration of 5-10μM is the saturating dose for L-type channels (Lorenzon and Foehring, 1995). In the presence of cytochrome C (0.01-0.1%) bath application of the selective N-type calcium channel blocker ω-conotoxin GVIA (Tsien *et al.*, 1988) (2μM, n=4), irreversibly reduced the duration of the action potential by 62.3 ± 16.9% (n=3, Figure 3.17D). The P/Q type channels are selectively blocked by the funnel-web spider venom ω-agatoxin IVA. In 3 SPN tested ω-Agatoxin IVA (100nm) reduced the duration of the action potential by 38.2 ± 23.1%. ω-conotoxin MVIIC is a non-specific N and P/Q type channel toxin (Hillyard *et al.*, 1992). The addition of cadmium (100μM) to the action potential in the presence of conotoxin MVIIC reduced its duration by 51.9 ± 12.8% and was termed the "residual" conductance.

3.3 Discussion

Data presented here represent the first attempt to define intrinsic passive and active membrane properties involved in regulating excitability of the sympathetic preganglionic neurons providing direct innervation of the catecholamine-secreting chromaffin cells. The conductances featured in the majority of AD-SPN include: a

transient outward rectification; an inward rectification; a low-threshold calcium conductance revealed upon caesium-loading of SPN; a sustained outward rectification; a high-threshold calcium conductance responsible for the shoulder on the repolarisation phase of the action potential.

3.31 Passive membrane properties of AD-SPN

The mean resting membrane potential of AD-SPN is within the range of values previously reported for SPN in neonatal rats using similar techniques (Dun and Mo, 1988; Pickering *et al.*, 1991; Logan *et al.*, 1996). The distribution of neuronal input resistance of AD-SPN revealed two peaks at high and low input resistances. Low input resistance in SPN has been linked to the presence of electrotonic coupling (Logan *et al.*, 1996) and see Chapter 4.

3.32 Fast transient outward rectification

AD-SPN express TOR comprising two potassium conductances with distinct time courses and pharmacology. The fast component was sensitive to 4-aminopyridine and changes in extracellular and intracellular potassium ion concentration, but was insensitive to extracellular barium and TEA. 4-aminopyridine, up to 4mM, blocks only a relatively fast component in SPN described here and previously (Pickering *et al.*, 1991; Miyazaki *et al.*, 1996). Surprisingly, was the TOR's relative insensitivity to intracellular caesium. The D-conductance is a transient outward rectifier that is sensitive to low micromolar concentrations of 4-aminopyridine and decays with a long (up to 5 seconds) time course (Storm, 1990). In this study, insensitivity of the TOR to low concentrations of 4-aminopyridine negates the involvement of a D-type conductance and supports the

presence of an A-type conductance, similar to that described previously in SPN in adult cat (Dembowsky *et al.*, 1986; Yoshimura *et al.*, 1986b), guinea-pig (Inokuchi *et al.*, 1993c), neonatal rat (Pickering *et al.*, 1991; Miyazaki *et al.*, 1996) and other central neurons (Rogawski, 1985).

A-type potassium conductances contribute to early spike repolarisation thus delaying the return to threshold and contributing to repetitive action potential firing (Rogawski, 1985; Storm, 1990; Takahashi, 1990). Voltage-clamp recordings from SPN suggest A-type channels are released from inactivation by hyperpolarisation and activated by depolarisation and, together with the intermediate afterhyperpolarising potential, act to control firing frequency (Miyazaki *et al.*, 1996). In AD-SPN the A-type conductance could act to regulate firing frequency by regulating spike repolarisation and by contributing to the afterhyperpolarising potential.

3.33 Slow transient outward rectification

The slower component of the TOR in AD-SPN was blocked by high concentrations of barium and was pharmacologically separable from the A-conductance by its insensitivity to 4-aminopyridine. Similar conductances with longer activation and inactivation kinetics than the A-type have been identified in other central neurons, including magnocellular neurosecretory cells in slices (Li and Ferguson, 1996) and supraoptic nucleus neurons in culture (Cobbett *et al.*, 1989).

The membrane potential range for activation of the slow TOR in AD-SPN suggests a pivotal role in regulating the frequency of firing of AD-SPN. Indeed the repolarising phase of the action potential and activation of the afterhyperpolarising potential may be sufficient to remove inactivation and subsequently activate this

conductance thus prolonging the return to resting potentials (Yoshimura *et al.*, 1986a; Spanswick and Logan, 1990a; Sah and McLachlan, 1995). Although the pharmacology of the slow component of the TOR negates the presence of a typical D-conductance, similar time courses and voltages of activation may preclude similar functions (Storm, 1990). The long duration of the D-conductance may provide a window for temporal integration (Storm, 1990). In AD-SPN, the activation of the slow TOR during the afterhyperpolarising potential is consistent with the prolonged (several seconds) afterhyperpolarising potential observed in SPN (Yoshimura *et al.*, 1986a; Spanswick and Logan, 1990a).

3.34 Ion channels mediating transient outward rectification

By the utilisation of molecular cloning techniques and subsequent artificial expression of identified proteins, rapid progress has been made in identifying not only distinct subunits of the 2 potassium channel families but also regulatory domains within the subunits and extrinsic cellular modulators of channel kinetics (Jan and Jan, 1997). The voltage dependent potassium channels comprise 6 transmembrane spanning domains in each α-subunit, forming the pore of the channel. In the mammalian nervous system, at least 18 genes encode the α-subunit grouped in 6 subfamilies; Kv 1.1-1.7 (Shaker), Kv 2.1-2.2 (Shab), Kv 3.1-3.4 (Shal), KCND1/Kv4.1,KCND2/Kv 4.2 and the splice variants KCND3S and 3L (Kv4.3), HERG (ether-a-go-go), maxi K (slowpoke/slo) while 4 mammalian β-subunits result from alternative splicing of a single gene and a related gene and include Kvβ1.1, Kvβ1.2, Kvβ1.3 and Kvβ2.1 (see Jan and Jan, 1997). In addition, four Kv channel interacting proteins (KChIP 1-4) have been cloned that possess

calcium binding domains and specifically bind to the cytoplasmic amino terminal of the Kv4 α-subunits to modulate channel kinetics (An *et al.*, 2000), thus are believed to be the β-subunits.

The α-subunits of the channels mediating the A-type conductance are encoded by the Kv4 (KCND1-3) gene family (Serodio *et al.*, 1996; Serodio and Rudy, 1998; Isbrandt *et al.*, 2000). The expression of Kv 4.2 mRNA is highly correlated with the expression of A-type potassium channels in the basal ganglia and basal forebrain (Tkatch *et al.*, 2000) and A-type potassium channels in striatonigral dopaminergic neurons have properties consistent with heterologously-expressed Kv4/KChIP potassium channels (Liss *et al.*, 2001). Since channels expressed from Kv4 alone posses similar, but not identical properties, to native A-type conductances, is it probable that KChIPs are associated with the Kv4 α-subunits (An *et al.*, 2000). Indeed, functional A-type channel complexes are formed in the membranes of cerebellar granule cells by co-expression of Kv4.3 and KChIP 1 subunits (Holmqvist *et al.*, 2001). Added kinetic diversity is conferred upon A-type channels by selective expression of KChIP splice variants, which determine the voltage of activation, the slowing of inactivation and rate of recovery from inactivation (An *et al.*, 2000; Bahring *et al.*, 2001; Ohya *et al.*, 2001). The splice variant KChIP 4a contains a K-channel inactivation suppressor (KIS) domain that eliminates the fast inactivation kinetics of Kv4.3 mediated currents, prolonging open time of the channels , hence slowing inactivation (Holmqvist *et al.*, 2002). Thus the kinetics of the channels mediating transient outward rectifiers are both diverse and modifiable, and can be controlled by differential expression of Kv α-subunits with splice varients of the KChIP regulatory β-subunits. Therefore tailoring channel expression and kinetics to function is

likely to be the "norm" within the central nervous system and we can only postulate that the unusually long transient outward rectifier observed in AD-SPN pertains to regulating their firing frequency, via activation subsequent to action potential firing.

3.35 Sustained outward rectification

SOR was observed in all AD-SPN in response to depolarising current pulses from around –50mV. At least 3 pharmacologically distinct components contributed to this rectification; a) a transient component sensitive to 4-aminopyridine and similar to the A-conductance described above b) a sustained component sensitive to calcium channel block or low calcium containing aCSF and c) a sustained component sensitive to quinine but insensitive to 4-aminopyridine, TEA, barium and calcium influx.

The SOR has been previously observed with intracellular recordings from SPN in T_2-T_3 from spinal cord slices from adult cats (Yoshimura *et al.*, 1986b). However this conductance was not classified. By utilising voltage-clamp studies of SPN 3 components of the slow outward rectification observed in response to depolarising step commands were identified as 1) the delayed rectifier (I_K) 2) a calcium-dependent transient current (I_{Ca}) and 3) a calcium-dependent sustained current contributing to the intermediate afterhyperpolarising potential (Miyazaki *et al.*, 1996). TEA has been shown previously to completely abolish outward rectification in SPN (Miyazaki *et al.*, 1996). However, TEA had no effect on a component of the SOR (that was isolated in the presence of non-selective calcium channel blockers, 4-aminopyridine, barium).

The outward rectifying conductances that are mediated by M-channels exhibit similar kinetics to the SOR observed in AD-SPN and are identified pharmacologically by a strong sensitivity to muscarinic agonists and to extracellular TEA, barium and calcium.

Although muscarine-insensitive M-like conductances have been reported in oxytocinergic magnocellular neurons (Stern and Armstrong, 1997), the insensitivity of the SOR observed in AD-SPN to barium and TEA argues against an involvement of M-like conductances.

To characterise the isolated SOR the effects of quinine were tested. Quinine blocks a range of potassium currents including a rapidly inactivating A-current, non-inactivating M-current and a slowly inactivating delayed rectifier (I_K) in bullfrog sympathetic neurons (Imai *et al.*, 1999). These currents were differentially sensitive to quinine with the IC_{50} for block of I_K in bullfrog sympathetic neurons being within the range of concentrations used in this study to block the outward rectification. Characterisation of the properties of the quinine-sensitive SOR conductance in AD-SPN were attempted. Insensitivity to modulation of the sodium gradient but sensitivity to the potassium gradient indicates potassium flux through the channels mediating this conductance. Interestingly, persistance of this conductance in the presence of internal caesium suggests that the current may be carried by caesium ions thus indicating permeability to both caesium and potassium. Whilst not a common feature, several studies report caesium permeability of outwardly rectifying, slowly inactivating currents revealed by voltage-clamp studies. This is evident in subthalamic nucleus neurons (Wigmore and Lacey, 2000), in avian nucleus magnocellularis (Rathouz and Trussell, 1998); dorsal root ganglion neurons (Trequattrini *et al.*, 1996); bullfrog sympathetic neurons (Block and Jones, 1997) and Kv1.5 channels expressed in cell lines (Fedida *et al.*, 1999). Unlike the quinine-sensitive component of the outward rectification observed here, outward rectifying potassium conductances and corresponding currents are generally blocked by TEA, barium and 4-aminopyridine, (e.g. Huguenard and Prince,

1991; Brew and Forsythe, 1995; Martina *et al.*, 1998; Wigmore and Lacey, 2000) including those in SPN (Miyazaki *et al.*, 1996).

3.36 Ion channels mediating sustained outward rectification

Outwardly rectifying potassium channels, as voltage dependent channels, can be formed from several gene families such as those described in section 3.34 and include Kv1, Kv2, Kv3, ether-a-go-go and Kv4 (KNCQ) (Jan and Jan, 1997). Although the properties of these channels can vary according to co-expression of auxillary β-subunits (Blaine and Ribera, 1998; Mathie *et al.*, 1998), the pharmacology of the quinine-sensitive sustained outward rectification in AD- SPN is not consistent with the properties of these channels, and therefore its molecular correlates are unlikely to reside in this gene family.

A superfamily of potassium channels has been identified recently that has an unusual pharmacology in that they are relatively insensitive to classical potassium channel blockers. These are the 2PDKC superfamily that, to date, includes TWIK-1, TWIK-2, KT3.2 and KT3.3, TASK-1, TASK-2, TASK-3, TASK-4, TREK-1, TREK-2, THIK-1 and THIK-2 and KCNK-7 (see Goldstein *et al.*, 2001 for review and references). Due to significant open probability at negative membrane potentials these channels are believed to contribute to the negativity of resting membrane potentials in neurons (Lesage and Lazdunski, 2000). Although none of the 2PDKC family express classical voltage sensors a proportion of these channels, for example TREK-1; TWIK-1 and TASK channels (Decher *et al.*, 2001; Meadows and Randall, 2001) exhibit some voltage-sensitivity thus indicative of functions outside those associated with setting resting membrane potential. As 2PDKC are modulated by pH, arachidonic acid and many of the cinchona alkaloids that include quinine e.g. TASK-3 (Meadows and Randall, 2001), these

pharmacological manipulations were carried out on the quinine-sensitive SOR present in AD-SPN. The effects of pH and sensitivity to quinine are consistent with the pharmacology of 2PDKCs. However the voltage of activation of the sustained outward rectifier in AD-SPN, and a block as opposed to activation by arachidonic acid (as observed for some 2PDKCs (Goldstein *et al.*, 2001), precludes the involvement 2PDKCs in the SOR in AD-SPN. As changes in pH (Tombaugh and Somjen, 1996) and arachidonic acid (i.e. Holmqvist *et al.*, 2001) can modulate a range of ion channels including other types of potassium channels, identifying a molecular correlate for the quinine-sensitive sustained outward rectification in AD-SPN is not possible at this time.

Functionally, the quinine-sensitive component of the SOR appears to be important in mediating spike repolarisation in AD-SPN. Quinine delayed the repolarisation of the action potential even under conditions where other conductances were blocked with TEA, calcium and 4-aminopyridine. These data suggest spike repolarisation in SPN to be complex involving several separate potassium conductances. The apparent sensitivity of the SOR to pH may have important functional consequences as both physiological and pathophysiological changes in the pH may be detected and registered in the firing pattern of SPN leading to sympathetic-mediated responses to restore the internal environment (see Chapter 7.53). Further detailed pharmacological and voltage-clamp experiments coupled with a single-cell molecular approach are required to clarify the molecular identity and role of these potassium conductances in regulating excitability of AD-SPN.

3.37 Inward rectification

The inward rectifier, originally named "rectification anomale" (Katz, 1949) after its ability to allow potassium influx to the neuron against prevailing electrochemical

gradients, was present in the majority of AD-SPN. The remaining 11% of neurons, in which the presence of the inward rectifier could not be discerned, exhibited evidence of electrotonic coupling (see Chapter 4). Therefore, the possibility exists that the inward rectifier was masked by low input resistances in these SPN. The inward rectifying conductance is known to play a significant role in regulating the resting membrane potential and that membrane depolarisation is observed upon block of the inward rectification suggest this may also be true in SPN. In addition the inward rectifier can be modulated by hormones, neurotransmitters through the activation of specific G-proteins, and the metabolic state of the cell (Jan and Jan, 1997). Vertebrate neurons contain 3 types of inward rectification; the anomolous rectifier (Constanti and Galvan, 1983), I_h (Yanagihara and Irisawa, 1980) which is a mixed sodium/potassium conductance that has also been designated I_f (Brown and Difrancesco, 1980) in cardiac or I_q (Halliwell and Adams, 1982) in hippocampal neurons and a chloride ion mediated inward rectification (Madison *et al.*, 1986). The high sensitivity of the inward rectification in SPN to barium, time independence and mediation by potassium ions (Hagiwara *et al.*, 1978; Constanti and Galvan, 1983) confirms that the inward rectification in SPN is of the anomolous type.

At least 12 genes have been identified that encode the inward rectifier (Doupnik *et al.*, 1995), that give rise to seven families of subunits that have been termed $K_{IR}1$-7. The mRNA have distinct patterns in expression in the mammalian central nervous system (Bredt *et al.*, 1995; Karschin *et al.*, 1996). Inward rectifying channel subunits have two transmembrane spanning domains and four subunits are believed to be required to form a functional channel. $K_{IR}2$ (specifically $K_{IR}2.1$ and 2.3), $K_{IR}4$ and $K_{IR}7.1$ channels are strong inwardly rectifying channels involved in setting the membrane potential, buffering extracellular potassium and modulating the waveform of the action potential in neurons.

$K_{IR}3$ comprise those channels that can be modulated by G-proteins while $K_{IR}6$ correspond to the adenosine trisphosphate dependent potassium channel family. Due to the strength of rectification, it is likely that the channels that mediate inward rectification in AD-SPN include subunits from the $K_{IR}2$, 4 or 7 families.

3.38 Low threshold spike

The activation of the TOR in SPN masked the low threshold spike. Therefore the full low threshold spike was observed upon the block, or reversing polarity, of the TOR. That the low threshold spike in SPN is mediated by low voltage activated calcium channels is suggested by; 1) a low voltage of activation, 2) sensitivity to extracellular calcium, 3) sensitivity to extracellular nickel and 4) similarity in shape to the low voltage activated calcium channels in other neurons (e.g. Carbone and Lux, 1984; Tsien *et al.*, 1988). Furthermore the low threshold spike promotes burst firing activity in AD-SPN and contributes to the afterdepolarising potential. Upon reaching threshold, the afterdepolarising potential can facilitate further sodium-driven action potential firing (White *et al.*, 1989).

Similar bursting activity mediated by the low threshold spike has been reported in many mammalian neurons, (see Perez-Reyes, 1999). The necessity for external input to reveal bursting activity has termed these endogenous pacemakers as "conditional bursters" (Selverston and Moulins, 1985). In addition to full bursts of activity, the low threshold spike has been observed to generate low-amplitude intrinsic neuronal oscillations, to promote the elevation of calcium entry, and to boost dendritic potentials (Huguenard, 1996; Ertel and Ertel, 1997). T-type channels are proposed to be located primarily throughout the dendritic tree in a variety of neurons (Munsch *et al.*, 1997;

Destexhe *et al.*, 1998), thus the generation of bursting activity is likely to be modified by ionic channels placed on proximal dendrites or at the soma. In AD-SPN the low threshold spike initiated dendritically would be subject to modulation by somatically placed intrinsic potassium channels (see Chapter 7.42A)

3.39 Ion channels mediating the low threshold spike

The deciphering of channels and subunits mediating the low threshold spike has been challenging due to the heterogeneity of the channels and lack of specific pharmacological tools (Ertel and Ertel, 1997). However careful scrutiny of the GenBank led to the cloning of three subunits α_1G , α_1H and α_1I (Klugbauer *et al.*, 1999; Williams *et al.*, 1999) also termed Cav3.1, Cav3.2, Cav3.3 (Cribbs *et al.*, 1998; Perez-Reyes *et al.*, 1998; Lee *et al.*, 1999b) which are believed to be the molecular substrates of the T-type calcium channel that mediates the low threshold spike (Carbone and Lux, 1984; Huguenard, 1996). In the spinal cord mRNA for α_1G is dominant (Talley *et al.*, 1999) and cloned channels comprising α_1G subunits are less sensitive to nickel (IC_{50}=250μM) than those comprised of α_1H (IC_{50}=13μM, Lee *et al.*, 1999a). Therefore subunit specificities within the T-type channel may account for the high concentrations required to block the low threshold spike in this study. Further classification could result from either the discovery or development of antagonists specific to subunits of the T-type channel, since there are none at present, or by utilising a single – cell molecular approach to SPN.

3.40 High threshold spike

AD-SPN all exhibit a high voltage activated calcium conductance. In SPN, both P/Q and N-type and possibly R-type channels, but not L-type, are present. While it has been proposed that P- and Q- type channels are separate channels distinguished by differential sensitivities to ω-conotoxin GVIA (Randall and Tsien, 1995), it is also believed that these are alternative splice variants (see Dolphin, 1995). Therefore they were classified as P/Q in this study.

The contribution of the high voltage activated channels to the total calcium conductance varied considerably within the SPN population occluding definitive quantative analysis. Besides an insufficient block of the repolarising potassium conductances or of the calcium channels themselves, such differences could reflect channel heterogeneity between individual SPN, since recordings were likely obtained from multiple functional groups. It is doubtful if voltage-clamp experiments could yield further quantitative data since space clamp error would likely be considerable given both extensive dendritic arbourisations in SPN and the high degree of electrotonic coupling between AD-SPN (see Chapter 4).

Functionally, calcium influx through high voltage activated channels is required for many intracellular events including potential activation of the calcium-dependent potassium conductances that mediate the afterhyperpolarising potential (Yoshimura *et al.*, 1986a, see Chapter 4). Furthermore, differential coupling of high voltage activated channels to signalling mechanisms have been reported, e.g. N-type calcium channels, but not L-type, are coupled to calcium- activated potassium channels in motor neurons (Viana *et al.*, 1993). A rise in intracellular calcium may also activate intracellular messengers, i.e. neuronal nitric oxide synthase present in AD-SPN (Blottner and

Baumgarten, 1992), protein kinases including calcium-calmodulin kinse II and calcium binding proteins including calretinin (Edwards *et al.*, 1996). These downstream effects of calcium entry may contribute to the strengthening of synapses, induce calcium release from intracellular stores, regulate the degree of gap junction coupling (see Chapter 4) or if in excess contribute to neurotoxicity.

3.5 Summary

Data presented here are the first report on the intrinsic conductances specific to AD-SPN, the final central command output to the chromaffin cells of the adrenal medulla. Data indicate that AD-SPN, for the most part, represent a homogeneous population with respect to expression of active intrinsic membrane conductances that include: a transient outward rectification (in 96% of AD-SPN); an inward rectification (in 89% of AD-SPN); a low-threshold calcium conductance (in 98% of AD-SPN revealed upon blockade of the transient outward rectifiers); a sustained outward rectification (in 96% of AD-SPN); a high-threshold calcium conductance responsible for the shoulder on the repolarisation phase of the action potential. That at least three potassium conductances contribute to determining the action potential waveform indicates the complexities and intricacies that may arise from individual modulation of the channels mediating these conductances. Furthermore calcium influx can both generate burst firing activity through the low threshold spike and determine the action potential duration and subsequent afterhyperpolarising and depolarising potentials. The following chapter investigates a prominent feature intrinsic to AD-SPN that contributes to generating neuronal activity: electrotonic coupling.

Table 3.1 Membrane properties of AD-SPN

The table summarises data obtained from 54 neurons identified as AD-SPN. Results are expressed as mean ± standard deviation except for descriptive data. Those AD-SPN expressing a particular conductance are shown as a percentage of total AD-SPN population.

Membrane Property		n
Resting membrane potential	-62.2 ± 5.7mV	54
Input resistance	410 ± 241MΩ	54
Action potential amplitude	88.5 ± 15.6mV	54
Action potential duration	5.7 ± 1.8ms	54
Afterhyperpolarisation amplitude	25.9 ± 6.8mV	54
Afterhyperpolarisation 90-10% decay time	297.7 ± 150.2ms	54
Presence of shoulder on action potential repolarisation phase	100%	54/54
Presence of transient outward rectification	96%	52/54
Presence of anomalous inward rectification	89%	48/54

Table 3.1

Figure 3.2 Distribution of passive membrane properties of AD-SPN

Frequency histograms summarise the distribution of A, resting membrane potential (R.M.P.), B, input resistances and C, membrane time-constants recorded in AD-SPN.

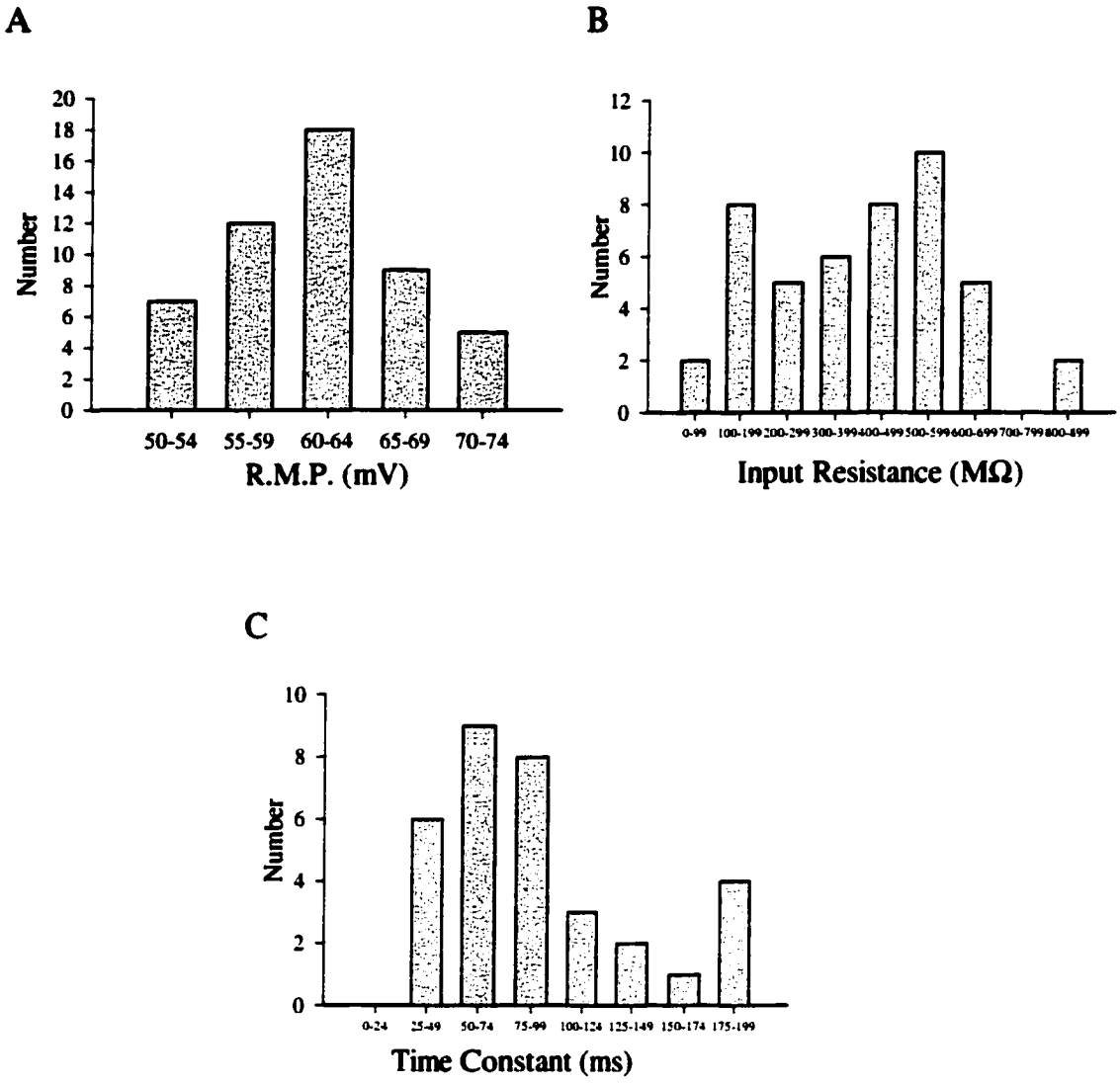
A
B
C
Number
R.M.P. (mV)
50-54
55-59
60-64
65-69
70-74
Input Resistance (MΩ)
Time Constant (ms)
0-24
25-49
50-74
75-99
100-124
125-149
150-174
175-199

Figure 3.2

Figure 3.3 Characteristic active membrane properties of AD-SPN

A, Superimposed whole-cell current clamp recordings of voltage responses to intracellular current pulses reveal three typical properties: 1) instantaneous inward rectification (star) observed as a decrease in voltage response to linearly increasing current pulse injection, 2) transient outward rectification (closed square) observed as a delayed return to rest of the membrane responses to injection of current pulses, 3) a pronounced shoulder on the repolarising phase of the action potential (inset, cross). B, a steady-state current-voltage curve plotted at the end of membrane responses to current injection of the neuron shown in A reveals a strong inward rectification activated at around –80mV.

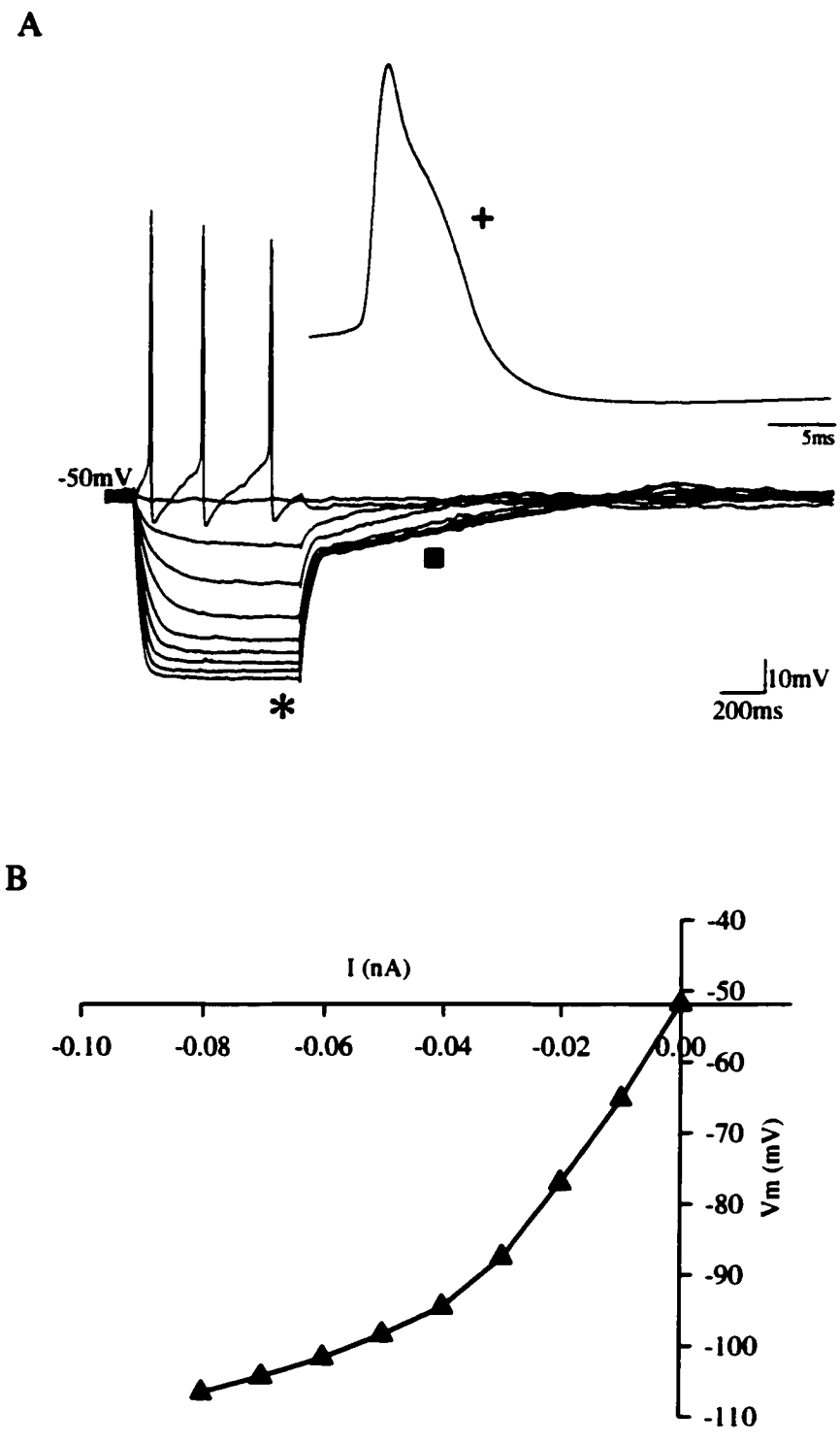
A
+
5ms
-50mV
10mV
200ms
*
B
I (nA)
-0.10
-0.08
-0.06
-0.04
-0.02
0.00
-40
-50
-60
-70
-80
-90
-100
-110
Vm (mV)

Figure 3.3

Figure 3.4 Sensitivity of the instantaneous inward rectification to extracellular barium and intracellular caesium

A, Superimposed whole-cell current clamp recordings of voltage responses to intracellular current pulses (-200 to 100pA, 20pA increments) in the presence of TTx (0.5μM). Note instantaneous inward rectification activated in response to large amplitude current pulses (i, star) that is reduced in the presence of extracellular barium (ii, star). In addition the sustained outward rectifier, activated at membrane potentials positive to –40mV is insensitive to barium. B, Steady-state current-voltage curves in control (closed circles, n=6) show pronounced inward rectification that is subsequently blocked by the presence of barium (closed squares, n=6). Also shown is the current-voltage curve for caesium-loaded neurons (closed triangles, n=12). Note the absence of instantaneous inward rectification.

Ai

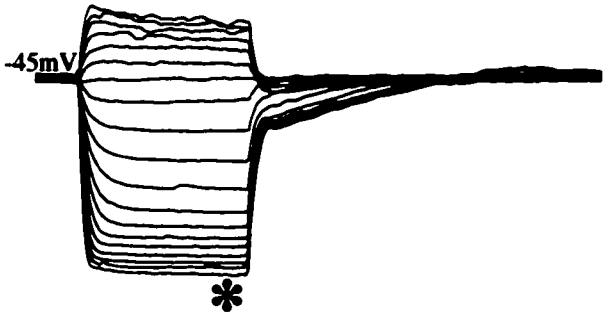

Control (TTx, 0.5μM)

Aii

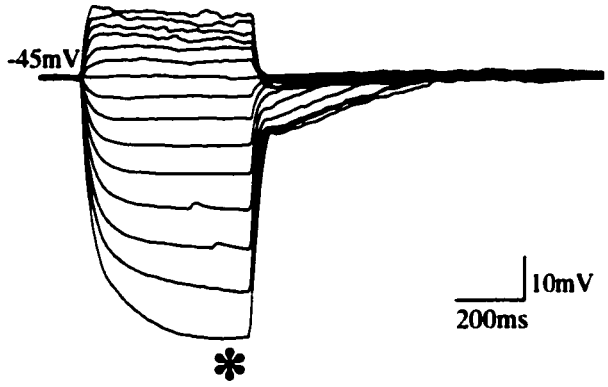

Barium (100μM)

B

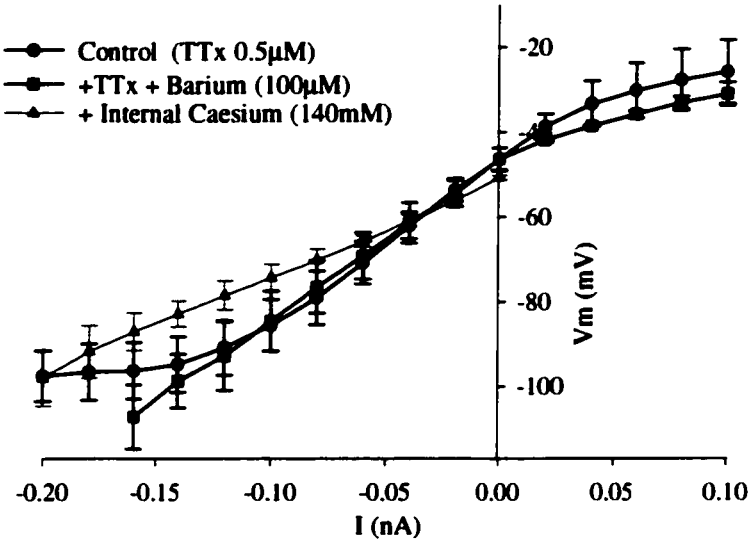

Figure 3.4

Figure 3.5 Sensitivity of the transient outward rectification to extracellular barium and 4-aminopyridine

A (i), transient outward rectification manifest as a delayed return to rest at the break of the membrane response to hyperpolarising current pulses (20pA increments) is reduced in the presence of barium (ii). Subsequent addition of 4-aminopyridine reduced further the remaining transient outward rectification (iii). B, Superimposed voltage responses from two separate neurons showing a fast component of the outward rectification sensitive to 4-aminopyridine (i) and a slower component sensitive to barium (ii). C, transient outward rectification (arrow) is observed upon injecting depolarising current pulses (20pA increments) from hyperpolarised membrane potentials (-100mV), achieved by the injection of hyperpolarising current pulses (-100pA).

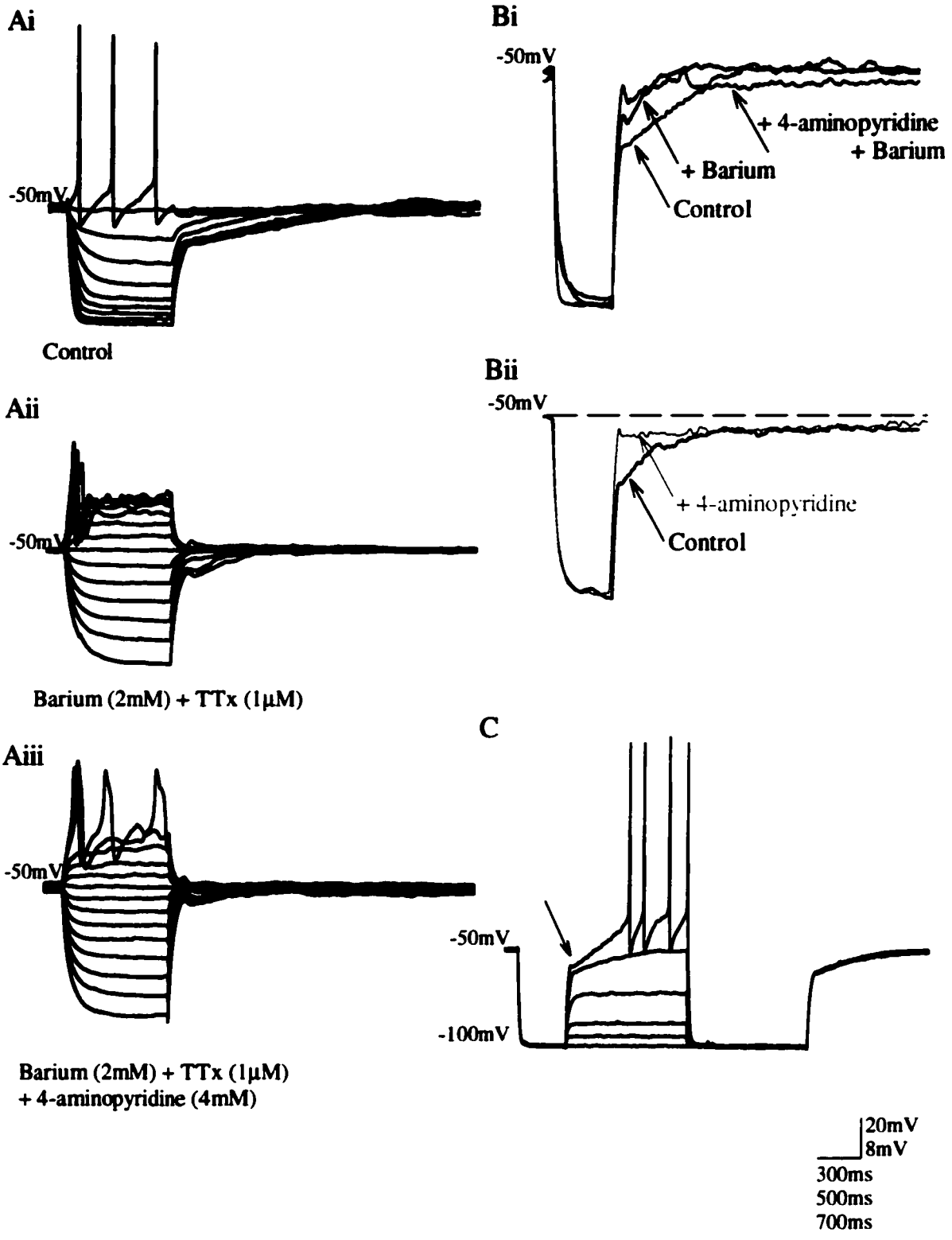
Ai
-50mV
Control
Aii
-50mV
Barium (2mM) + TTx (1μM)
Aiii
-50mV
Barium (2mM) + TTx (1μM)
+ 4-aminopyridine (4mM)
Bi
-50mV
+ 4-aminopyridine
+ Barium
+ Barium
Control
Bii
-50mV
+ 4-aminopyridine
Control
C
-50mV
-100mV
20mV
8mV
300ms
500ms
700ms

Figure 3.5

Figure 3.6 Effects of reducing extracellular potassium concentration on the expression of the transient outward rectification and the inward rectification

A, Superimposed whole-cell current clamp recordings of voltage responses to intracellular current pulses (-120 to 100pA, 20pA increments) in the presence of TTx (0.5μM) show instantaneous inward rectification (star) and transient outward rectification (closed square) in the presence of 3.1mM extracellular potassium. B, In nominally potassium-free aCSF, note the increased expression of the transient outward rectification (closed square) and reduced expression of the instantaneous inward rectification (star).

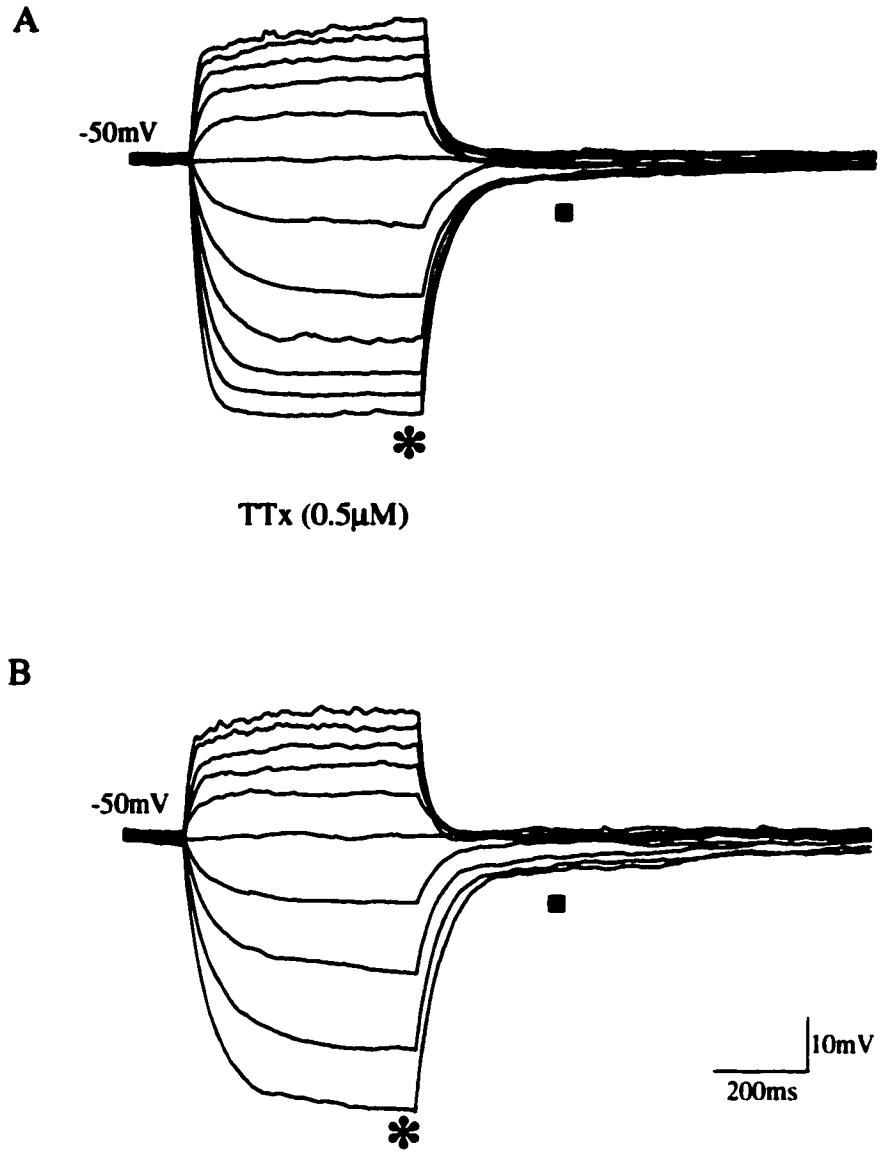
A
-50mV
TTx (0.5μM)
B
-50mV
10mV
200ms
TTx + nominally potassium-free aCSF

Figure 3.6

Figure 3.7 Sensitivity of the caesium induced rebound depolarisation to extracellular potassium

A, In the presence of 140mM internal caesium and TTx (1μM) membrane responses were evoked by injection of rectangular wave current pulses (-220 to +280pA, 20pA increments). Note the rebound depolarisation (Ai, arrow) whose voltage of activation is reduced in the presence of nominally potassium-free aCSF (Aii, arrow). B, Voltage responses in the presence of 140mM internal caesium and TTx (1μM) show the rebound depolarisation (Bi, arrows) that is reduced in the presence of nominally potassium-free aCSF (Bii, arrows). Membrane responses were evoked by the injection of depolarising current pulses (20pA increments) from hyperpolarised potentials (-100mV, with injection of –180pA current pulse). Note the presence of spontaneous miniature postsynaptic potentials.

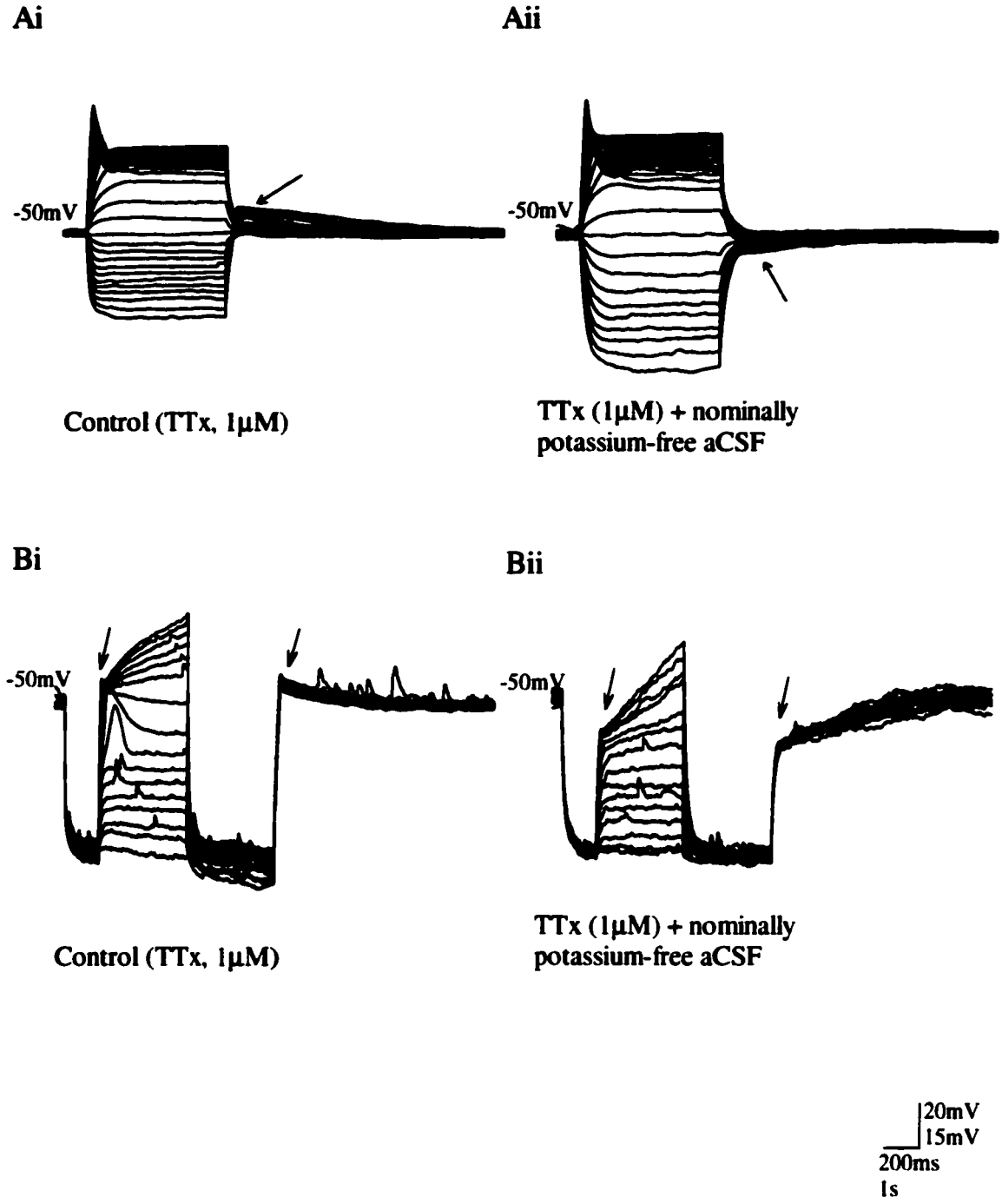
Ai
Aii
-50mV
-50mV
Control (TTx, 1μM)
TTx (1μM) + nominally potassium-free aCSF
Bi
Bii
-50mV
-50mV
Control (TTx, 1μM)
TTx (1μM) + nominally potassium-free aCSF
20mV
15mV
200ms
1s

Figure 3.7

Figure 3.8 Sensitivity of the caesium induced rebound depolarisation to 4-aminopyridine, external calcium and external caesium.

A, Superimposed voltage responses in the presence of 140mM internal caesium evoked by injecting depolarising current pulses (20pA) from hyperpolarised potentials (approx –100mV by the injection of -100pA current pulses). Note the activation of the rebound depolarisation (Ai, stars) that is blocked by 4-aminopyridine (4mM), revealing a high voltage activated spike (stars, Aii). Aiii, superimposed voltage responses from i and ii reveal the low threshold spike upon addition of 4-aminopyridine. B, Superimposed voltage responses in the presence of 140mM internal caesium and TTx (1μM) evoked by injection of incrementing current pulses (20pA, -120 to 140pA). The rebound depolarisation is evoked on the break of hyperpolarising current pulses (Bi), and is insensitive to nominally calcium-free aCSF (Bii) and 1mM external caesium (Bii). Note the insensitivity of the sustained outward rectifier evoked at potentials positive to -40mV to nominally calcium-free aCSF (Bii) and 1mM external caesium (Bii).

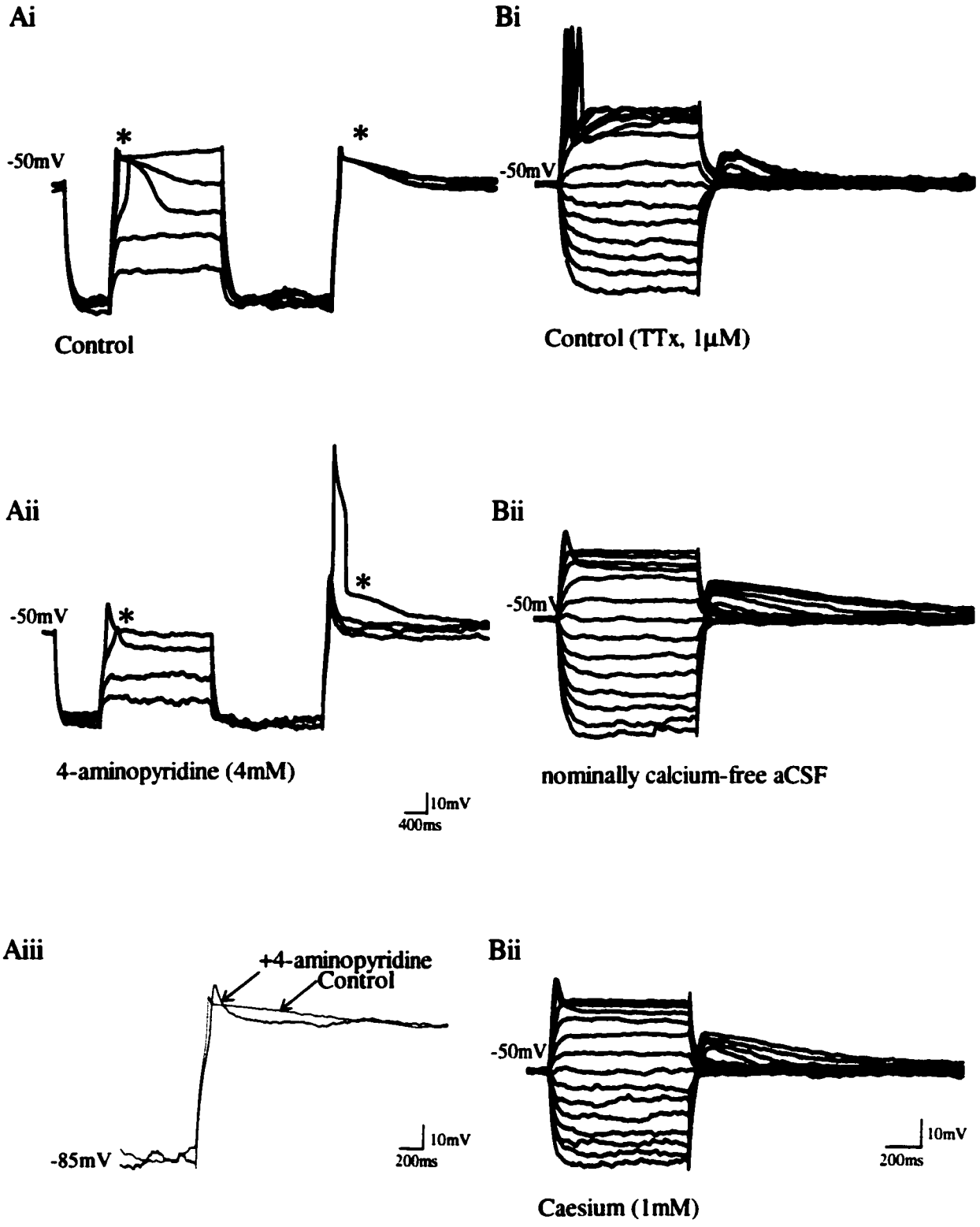
Ai
Bi
-50mV
*
*
-50mV
Control
Control (TTx, 1μM)
Aii
Bii
-50mV
*
*
-50mV
4-aminopyridine (4mM)
nominally calcium-free aCSF
10mV
400ms
Aiii
Bii
+4-aminopyridine
Control
-85mV
10mV
200ms
-50mV
10mV
200ms
Caesium (1mM)

Figure 3.8

Figure 3. 9 Sensitivity of the low threshold spike to nickel

Ai, In the presence of TTx (0.5μM), superimposed voltage responses show a rebound excitation (i, arrow) on the break of hyperpolarising current pulses (-160 to 80pA, 20pA increments). Aii, The rebound excitation is blocked upon addition of nickel (2mM). Bi, In the presence of internal caesium (140mM) and external TTx (1μM) membrane responses to injection of depolarising current pulses from hyperpolarised holding potentials (-100pA to −100mV, 20pA increments) reveal the low threshold spike (arrows). Bii, The low threshold spike is blocked upon addition of nickel (2mM).

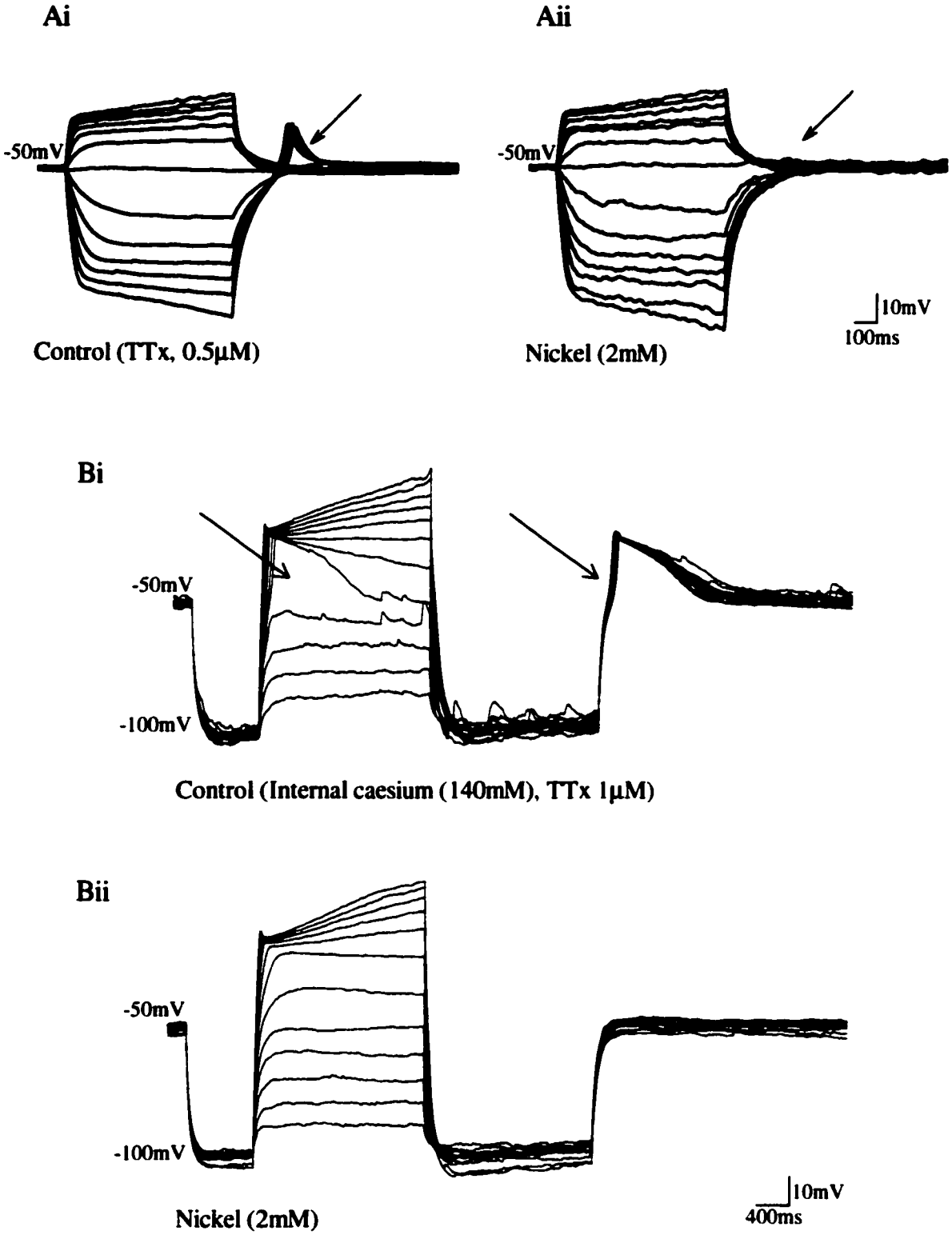
Ai
Aii
-50mV
-50mV
10mV
100ms
Control (TTx, 0.5µM)
Nickel (2mM)
Bi
-50mV
-100mV
Control (Internal caesium (140mM), TTx 1µM)
Bii
-50mV
-100mV
10mV
400ms
Nickel (2mM)

Figure 3.9

Figure 3.10 Burst firing activity is revealed by internal caesium

A, In the presence of 140mM internal caesium a continuous voltage trace shows spontaneous bursting activity. Expanded traces (ii and iii, indicated by bars in i and ii) show periods of hyperpolarisation followed by rapid depolarisation crowned with action potentials. B, Single spontaneous action potentials recorded in the presence of 140mM internal caesium from holding levels of –50mV may show a prominent afterdepolarising potential (i) and from holding levels of –80mV an extended period of depolarisation (ii) following repolarisation of the action potential.

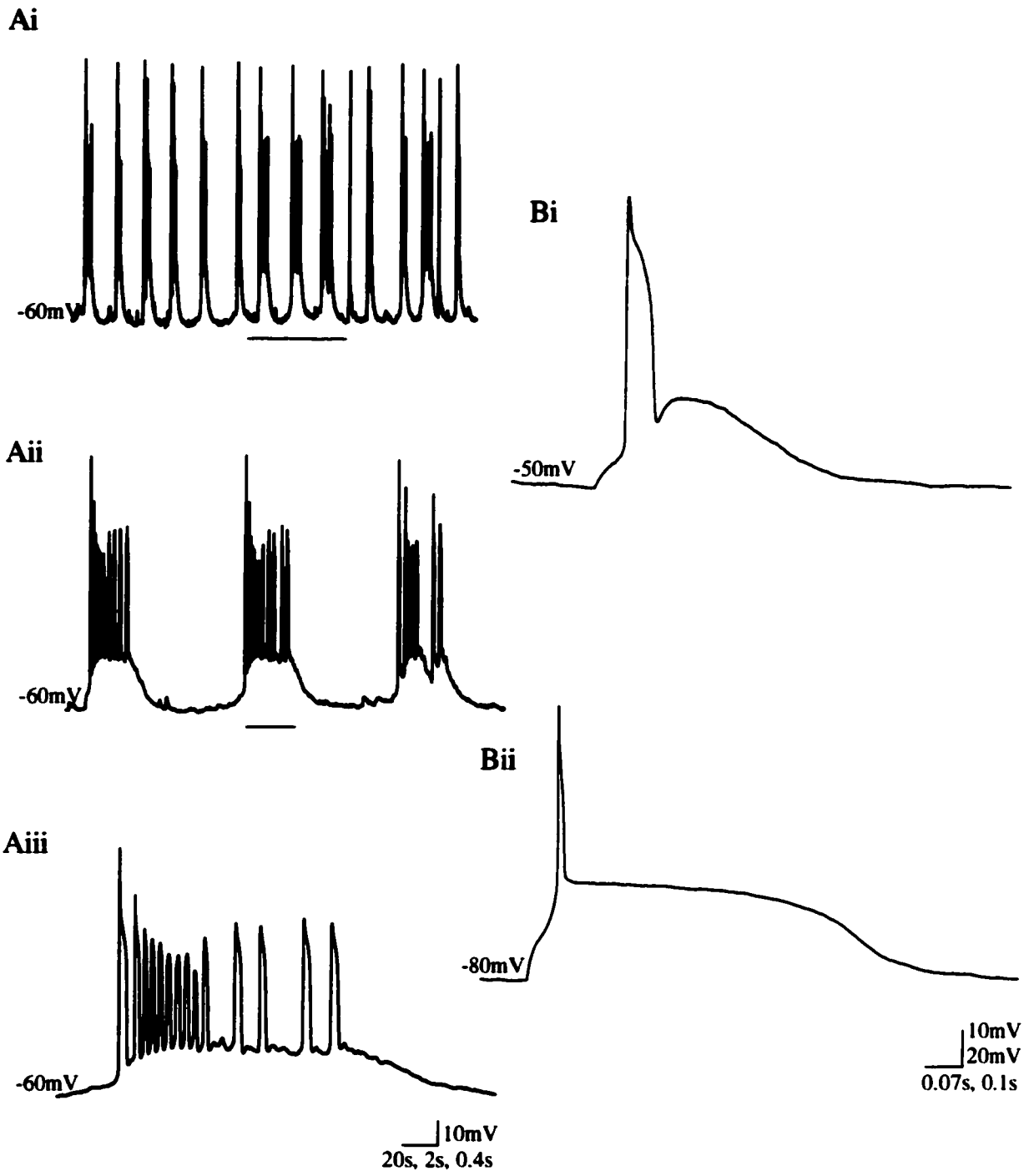
Ai
-60mV
Bi
-50mV
Aii
-60mV
Bii
-80mV
Aiii
-60mV
10mV
20s, 2s, 0.4s
10mV
20mV
0.07s, 0.1s

Figure 3.10

Figure 3.11 Burst firing induced by internal caesium: sensitivity to nickel

A, In the presence of 140mM internal caesium, spontaneous bursting activity is observed. At holding potentials of -70mV, bursts are shorter and more frequent than those occurring from holding potentials of –50mV. B, Bursting activity is blocked upon addition of nickel. C, Upon wash of nickel bursting activity returns. All traces are from the same neuron.

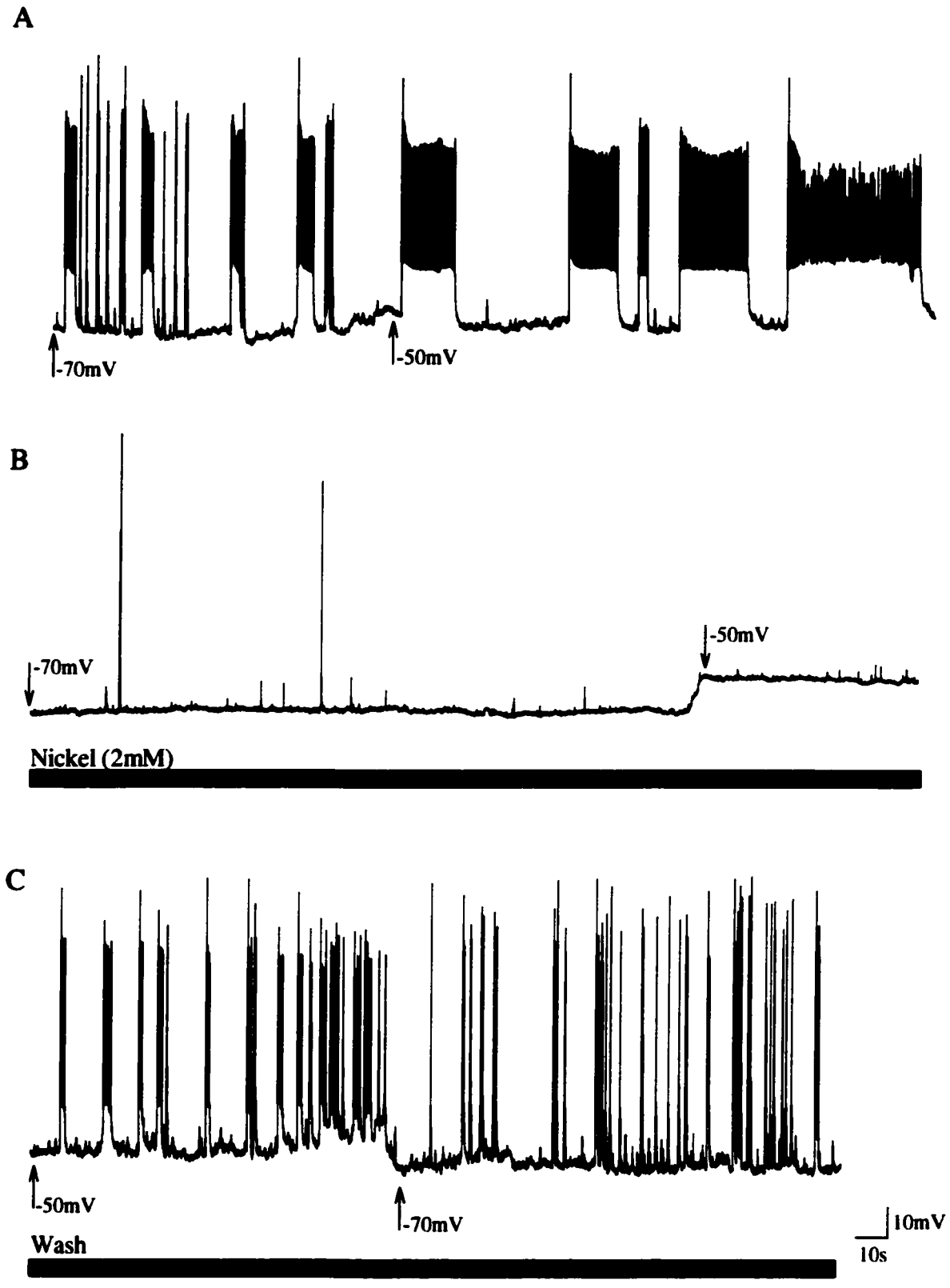

Figure 3.11

Figure 3.12 The sustained outward rectifier: sensitivity to potassium ion concentrations

Ai, Superimposed voltage responses evoked by injection of depolarising current pulses (10pA, i and ii, 2pA, iii) in control external potassium (3.1mM) show sustained outward rectification at voltages positive to –40mV. Aii, Addition of nominally potassium-free aCSF produced minimal change in sustained outward rectification. Aiii, Upon subsequent addition of high external potassium aCSF (15mM) a decrease in input resistance and absence of sustained outward rectification was observed. All membrane responses were evoked in the presence of TTx (1μM), TEA (30mM), nickel (2mM) and 4-aminopyridine (4mM). B, Current- voltage curves plotted under control external potassium (3.1mM), low external potassium (0.6mM) and high external potassium (15mM). Note the absence of rectification under high external potassium conditions (n=3).

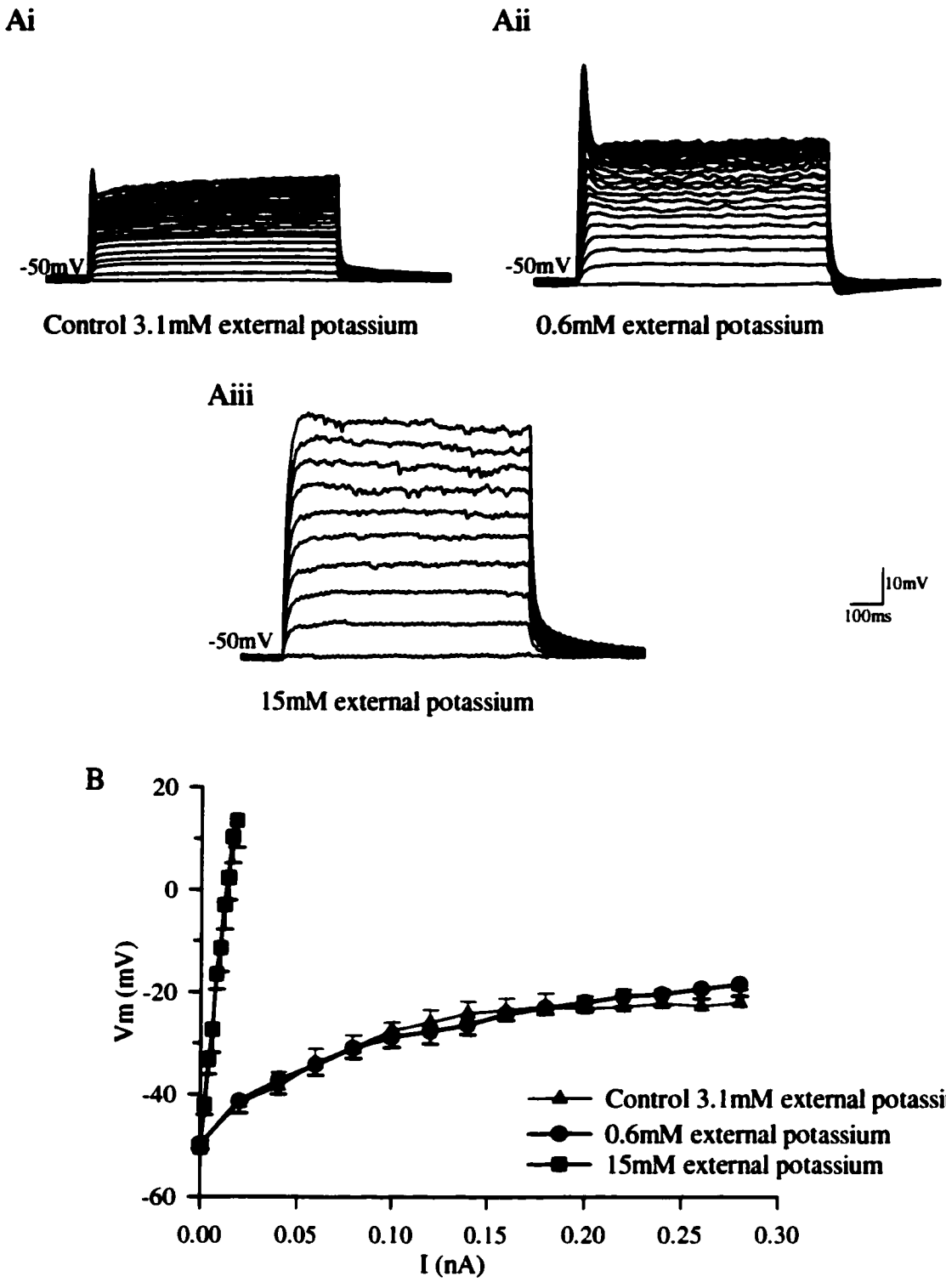
Ai
Aii
-50mV
-50mV
Control 3.1mM external potassium
0.6mM external potassium
Aiii
-50mV
10mV
100ms
15mM external potassium
B
20
0
-20
-40
-60
Vm (mV)
0.00
0.05
0.10
0.15
0.20
0.25
0.30
I (nA)
Control 3.1mM external potassium
0.6mM external potassium
15mM external potassium

Figure 3.12

Figure 3.13 The sustained outward rectifier is composed of three conductances

A, Voltage responses to depolarising current pulses (10pA) obtained in the presence of TTx (1μM) show sustained outward rectification (Ai). Aii, an initial component of the sustained outward rectification is blocked by cobalt (2mM). Aiii, a transient decaying phase is blocked upon subsequent addition of 4-aminopyridine (4mM). Aiv, the remaining outward recitification is insensitive to TEA (30mM). Bi, Current-voltage relations from the data in A taken at the peak amplitude of the notch (*). Note the decrease in the gradient of the plots obtained in the presence of cobalt and 4-aminopyridine. Bii, Current-voltage relations taken at the steady state peak amplitude of the membrane response (Bii, +) show insensitivity to the pharmacological manipulations in A.

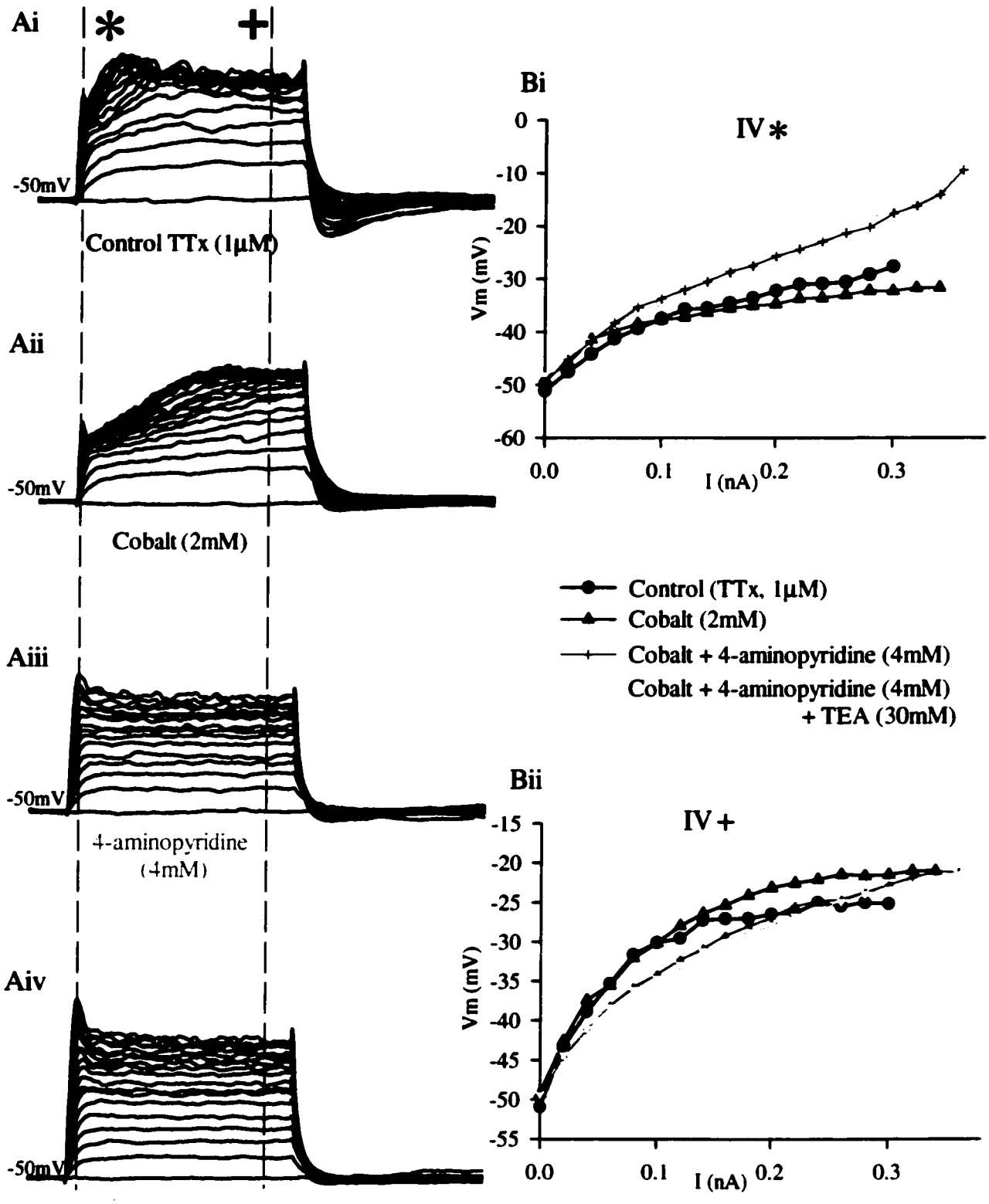
Ai
*
+
-50mV
Control TTx (1μM)
Aii
-50mV
Cobalt (2mM)
Aiii
-50mV
4-aminopyridine
(4mM)
Aiv
-50mV
Bi
IV*
Vm (mV)
0
-10
-20
-30
-40
-50
-60
0.0
0.1
I (nA)
0.2
0.3
Control (TTx, 1μM)
Cobalt (2mM)
Cobalt + 4-aminopyridine (4mM)
Cobalt + 4-aminopyridine (4mM)
+ TEA (30mM)
Bii
IV+
Vm (mV)
-15
-20
-25
-30
-35
-40
-45
-50
-55
0.0
0.1
I (nA)
0.2
0.3

Figure 3.13

Figure 3.14 Pharmacology of the sustained outward rectifier

Ai, Voltage responses evoked by the injection of depolarising intracellular current pulses (10pA) in the presence of 4mM internal QX-314 reveal high threshold spikes. Aii, Upon the addition of 2mM nickel the high voltage activated spikes are blocked revealing the sustained outward rectifier. Aiii, The addition of 4mM 4-aminopyridine reduced the initial transient component of the sustained outward rectification. Note the voltage of activation is between –5mV and 0mV. Bi, Voltage responses evoked in the presence of 140mM internal caesium by the injection of depolarising intracellular current pulses (20pA) reveal high threshold spikes. Bii, High threshold spikes are absent upon the removal of calcium from the aCSF, revealing sustained outward rectification Biii, The sustained outward rectification is not sensitive to a reduced sodium gradient (60mM) but is completely blocked with quinine (100μM, iv). Note the expanded voltage scale in Biv. C, Current-voltage relations showing the input resistance, measured as the mean between two points within steady-state potentials, of the sustained outward rectification under control conditions (circles, n=12), in 4mM internal QX 314 (triangles, n=5) and 140mM internal caesium (squares, n=12). Note the shift in voltage of activation in the presence of internal QX 314.

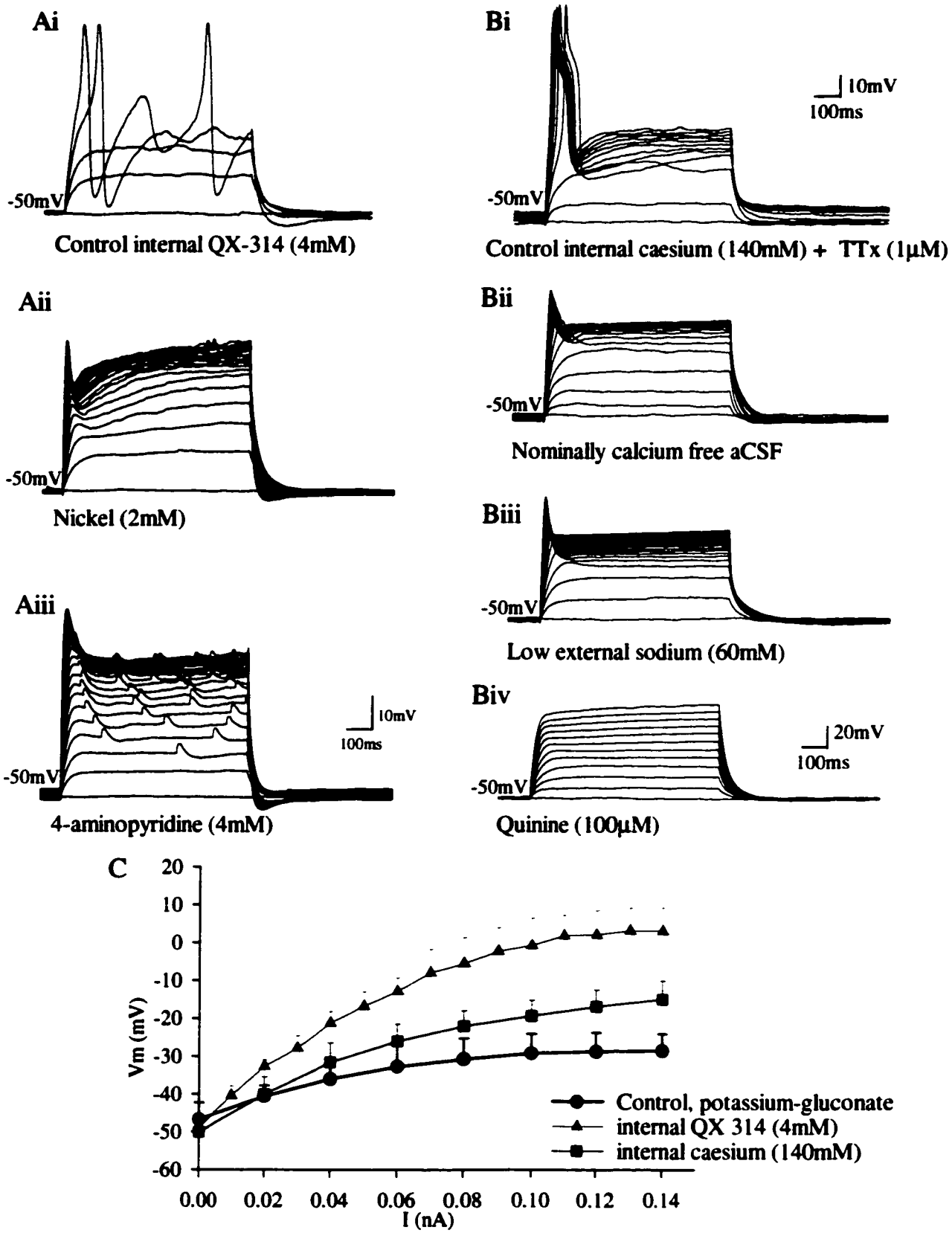
Ai
-50mV
Control internal QX-314 (4mM)
Bi
10mV
100ms
-50mV
Control internal caesium (140mM) + TTx (1μM)
Aii
-50mV
Nickel (2mM)
Bii
-50mV
Nominally calcium free aCSF
Biii
-50mV
Low external sodium (60mM)
Aiii
10mV
100ms
-50mV
4-aminopyridine (4mM)
Biv
20mV
100ms
-50mV
Quinine (100μM)
C
Vm (mV)
20
10
0
-10
-20
-30
-40
-50
-60
0.00
0.02
0.04
0.06
0.08
0.10
0.12
0.14
I (nA)
Control, potassium-gluconate
internal QX 314 (4mM)
internal caesium (140mM)

Figure 3.14

Figure 3.15 The sustained outward rectifier: partial reduction by low external pH and arachidonic acid

Ai, Superimposed voltage responses to intracellular current pulses (20pA) in the presence of TTx (1μM) show sustained outward rectification. Aii, Addition of low external pH 6.2 shifted the voltage of activation of the sustained outward rectification to more positive membrane potentials. Aiii, Graphical representation of the current-voltage relations in the presence of external pH 7.4 (squares) and external pH 6.2 (triangles). B, Membrane responses evoked by injection of depolarising current pulses (10pA) in the presence of TTx (1μM), nickel (2mM) and 4-aminopyridine (4mM) reveal sustained outward rectification. Bii, The addition of arachidonic acid (100μM) reduced the sustained outward rectification. Biii, Graphical representation of the current-voltage relations in control (circles) and arachidonic acid (triangles, n=3).

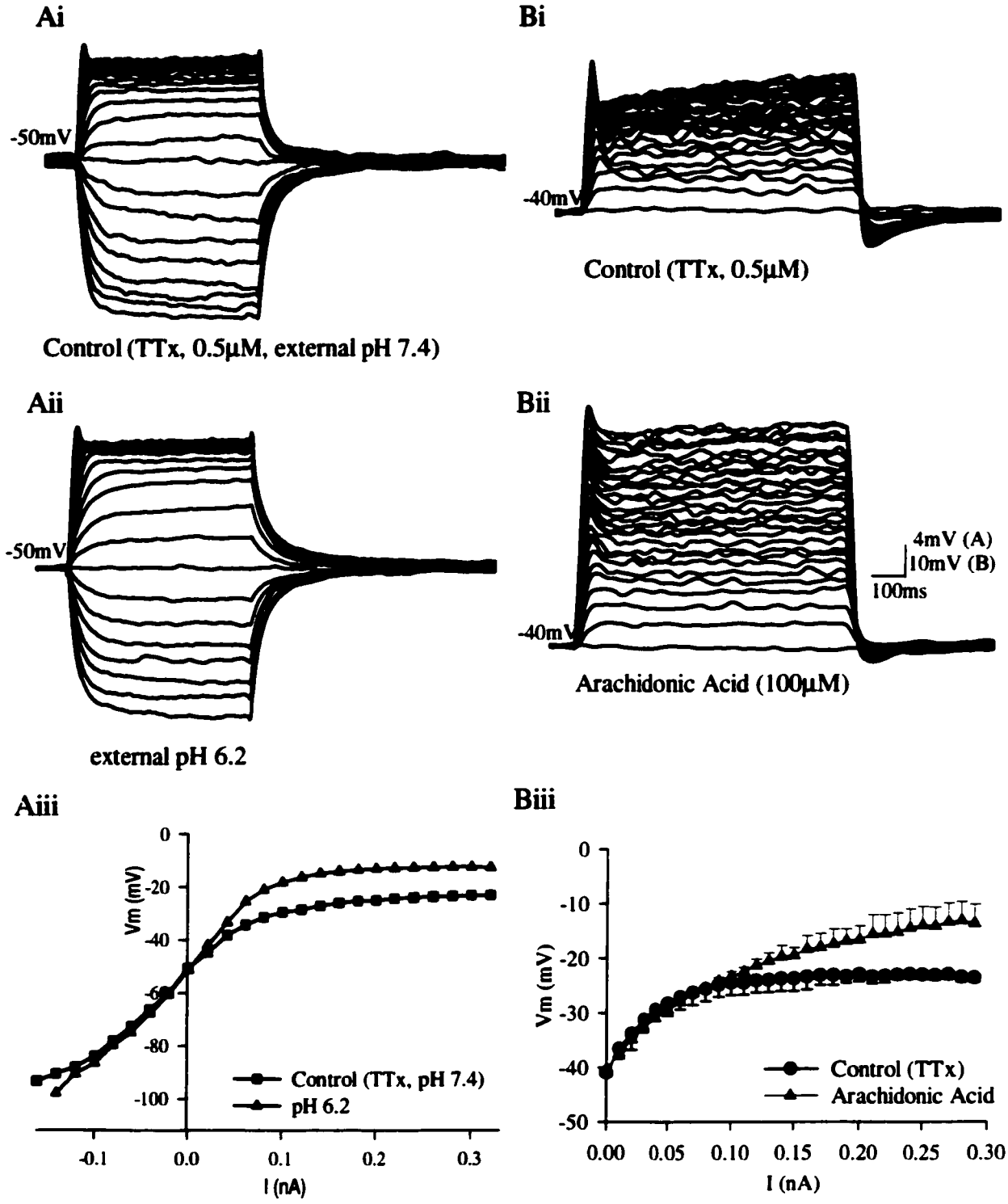
Ai
-50mV
Control (TTx, 0.5µM, external pH 7.4)
Bi
-40mV
Control (TTx, 0.5µM)
Aii
-50mV
external pH 6.2
Bii
-40mV
4mV (A)
10mV (B)
100ms
Arachidonic Acid (100µM)
Aiii
Vm (mV)
0
-20
-40
-80
-100
-0.1
0.0
0.1
0.2
0.3
I (nA)
Control (TTx, pH 7.4)
pH 6.2
Biii
Vm (mV)
0
-10
-20
-30
-40
-50
0.00
0.05
0.10
0.15
0.20
0.25
0.30
I (nA)
Control (TTx)
Arachidonic Acid

Figure 3.15

Figure 3.16 Outward rectification contributes to action potential duration and afterhyperpolarising potential amplitude

Traces show superimposed averaged (n>10 sweeps) antidromic spikes evoked by electrical stimulation (9V, 5ms, 0.05Hz) of the ventral roots at the exit zone in the presence of D-AP5 (10μM), NBQX (5μM), bicuculline (10μM) and strychnine (2μM). Ai, the antidromic spike (1) is prolonged in the presence of 30mM TEA (2) and further extended in the presence of 4mM 4-aminopyridine (3). Aii, Data from Ai on a slower time base shows the reduction in afterhyperpolarising potential in 4-aminopyridine (3) from that in TEA (2) and control (1). B, In a different neuron, the evoked antidromic spike (1) is prolonged in the presence of 2mM barium and 4mM 4-aminopyridine (2) and further extended in the presence of 100μM quinine (3).

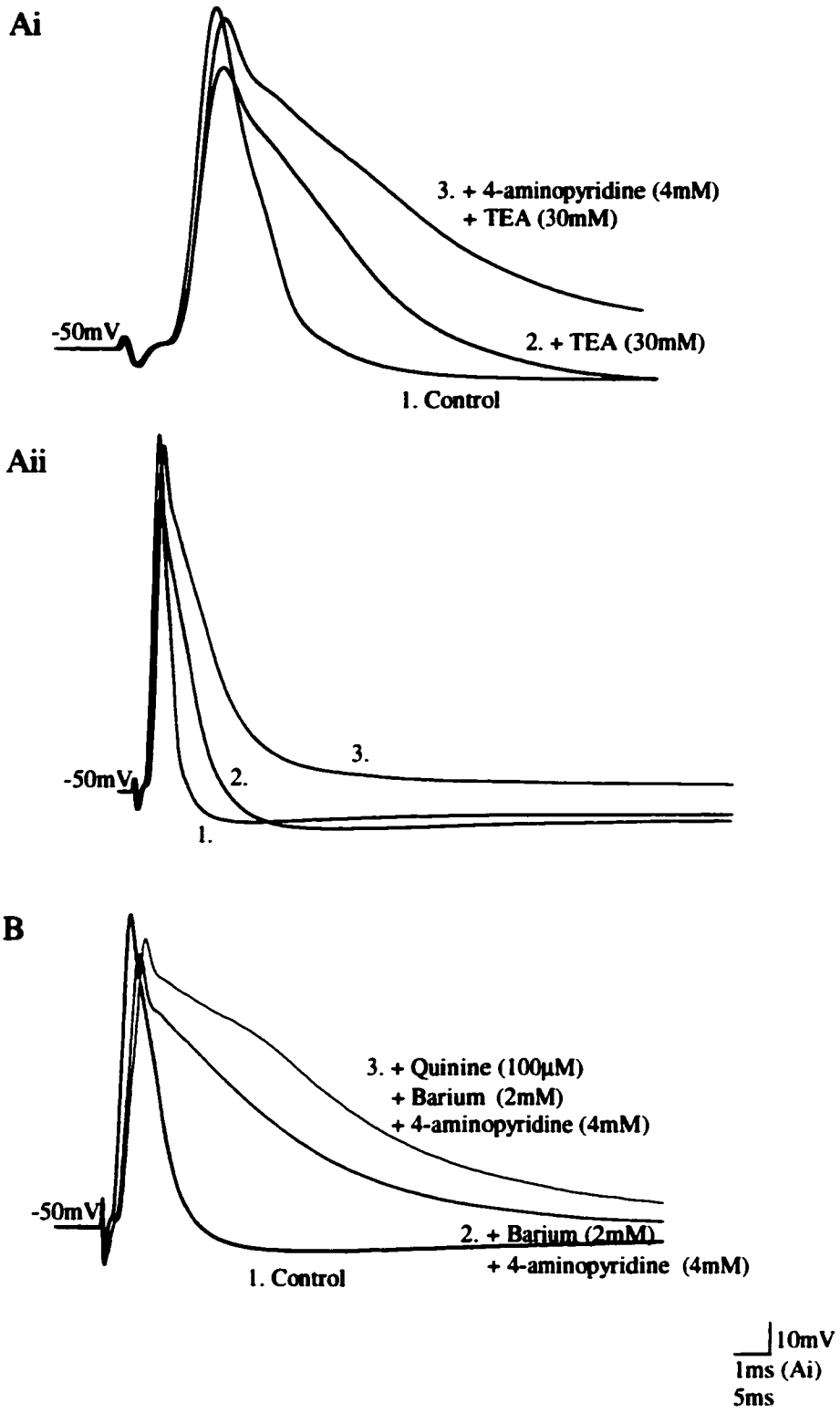
Ai
3. + 4-aminopyridine (4mM)
+ TEA (30mM)
-50mV
2. + TEA (30mM)
1. Control
Aii
-50mV
3.
2.
1.
B
3. + Quinine (100µM)
+ Barium (2mM)
+ 4-aminopyridine (4mM)
-50mV
2. + Barium (2mM)
+ 4-aminopyridine (4mM)
1. Control
10mV
1ms (Ai)
5ms

Figure 3.16

Figure 3.17 Pharmacology of the high voltage activated spike

A, Superimposed action potentials showed an increase in duration upon increasing external barium concentrations (1-5mM). B, Superimposed averaged (n≥8) antidromic spikes evoked by electrical stimulation (7V) of the ventral roots at the exit zone showed an increase in duration upon the addition of increasing (10-30mM) concentrations of TEA. C, Traces show superimposed averaged (n≥12) antidromic spikes. The control spike (1) is extended in duration by the addition of barium (2mM, 2). Subsequent addition of nimodipine (10μM) did not reduce the duration (3). D, Superimposed averaged (n≥12) antidromic spikes were evoked in the presence of 140mM internal caesium. The control action potential (1) is enhanced in duration upon addition of extracellular barium (2mM, 2). The addition of cytochrome C (0.1%) had no effect on the duration of the action potential (3). Subsequent addition of Conotoxin GVIA (2μM) reduced the duration of the action potential (4) and cadmium (100μM) blocked the remaining calcium component (5).

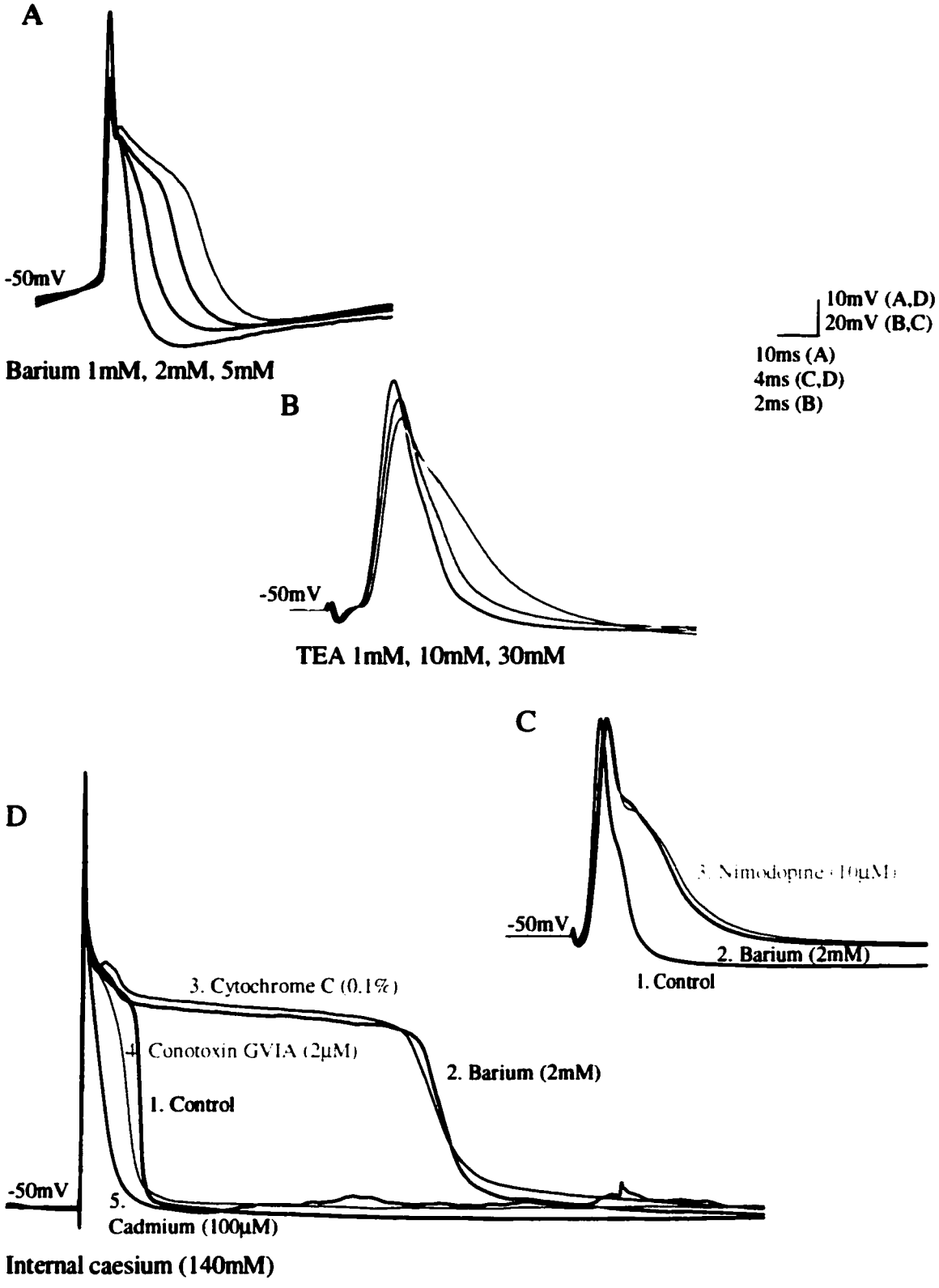
A
-50mV
Barium 1mM, 2mM, 5mM
10mV (A,D)
20mV (B,C)
10ms (A)
4ms (C,D)
2ms (B)
B
-50mV
TEA 1mM, 10mM, 30mM
C
-50mV
2. Barium (2mM)
1. Control
D
3. Cytochrome C (0.1%)
+ Conotoxin GVIA (2μM)
2. Barium (2mM)
1. Control
-50mV
5.
Cadmium (100μM)
Internal caesium (140mM)

Figure 3.17

CHAPTER 4

ELECTROTONIC COUPLING IN ADRENOMEDULLARY SYMPATHETIC PREGANGLIONIC NEURONS

4.1 Introduction

Electrotonic coupling was first identified in invertebrates (Watanabe, 1958; Furshpan, 1959) and subsequently in vertebrates, in both the peripheral and central nervous systems, a feature of both neurons (Korn *et al.*, 1973; Llinas *et al.*, 1974; MacVicar and Dudek, 1981; Mann-Metzer and Yarom, 1999) and glia (Schwartzkroin and Prince, 1979; Massa and Mugnaini, 1982). Originally proposed to mediate endogenous electrical and biochemical communication during development (Kandler and Katz, 1995; 1998, Fulton 1988, Connors 1983), it is now evident that in specific populations of neurons electrotonic coupling persists into adulthood, where it is believed to co-ordinate and synchronise neuronal output (Draguhn *et al.*, 1998; Galarreta and Hestrin, 1999; Mann-Metzer and Yarom, 1999; Landisman *et al.*, 2002).

In vertebrates, the molecular substrates mediating electrical coupling are gap junction channels composed of connexin proteins (Bruzzone *et al.*, 1996; Kumar and Gilula, 1996). Currently, fourteen connexins have been identified and named according to their molecular weight. Neurons are known to synthesise connexins 26, 32, 36, 43 and 47, each of which may confer specific properties on the channels in which they are incorporated. These properties include phosphorylation sites (Yahuaca *et al.*, 2000), pH (Spray *et al.*, 1981), calcium, voltage dependence (Moreno *et al.*, 1994) and modulation by neurotransmitters and second messengers (McMahon, 1994; Velazquez *et al.*, 1997).

Within one cell, six connexin proteins are required to form a hexameric structure with a central aqueous pore, called a connexon or hemichannel. Hemichannels from opposing cells interact to allow direct cytoplasmic communication. The clustering of multiple channels in closely packed hexameric or pentameric structures forms a gap junction (Revel *et al.*, 1992; Hoh *et al.*, 1993).

Electrotonic coupling is also present within the autonomic nervous system, in particular within a subpopulation of thoracolumbar SPN (Logan *et al.*, 1996; Nolan *et al.*, 1999) where electrotonically coupled neurons displayed spontaneous biphasic oscillations in membrane potential.

The present study was undertaken to address the presence of electrotonic coupling in a population of SPN that had been retrogradely labeled with a dye placed in the adrenal medulla, the AD-SPN. The results presented in this chapter identify and describe some of the properties of electrotonically coupled AD-SPN and provide insight into a mechanism by which highly complex firing patterns may arise from a network of coupled AD-SPN. Preliminary evidence is also presented that suggests a role for intracellular calcium in regulating both spontaneous activity and electrotonic coupling.

4.2 Results

Of the 54 SPN identified as adrenomedullary by the presence of double labeling (described in Chapter 3) 40 neurons (74%) displayed one or more of the following properties that are consistent with the presence of electrical coupling;

a) spontaneous oscillations in membrane potential (Figures 4.2, 4.14Ci)

b) short latency depolarisations (Figure 4.3)

c) direct current transfer between AD-SPN (Figures 4.4, 4.5, 4.8, 4.11)

A verification that properties a) and b) are indicative of electrotonic coupling comes from their demonstration in SPN that permit direct current transfer (c).

This chapter includes data from 54 single and 3 pairs of AD-SPN. Also included are data demonstrating the influence of an electrotonically coupled network on the properties of individual neurons and data obtained under modified calcium conditions. These data were obtained from 6 pairs of electrotonically coupled SPN all located in T_7-T_{10} spinal levels but unidentified because of lack of retrograde tracer.

4.21 Membrane properties of electrotonically coupled AD-SPN

The mean resting membrane potential of AD-SPN bearing one or more of the properties mentioned above was -61.7 ± 5.6 mV, ranging between -72 and -50 mV, and showing a normal distribution similar to that of the total AD-SPN population (n=54, Figure 4.1A). The mean input resistance of these neurons was 296.7 ± 146.2 MΩ. The distribution of input resistances tended towards low resistances (Figure 4.1B). The resting membrane potentials of the electrotonically coupled and putative non-coupled AD-SPN (-60.7 ± 5.6 mV, n=39 and –60.4 ± 2.3mV, n=11 respectively) was not significantly different (P>0.2). However the differences in input resistance between coupled (296.7 ± 146.2 MΩ, n=32) and putatively non-coupled (544.2 ± 158.6 MΩ, n=9) SPN reached significance with P=0.001 (2-tailed, 2 sample unequal variance). It is appreciated that a lack of evidence of electrotonic coupling does not imply the absence of coupling so underestimates of the extent of coupling between SPN are likely. Subsequently the above groupings are arbitary. The time constant was 134.8 ± 39.5ms (n=6), estimated by fitting

double exponentials to the membrane voltage charging curves induced by injection of small, hyperpolarising rectangular-wave current pulses.

4.22 Oscillations in membrane potential

In electrotonically coupled AD-SPN, 3 types of spontaneous activity were observed, all of which were stable over prolonged recording periods (<6 hours). Eleven neurons displayed bursting activity characterised by brief discharges of 2-8 action potentials followed by a long (1.5 to 20s) silent phase coincident with a large amplitude and prolonged hyperpolarisation of the membrane (Figure 4.2). Twenty four neurons displayed single action potentials that occurred in a rhythmical or random fashion (Figure 4.9A). The randomly occurring action potentials were "striking" in the variability of their afterhyperpolarising potential waveform that within one neuron ranged from a mean amplitude of 25.4±1.6mV to 11.9 ±0.5mV and tau of decay of 20.1 ± 3.5s to 0.5 ±0.1s. A third feature common to both the above were subthreshold oscillations in membrane potential observed both spontaneously and upon hyperpolarisation of the membrane of active neurons (Figure 4.2). Oscillations differed from spontaneous postsynaptic potentials in that they displayed a characteristic "biphasic" waveform consisting of an initial small depolarising transient (1-4mV) followed by a pronounced hyperpolarising component (Figure 4.2Bii). At resting levels spontaneous oscillation frequencies ranged between 0.09 and 0.71Hz (mean = 0.35 ± 0.27Hz, n=10). Hyperpolarisation of the membrane resulted in a decrease in their frequency and no reversals were obtained (Figure 4.2Bi). For example in a fast oscillating SPN the frequency decreased from 3.33Hz at –40mV to 0.83Hz at –100mV. In a slow oscillating SPN a 20mV

hyperpolarisation induced a decrease in oscillation frequency from 6.6Hz to 5Hz. In some SPN where multiple rhythms (or waveforms) were observed (Figure 4.12Ci), a selective fall out of particular waveforms (selective filtering) was observed upon hyperpolarisation.

4.23 Short latency depolarisations

In single electrode recordings it is possible to infer direct current transfer by evoking a short latency depolarisation (SLD) via antidromic stimulation (Walton and Navarrete, 1991; Logan *et al.*, 1996). Electrical stimulation (3-11V, 0.1ms, 0.25- 0.1Hz) of the ventral roots at the exit zone in the ventral horn induced an antidromic spike in 32 of 34 SPN. Although none turned out to be retrogradely labeled, antidromic activation evoked a subthreshold SLD (Figure 4.3A). SLDs were evoked at subthreshold stimulus intensities in 6 of 6 SPN tested, as well as in 5 of 7 SPN recorded in the presence of intracellular QX 314 (4mM, Figure 4.3B). Since there was no difference in the properties of the SLD revealed under each of these conditions data were pooled. SLDs had a biphasic waveform with a peak to peak amplitude of 14.4 ± 4.45mV (range = 9.2 to 21.6mV) and a mean latency of 1.01 ± 0.18ms (n=11). SLDs typically exhibited a graded response to increasing stimulus intensity. While resistant to membrane hyperpolarisation to –100mV (Figure 4.3C), hyperpolarisation reduced the amplitude of the inhibitory component from 18.9 at –40mV to 4mV at –80mV (n=2, Figure 4.3Cii). These results compare favourably to those obtained previously in SPN (Logan *et al.*, 1996) and in motor neurons (Walton and Navarrete, 1991).

That the SLD is due to electrotonic coupling is indicated by fulfillment of at least three of the following criteria; A) a shorter latency than that of monosynaptic PSPs, the difference reflecting electrical current transfer versus chemical transmission, B) insensitivity to membrane hyperpolarisation, C) graded response to increasing voltage stimulation, D) ability to follow high frequency stimulation, E) resistance to collision with an action potential from the soma, F) insensitivity to removal of calcium from the aCSF (Walton and Navarrete, 1991).

4.24 Paired recordings from AD-SPN

In this series of experiments, simultaneous whole cell recordings obtained from nine pairs of SPN, including three pairs of positively identified AD-SPN, demonstrated direct current transfer. Injection of current pulses (-140 to 40pA, 800ms, 0.1Hz) into one SPN resulted in voltage deflections in both SPNs (Figure 4.4, 4.5). Current transfer was inferred to be bi-directional; thus either neuron could be termed the pre- or post- synaptic neuron, depending on which one was the driving neuron. In each pair, the membrane potential deflection was smaller and the time course of voltage change was slower in the postsynaptic SPN; compare the presynaptic tau of 33.4 ±6.1ms to the postsynaptic tau of 149.8 ± 33.2ms (n=8, Figure 4.4). Current injection that caused the membrane voltage to reach threshold and generate an action potential in the presynaptic SPN was simultaneously associated with a characteristic biphasic oscillation in membrane potential in the postsynaptic SPN (Figure 4.4).

An indication of the amount of current transfer between two electrotonically coupled neurons is given by the *coupling co-efficient*, i.e. the ratio of the amplitude of the

postsynaptic to presynaptic potential change (Bennett, 1966, see Chapter 2.6). In AD-SPN, the coupling coefficient ranged from 0.08 to 0.43 (Table 4.6A); similar to those obtained from 6 pairs of electrotonically coupled SPN unidentified as to their target projection (range 0.146 to 0.537, Table 4.7A). An example of electrotonic coupling in AD-SPN with relatively high coupling coefficients (strong coupling) is shown in Figure 4.4 and coupling with low coupling coefficients (weak coupling) in Figure 4.5. *Junctional conductance* is a measure of current transfer that takes into account not only the coupling coefficient but also the input resistance of the two neurons. The junctional conductance can be calculated by incorporating the steady state input resistances and the coupling coefficients into a mathematical equation in which each neuron is represented by a single compartment joined by a resistor representing the electrotonic junction (Bennett, 1966, 1977, see Chapter 2.6). The junctional conductance for AD-SPN ranged between 0.23 and 4.45nS (Table 4.6A) and compared favourably with that for unidentified SPN (range 0.58 to 5.54nS, Table 4.7A).

Previous studies (Furshpan, 1959; Nolan *et al.*, 1999) have demonstrated that current may be transmitted more readily in one direction within a pair of coupled neurons, a feature endowing the electrotonic junction with rectifying properties (Furshpan, 1959; Auerbach and Bennett, 1969; Bennett, 1977). The *coupling coefficient ratio* and *junctional conductance ratio* are reflections of the equality of current transfer with the latter taking into account the input resistance of the two neurons. Ratios of coupling coefficient, junctional conductance and input resistance are defined as the largest to the smallest value. In AD-SPN, a coupling coefficient ratio close to 1 (mean = 1.10 ± 0.08, n=3 pairs, Table 4.6B) implied non-rectifying electrotonic junctions. However, in the 6 pairs of unidentified electrotonically coupled SPN the coupling

coefficient ratio deviated from unity (mean = 1.45 ± 0.26, Table 4.7B), indicating that current passage between a pair may be preferential. Without a larger sample of AD-SPN, the significance of these differences cannot be assessed.

Rectification of current flow between 2 cells may be determined either by the intrinsic properties of the electrotonic junction (i.e. molecular nature of the connexins) or as a consequence of differences in input resistance between any pair. While the former remains to be characterised in SPN, data is available on the input resistance ratio. In AD-SPN, the input resistance ratios in 2 of the 3 pairs were calculated to be close to unity (1.11 and 1.18), in keeping with junctional conductance ratios of 1.16 and 1.23, suggesting the electrotonic junctions between these particular AD-SPN were non-rectifying. The remaining pair possessed an input resistance ratio of 1.46 and junctional conductance ratio of 1.78, (Table 4.6B) indicating that current transfer between the pair was unequal. In the 6 pairs of unidentified electrotonically coupled SPN, the input resistance ratios ranged from 1.15 to 2.07 (mean 1.64 ± 0.36, Table 4.7B). These data suggest that the rectification indicated by the coupling coefficients can be attributable to differences in input resistance within a pair of SPN. Furthermore the junctional conductance ratios, that compensate for differences in input resistance, are close to unity (mean = 1.17 ± 0.21, n=6 pairs, Table 4.7B). Differences in input resistance do not rule out the presence of an intrinsically rectifying junction. For AD-SPN, based on the data presented here, it is suggested that the junctions are non-rectifying and formed between cells of similar input resistances. However that relatively strong rectification was observed in 2 of 6 pairs of unidentified electrotonically coupled SPN raises the possibility of the small sample size creating bias in the data.

4.25 Electrotonic coupling and synchronous firing

Electrotonic coupling can facilitate synchronous firing between neurons, and has been observed in inhibitory interneurons in the cortex (Galarreta and Hestrin, 1999), in inferior olive neurons (Llinas and Yarom, 1981), neurons in the locus coeruleus (Williams and Marshall, 1987), cerebellar cortex (Mann-Metzer and Yarom, 1999) and thalamic reticular nucleus (Landisman *et al.*, 2002). This also appears to be the situation in AD-SPN. When action potentials were evoked by injection of suprathreshold current pulses (120-220pA, 500ms, 0.1Hz) into presynaptic neurons, simultaneous oscillations in membrane potential were observed in the postsynaptic neuron (Figure 4.8). Oscillations became synchronous action potentials when suprathreshold current pulses were injected into postsynaptic neurons (n=3, Figure 4.7C). The fact that synchronous firing was observed both for low frequency (0.54 Hz) and high frequency firing (3.2 Hz) rates indicates that frequency is not a modifying factor in synchronous activity.

4.26 Firing patterns of electrotonically coupled AD-SPN

As noted above (Section 4.22, Figure 4.2) in single electrode recordings of AD-SPN, spontaneous action potential firing could either form distinct bursting patterns (Figure 4.2A) or more irregular firing patterns (Figure 4.9A). The burst pattern comprised 2-7 action potentials at a frequency of 2.8 ± 1.0 Hz (range 1.47-5Hz, from 6 SPN). The striking feature of burst firing activity was the variability of afterhyperpolarising potential waveform (Figure 4.9). These differences in afterhyperpolarising potential amplitude and duration can be seen by comparing afterhyperpolarising potential amplitude and decay times during and after bursting activity and plotting these variables against each other (An example is given in Figure 4.10A). Termination of firing was associated with long

duration (1.6s ± 0.4s compared to 0.7 ± 0.1s) and larger amplitude (24.1 ± 2.4 mV compared to 19.8 ± 1.1 mV, n=16, P<0.001 from single electrode recording) afterhyperpolarising potential than those during the burst (Figure 4.9A) as indicated by the cluster of points to the top right of the graph in Figure 4.10A. A better appreciation of the influence of the afterhyperpolarising potential on the neuronal firing pattern in SPN can be gained from examination of the spontaneous activity in pairs of electrotonically coupled SPN, where burst firing is a feature of one SPN. In Figure 4.9B for example, note that termination of burst firing activity in SPN 2 was concurrent with action potential firing in both SPN. Upon synchronous firing, the peak amplitude of the afterhyperpolarising potential in the bursting SPN increased (from 22.8 ± 3.5mV to 15.3 ± 2.8mV, a 149% increase) and tau of decay increased (from 463.9 ± 158.6ms to 183.0 ± 36.5ms, a 253.5% increase, n= 3 pairs, Figure 4.9C). These data can be plotted against each other to reveal distinct groups (Figure 4.10B). Increases in afterhyperpolarising potential properties within a pair were asymetrical, evidenced by a greater increase in peak amplitude (9.5 ± 1.5 %) and tau of decay (133.3 ±19.2%, n=2 pairs) for one SPN in the pair. These data suggest that synchronous firing induced by electrotonic coupling enhanced both the duration and amplitude of the afterhyperpolarising potential present during the burst. As a result of the enhanced afterhyperpolarising potential further action potential firing is prevented. Conversely a common feature of the large amplitude afterhyperpolarising potentials was that coupled neurons fired synchronously. Thus data suggest that the burst firing may be an emergent property of the electrotonically coupled network which is dependent on the expression of intrinsic membrane properties.

To test the influence of isopotentiality (i.e. equality of membrane potential) on pre- and post-synaptic waveforms, the effects of membrane hyperpolarisation on input resistance were investigated. In simultaneous recordings from 2 pairs of electrotonically coupled SPN, current pulses (-140 to 40pA, 800ms, 0.1Hz) were injected into the presynaptic neuron which was held at a constant membrane potential (V_h= -50mV) and the postsynaptic neuron was held at varying membrane potentials (V_h= - 40 to –100mV, 10mV increments, Figure 4.11). At each holding potential, the steady-state voltage amplitude in both pre- and post- synaptic neurons were measured and plotted against the current injected (Figure 4.12). Upon moving the postsynaptic neuron away from isopotentiality, data revealed a decrease in the voltage response of both the pre- and post-synaptic neurons to current injection. In the presynaptic neuron the input resistance decreased at steady state potentials (pair one from 338.5 to 314.3 MΩ, pair two from 419.3 to 410.3) and at membrane potentials negative to –70mV (pair one from 154.7 to 151.1, pair 2 from 125.4 to 121.8MΩ). The gradient of the line fitting the amplitude of the voltage response to injection of presynaptic current pulses upon hyperpolarisation of the membrane in the receiving cell decreased at steady state membrane potentials (pair one from 33.3 to 24.1, pair two from 63.6 to 12.3) and at hyperpolarised potentials (pair one from 16.0 to 12.3, pair two 57.2 to 9.1) (Figure 4.12, n=2 pairs). The increase in input resistance at isopotentiality is concomitant with the reduction of current flow between the pair of neurons. This effect applied in both directions (Figure 4.11, 4.12). Therefore, these data indicate that the activity within the electrotonically coupled network determines the input resistance of the individual neurons.

4.27 Calcium and electrotonic coupling

Calcium has a prominent role at several levels in regulating neuronal excitability, including actions on intracellular signaling cascades (e.g. calcium dependent kinases), release of calcium from intracellular stores, and regulation of gap junction coupling (Berridge, 1998). In AD-SPN, routes for calcium entry include high voltage activated N- and P-type channels, low voltage activated T-type channels (Chapter 3) and NMDA receptors (Chapter 5). The availability of paired recordings from electrotonically coupled neurons provided an opportunity to test how these SPN would respond to changes in internal calcium concentrations. Data presented are from 2 pairs of electrotonically coupled SPN that exhibited spontaneous action potential firing. One SPN in each pair exhibited bursts of action potentials, the terminations of which were synchronous with action potential firing in the coupled SPN.

A) The effects of caffeine

Caffeine (10mM), can induce calcium release from the endoplasmic reticulum (Sawynok and Yaksh, 1993). Bath application of caffeine evoked a 3-4mV hyperpolarisation and cessation in spontaneous firing and oscillatory activity in both pairs (Figure 4.13A, B). Spontaneous activity did not return even when the membrane potential was returned to resting levels by injection of positive current. During this caffeine-induced response, the coupling coefficient decreased (in Pair A from 0.22 to 0.12 and from 0.17 to 0.10, in Pair B from 0.56 to 0.32 and from 0.17 to 0.10), the junctional conductance decreased (in Pair A from 0.87 to 0.80nS and from 0.84 to 0.58nS, in Pair B from 1.43 to 0.53nS and from 0.89 to 0.67nS) and a decrease in input resistance was observed (in Pair A from 210.2 to 174.7MΩ and from 271.8 to 156.0MΩ, in Pair B from

205.2 to 158.5MΩ, Table 4.15). One neuron exhibited an increase in input resistance (Pair B 463.2 to 628.1MΩ). Interestingly the junctional conductance decreased by a further 30.9% in one direction of current transfer compared to the reverse direction. This feature is termed unilateral modulation in this study. In Pair A, this is believed to be a direct effect on the junctional conductance since both coupling coefficient and input resistance ratios decreased (from 1.33 to 1.22 and from 1.29 to 1.12) while the junctional conductance ratio increased (from 1.04 to 1.38, Table 4.16). Pair B showed a decrease in ratios of coupling coefficients and junctional conductance (3.28 to 3.19 and 1.61 to 1.28 respectively), and an increase in input resistance ratio (2.26 to 3.96, Table 4.16). Therefore, the reduction in junctional conductance may be contributed to by a unilateral increase in input resistance.

B) The effects of BAPTA-AM

BAPTA-AM (10-15μM) is a membrane permeable high-affinity free calcium chelater (Niesen *et al.*, 1991). When applied in 2 pairs subsequent to exposure to caffeine, spontaneous neuronal activity returned, first with oscillations in membrane potential, then with synchronous firing of action potentials. One SPN in each pair exhibited bursts of action potentials, the terminations of which were synchronous with action potential firing in the coupled SPN (Figure 4.13C, n=2). The coupling coefficient of current transfer increased in BAPTA-AM (in Pair A from 0.12 to 0.16, in Pair B from 0.32 to 0.42, and from 0.101 to 0.157). The coupling coefficients of the reverse direction in Pair A were not significantly different (from 0.101 to 0.105, Table 4.15). An increase in input resistance was observed in 3 of 4 neurons (in Pair A, SPN 1 from 174.6 to 180.2M Ω

and SPN 2 from 156.0 to 286.6 MΩ, in Pair B SPN 1 from 158.4 to 202.5 MΩ, note SPN 2 decreased input resistance from 628.1 to 502.1 MΩ, Table 4.15). Junctional conductance in 3 of 4 directions increased (in Pair A from 0.58 to 0.60, from 0.80 to 0.60, in Pair B from 0.52 to 0.90 and from 0.67 to 0.82) upon the addition of BAPTA-AM (Table 4.15). The possible contribution of changes in input resistance to the increase in junctional conductance and unilateral modulation of the junction were investigated by calculating the ratios for the coupling coefficients, input resistance and junctional conductance for each pair (Table 4.16). Interestingly a shift toward equality in current transfer between SPN in both pairs was observed upon the addition of BAPTA-AM. In Pair B, this was achieved by a reduction of the high ratios for both coupling coefficient and input resistance (from 3.19 to 2.69 and from 3.96 to 2.47 respectively), resulting in a junctional conductance ratio near unity (1.09 from 1.28). In Pair A the junctional conductance ratio was brought close to unity (1.01 from 1.38) by an increase in coupling coefficient and input resistance ratios (from 1.22 to 1.47 and from 1.12 to 1.49, respectively, Table 4.15). These data indicate that a decrease in internal calcium tends to drive the electrotonic junctions towards a more open state. In addition, data suggest that the electrotonic junctions may be regulated unilaterally by calcium.

C) The effects of calcium-free aCSF

A further reduction of intracellular calcium was achieved by removing calcium from the extracellular solution, thereby enhancing the electrochemical gradient for calcium ions to flow out of the cell. Within 5 minutes of nominally calcium-free aCSF being applied subsequent to BAPTA-AM, high frequency (7.25 and 2.5Hz) firing was

induced, abolishing the previous burst-like pattern of activity (Figure 4.14). Hyperpolarisation of the membrane revealed oscillations in membrane potential underlying action potential firing (Figure 4.14C). Interestingly the 2 waveforms of oscillations present in control situations were absent in nominally calcium free aCSF. Instead oscillations were smaller (7.25 ± 1.1mV) in calcium free aCSF compared to pre-response levels (14.7 ± 1.5mV and 2.5 ± 0.6mV) but were approximately of the same frequency (2.43Hz compared to 2.2Hz) as that of the control. The coupling coefficients and junctional conductances in both directions of current transfer increased (0.42 to 0.54 and 0.15 to 0.20 respectively), and in one direction increased more than the other (Table 4.15). The increased input resistance and coupling coefficient ratios in nominallly calcium-free aCSF (from 2.48 to 3.47 and from 1.09 to 1.35, respectively, Table 4.16) suggest unilateral regulation of the junctions, a feature that may impart directionality to current transfer.

4.3 Discussion

4.31 Properties of electrotonic coupling in AD-SPN

At least 75% of AD-SPN demonstrate evidence consistent with electrotonic coupling. This is most convincing when there is evidence for direct current transfer, where an action potential generated in a presynaptic cell is seen to be mirrored by an oscillation in membrane potential in the postsynaptic neuron. Oscillations typically display a biphasic waveform that consists of an initial depolarising component and a longer hyperpolarising component. This characteristic waveform arises from the electrotonic junction acting as a low pass filter, with a cut-off point at about 1Hz in SPN

(Nolan *et al.*, 1999). Hence, the rapid depolarising phase of the action potential in the presynaptic neuron becomes truncated upon transmission through the electrotonic junction and is seen as a small depolarising transient in the postsynaptic cell. By contrast, the slower presynaptic afterhyperpolarising potential is faithfully transmitted to the postsynaptic cell. These resemble oscillations in membrane potential observed in the locus coeruleus (Christie *et al.*, 1989); cerebellar cortex (Mann-Metzer and Yarom, 1999); visual cortex (Venance *et al.*, 2000); snail, *Lymnaia stagnalis* (Egelhaaf and Benjamin, 1983) and molluscs *Navanax inermis* (Levitan *et al.*, 1970) and *Tritonia diomedia* (Getting and Willows, 1973).

The presence of oscillations in membrane potential during single electrode recordings indicated the presence of an electrotonically coupled SPN. However, as the activity of individual neurons determines the degree of oscillatory activity in the network the lack of oscillations may reflect a "depressed" network in which no SPN are firing, rather than the absence of electrotonic coupling. Therefore the number of AD-SPN reported to be electrotonically coupled in this study may be an under representation.

The activation of multiple SPN axons by ventral root stimulation induces a SLD in electrotonically coupled SPN in this study, as well as previous studies (Logan *et al.*, 1996). That this biphasic postsynaptic potential is due to electrotonic coupling is indicated by several observations. Electrotonic oscillations have shorter latencies than monosynaptic PSPs and membrane polarisation was unable to reverse the oscillations. The reduction in frequency of oscillations observed at hyperpolarised potentials is likely to be a result of current spread throughout the network preventing neighbouring cells from reaching threshold. In addition the lack of isopotentiality within the network may reduce the input resistance contributing to a dampening of the excitability of individual

cells. In contrast to chemically mediated synaptic transmission, spontaneous and evoked oscillations were not blocked by removal of extracellular calcium shown here and in SPN previously (Spanswick and Logan, 1990b; Logan *et al.*, 1996). Under these conditions the calcium-activated potassium conductances that mediate the afterhyperpolarising potential will not be activated, thus reducing the afterhyperpolarising potential and the amplitude and duration of the hyperpolarising component of the oscillation (Walton and Navarrete, 1991).

The variation in oscillation size and frequency may be attributable to a number of factors; the number of neurons firing in synchrony, summation of afterhyperpolarising potentials, activation of intrinsic conductances, the properties and location of the electrotonic junctions and the influence of the coupled network. These are discussed in detail later with respect to the generation of burst firing activity.

4.32 Properties of electrotonic junctions

The unequivocable method of demonstrating the presence of electrotonic coupling by simultaneously recording from pairs of central neurons permits a characterisation of the properties of the electrotonic junction and nuances of current transfer. The strength of current transfer is indicated by the coupling coefficient. In central nervous system neurons, this may range from relatively weak (coupling ratio <0.1) to relatively strong (coupling ratio > 0.4). Within a given cell type the norm appears to be a range of coupling coefficients. For example, coupling coefficients for inhibitory interneurons in the neocortex range from 0.03 to 0.41 (Galarreta and Hestrin, 1999), while those between supraoptic nucleus neurons range from 0.05 to 0.2 (Yang and Hatton, 1988). Coupling coefficients for AD-SPN (range 0.08 to 0.43) are within the range of those from SPN

unidentified as to their target, as recorded here (range 0.14 to 0.53) and elsewhere (range 0.02 to 0.48; Nolan *et al.*, 1999).

Junctional conductance is a quantitative measure of current transfer between pairs of electrotonically coupled neurons. It assumes that neurons can be represented by a single compartment and that electrotonic junctions are located at the soma (Bennett, 1966, 1977). Extensive dendritic branching (Dembowsky *et al.*, 1985a; Cabot and Bogan, 1987; Forehand, 1990) and double-fits of exponentials to calculate tau values (Pickering *et al.*, 1991, and see chapter 3), suggest that SPN are not likely to be single compartments. In addition, the placement of electrotonic junctions may not be somatic (see Logan *et al.*, 1996). Therefore the values of junctional conductance based on such a model may be but a rough estimate of actual current transfer. Nonetheless, use of such a model yields junctional conductances ranging between 0.23 and 5.54nS in 3 pairs of AD-SPN and 6 pairs of unidentified SPN. This range extends beyond that reported previously for pairs of SPN (from 0.2 to 2.9nS, Nolan *et al.*, 1999) for reasons that remain to be determined.

In purely electrotonic neuronal circuits, rectifying junctions could allow selective transfer of current in a particular direction, a function that is fulfilled by chemical interactions at the classical synapse. Therefore rectification and also asymmetry of current transfer could add directionality and specificity to an electrotonically coupled network. These features are common in non-mammalian circuits, examples coming from preferential current transfer from the lateral and median giant fibres to the motor fibre in the crayfish (Furshpan and Potter, 1959) and also from the giant fibres to the motor fibres in the hatchetfish (Auerbach and Bennett, 1969). In both cases, rectification serves to prevent back excitation of the innervating fibres whilst still permitting mass activation

of the motor fibres. Rectifying junctions are also present in the leech, Aplysia, and horseshoe crab Limulus (see Bennett, 1977).

The equality, or property of rectification, of current transfer between a pair of neurons is reflected in ratios of the coupling coefficients. The closeness to unity of the coupling ratios in AD-SPN are indicative of non-rectifying electrotonic junctions. Indeed coupling coefficient ratios of up to 1.25 have been considered indicative of non-rectifying electrotonic junctions, evoking symmetrical current transfer between inhibitory neurons in the molecular layer of the cerebellar cortex (Mann-Metzer and Yarom, 1999). This could include 2 of 3 pairs of AD-SPN. The fact that one pair of AD-SPN exhibited substantial differences in their input resistance (as indicated by high ratios of input resistance (1.46) and junctional conductance (1.78)) could suggest an intrinsically rectifying electrotonic junction. Interestingly, the majority (5 of 6) of the other electrotonically coupled pairs of SPN (those that were unidentified as to their target of innervation) possessed coupling coefficients ratios and input resistance ratios greater than 1.3. These data indicate an inequality of current transfer (rectification) that is likely due to differences in input resistance, rather than properties of the electrotonic junction. This is supported by a closeness to unity of junctional conductance ratios. Previous studies in SPN indicate that over half of the electrotonically coupled pairs exhibited rectifying current transfer that could be attributed to the differences in input resistance between any pair (Logan *et al.*, 1996; Nolan *et al.*, 1999). To date, this is the only known report of rectifying current transfer in mammalian central neurons. Regardless of whether rectification is intrinsic to the junction or arises from differences in input resistance, its purpose is to permit preferential current transfer between cells thus giving rise to a hierarchical arrangement within the network (see Bennett, 1977).

4.33 Where are the electrotonic junctions?

The locations of the electrotonic junctions are likely to determine their impact on neuronal integration and excitability. Points of contact between two electrotonically coupled neurons have been assessed from dye fill transfers, from ultrastructural visualisation of typical gap junction profiles, from electrophysiological timing, and by computer modeling studies. In the majority of coupled neurons, it is proposed that electrotonic junctions are placed somatically or on proximal dendrites. These include dentate gyrus neurons (Dudek, 1983), neocortical neurons (Sloper and Powell, 1978), locus coeruleus neurons (Ishimatsu and Williams, 1996), spinal motor neurons (Matsumoto *et al.*, 1989; van der Want *et al.*, 1998) and GABAergic CA1 neurons in the hippocampus (Fukuda and Kosaka, 2000). In an earlier study (Logan *et al.*, 1996) it was suggested that electrotonic junctions between SPN were located on the proximal dendrites, based on a) a fast or faster latency of the SLD compared to the soma-dendritic component of the antidromic action potential, b) the identical or higher thresholds of the action potential compared to the evoked oscillation, c) simultaneous discharge of action potentials in both coupled neurons.

Recently, an axonal location for electrotonic junctions has been postulated and confirmed electrophysiologically in CA3 neurons in the hippocampus. Electrotonic junctions placed on the axon give rise to oscillations in membrane potential that consist of only an excitatory component (Bennett *et al.*, 1967; Draguhn *et al.*, 1998; Bennett, 2000). In the CA3 region, as few as 1.6 gap junctions strategically located between axons induce fast electrotonic potentials that serve to facilitate and co-ordinate highly synchronous (200Hz) activity (Draguhn *et al.*, 1998; Traub and Bibbig, 2000). The low pass filtering properties, determined by the membrane area and electrotonic junction, are

reduced for electrotonic contacts made at an axonal compared to somatic or dendritic location (see Traub and Bibbig, 2000). Therefore spikelets in the postsynaptic axon, resulting from presynaptic action potentials, have faster rise times. If the junctional conductance is large enough, spikelets evoke a postsynaptic action potential that propagates antidromically to the somata of the coupled neuron. Highly synchronous oscillatory activity is determined by the topography (axonal contacts) and the time taken for an action potential in one cell to induce a spike in a neighbouring axon (Draguhn *et al.*, 1998; Traub *et al.*, 1999; Traub and Bibbig, 2000). Axonal location of electrotonic junctions therefore may facilitate very specific functions of neuronal co-ordination and synchronisation.

This neuronal activity pattern facilitated by an axonal location for electrotonic contact contrasts dramatically to that observed in AD-SPN which consists of distinct bursting and rhythmically slow firing. Furthermore the inhibitory phase of the biphasic waveform of the SLD and spontaneous oscillations in membrane potential observed in AD-SPN corresponds to the afterhyperpolarising potential in the neighbouring cell; these are not seen in axons and therefore the electrotonic junctions can not be axonic.

4.34 Dye coupling

Dye transfer has frequently been associated with the presence of electrotonic coupling mediated by gap junctions, and after the synthesis of Lucifer Yellow it became a popular means of assessing the presence and extent of electrotonic coupling, (see Dudek, 1983). Interestingly, despite the irrefutable evidence for electrotonic coupling presented here and elsewhere (Logan *et al.*, 1996; Nolan *et al.*, 1999), no incidence of dye transfer between SPN has been reported. Throughout the experiments reported here, various dyes

were included in the patch pipette including Lucifer Yellow (molecular weight = 443, charge = -1 threshold conductance ≈ 2nS (Dermietzel, 1996)) and the fluorescent Alexa dyes which carry a net charge of –1. The size and composition of these dyes varies; Alexa 594 has a molecular weight of 759 and contains 5 conjugated aromatic rings, Alexa 480 has a molecular weight of 570 and has 3 aromatic rings while Alexa 350 has a molecular weight of 349 and contains 2 conjugated aromatic rings.

Electrotonic coupling in the absence of dye transfer has now been documented in other central neurons including the neocortex and thalamic reticular nucleus (Gibson *et al.*, 1999; Landisman *et al.*, 2002). Conversely, in motor neurons, dye coupling has been reported with a no evidence for electrotonic coupling (Chang *et al.*, 2000b). With a junctional conductance between AD-SPN as large as 4.45nS (this study), one might have expected that Lucifer Yellow could pass through the junction. It is possible that the specific connexin composition of the gap junctions confers its permeability features (Veenstra, 1996). Artificial expression of connexin proteins in osteoblast cell lines indicates that gap junctions composed of connexin 45 are less permeable to negatively charged dyes than those composed of connexin 43 (Steinberg *et al.*, 1994). Artificial expression of connexin 43 formed highly permeable junctions for all 3 Alexa dyes while those composed of connexin 26 showed selective permeability for Alexa 350 and junctions synthesised from connexin 32 were of intermediate permeability (Nicholson *et al.*, 2000). Co-expression of connexins 45 and 43 reduced dye coupling but increased electrical coupling (Koval *et al.*, 1995). Apparently, the carboxy terminal tail of the connexin molecule is important in determining both permeability and interactions with other connexins (Koval *et al.*, 1995). Of the connexins known to be present in neurons in the central nervous system, connexins 36 and 47 are abundantly expressed in the gray

matter in the spinal cord including the intermediolateral cell column (Sohl *et al.*, 1998; Teubner *et al.*, 2001). Furthermore the somata and dendrites of neurons in the spinal cord exhibit immunoflourescence for connexin 36 but not connexins 32 or 43 (Rash *et al.*, 2000). Therefore, of the known connexins, electrotonic coupling in SPN may be mediated by gap-junctions composed of connexins 36 or 47. To date, information on the permeability characteristics of junctions formed by these connexins remains to be determined.

4.35 The function of electrotonic coupling

A) Synchronisation of neuronal activity

Two attributes distinguish electrotonic coupling from its chemical counterpart: short latencies and reciprocity. Therefore it is not surprising that neuronal systems that rely on speed and mass activation /synchrony utilise electrotonic communication. Fast activation promotes survival in the escape response of hatchetfish (Auerbach and Bennett, 1969) and in the tail flip response of the crayfish where coactivation of many fibres are required (see Edwards *et al.*, 1999). In the mammalian central nervous system, the cerebellum is a site where rapid transfer of information is required to control fine co-ordinated movements. Here, electrotonically coupled neuronal networks are proposed to be involved in the synchronous inhibition of cerebellar climbing fibre input to the purkinje neurons (Mann-Metzer and Yarom, 1999) and in putative "timing" circuits in the inferior olive, a source of input to the climbing fibres (see Dermietzel and Spray, 1993). In the hippocampus, axonal gap junctions act as a signal generator for highly synchronous 200Hz oscillations (Draguhn *et al.*, 1998; Traub and Bibbig, 2000), deemed important for cognitive function. Within the spinal cord, multiple oscillators have been

proposed to mediate characteristic and highly synchronous sympathetic nerve activity (Chang *et al.*, 1999a; Chang *et al.*, 2000a). Therefore it is highly probable that electrotonic coupling can facilitate synchronous firing in AD-SPN, promoting neuronal activity relevant to the secretion of catecholamines from the adrenal medulla under conditions of urgency.

B) Burst firing neuronal activity

Reciprocity of current transfer throughout a network promotes synchrony of single action potentials (as described above) and also promotes synchronisation of bursts, particularly in cases where firing is asynchronous (Bennett, 1977). In the marine molluscs *Tritonia Diomedia* and *Helisoma* bursting is proposed to arise from mutual interactions within the coupled network (Willows *et al.*, 1973; Getting and Willows, 1974). As observed in this study, electrotonic coupling between AD-SPN facilitates the generation of complex burst firing patterns of neuronal activity that rely on synchronous firing. As one SPN is firing, the average depolarisation within the network increases thus drawing the whole network towards threshold. Upon synchronous action potential firing an enhanced and prolonged afterhyperpolarising potential inhibits all activity, producing the silent phase of the burst and the level of excitability is re-set. Therefore bursting activity in SPN is self-limiting based on reciprocity of current transfer that promotes an inherent tendency towards synchronous firing. This burst firing neuronal activity is similar to that observed utilising single electrode recordings in SPN in neonatal rat *in vitro* (Spanswick and Logan, 1990a, b; Logan *et al.*, 1996; Nolan *et al.*, 1999) adult cat *in vivo* (Mannard and Polosa, 1973) and *in vitro* upon application of noradrenaline (Yoshimura *et al.*, 1987a).

The conversion of asynchronous action potential firing into a bursting mode of activity is facilitated by an afterhyperpolarising potential that is enhanced by the existence of an electrotonically coupled network. A network-like situation can be represented by a model in which coupled neurons are placed in parallel, each with their own resistance and capacitance and a resistance representing the electrotonic junction (Figure 4.17). Such a model predicts that the input resistance of a neuron would be predominantly determined by the number of coupled neurons (parallel resistance pathways) and their coupling coefficients and not by the specific membrane resistance and capacitance of the individual neuron. If two neurons are isopotential then the current flow through the junctions would be minimal, indicated as one less current pathway in the model. This would result in an apparent increase in input resistance. Therefore during synchronous firing when the neurons are isopotential, little or no current would be flowing through the junctions and the afterhyperpolarising potential would be prolonged in both amplitude and duration, due to the increase in input resistance.

According to this model, synchronous firing and an enhanced afterhyperpolarising potential is governed by the extent of current shunt through the electrotonic junctions. Non-isopotentiality within the network creates attenuation of single neuronal membrane potentials across the electrotonic junctions. However as more SPN are recruited (via reciprocal depolarisation), synchronous firing would induce isopotentiality within the network. Isopotentiality ensures minimal current shunt across the junction and an apparent increase in input resistance would facilitate a larger afterhyperpolarising potential, ending the burst. It could be postulated that the variation of afterhyperpolarising potentials during a burst reflects varying degrees of isopotentiality in the network. In addition to the degree of isopotentiality, the number of SPN within a

network would determine the extent of current flow across the junction. Therefore the burst firing activity in SPN could arise from these regenerative electrical interactions within the network , in a similar manner to those in *Tritonia Diomedia* (Willows *et al.*, 1973; Getting and Willows, 1974). This model has inherent limitations in that it assumes equality within the network regarding coupling coefficients and input resistance and negates the contribution of the cable properties to potentials recorded. Recordings from all electrotonically coupled neurons in the network and detailed ultrastructural studies pinpointing points of electrical contact would be required to clarify and refine this model.

4.36 Calcium, electrotonic coupling and firing patterns

Previous studies indicate that internal calcium can close gap junctions (Rose and Loewenstein, 1975; Baux *et al.*, 1978; McMahon and Mattson, 1996) and artificially expressed hemichannels can be blocked by extracellular calcium ions (Zhang and McMahon, 2001). Regenerative calcium waves that pass though gap junctions are known to play a role in shaping neuronal connections in cortical and retinal circuits during development (Roerig and Feller, 2000). Spontaneous and induced regenerative calcium waves can also propagate through an electrotonically coupled network of glial cells (Verkhratsky *et al.*, 1998). Therefore in light of these studies, a precursory evaluation of a role for calcium ions in electrotonically coupled SPN was investigated.

The data presented here indicate that calcium ions regulate electrotonic coupling in SPN. That the internal calcium concentration is critical in controlling both firing patterns and the strength of electrotonic coupling between SPN is indicated by the effects of caffeine (increasing internal calcium), BAPTA-AM (decreasing internal calcium), and nominally calcium-free aCSF (further decreasing internal calcium). The endoplasmic

reticulum (or intracellular stores) houses 2 ligand gated receptors, inositol trisphosphate and ryanodine receptors, that control the release of calcium into the intracellular space (Berridge, 1998). Caffeine enhances the sensitivity of ryanodine receptors to calcium ions therefore inducing calcium release (Rousseau and Meissner, 1989). The complete cessation of spontaneous activity and decrease in coupling coefficients and junctional conductances upon addition of caffeine to SPN suggest partial closure of the electrotonic junctions. Interestingly the increase in the junctional conductance ratio suggests unilateral modulation by calcium ions giving rise to preferential current transfer; a form of induced rectification. In one pair, this rectification may be contributed to by increases in the difference of input resistances between the 2 SPN. Caffeine is known to have a number of non-specific actions at concentrations of 10mM. These include prolongation of action potential and time to peak of the slow afterhyperpolarising potential while reducing peak amplitude (Seutin *et al.*, 2000), possibly facilitated through antagonism of adenosine receptors that activate a small conductance potassium channel (Daly *et al.*, 1983). Although this may have occurred in this study, the changes in spontaneous activity coupled to modulation of coupling co-efficients and junctional conductances and the fact that these effects can be offset upon subsequent application of BAPTA-AM argue that caffeine acted primarily to raise internal calcium.

Caffeine applied at 10mM completely depletes internal stores (Sandler and Barbara, 1999; Seutin *et al.*, 2000). However as the endoplasmic reticulum is situated close enough to the plasma membrane to allow rapid refilling (see Berridge, 1998), continuous calcium induced calcium release could occur. The extent of calcium release and thus internal calcium concentrations is difficult to discern and depends on many factors outside of experimental control. For example, both the concentration of calcium

in the endoplasmic reticulum and the sensitivity of the ryanodine and inositol trisphosphate receptors are influenced by the intracellular factors that include calcium buffers, second messengers, and activation of membrane receptors.

A return to spontaneous burst firing, accompanied by increases in coupling coefficients and junctional conductance, was observed upon decreasing intracellular calcium by the addition of BAPTA-AM. Modulation of both the coupling coefficient and input resistance ratios equalised current transfer between the pairs of SPN, indicated by junctional conductance ratios close to unity. For this to be achieved the differences in input resistance on either side of the junction were compensated for by unilateral modulation of the electrotonic junction.

Burst firing gave way to high frequency firing upon removal of calcium ions from the aCSF. The accompanying rise in coupling coefficients and junctional conductance were indicative of electrotonic junction opening. Although the input resistance of each SPN fell, the input resistance ratios increased, suggesting preferential current flow between the pair. The differences in input resistance may account for the increase in junctional conductance ratio. Disregarding the mechanism, unilateral modulation in the absence of internal calcium gives rise to rectification across the electrotonic junction.

The modulation of oscillation waveform in nominally calcium free aCSF may be accounted for by equality of current spread throughout the network. In addition, the lack of activation of the calcium activated potassium conductances that mediate the afterhyperpolarising potential would dramatically shorten the interspike interval and thus oscillation frequency. Such a dramatic effect of nominally calcium free aCSF may in part be contributable to by a rebound change in intracellular pH, which is observed to alter the

incidence of dye coupling in the CA1 neurons in the hippocampus (Church and Baimbridge, 1991).

4.37 Functional implications of calcium modulation of neuronal activity

Calcium influx during the action potential is sufficient to induce calcium release from internal stores especially during sustained firing (Kano *et al.*, 1995; Shmigol *et al.*, 1995; Cohen *et al.*, 1997). Several consequences of this rise in calcium can be considered in relation to burst firing and electrotonic junction regulation.

The slow phase of the afterhyperpolarising potential of SPN comprises two calcium-dependent potassium conductances: an initial fast component sensitive to apamin, and a later component sensitive to phenylephrine and ryanodine (Spanswick and Logan, 1990a; Inokuchi *et al.*, 1993b). SK-type calcium-dependent potassium channels may mediate the fast apamin sensitive component (Inokuchi *et al.*, 1993b). BK -type calcium -dependent potassium channels may mediate the ryanodine sensitive component (Sah and McLachlan, 1991, 1992). The selective activation of those distinct calcium-dependent potassium channels in SPN may depend on the source of intracellular calcium. In the dorsal motor nuclues of the vagus and in sympathetic neurons, internal calcium that comes from high voltage activated calcium channels may activate the apamin-sensitive potassium channels while that from intracellular stores may activate the channels responsible for the late slow component (Sah and McLachlan, 1991; Jobling *et al.*, 1993). During a burst of action potentials in SPN, the rise in intracellular calcium through high voltage activated N- and P- type calcium channels (see Chapter 4) may not be sufficient to activate the slow afterhyperpolarising potential, thereby partly accounting for short duration afterhyperpolarising potentials observed during a burst. This calcium

influx could act to prime the intracellular stores. When the internal calcium concentration reaches a level sufficient to activate the ryanodine and inositol trisphosphate receptors, calcium extrusion from the intracellular could activate slow afterhyperpolarising potentials that would contribute to terminating the burst. Concurrently, a large increase in intracellular calcium might close the electrotonic junctions and, in conjunction with synchronicity within the network (isopotentiality), reduce current flow across the junctions leading to an increase in input resistance. Should intracellular calcium regulate junctional conductance preferentially in one direction, thus imparting directionality (or a heirarchical organisation) to the network, this would add on an additional level of complexity.

The properties of burst firing may be contributed to by the activation of transient outward rectification (TOR, see chapter 3). The repolarising phase of the action potential may be sufficient to release inactivation and permit activation, thus prolonging the interburst interval and the return to threshold. Therefore, differential expression and selective activation of the conductances mediating the afterhyperpolarising potential, distinct activation of intrinsic potassium conductances, and physiological modulation of any of these conductances will precisely control the afterhyperpolarising potential waveform. In addition the network (and the properties of the junctions) will integrate each neuron's activity and formulate the appropriate output (bursting) activity.

4.4 Summary

A minimum of 74% of SPN that innervate the adrenal medulla possess the criteria attributable to electrotonic coupling, identified during single electrode recording in AD-SPN and further supported by simultaneous recordings from pairs of AD-SPN. The

biphasic oscillations in membrane potential impart intrinsic pacemaker-like properties to SPN while the presence of an electrotonically coupled network facilitates synchronous firing and complex burst firing patterns. The direct connectivity between SPN in a network dictates that changes in electrical activity in one SPN will affect its neighbours. Therefore a model was proposed and confirmed whereby isopotentiality induces a reduction of current shunt throughout the network, thus enhancing the localised change in potential and transmission throughout the network. Such a mechanism may contribute to the enhanced afterhyperpolarising potential required to terminate burst firing. The importance of calcium was highlighted by changes in spontaneous activity and modifications in junctional conductance between SPN upon modulations of free intracellular calcium. Noteworthy are the data that suggest unilateral regulation of electrotonic coupling by calcium, thus bestowing directionality within the network

Figure 4.1 A comparison of the distribution of passive membrane properties of electrotonically coupled AD-SPN with the whole population of AD-SPN.

Frequency histograms summarise the distribution of passive membrane properties of AD-SPN. A, distribution of resting membrane potentials (mV) of AD-SPN. B, distribution of input resistances (MΩ) recorded in AD-SPN. Note fewer electrotonically coupled AD-SPN with high input resistances.

A

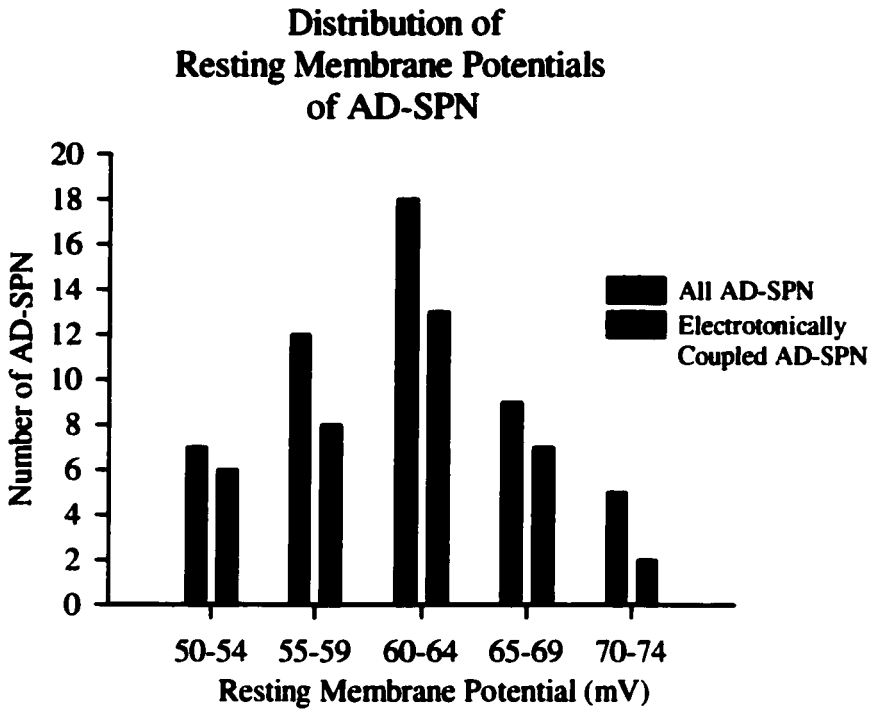
Distribution of
Resting Membrane Potentials
of AD-SPN
Number of AD-SPN
20
18
16
14
12
10
8
6
4
2
0
All AD-SPN
Electrotonically
Coupled AD-SPN
50-54
55-59
60-64
65-69
70-74
Resting Membrane Potential (mV)

B

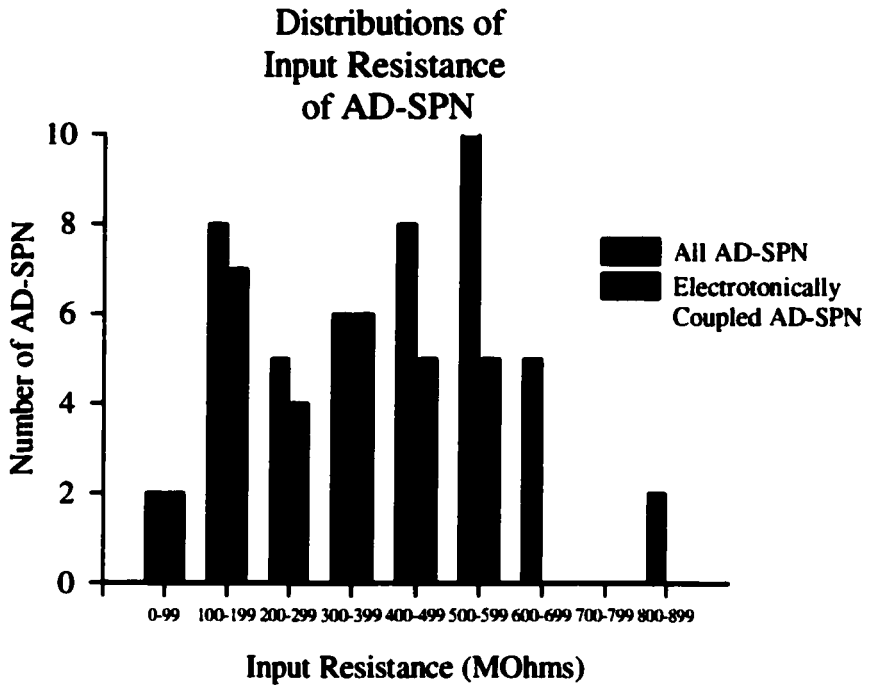
Distributions of
Input Resistance
of AD-SPN
Number of AD-SPN
10
8
6
4
2
0
All AD-SPN
Electrotonically
Coupled AD-SPN
0-99
100-199
200-299
300-399
400-499
500-599
600-699
700-799
800-899
Input Resistance (MOhms)

Figure 4.1

Figure 4.2 Characteristics of oscillations in membrane potential in AD-SPN

A, Voltage traces from the same AD-SPN. Note the spontaneous burst at resting membrane potentials (-50mV). Hyperpolarisation of the neuron (-70 mV, -80mV) by injection of constant negative current revealed spontaneous regular oscillations in membrane potential. Bi, in another AD-SPN hyperpolarisation of the membrane had little effect on the amplitude of the oscillations in membrane potential, but decreased frequency. The transient depolarising spikes are chemical potentials. Bii, an enlarged oscillation in membrane potential from the same neuron as Bi shows the characteristic "biphasic" waveform consisting of a small depolarising transient followed by a large hyperpolarising component.

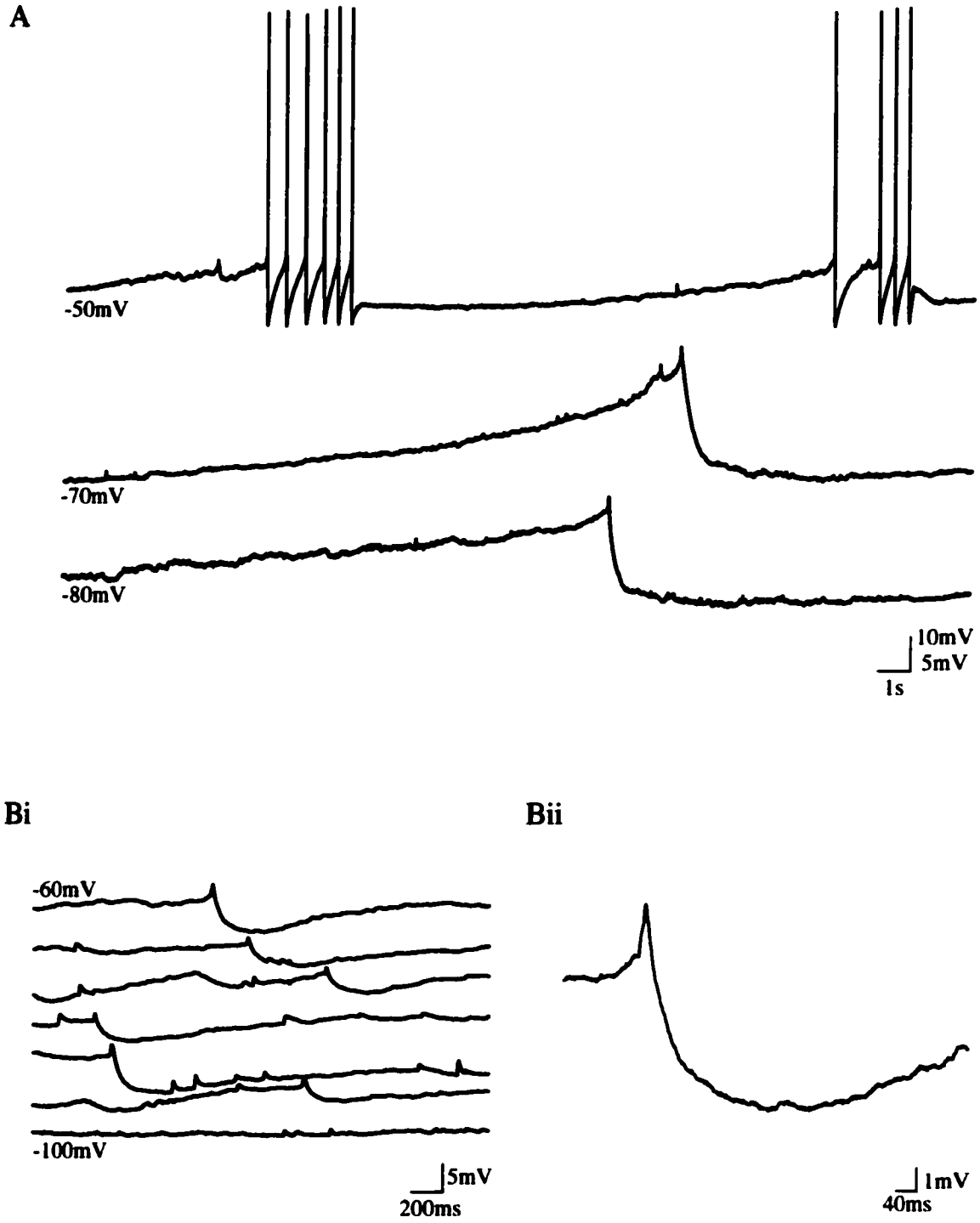
A
-50mV
-70mV
-80mV
10mV
5mV
1s
Bi
-60mV
-100mV
5mV
200ms
Bii
1mV
40ms

Figure 4.2

Figure 4.3 Antidromically evoked short latency depolarisations

A, Superimposed voltage responses to ventral horn stimulation show an antidromic spike evoked in response to a high voltage stimulation (12V) and a short latency depolarisation (SLD) evoked by a lower voltage (6V). B, In the presence of internal QX 314 (4mM), ventral horn stimulation evoked an antidromic spike immediately upon whole-cell recording. Within 5 minutes, the spike was blocked by QX 314, leaving a small biphasic component. The SLD exhibited a graded response to increased stimulus intensity (3-11V). Note the constant latencies of the SLD (B inset). C, In the presence of internal QX 314 the depolarising component of the SLD evoked by antidromic stimulation (6V) was insensitive to membrane hyperpolarisation while the hyperpolarising component was reduced upon successive membrane hyperpolarisation (range -45 to –110mV). Data from this neuron is plotted graphically in Cii.

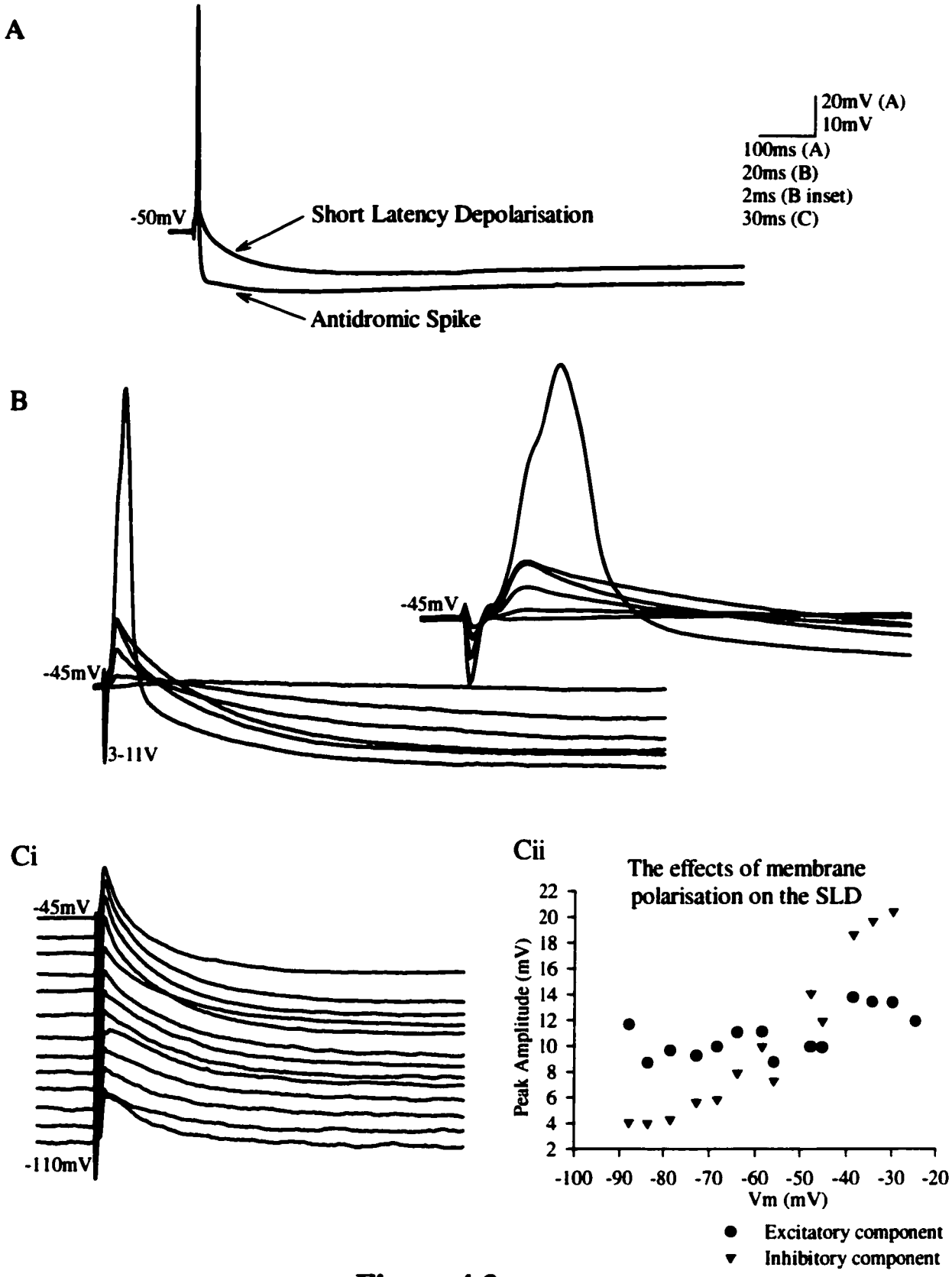
A
20mV (A)
10mV
100ms (A)
20ms (B)
2ms (B inset)
30ms (C)
-50mV
Short Latency Depolarisation
Antidromic Spike
B
-45mV
-45mV
3-11V
Ci
-45mV
-110mV
Cii
The effects of membrane polarisation on the SLD
Peak Amplitude (mV)
22
20
18
16
14
12
10
8
6
4
2
-100 -90 -80 -70 -60 -50 -40 -30 -20
Vm (mV)
Excitatory component
Inhibitory component

Figure 4.3

Figure 4.4 Strong symmetrical voltage independent coupling between AD-SPN

A, Simultaneous recordings from two electrotonically coupled AD-SPN showing bi-directional current transfer between the pair. Rectangular wave current pulses (40pA increments, -240pA to120pA, 800ms) injected into the presynaptic neuron (Ai, Aii) induced corresponding voltage deflections in both neurons. Note biphasic oscillations in membrane potential in the postsynaptic neuron corresponded to action potential firing in the presynaptic cell induced by positive current injection driving the presynaptic neuron to threshold. B, plots of the relationship between the injected current and the steady-state membrane potential response for current transfer between SPN 1 and 2 (Bi) and between SPN 2 and 1 (Bii).

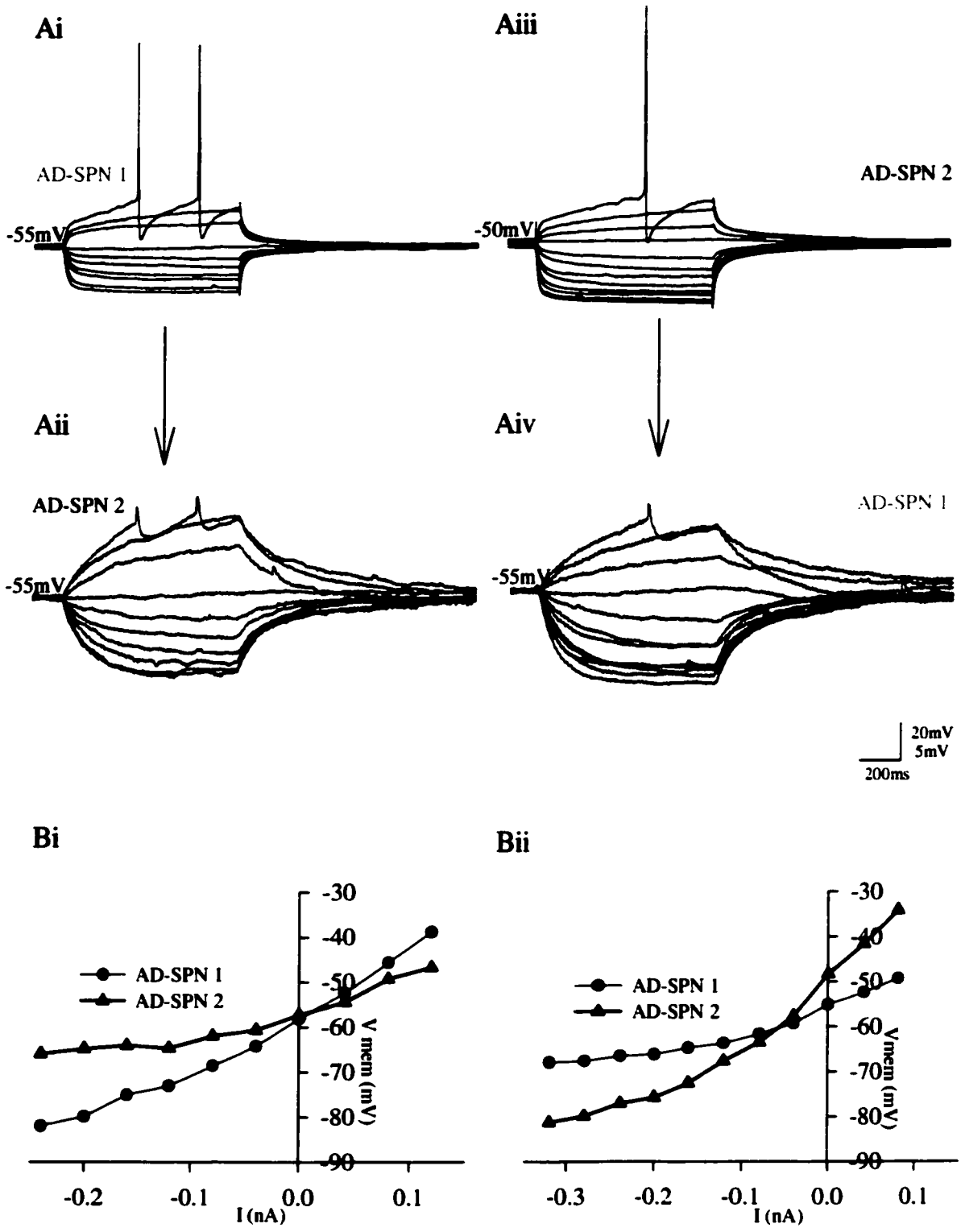
Ai
AD-SPN 1
-55mV
Aiii
AD-SPN 2
-50mV
Aii
AD-SPN 2
-55mV
Aiv
AD-SPN 1
-55mV
20mV
5mV
200ms
Bi
AD-SPN 1
AD-SPN 2
-30
-40
-50
-60
-70
-80
-90
V mem (mV)
-0.2
-0.1
0.0
0.1
I (nA)
Bii
AD-SPN 1
AD-SPN 2
-30
-40
-50
-60
-70
-80
-90
V mem (mV)
-0.3
-0.2
-0.1
0.0
0.1
I (nA)

Figure 4.4

Figure 4.5 Weak symmetrical voltage independent coupling between AD-SPN

A, simultaneous recordings from two electrotonically coupled AD-SPN showing bi-directional current transfer between the pair. Rectangular wave current pulses (20pA increments,-160pA to 20pA, 800ms) injected into the presynaptic neuron (Ai, Aiii) induced corresponding voltage deflections in both neurons. B, plots of the relationship between the injected current and the steady-state membrane potential response for current transfer between SPN 1 and 2 (Bi) and between SPN 2 and 1 (Bii).

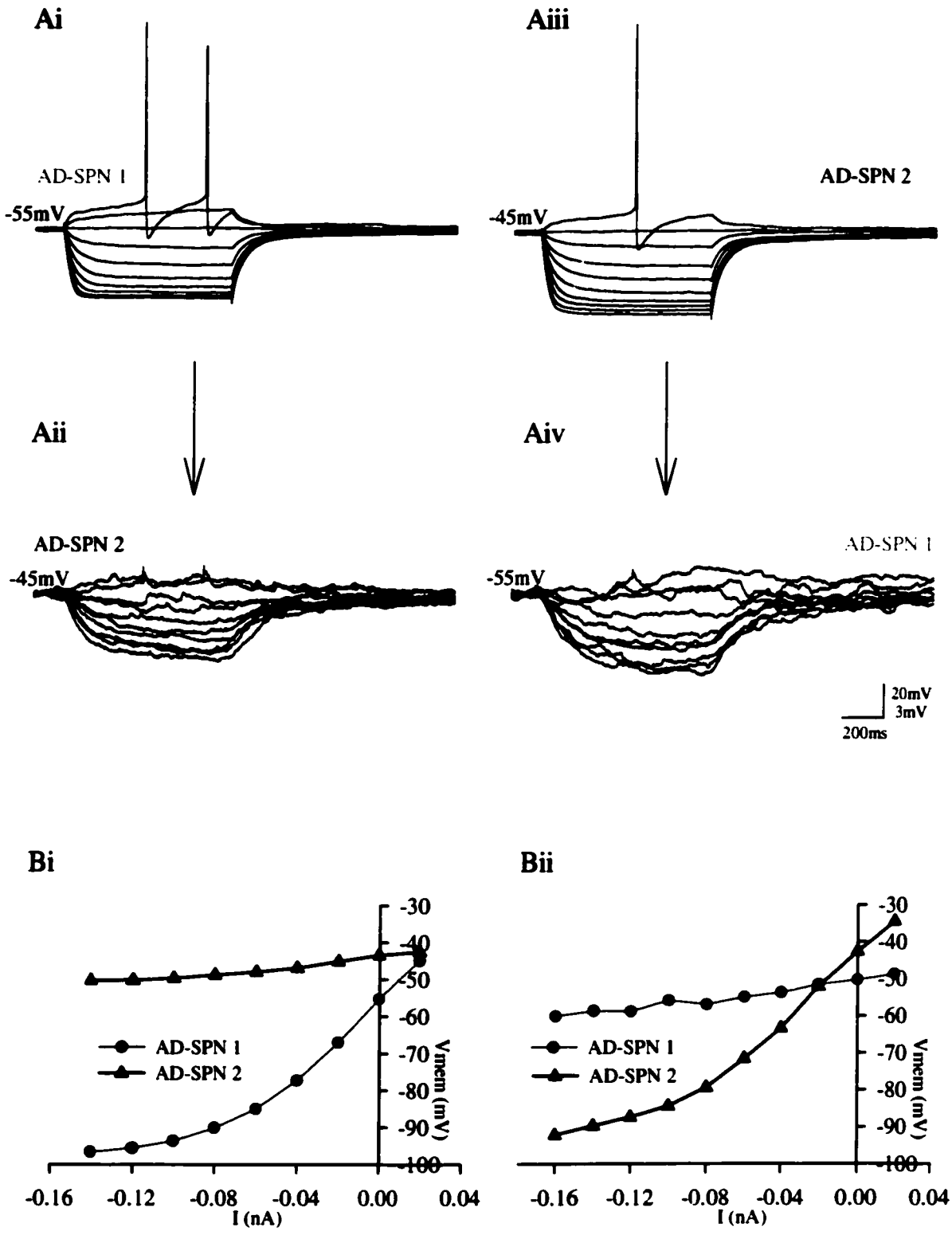
Ai
AD-SPN 1
-55mV
Aiii
AD-SPN 2
-45mV
Aii
AD-SPN 2
-45mV
Aiv
AD-SPN 1
-55mV
20mV
3mV
200ms
Bi
AD-SPN 1
AD-SPN 2
-30
-40
-50
-60
-70
-80
-90
-100
Vmem (mV)
-0.16
-0.12
-0.08
-0.04
0.00
0.04
I (nA)
Bii
AD-SPN 1
AD-SPN 2
-30
-40
-50
-60
-70
-80
-90
-100
Vmem (mV)
-0.16
-0.12
-0.08
-0.04
0.00
0.04
I (nA)

Figure 4.5

Table 4.6 Measurements of coupling coefficients, input resistance and junctional conductance and their ratios for each pair of AD-SPN

Tables show A, Coupling coefficients calculated as the ratio of the postsynaptic to presynaptic potential change. The input resistance was calculated at steady state potentials. The junctional conductance was calculated by incorporating the input resistance and coupling coefficients into a model in which the cell is represented by a single compartment joined to its neighbour by a resistance representing the electrotonic junction. B, the ratios (largest : smallest) calculated for coupling coefficients, input resistance and junctional conductance for each pair of electrotonically coupled AD-SPN. Note ratios deviating significantly from unity likely represent rectification between the pair of AD-SPN.

A

		Coupling Coefficient (k)	Input Resistance (MΩ)	Junctional Conductance (nS)
Pair 1	1→2	0.117	528.906	0.249
	2→1	0.148	474.412	0.286
Pair 2	1→2	0.415	133.429	2.501
	2→1	0.427	195.965	4.451
Pair 3	1→2	0.081	358.604	0.273
	2→1	0.079	303.317	0.225
	Average	0.211	332.439	1.331
	Stdev	0.164	153.960	1.772

B

	Coupling Coefficient Ratio	Input Resistance Ratio	Junctional Conductance Ratio
Pair 1	1.273	1.115	1.149
Pair 2	1.027	1.469	1.780
Pair 3	1.027	1.182	1.211
Average	1.109	1.255	1.380
Stdev	0.142	0.188	0.348

Table 4.6

Table 4.7 Measurements of coupling coefficients, input resistance and junctional conductance and their ratios for pairs of SPN unidentified as to their target

Tables show A, Coupling coefficients calculated as the ratio of the postsynaptic to presynaptic potential change. The input resistance was calculated at steady state potentials. The junctional conductance was calculated by incorporating the input resistance and coupling coefficients into a model in which the cell is represented by a single compartment joined to its neighbour by a resistance representing the electrotonic junction. B, the ratios (largest : smallest) calculated for coupling coefficients, input resistance and junctional conductance. Note ratios deviating significantly from unity likely represent rectification between the pair of SPN.

A

		Coupling Coefficient (k)	Input Resistance (MΩ)	Junctional Conductance (nS)
Pair 1	1 → 2	0.146	367.473	0.889
	2 → 1	0.202	177.523	0.580
Pair 2	1 → 2	0.226	210.217	0.870
	2 → 1	0.169	271.801	0.837
Pair 3	1 → 2	0.446	153.341	4.418
	2 → 1	0.522	132.394	4.536
Pair 4	1 → 2	0.532	121.101	2.694
	2 → 1	0.272	235.210	2.635
Pair 5	1 → 2	0.537	85.833	4.124
	2 → 1	0.386	157.095	5.543
Pair 6	1 → 2	0.456	84.525	3.908
	2 → 1	0.309	134.490	4.314
	Average	0.350	177.584	2.946
	Stdev	0.147	82.294	1.768

B

	Coupling Coefficient Ratio	Input Resistance Ratio	Junctional Conductance Ratio
Pair 1	1.383	2.070	1.532
Pair 2	1.337	1.292	1.039
Pair 3	1.170	1.158	1.026
Pair 4	1.955	1.942	1.022
Pair 5	1.391	1.830	1.344
Pair 6	1.476	1.591	1.104
Average	1.452	1.647	1.178
Stdev	0.266	0.365	0.212

Table 4.7

Figure 4.8 Electrotonic coupling promotes synchronous firing between AD-SPN

Traces from simultaneous recordings of a pair of electrotonically coupled SPN show single trials of membrane responses to injection of positive current pulses (SPN 1; 30pA, SPN 2; 80pA, 5s). Injection of current into the presynaptic neuron (SPN 1 in A and SPN 2 in B) evoked characteristic oscillations in membrane potential in the postsynaptic SPN. C, simultaneous injection of current pulses into both SPN facilitated synchronous firing.

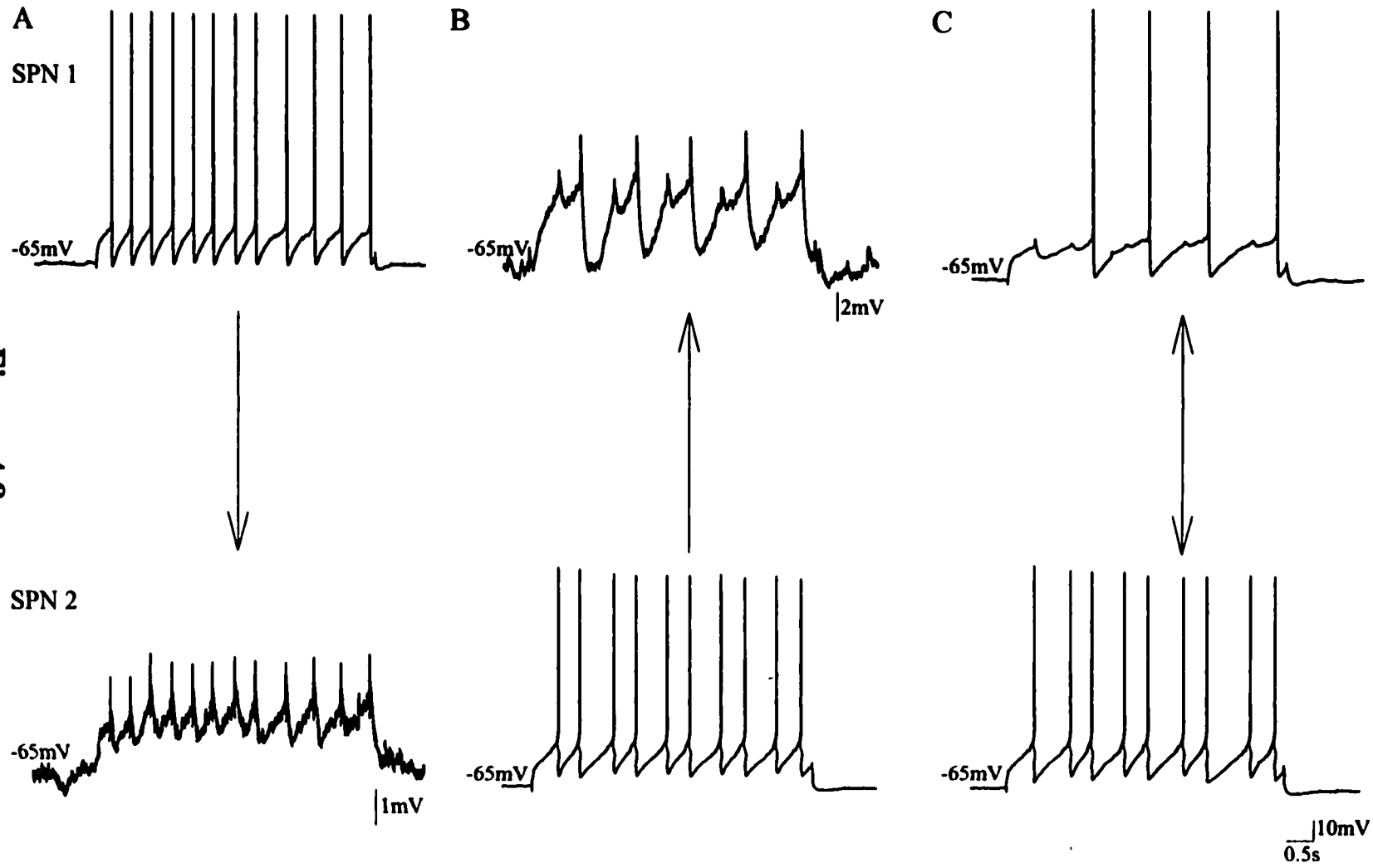

Figure 4.8

Figure 4.9 Afterhyperpolarising potentials and burst firing patterns

A, a single electrode recording from a SPN shows spontaneous firing interspersed with variable afterhyperpolarising potential waveforms. Note the oscillations in membrane potential indicating electrotonic coupling. B, simultaneous recordings from a pair of electrotonically coupled SPN show spontaneous activity. Note the synchronicity of action potential firing in SPN 1 (Bi) with termination of bursting activity in SPN 2 (Bii). Ci, afterhyperpolarising potential from SPN 1 in Bi on a faster time base. Cii, superimposed afterhyperpolarising potentials from SPN 2 taken during the burst (1. intraburst afterhyperpolarising potential) and upon termination of the burst and synchronous firing with SPN 1 (2. interburst afterhyperpolarising potential).

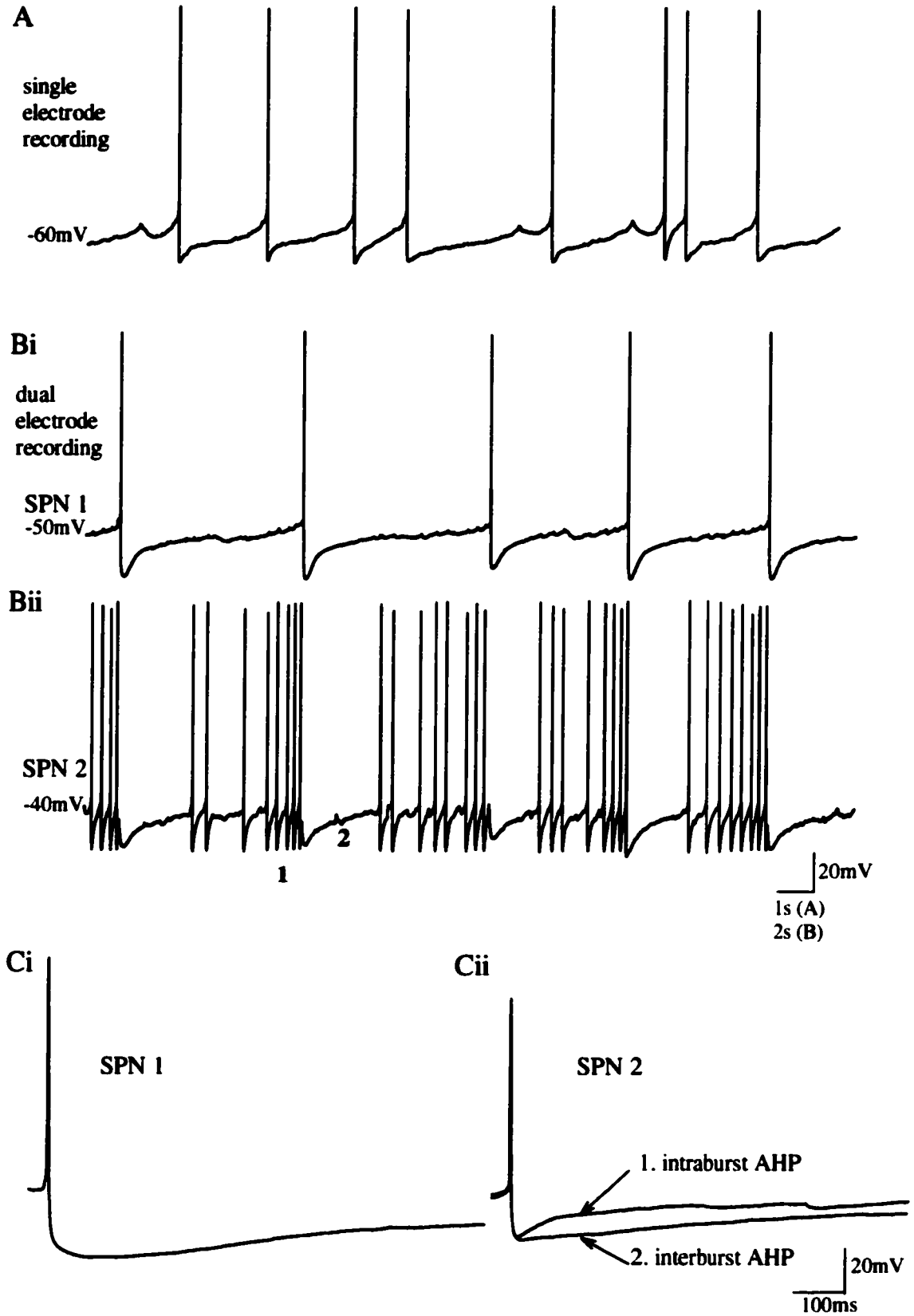
A
single
electrode
recording
-60mV
Bi
dual
electrode
recording
SPN 1
-50mV
Bii
SPN 2
-40mV
1
2
20mV
1s (A)
2s (B)
Ci
SPN 1
Cii
SPN 2
1. intraburst AHP
2. interburst AHP
20mV
100ms

Figure 4.9

Figure 4.10 Cluster analysis of the variations in afterhyperpolarising potentials in electrotonically coupled SPN.

A, plot of peak amplitude versus 90-10% decay time of the afterhyperpolarising potential from a single electrode recording of an electrotonically coupled SPN. Note a population of afterhyperpolarising potentials to the upper right of the plot with large amplitudes and long tau of decay times. B, plot of peak amplitude versus 90-10% decay time of the afterhyperpolarising potential from the pair of electrotonically coupled SPN shown in Figure 5.7B. Data fall into 3 distinct groups.

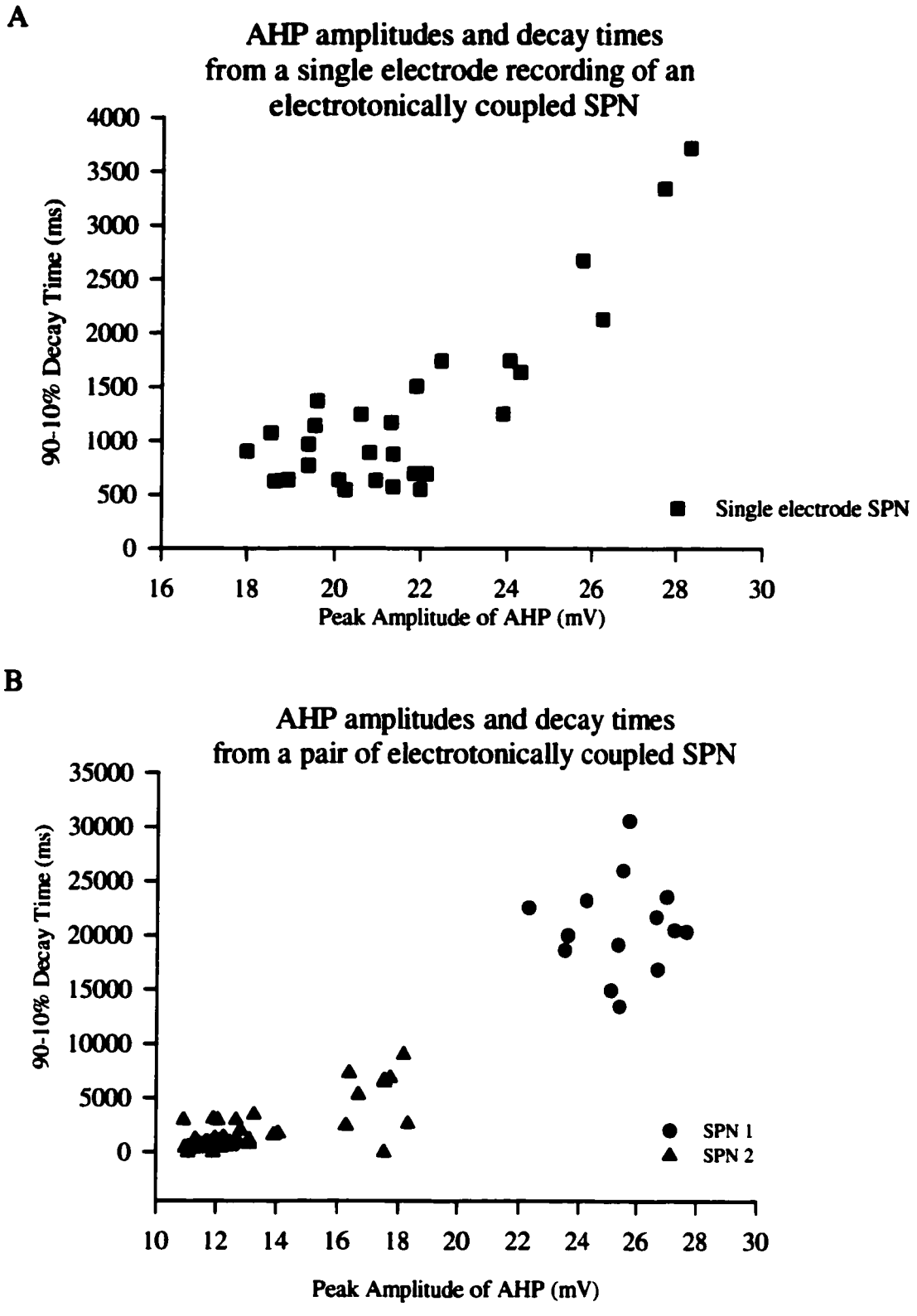
A
AHP amplitudes and decay times
from a single electrode recording of an
electrotonically coupled SPN
90-10% Decay Time (ms)
4000
3500
3000
2500
2000
1500
1000
500
0
16
18
20
22
24
26
28
30
Peak Amplitude of AHP (mV)
Single electrode SPN
B
AHP amplitudes and decay times
from a pair of electrotonically coupled SPN
90-10% Decay Time (ms)
35000
30000
25000
20000
15000
10000
5000
0
10
12
14
16
18
20
22
24
26
28
30
Peak Amplitude of AHP (mV)
SPN 1
SPN 2

Figure 4.10

Figure 4.11 Effect of membrane polarisation on input resistance in a pair of electrotonically coupled SPN

Traces show simultaneous recordings from a pair of electrotonically coupled SPN. A, superimposed voltage responses to injection of rectangular wave current pulses (20pA increments, -200pA to 40pA, 800ms, 0.1Hz) into SPN 1 held at –60mV. Note that as the postsynaptic neuron (SPN 2) is moved from isopotentiality the amplitude of voltage response decreased. B, superimposed voltage responses to injection of rectangular wave current pulses (20pA increments, -200pA to 60pA, 800ms, 0.1Hz) into SPN 2 held at –60mV. Note that as the postsynaptic neuron (SPN 1) is moved from isopotentiality the amplitude of voltage response decreased. Action potentials truncated for clarity.

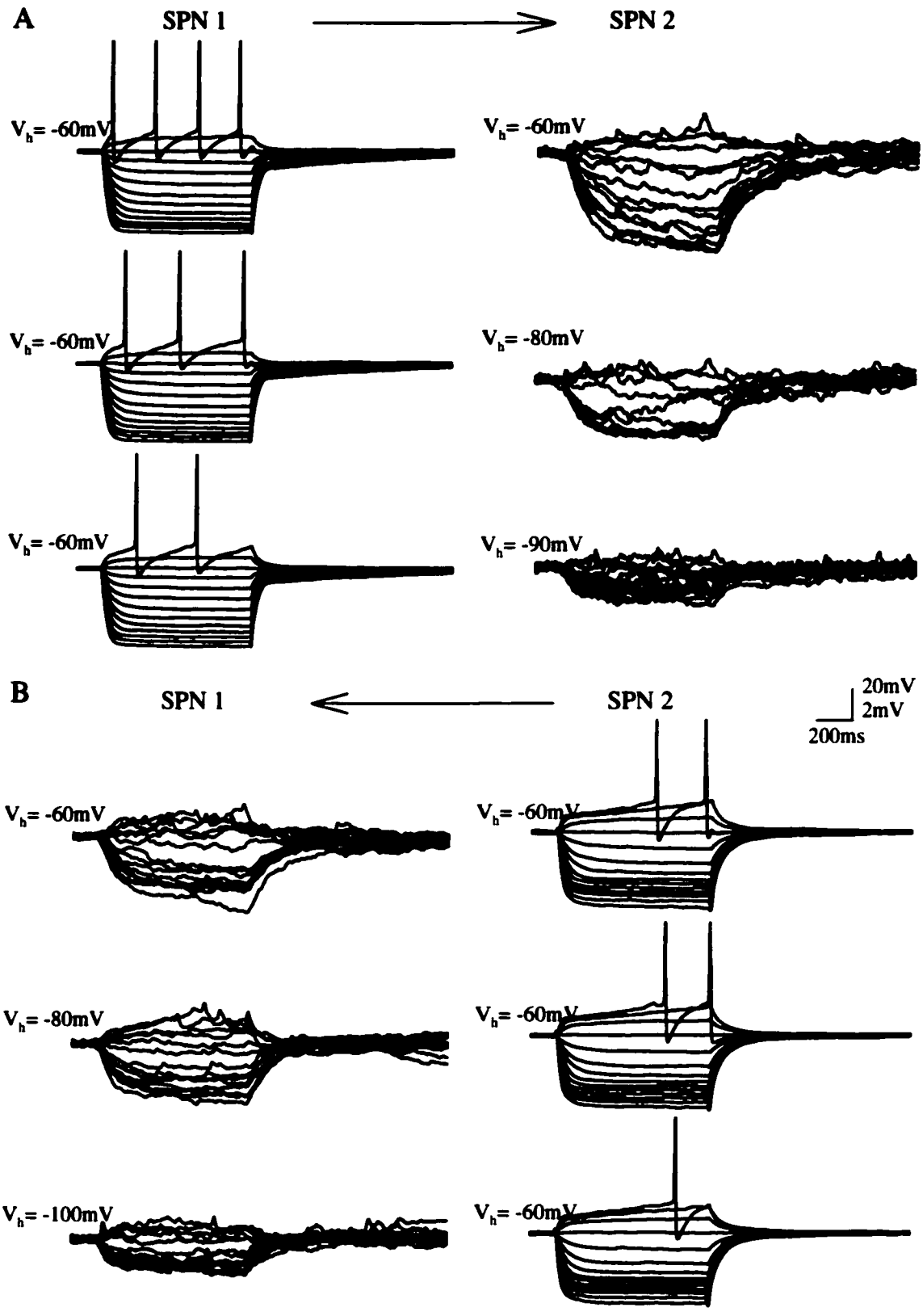
A
SPN 1
SPN 2
V_h= -60mV
V_h= -60mV
V_h= -60mV
V_h= -80mV
V_h= -60mV
V_h= -90mV
B
SPN 1
SPN 2
20mV
2mV
200ms
V_h= -60mV
V_h= -60mV
V_h= -80mV
V_h= -60mV
V_h= -100mV
V_h= -60mV

Figure 4.11

Figure 4.12 Effect of membrane polarisation on input resistance in a pair of electrotonically coupled SPN

Plots of the amplitude of voltage responses against current injection for both the presynaptic (Ai, Bi) and postsynaptic neurons (Aii, Bii) as the cells were moved away from isopotentiality. Note that the postsynaptic neurons showed a decrease in amplitude response as the membrane was successively hyperpolarised. C, superimposed voltage responses of the presynaptic neuron to current pulses (Ci, SPN 1; 40pA and Cii, SPN 2; 80pA, 800ms) when neurons were isopotential and when the postsynaptic neuron is held at –90-100mV. Note the increased voltage response upon isopotentiality.

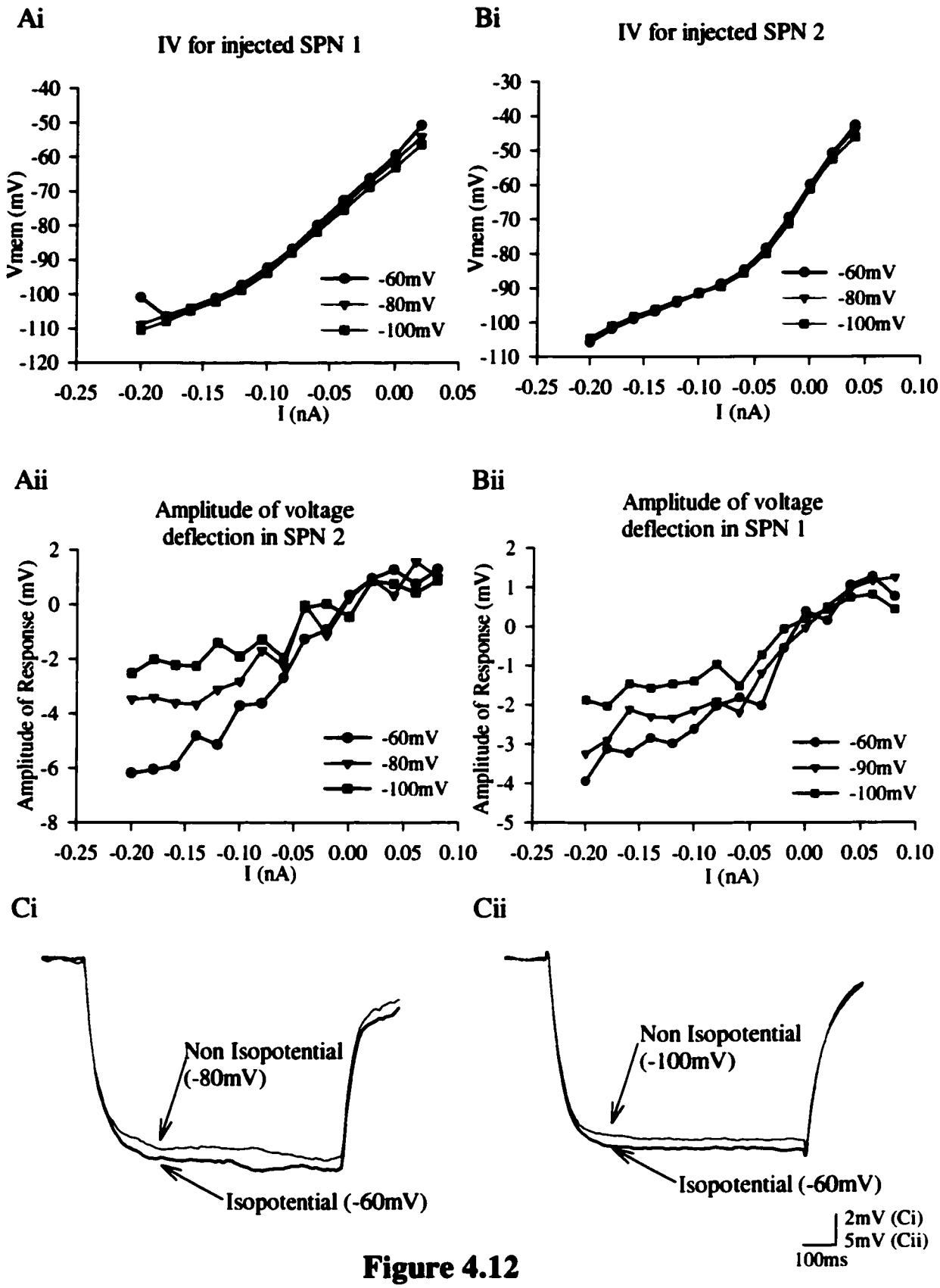
Ai
IV for injected SPN 1
Vmem (mV)
I (nA)
-60mV
-80mV
-100mV
Bi
IV for injected SPN 2
Vmem (mV)
I (nA)
-60mV
-80mV
-100mV
Aii
Amplitude of voltage deflection in SPN 2
Amplitude of Response (mV)
I (nA)
-60mV
-80mV
-100mV
Bii
Amplitude of voltage deflection in SPN 1
Amplitude of Response (mV)
I (nA)
-60mV
-90mV
-100mV
Ci
Non Isopotential (-80mV)
Isopotential (-60mV)
Cii
Non Isopotential (-100mV)
Isopotential (-60mV)
2mV (Ci)
5mV (Cii)
100ms

Figure 4.12

Figure 4.13 Effects of internal calcium concentration manipulations on spontaneous activity in a pair of electrotonically coupled SPN

Traces show samples from a continuous record of spontaneous activity in a pair of electrotonically coupled SPN. A, Control shows the presence of bursting behaviour in SPN 1 and single action potential firing in SPN 2 that is synchronous with the termination of burst firing in SPN 1. The addition of caffeine (10mM) induced cessation of spontaneous activity B, No spontaneous activity is observed in the presence of caffeine. C, The addition of BAPTA-AM (12μM) induced spontaneous activity consisting of burst firing in SPN 1 and single action potential firing in SPN 2 that is coincident with the termination of burst firing in SPN 1. This pattern of activity is similar to that of controls.

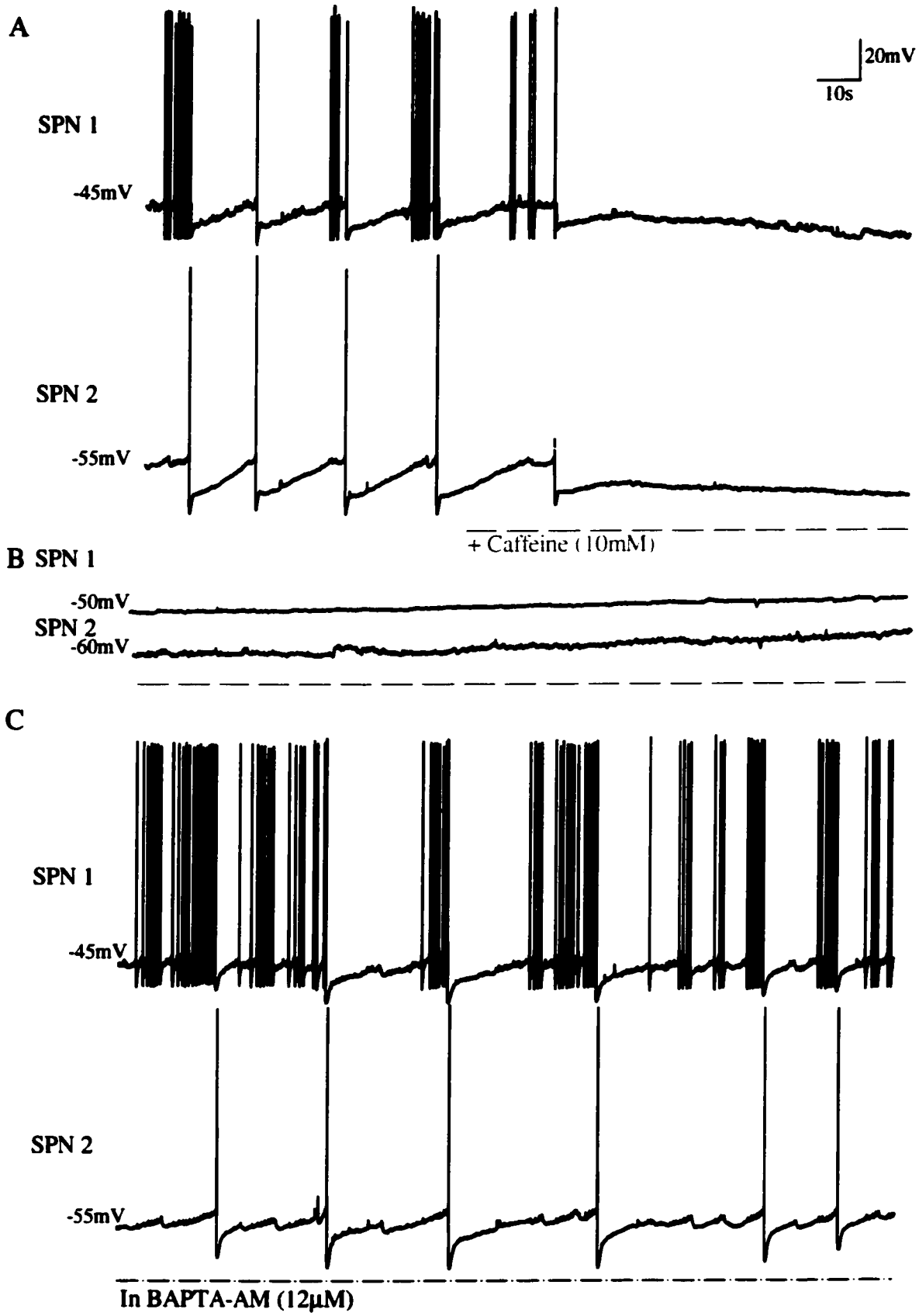
A
20mV
10s
SPN 1
-45mV
SPN 2
-55mV
+ Caffeine (10mM)
B SPN 1
-50mV
SPN 2
-60mV
C
SPN 1
-45mV
SPN 2
-55mV
In BAPTA-AM (12μM)

Figure 4.13

Figure 4.14 Effects of nominally calcium- free aCSF on spontaneous activity in a pair of electrotonically coupled SPN

Traces A and B show samples from a continuous record of spontaneous activity in a pair of electrotonically coupled SPN. A, Control shows single action potential firing in SPN 1 that is synchronous with the termination of burst firing in SPN 2. B, Upon the addition of nominally calcium-free aCSF the patterned (bursting and single action potential firing) activity is replaced by high frequency firing in both SPN. Ci, The control shows spontaneous oscillations in membrane potential revealed upon hyperpolarisation of the membrane. Note the 2 rhythms. Cii, Nominally calcium-free aCSF modulates the waveform of the oscillations. Note the loss of 2 rhythms and the loss of hyperpolarising component.

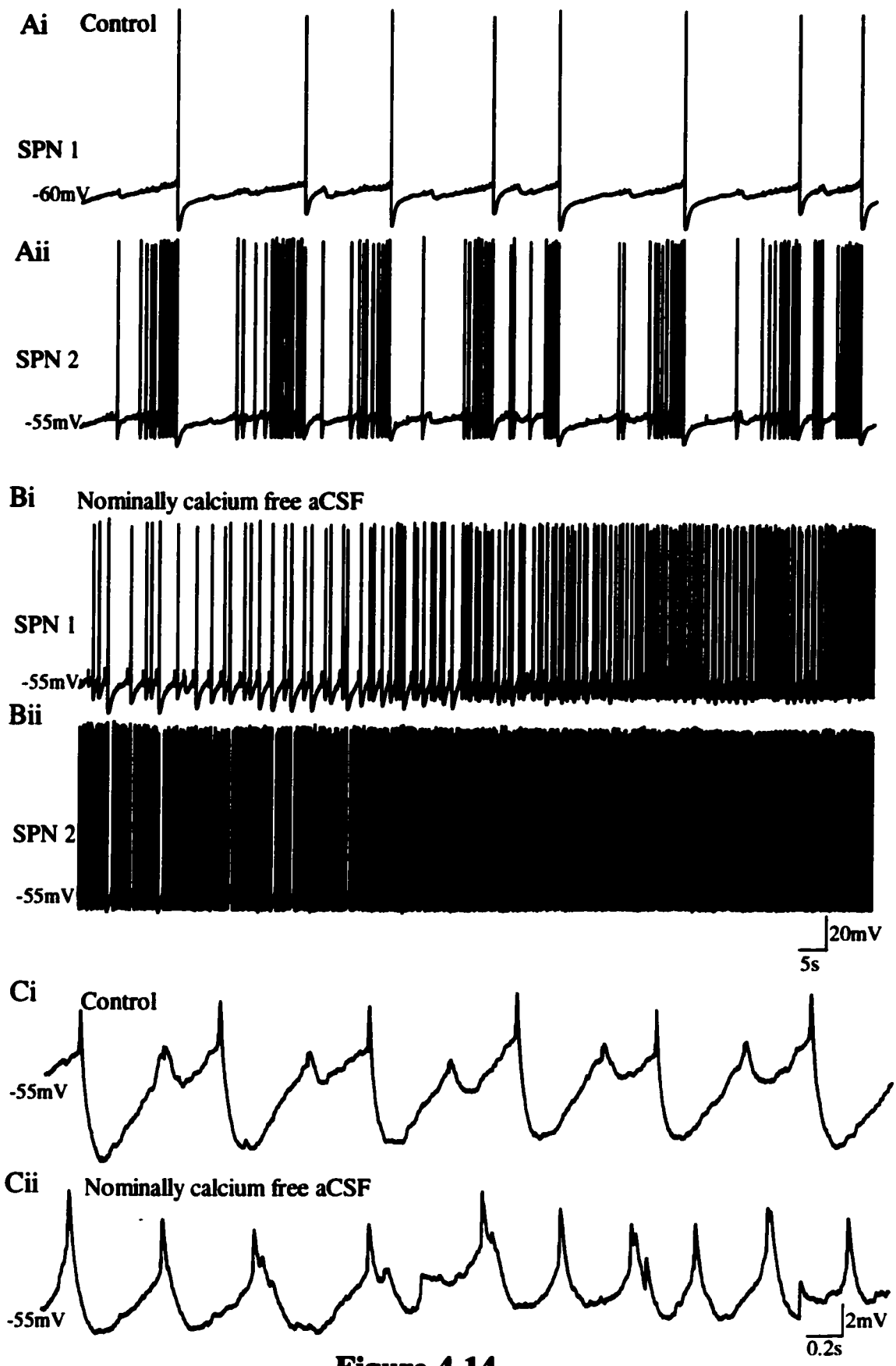
Ai
Control
SPN 1
-60mV
Aii
SPN 2
-55mV
Bi
Nominally calcium free aCSF
SPN 1
-55mV
Bii
SPN 2
-55mV
20mV
5s
Ci
Control
-55mV
Cii
Nominally calcium free aCSF
-55mV
2mV
0.2s

Figure 4.14

Table 4.15 Measurements of coupling coefficients, input resistance and junctional conductance from simultaneously recorded pairs of electrotonically coupled SPN under modified calcium concentrations

Table indicates the measurements from experiments where internal calcium was increased by the application of caffeine (10mM), decreased by the addition of BAPTA-AM (12-15μM) and decreased further by the removal of external calcium. The coupling coefficient was calculated as the ratio of the postsynaptic to presynaptic potential change. The input resistance was calculated at steady state potentials. The junctional conductance was calculated by incorporating the input resistance and coupling coefficients into a model in which the cell is represented by a single compartment joined to its neighbour by a resistance representing the electrotonic junction.

Pair A		Coupling Coefficient (k)	Input Resistance (MO)	Junctional Conductance (nS)
Control	1 → 2	0.226	210.217	0.870
	2 → 1	0.169	271.801	0.837
Caffeine	1 → 2	0.123	174.692	0.804
	2 → 1	0.101	156.003	0.584
BAPTA-AM	1 → 2	0.105	268.660	0.600
	2 → 1	0.155	180.193	0.605

Pair B		Coupling Coefficient (k)	Input Resistance (MO)	Junctional Conductance (nS)
Control	1 → 2	0.557	205.232	1.429
	2 → 1	0.170	463.200	0.889
Caffeine	1 → 2	0.323	158.457	0.528
	2 → 1	0.101	628.073	0.675
BAPTA-AM	1 → 2	0.422	202.547	0.903
	2 → 1	0.157	502.104	0.825
0mM $[Ca^{2+}]_o$	1 → 2	0.544	87.841	2.005
	2 → 1	0.201	305.173	2.711

Table 4.15

Table 4.16 Ratios of coupling coefficient, input resistance and junctional conductance measurements from simultaneously recorded pairs of electrotonically coupled SPN under modified calcium concentrations.

Table indicates the ratios (largest : smallest) calculated for coupling coefficients, input resistance and junctional conductance for each pair of electrotonically coupled SPN in Table 4.15 under different calcium manipulations.

CONTROL	Coupling Coefficient Ratio	Input Resistance Ratio	Junctional Conductance Ratio
Pair A	1.334	1.293	1.039
Pair B	3.283	2.257	1.606

CAFFEINE	Coupling Coefficient Ratio	Input Resistance Ratio	Junctional Conductance Ratio
Pair A	1.220	1.120	1.378
Pair B	3.193	3.964	1.277

BAPTA-AM	Coupling Coefficient Ratio	Input Resistance Ratio	Junctional Conductance Ratio
Pair A	1.476	1.491	1.009
Pair B	2.692	2.479	1.095

0mM $[Ca^{2+}]_0$	Coupling Coefficient Ratio	Input Resistance Ratio	Junctional Conductance Ratio
Pair B	2.712	3.474	1.352

Table 4.16

Figure 4.17 Electrical circuit modeling an electrotonically coupled network of cells. The model shows a single cell (A) electrotonically coupled in parallel to N other similar cells. R_1 and C are the membrane resistance and capacitance for each cell while R_2 is the coupling resistance. The input resistance R_{IN} for cell A at steady state potentials decreases as the number of cells (N) increases.

(from Getting and Willows, 1973, 1974)

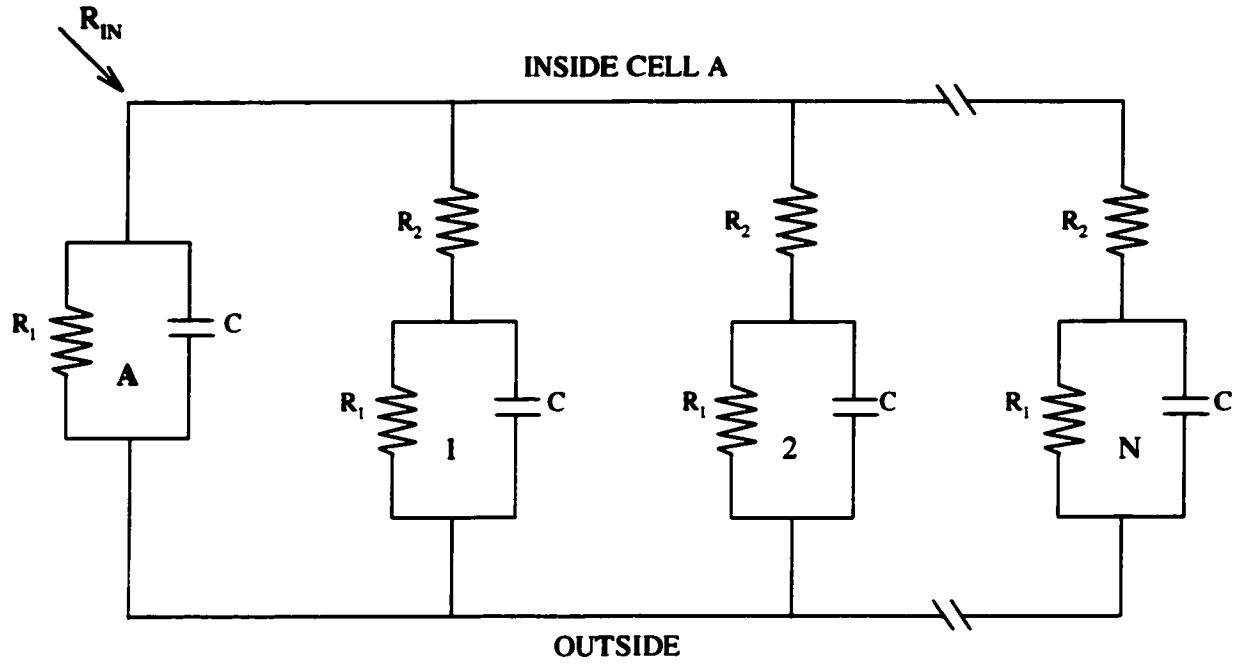

$$R_{IN} = \frac{R_1 (R_1 + R_2)}{(N+1) R_1 + R_2}$$

From Getting and Willows (1973)
Brain Research, p424-29

Figure 4.17

CHAPTER 5

DESCENDING FAST (AMINO-ACID MEDIATED) SYNAPTIC TRANSMISSION IN ADRENOMEDULLARY SYMPATHETIC PREGANGLIONIC NEURONS

5.1 Introduction

Catecholamine secretion from adrenomedullary chromaffin cells is determined by information encoded in the firing frequency and pattern of the preganglionic neuronal input. In turn, the firing patterns of AD-SPN are a reflection of neuronal excitability that is dynamically determined by both intrinsic properties, identified in the preceeding chapters, and synaptic inputs, investigated in the following chapters.

In the autonomic nervous system, the reflex firing and tonic background firing in SPNs *in vivo* in cat has been attributed to summating fast EPSPs (Dembowsky *et al.*, 1985b). Fast EPSPs evoked in SPN by electrical stimulation of the rostral ventrolateral medulla (Deuchars *et al.*, 1997) are mediated by glutamate. Stimulation of both lateral funiculi, where axons from supraspinal regions descend towards the intermediolateral cell column (Carlsson, 1964; Anderson *et al.*, 1989) and ipsilateral dorsal horn, where afferents terminate on interneurons that innervate SPN, evokes fast EPSPs that are blockable by glutamate receptor antagonists (Spanswick *et al.*, 1998). Exogenous application of L-glutamate excites SPN whether applied iontophoretically *in vivo* (Backman and Henry, 1983a) or superfused in a slice preparation (Yoshimura and Nishi, 1982; Shen *et al.*, 1990; Spanswick and Logan, 1990a; Inokuchi *et al.*, 1992c). Ultrastructural immunohistochemical studies confirm direct contact of glutamatergic

synapses, and glutaminase reactive synapses on SPN somata (Llewellyn-Smith *et al.*, 1992; Chiba and Kaneko, 1993).

There has been some controversy regarding the subtype of postsynaptic receptors mediating the fast EPSP in SPN. In rat, initial studies suggested that NMDA receptors might mediate synaptic transmission from the dorsal horn (i.e. segmental) whereas non-NMDA receptors might mediate synaptic transmission from descending sources (Shen *et al.*, 1990; Sah and McLachlan, 1995). However subsequent studies have demonstrated dual component fast EPSPs involving both NMDA and non-NMDA receptors in excitatory input from both descending and segmental sources in both neonatal rat (Krupp and Feltz, 1995; Spanswick *et al.*, 1998) and adult cat (Inokuchi *et al.*, 1992c). It remains to be seen if heterogeneity exists in the ratio of NMDA to non-NMDA receptors in any given input, a feature that could reflect target or function specificity.

Fast IPSPs can be evoked in SPN by electrical stimulation of the lateral funiculi in cat (Inokuchi *et al.*, 1992b), and in rat (Krupp and Feltz, 1993) and of the rostral ventrolateral medulla in rat (Deuchars *et al.*, 1997). GABA immunoreactivity is observed in the intermediolateral cell columns (Yoshimura and Nishi, 1982; Backman and Henry, 1983a) and in nerve terminals that contact AD-SPN initial segment axons, somata, proximal and distal dendrites (Bogan *et al.*, 1989; Cabot *et al.*, 1995; Llewellyn-Smith *et al.*, 1998). Bath application of GABA to SPN induces an inward current mediated by chloride ions (Backman and Henry, 1983a; Inokuchi *et al.*, 1992b; Krupp and Feltz, 1993). The current mediating this hyperpolarisation and the fast IPSPs evoked by lateral funiculi stimulation can be blocked by a $GABA_A$ receptor antagonist, bicuculline. This study is focussed on the $GABA_A$ receptor-mediated postsynaptic potentials evoked by

electrical stimulation of the ipsilateral and contralateral funiculi (iLF and cLF respectively) in both AD-SPN and SPN unidentified as to their target.

5.2 Results

5.21 Fast excitatory synaptic transmission to AD-SPN

All AD-SPN (n=50 of 50) and all unidentified SPN (n= 62) tested displayed fast excitatory postsynaptic potentials (EPSPs) following electrical stimulation (1 pulse, 3-11V, 5ms, 0.25- 0.1Hz) of the medial edge of the iLF and cLF. In AD-SPN, fast EPSPs evoked from both funiculi had constant rise times, graded response to increasing stimulus intensity and followed 10Hz stimulation (Figure 5.1A, C), features consistent with a monosynaptic origin. Latencies were significantly shorter on fast EPSPs evoked from the iLF than from the cLF (0.8 ± 0.3ms compared to 4.5 ± 0.6 ms, $P<0.001$, n=22, Figure 5.1Aiii). The mean rise times of fast EPSPs resulting from stimulation of both the iLF and cLF stimulation were similar (4.9 ±1.5 ms and 5.9 ± 1.1ms respectively, $P>0.1$, n=22). From holding potentials just negative to resting levels, –60 to –65mV, the peak amplitudes of fast EPSPs from the iLF and cLF were 8.7 ± 3.0mV and 5.2 ± 1.8mV respectively (n=24). The decay times of the fast EPSP were variable within both iLF and cLF ranging from 86ms to 467ms (mean iLF 234.8 ± 173.9ms, mean cLF 232.2 ± 124.5ms, mean all 215.0 ± 120.9ms, n=24). The properties of the fast EPSPs recorded from AD-SPN are summarised below in Table 5.2.

	iLF	cLF	n
Latency (ms)	0.8 ± 0.3	4.5 ± 0.6	22
Rise Time (ms)	4.9 ± 1.5	5.9 ± 1.1	22
Peak Amplitude (mV)	8.7 ± 3.0	5.2 ± 1.8	24
Tau of Decay (ms)	234.8 ± 173.9	232.2 ± 124.5	24

Table 5.2 Summary of properties of fast EPSPs evoked in AD-SPN.
Fast EPSPs were evoked in AD-SPN by electrical stimulation of the ipsilateral and contralateral funiculi (iLF and cLF respectively). Latency was calculated from the end of the stimulus artifact to the start of the rise of the fast EPSP. Rise time represents the 10-90% time to reach peak amplitude. The decay time represents the tau of decay for a single exponential fit of the decaying phase of the fast EPSP.

5.22 A Non-NMDA receptor mediated component of the fast EPSP

To address the possible role of non- NMDA receptor-mediated components of the fast EPSP, the effects of excitatory amino acid antagonists were tested on monosynaptic EPSPs evoked from both lateral funiculii. Strychnine (2μM), bicuculline (10μM) were included in the perfusate to avoid any possible contamination of the EPSPs by simultaneously activated IPSPs. D(-)-2-Amino-5-phosphonopentanoic acid (D-AP5, 10μM) was included to block NMDA receptor-mediated components. From holding potentials of -60 to -65mV the fast decaying component of the EPSP evoked from both iLF and cLF was completely blocked by the non-NMDA receptor antagonists 2,3-Dioxo-6-nitro-1,2,3,4-tetrahydrobenzo(f)quinoxaline-7-sulfonamide (NBQX, 5μM) or 6-Cyano-7-nitroquinoxaline-2,3-dione (CNQX, 10μM) in all SPN tested (n= 14 NBQX, n=6 CNQX, Figure 5.3A). This fast component was also blocked by the α-amino-3-hydroxy-5-methyl-4-isoxazole-proprionate (AMPA) specific noncompetitive antagonist 1-(4-

aminophenyl)-4-methyl-7,8-methylenedioxy-5H-2,3-benzodiazepine (GYKI) 52466 in a dose dependent manner (1-100μM, n=4, Figure 5.3B). The isolated non-NMDA receptor mediated component of the fast EPSP had a rise time of 5.4 ± 2.1 ms, peak amplitude of 5.4±1.8mV and tau of decay of 23.7±14.1ms (n=8). Upon hyperpolarisation of the membrane by injection of constant negative current, the non-NMDA receptor mediated component increased in amplitude progressively (-50 to –110mV, n=8, Figure 5.3Ci). The reversal potential, extrapolated from plots of the peak amplitude against membrane voltage was -31.6 ± 8.0mV (n=8). An example is shown in Figure 5.3Cii.

5.23 A NMDA receptor mediated component of the fast EPSP

In the presence of NBQX (5μM) to block non-NMDA receptor mediated EPSPs and bicuculline (10μM) and strychnine (2μM) to block any IPSPs, stimulation in the iLF and cLF evoked a fast EPSP with a rise time of 37.4 ± 7.7ms and tau of decay of 244.6 ± 57.8ms (n=7, Figure 5.4A). There were no differences in the rise time or decay times between iLF and cLF, therefore data were pooled. Both properties were significantly different when compared to the non-NMDA receptor mediated component ($P<0.001$). The peak amplitude of this component at holding potentials just negative to rest (-60 to –65mV) varied between 0.5 and 9.0mV (mean = 4.2 ± 2.8mV, n = 12). This component was confirmed to be mediated by NMDA receptors by its sensitivity to D-AP5 (10μM, n=8, Figures 5.4A, 5.3A).

NMDA receptors are gated by magnesium ions (Nowak *et al.*, 1984). In control aCSF, membrane hyperpolarisation resulted in a linear decrease in the peak amplitude of the NMDA-receptor mediated fast EPSP (n=8, Figure 5.5A, 5.5C). Removal of

magnesium from the aCSF altered the waveform of the NMDA component in 6 of 8 SPN tested. Since there were no significant differences in data from iLF and cLF, data were pooled. The rise time in magnesium free acCSF was faster (28.5 ± 13.7ms) than that in magnesium-containing aCSF (37.4 ± 7.7ms). This initial fast rising phase cumulated in a notch (17.8 ± 8.8mV) that could generate an action potential (Figures 5.4Ai, Bi), that was followed by a plateau (peak amplitude = 14.4 3 ± 2.5 mV, duration = 399 ± 44.2ms, Figures 5.4A, B). This plateau induced action potential firing comprising 5-7 spikes. The cessation of firing was determined by the decay phase of the PSP that, from the end of the plateau, had a tau of 841.8 ± 122.3ms (n=6). The addition of D-AP5 (20μM) completely blocked this component of the fast EPSP in magnesium free aCSF (n=6, Figure 5.4A).

The voltage sensitivity of the NMDA receptor mediated EPSP was investigated in magnesium free aCSF. In 7 of 8 SPN, the peak amplitude of the NMDA receptor meditated EPSP decreased upon successive hyperpolarisation of the membrane in magnesium free external conditions (n= 7 of 8) (Figure 5.5B, Cii).

5.24 Fast inhibitory synaptic transmission in a subpopulation of SPN

Fast IPSPs were evoked in AD-SPN (n=5) and unidentified SPN (n= 3) by low frequency electrical stimulation (1 pulse, 3-11V, 5ms, 0.25- 0.1Hz) of the fibres in the ipsilateral and contralateral funiculi (iLF and cLF respectively). Since fast IPSPs evoked in SPN from both lateral funiculi were masked by the fast EPSP (n=6 of 8), D-AP5 (10μM) and NBQX (5μM) were added to the aCSF. Fast IPSPs displayed constant rise times, a graded response to increasing stimulus intensity and no failures upon high frequency stimulation (Figures 5.6A, 5.6B), consistent with a monosynaptic origin. The

fast IPSP had a significantly shorter latency when evoked from the iLF (1.54 ±0.34 ms, n=7) compared to that evoked by stimulation of the cLF (4.55 ± 1.20 ms, n=7, P<0.01). From iLF and cLF, the mean rise time and decay times of the fast IPSPs were 16.44 ± 2.34ms and 117.11 ± 28.55ms, respectively (n=5). From resting or holding potentials close to threshold (-45 to –50mV) the peak amplitude of the fast IPSP was 4.46 ± 1.9 mV (n=5). Hyperpolarisation of the membrane induced a reversal of the fast IPSP at –58.2 ± 3.9mV (Figure 5.6C), which is close to the reversal potential for chloride ions under our recording conditions (-55mV). The fast IPSP was confirmed as being mediated by $GABA_A$ receptors by its sensitivity to bicuculline (10μM, Figure 5.6D, n=8). The application of strychnine (1-2μM) before (n=4) the addition of bicuculline had no significant effect on the amplitude of the fast IPSP.

Interestingly in the majority of SPN, held near threshold, the rebound of the fast IPSP could overshoot resting levels to evoke an action potential (Figures 5.6B).

5.25 The biphasic component and fast EPSPs

In AD-SPN that showed evidence (see Chapter 4) of electrotonic coupling, electrical stimulation (1 pulse, 3-11V, 5ms, 0.25- 0.1Hz) of the iLF and cLF could evoked a PSP that was biphasic in nature i.e. displayed both depolarising and hyperpolarising components (n = 8 iLF, n=8 cLF, Figure 5.7A). The inhibitory receptor antagonists bicuculline and strychnine had no influence on any part of the biphasic PSP. The depolarising component consisted of an initial slow rising component (rise time = 6.0 ± 1.7ms, peak = 8.7 ± 1.8mV), that displayed a notch or additional depolarising component (peak amplitude = 1.1 ±0.6mV, see Figure legend 5.7) at its peak that could

reach threshold for action potential generation. In the absence of action potential generation, fast repolarisation from the notch peak (tau of decay = 24.7 ± 9.4ms, n= 9) was followed by a hyperpolarising component (range –0.8mV to -10.6mV, mean = -4.5 ± 3.7 mV). In addition the biphasic PSP was observed rising from both the isolated NMDA receptor mediated component (Figure 5.7B) and the isolated non-NMDA receptor mediated component and could itself reach threshold for action potential.

The biphasic PSP was observed in electrotonically coupled SPN (see Chapter 5) that showed evidence of spontaneous oscillations in membrane potential (n= 10) and those that were silent (n= 7). The biphasic PSP was not present in SPN that did not show evidence of electrotonic coupling (n=16). Since oscillations in membrane potential are a result of the filtering properties of the electrotonic junction on a presynaptic action potential (see Chapter 4), the effects of increasing stimulus intensity (i.e. subthreshold and suprathreshold) on PSPs evoked from both iLF and cLF in both electrotonically coupled and putatively non-coupled SPN were investigated. In all AD-SPN low stimulus intensities evoked a subthreshold EPSP from both lateral funiculi. In 6 electrotonically coupled AD-SPN, further increases in stimulus intensity to both lateral funiculi evoked a biphasic PSP, reflecting neighbouring coupled SPN reaching threshold for action potential generation in response to synaptic input (Figure 5.7B). In "non-coupled" AD-SPN the fast EPSP reached threshold without exhibiting the biphasic potential. These data were confirmed by utilising simultaneous recording from pairs of electrotonically coupled SPN and increasing stimulus intensity to induce action potential generation in one neuron of the pair. As shown in Figure 5.7C, action potential firing is concomitant with the biphasic PSP in the coupled neuron.

Utilising simultaneous recordings from pairs of electrotonically coupled SPN, the effects of isopotentiality were investigated on the properties of the EPSP. SPN 1 was held at constant voltage while SPN 2 was moved away from the holding potential of SPN 1 (see chapter 4). A 15mV shift away from isopotentiality induced a 17.9 ± 3.0% increase in rise time, a 15.4 ± 4.8% decrease in peak amplitude and a 31.1 ± 2.4% decrease in the rate of rise of the fast EPSP (n=4).

5.3 Discussion

The data presented in this chapter indicate that AD-SPN receive monosynaptic fast synaptic input from fibres in both the ipsilateral and contralateral spinal cord. This fast synaptic transmission can be excitatory and mediated by both NMDA and non-NMDA receptors, separable by kinetics and pharmacology, or inhibitory and mediated by $GABA_A$ receptors. In addition the excitatory input may give rise to a biphasic potential that is a consequence of electrotonic coupling in SPN.

5.31 Origin of monosynaptic fibres innervating AD-SPN

A monosynaptic origin of the input from both lateral funiculi is implied by graded response to an increase in stimulus intensity, constant latencies and the absence of failures upon 10Hz stimulation. Significant differences between the latencies of iLF and cLF evoked PSPs suggest potentials from the cLF have a longer distance to travel before synapsing on SPN membrane. Similar rise times indicate that presynaptic fibres from both locations are contacting SPN at an equidistant point from the recording electrode, which presumably is at the soma. Synaptic contact on distal dendrites in the central gray

area or dendrites in the lateral funiculi area is perhaps unlikely as this would require either ipsi- or contra- lateral fibres to bypass the soma. The placement of synaptic input may determine its impact on electrical activity in the postsynaptic neuron. Therefore a somatic or proximal dendritic innervation of lateral funiculi fibres could exert autonomy over all incoming activity to SPN. Furthermore a somatic or proximal dendritic location for the fast IPSP would permit shunting (if the resting potential is above that for chloride ions) of any excitatory input that would otherwise reach threshold for action potential generation.

Higher brain regions send their axons to the spinal cord via the lateral funiculi from where they branch at right angles to send axon collaterals towards SPN in the intermediolateral cell column (Anderson *et al.*, 1989). A large proportion of these fibres decussate through the spinal gray matter to terminate in the contralateral intermediolateral cell column (Harrison, 1939; Dahlstrom, 1965; Ranson *et al.*, 1998). Fibres included in the lateral funiculi have their somata in the medulla oblongata, that includes the rostral ventrolateral and ventromedial medulla, A5 cell group, caudal raphe region, the midbrain periaqueductal gray matter and the hypothalamus, including the paraventricular nucleus and lateral hypothalamic area. Stimulation of the rostral ventrolateral medulla induces fast excitatory and inhibitory postsynaptic potentials in SPN in young neonatal rats (Deuchars *et al.*, 1995; Deuchars *et al.*, 1997). Upon spinal cord transection there is an acute loss in glutamate immunoreactivity in axon terminals in the rat intermediolateral cell column (Morrison *et al.*, 1989a; Llewellyn-Smith *et al.*, 1997a), suggesting a supraspinal origin of these fibres. Therefore it is highly likely that the fibres activated by electrical stimulation of both lateral funiculi in this study are of a supraspinal origin, possibly from the rostral ventrolateral medulla.

The lateral funiculii itself contains several discrete neuronal populations, and therefore the possibility of interneuronal innervation and activation merits attention. The lateral spinal neurons are located in the dorsal regions of the lateral funiculi throughout the spinal cord and send a predominantly ipsilateral projection to SPNs within the intermediolateral cell column of upper thoracic regions. However few terminations are noted in low thoracic regions. On the other hand, the scattered neuronal population within the lateral funiculi originating from a more ventral location in the cervical lateral funiculi innervate SPN at all thoracic levels. These neurons innervate SPN bilaterally but with an ipsilateral dominance (Jansen and Loewy, 1997). Pseudo rabies virus tracing studies indicate that both sets of neurons innervate SPN that project to the stellate ganglia and the authors state that similar results were obtained from injections to the adrenal medulla (Jansen *et al.*, 1995a). The strong innervation of AD-SPN from the cLF observed in this chapter suggests that if interneurons from the lateral funiculi were activated, they are more likely to be fibres from the scattered lateral funiculi cell group than the lateral spinal neurons. Injections of pseudo rabies virus into multiple sympathetic organs did not produce double labeled neurons in the lateral funiculi, thus precluding multiple organ innervation (Jansen *et al.*, 1995b). The lateral funiculi also contains ascending propriospinal inputs (Akeyson and Schramm, 1994) that may have been activated.

As fast EPSPs originating from the dorsal horn possess slower rise times than those from the lateral funiculi (Krupp and Feltz, 1995; Spanswick *et al.*, 1998), a dendritic point of contact for segmental input with SPN has been suggested. Were this to be the situation, somatic or proximal innervation by descending fibres could permit them to exert control over reflex segmental inputs generated at more distal dendritic sites.

5.32 A role for non-NMDA receptors in mediating the fast EPSP

The timecourse of the fast EPSP is determined by presynaptic variables, those affecting glutamate in the synaptic cleft, and the properties of the postsynaptic receptors themselves. In addition the properties of the receptors, namely affinity for the neurotransmitter, deactivation and desensitisation kinetics, will affect the EPSP timecourse. It is possible that fast inhibitory PSPs may distort the waveform of the fast EPSP, however this was unlikely in these experiments for several reasons. Firstly during experimentation it was observed that fast IPSPs were reliably evoked by placement of the stimulating electrode on the lateral edges of the lateral funiculi. The fast EPSPs recorded in AD-SPN were evoked by stimulation of the lateral funiculi at the medial border, close to the intermediolateral cell column. Secondly the rise and decay times of the fast EPSPs in AD-SPN given above are similar to those evoked in the presence of bicuculline and strychnine in SPN.

AMPA sensitive glutamatergic receptors mediate fast excitatory neurotransmission throughout the central nervous system. Differences in properties of the AMPA receptors are apparent in different functional neuronal pathways. For example hippocampal and neocortical principal neurons contain AMPA receptors that have low calcium permeability and desensitise slowly while AMPA receptors in interneurons from these same areas display high calcium permeability and desensitise rapidly (Colquhoun *et al.*, 1992; Hestrin, 1993; Jonas *et al.*, 1994). The similarity of the rise time of the isolated non-NMDA component to the rise time of compound fast EPSP in AD-SPN, suggests that all AD-SPN possess non-NMDA receptors that contribute to the fast EPSP. The decay time constant of the non-NMDA receptor mediated component in AD-SPN was relatively slow, being similar to that of principal neurons in the hippocampus and

neocortex (Colquhoun *et al.*, 1992; Hestrin, 1993; Jonas *et al.*, 1994) and is likely a reflection of the deactivation kinetics of the channels.

In AD-SPN, the non-NMDA receptor mediated fast EPSP was sensitive to antagonists NBQX, which exhibits a 30 fold selectivity for AMPA over kainate receptors (Sheardown *et al.*, 1990), CNQX, and GYKI 52466, that is highly selective for AMPA receptors (Donevan and Rogawski, 1993). A small EPSP component remained subsequent to addition of GYKI 52466. Glutamatergic receptors that are preferential to kainate activation over AMPA are documented in the central nervous system (Ozawa *et al.*, 1998), and may have a distinct role in synaptic transmission that occurs upon high frequency or "voltage" activation of their presynaptic fibres (Vignes and Collingridge, 1997; Li *et al.*, 1999). In the rat spinal cord, mRNA for subunits that comprise functional kainate receptors (GluR 5-7, KA 1, 2) are dramatically down regulated during the first 10 days of life resulting in undetectable levels in adult (Stegenga and Kalb, 2001). As the rats used in this study ranged from 11-15days it is unlikely that kainate receptors are present in the spinal cord and thus the fast EPSP remaining in GYKI 52466 is unlikely to be attributable to the activation of kainate receptors. The low sensitivity of the fast EPSP to GYKI 52466 indicates that an incomplete block of AMPA receptors can not be ruled out.

The non-NMDA receptor mediated component increased upon hyperpolarisation, as expected if the ionic conductance was mediated by both sodium and potassium ions. The extrapolated reversal potential (–30mV) was unusually low compared to that typically calculated by the Nernst equation for a mixed cation conductance (≈ 0mV). Interference of the amplitudes of the EPSPs upon membrane polarisation by the activation of the sustained outward rectifier at positive potentials and the inward rectifier

at negative potentials presents variables in distinguishing the ionic conductances by reversal potentials. In addition the presence of an electrotonically coupled network modifies the intrinsic properties, including the input resistance, of individual neurons [Getting, 1974 #775; see Chapter 4] and therefore is likely to alter the EPSP waveform, especially if synapses are located on dendrites.

5.33 AMPA receptor subunits

Functional AMPA receptors are oligomers composed of 4 or 5 subunits termed GluR1-4 that are genetically distinct (Keinanen *et al.*, 1990) and which determine the kinetics of the AMPA channel (Hollmann and Heinemann, 1994). During embryonic and developmental stages, the alternatively spliced flip form of the AMPA receptor predominates in the central nervous system, however the expression of the flop form increases from postnatal day 8 reaching adult levels by postnatal day 14 (Monyer *et al.*, 1991). As the flop rich receptors deactivate more quickly than flip rich receptors (Mosbacher *et al.*, 1994) it is likely that the AMPA receptors in SPN mediating the fast EPSP in this study are a combination of flip and flop forms. Therefore it may be expected that the time course of the EPSP will further decreases with age. However, this was out side the scope of this study. In heteromeric AMPA receptors, the inclusion of a single GluR2 subunit eliminates an otherwise calcium permeable AMPA receptor (Keinanen *et al.*, 1990; Jia *et al.*, 1996; Pellegrini-Giampietro *et al.*, 1997) and induces an outward rectifying channel from otherwise strong inward rectifying channels (see Hollmann and Heinemann, 1994). SPN from T_8 spinal cord areas are heterogenic regarding the expression of AMPA receptor subunits, with 92% of SPN immunoreactive for GluR1, 63% for GluR2 and 85% for GluR2/3 (McNair *et al.*, 1998). The presence of GluR4 in

the intermediolateral cell column has been debated (Tachibana *et al.*, 1994; McNair *et al.*, 1998; Grossman *et al.*, 1999). As a result, it is likely that a proportion of SPN contain outward rectifying AMPA receptors that are calcium impermeable. However as individual SPN possess different levels of each subunit, the composition of receptors the properties of EPSP waveform are likely to be hetergeneous.

It would be interesting to determine whether differences in subunit expression reflect SPN function, or even a subpopulation within a functional group that is activated in response to physiological stimuli of a particular kind. Indeed SPN partake in chemical specific pathways (Janig and McLachlan, 1992b) and calretinin is found in a subpopulation of AD-SPN projecting to the adrenal medulla, namely those projecting to noradrenergic containing chromaffin cells (Edwards *et al.*, 1996).

5.34 A role for NMDA receptors in mediating the fast EPSP

Co-localisation and co-activation of NMDA and AMPA receptors at central synapses has been documented (Jones and Baughman, 1988, 1991; Clements *et al.*, 1992). Indeed AMPA receptor activation is thought to be necessary to induce sufficient depolarisation to relieve the magnesium block of NMDA receptor channels to allow calcium and sodium influx (see Ozawa *et al.*, 1998). Furthermore this lends the NMDA receptor the properties to function as a coincidence detector of both pre- and post-synaptic activity. Interestingly, in AD-SPN, the NMDA receptor mediated component could be evoked both in the presence and absence of non-NMDA receptor activation.

In many areas of the central nervous system postsynaptic responses mediated by the activation of NMDA receptors have slower rise and longer decay times than that mediated by AMPA receptors (Hestrin *et al.*, 1990b; Keller *et al.*, 1991). This is also true

in AD-SPN. In AD-SPN, the fast activation of the non-NMDA component masks the slower activation of the NMDA component while the tau of decay of the NMDA receptor mediated component determines the decay of the compound EPSP evoked in AD-SPN. However the absence of a slow decaying potential does not exclude the presence of NMDA receptors since they may be blocked by external magnesium ions at resting membrane potentials (Nowak *et al.*, 1984 and see below).

The variability in peak amplitude of the NMDA receptor mediated component of the fast EPSP in SPN may indicate a differential contribution to the compound EPSP at resting potentials. The long tau of decay of the NMDA receptor mediated EPSP is determined by the high affinity binding of glutamate to the NMDA receptor resulting in prolonged binding, during which time the channel can open repeatedly (Hestrin *et al.*, 1990a; Lester *et al.*, 1990; Lester and Jahr, 1992). In addition the decay time is determined by desensitisation of the NMDA receptor (see Mayer, 1995). Furthermore particular expression of NMDA receptor subunits has been linked to differential expression of the forms of desensitisation (Monyer *et al.*, 1992; Krupp *et al.*, 1998). Therefore the time course of the EPSP in AD-SPN can be precisely controlled by both the intrinsic properties of the channel and also by external factors, detailed below.

5.35 Magnesium block of the NMDA receptor

The NMDA receptor channel exhibits unusual voltage sensitivity that is a consequence of a physiological block by magnesium ions (Nowak *et al.*, 1984), the extent of which is subunit specific. In the central nervous system, the removal of magnesium ions is required to activate the NMDA receptor, however in AD-SPN neurons a fast EPSP is evokable in extracellular magnesium. That the fast EPSP decreases with

hyperpolarisation of the membrane is typical of magnesium ion block. Magnesium ions act on an asparagine site deep within the channel pore (Nowak *et al.*, 1984; Ascher and Nowak, 1988), functioning as an open channel blocker, inducing rapid channel flickering between open and closed states, that may be responsible for the regenerative depolarisations associated with NMDA receptor activation (MacDonald *et al.*, 1982). In AD-SPN the absence of magnesium ions altered the waveform of the NMDA receptor mediated fast EPSP considerably, with faster rise times, depolarised plateaus that facilitated spiking and longer decay times. At hyperpolarised potentials fast EPSPs comprised several peaks.

In this study, the NMDA mediated component of the fast EPSP displayed voltage dependence even when magnesium was removed from the extracellular medium. Factors including an intracellular block of NMDA channels by magnesium ions (Johnson and Ascher, 1990), incomplete removal of external magnesium ions and the presence (or absence) of physiological modulatory molecules of the NMDA receptor (i.e. glycine, calcium, zinc, protons, D-serine, polyamines, nitric oxide) may contribute to the results observed here.

5.36 NMDA receptor subunits

Molecular cloning techniques have revealed the diversity of NMDA receptor subunits, with distinct properties, regulation and distribution, that are both developmentally and functionally controlled. In rat, 3 subunits families are identified to contribute to NMDA receptors; NMDA R1, NMDA $R2_{A-D}$, and NMDA R3, although the latter is believed to be developmentally down regulated. In the spinal cord NR1 mRNA was particularly abundant in comparison with the minimal amounts of mRNA for NR2

subunits (Tolle *et al.*, 1993; Watanabe *et al.*, 1994; Grossman *et al.*, 2000). Discrepancy exists with regard to exactly which of the NR2 subunits are expressed, with mRNA for $NR2_D$ in the lumbar region (Tolle *et al.*, 1993), $NR2_A$ and $NR2_B$ in SPN in the intermediolateral region (Grossman *et al.*, 2000), and $NR2_A$ in the cervical spinal cord (Watanabe *et al.*, 1994) being reported. The NR2 subunits are subject to developmental down regulation with only $NR2_A$ remaining after postnatal day 7 (Watanabe *et al.*, 1994). These studies agree however on the minimal amounts of NR2 subunit mRNA present, being just above background levels. Therefore it is possible that hitherto undescribed NMDA receptor subunits exist, or that NMDA receptors are composed of unique homomers of NR1 in the spinal cord.

Functional receptors composed of heteromeric NMDA receptor subunits are diverse in their magnesium, glutamate and glycine sensitivities. These shall be very briefly considered here. $NR2_A$ and $NR2_B$ subunits in conjunction with NR1 produce high conductance (40 –50pS), high magnesium sensitive channels (Monyer *et al.*, 1992; Stern *et al.*, 1992). In addition $NR2_B$ and especially $NR2_A$ when combined with NR1 produce channels that are subject to enhancement of calcium influx by protein kinase C (Kutsuwada *et al.*, 1992) and are implicated in long term potentiation. The NR1 itself contributes (via a single site containing an asparagine residue) to the calcium influx and calcium block, proton sensitivity and magnesium block conferred upon the channel and also determines the potency of the co-agonist glycine. Conversely, block by internal magnesium is independent of subunit expression (Li-Smerin *et al.*, 2000). The NR2 subunits determine the decay time constants which range from 120ms to 4800ms for $NR2_A$ to $NR2_D$. Therefore a wide range of distinct properties of the NMDA receptor channel may be determined by its subunit composition.

5.37 The neurotransmitter

It is commonly acknowledged, and often assumed, that L-glutamate is the primary ligand for NMDA, AMPA and kainate receptors. Within the intermediolateral cell column spontaneous efflux of L-aspartate was half that compared to glutamate, however field stimulation induced aspartate efflux that was double that of glutamate (Inokuchi *et al.*, 1992c). Furthermore aspartate excites SPN equally to and in a subpopulation preferentially to glutamate (Backman and Henry, 1983b). Therefore the release of L-aspartate, being considered to be a relatively pure NMDA receptor agonist (Patneau and Mayer, 1990), could select the activation of NMDA receptors and while increasing membrane excitability in its own right could also prime the neuron for further input. Several other endogenous molecules are known to activate NMDA receptors in the central nervous system, including N-acetylaspartylglutamate which is localised to cholinergic, glutamatergic, GABAergic, noradrenergic fibres and is released in a calcium dependent manner (Coyle, 1997), L-cysteinesulfinic acid, L-homocysteic acid while the neuromodulators and coagonists zinc, D-serine, glycine present and for AMPA/KA receptors, quisqualate and domoic acid are potential ligands.

5.38 NMDA versus non-NMDA receptor mediated fast EPSPs

From the data presented here, it is concluded that all AD-SPN receive a bilateral descending fast EPSP that is mediated by non-NMDA receptors, in particular AMPA receptors. The fast EPSPs with long (>50ms this study, >120ms, see Ozawa *et al.*, 1998) tau of decay, is likely to indicate the presence of a NMDA receptor mediated component in these AD-SPN. As shown here the NMDA component is subject to considerable block by magnesium ions at resting potentials, therefore it is possible that AD-SPN with short

tau of decay times do express a NMDA receptor mediated component. A similar situation occurs in the hippocampus where NMDA receptors contribute little to the EPSP at resting levels but are revealed upon high frequency stimulation, depolarisation or magnesium free conditions (Collingridge and Lester, 1989). Utilising the technique of reverse transcriptase-polymerase chain reaction (RT-PCR) at a single cell level would give insight into the mRNA synthesised by the neuron for specific glutamatergic subunits.

Visceral input destined for SPN enters through the dorsal roots and involves a multisynaptic pathway. An exclusive role for NMDA receptor-mediated excitation has been proposed for this pathway (Shen *et al.*, 1990). However a monosynaptic pathway from the dorsal horn has a dual component EPSP consisting of both NMDA and AMPA/Kainate receptors (Krupp and Feltz, 1995; Spanswick *et al.*, 1998). Similar discrepencies in the literature exist with regards to the receptors mediating the fast EPSP from the lateral funiculii. An exclusive role for AMPA/KA receptors has been suggested (Shen *et al.*, 1990), however the majority of reports indicate that this pathway is likely to be mediated by both NMDA and AMPA/KA receptors (Inokuchi *et al.*, 1992c; Krupp and Feltz, 1995; Spanswick *et al.*, 1998; this study). Such differences may arise from the diversity of location of recording (upper thoracic spinal cord (Sah and McLachlan, 1995), T_2-T_3 (Inokuchi *et al.*, 1992c), SPN projecting to the superior cervical ganglion (Spanswick *et al.*, 1998)), species (rat (Krupp and Feltz, 1995; Sah and McLachlan, 1995; Spanswick *et al.*, 1998) and cat (Inokuchi *et al.*, 1992c)) and age (adult (Inokuchi *et al.*, 1992c) or neonate (Krupp and Feltz, 1995; Sah and McLachlan, 1995; Spanswick *et al.*, 1998)). The widely differing affinities of the NMDA and AMPA receptors for glutamate could ensure differential activation (Patneau and Mayer, 1990).

These data are likely to represent the basic picture of fast excitatory synaptic transmission to SPN. Added complexity may arise in the form of species differences, developmental and differential regulation, and activity induced modulation of expression of subunits within each receptor. Finally it is interesting to speculate whether the target organ of innervation, and thus function, of SPN may dictate differences in receptor compositions. Indeed that AD-SPN receive more glutamatergic inputs (2/3) than those projecting to the superior cervical ganglion (1/2) (Llewellyn-Smith *et al.*, 1998) and that chemical coding of the basis of sympathetic function (Holets and Elde, 1982; Janig and McLachlan, 1992a, b) is apparent, enhances this possibility.

5.39 Fast inhibitory synaptic transmission

A bilateral descending monosynaptic fast inhibitory postsynaptic potential is present in a subpopulation of AD-SPN. Stimulation of both ipsi- and contra- lateral funiculi evoked a monosynaptic fast IPSP mediated by an influx of chloride ions through $GABA_A$ receptors. Therefore it is likely that GABA is the neurotransmitter released from the presynaptic terminal. Interestingly, when the SPN is near threshold, the decay phase of the fast IPSP over shoots to evoke an action potential. In this manner the response mediated by GABA may in fact serve to evoke delayed firing therefore in these circumstances could be considered excitatory. As the placement of the stimulating electrode is crucial in evoking the fast IPSP and that often it was masked by fast EPSPs the number of AD-SPN that receive this input may be higher than data indicate here.

GABAergic interneurons are present in the spinal cord, primarily in the dorsal horn (Todd and Sullivan, 1990). However studies utilising transynaptic viral tracers argue against these fibres directly innervating SPN (Cabot *et al.*, 1994), although *in vivo*

studies suggest a role for spinal GABA (Lewis and Coote, 1996). The absence of spontaneous GABAergic potentials in a transverse slice (Dun and Mo, 1989; Krupp and Feltz, 1993) compared to an *in vivo* preparation (Backman and Henry, 1983a), is likely due to severance of supraspinal descending GABAergic fibres. Indeed morphological data suggest prominent descending GABA input to AD-SPN (Bacon and Smith, 1988). Therefore GABA may come from a descending source (Krupp and Feltz, 1993).

The source of GABAergic innervation to SPN is likely to be from the rostral ventrolateral medulla, similar to the IPSPs present in unidentified SPN in neonatal rats of 2-5 days age (Deuchars *et al.*, 1997). However recent *in situ* hybridisation studies indicate that spinal projecting GABAergic neurons were located in very restricted areas of the rostral ventrolateral medulla, including the caudal part of the solitary nucleus, the parasolitary nucleus, the vestibular nuclei, the ventral medial medulla, the raphe nuclei, and parapyramidal area (Stornetta and Guyenet, 1999). In addition, studies utilising the technique of single cell RT-PCR have indicated a distinct lack of glutamic acid decarboxylase and the GABA transporter 1 in neurons located in the rostral ventrolateral medulla (Comer *et al.*, 1999). Therefore, the rostral ventrolateral medulla may a send a small proportion of GABAergic containing fibres to the spinal cord. In theory other supraspinal centres may also contribute to this projection, however very little is known about these.

Nineteen different mammalian subunit genes (α_{1-6}, β_{1-4}, χ_{1-3}, δ, ε, π and ρ_{1-3}) have been identified for $GABA_A$ receptors (Barnard *et al.*, 1998) with alternative splicing increasing diversity and conferring unique biophysical and pharmacological properties upon the receptor (Macdonald and Olsen, 1994; Haas and Macdonald, 1999). Neurons in the spinal cord express at least 4 α subunits, while β_3 and χ_3 are ubiquitously expressed

(Macdonald and Olsen, 1994). Mature motorneurons in the rat ventral horn contain $\alpha_2\beta_3\chi_2$ transcripts while dorsal horn neurons coexpress the $\alpha_3\beta_3\chi_2$ transcripts (Ma *et al.*, 1993). The data from Ma *et al.*, (1993) show little immunoreactivity for α_2 or α_3 mRNA, however GABA immunoreactivity is shown throughout the intermediate gray region. Despite the focus of their study at cervical levels of the spinal cord, these data suggest that SPN may utilise α subunits other than α_2 or α_3. The receptor subunits specific to each neuronal type may confer unique properties adapted to the purpose and function of that neuron.

5.40 The effect of electrotonic coupling on chemical synaptic input

In AD-SPN the biphasic PSP is a result of the low pass filter properties of the electrotonic junction filtering the action potential and ensuing afterhyperpolarising potential throughout the network, which is superimposed on the subthreshold fast EPSP. This was indicated by single electrode recordings and confirmed by dual recordings. That the timing of an action potential resulting from synaptic input can be signaled throughout a network (in the form of a biphasic PSP) provides transient synchrony, amplification of the incoming input and, as a result of the filtered afterhyperpolarising potential, overrides individual neurons synaptic activity. Indeed as more SPN fire action potentials the afterhyperpolarisation will be enhanced, partly due to a decrease in input resistance (Chapter 4) and possible summation, inducing a larger hyperpolarising phase of the biphasic PSP. This may prevent temporal summation of further synaptic input. On the other hand, the depolarising notch provides a window of high excitability in which summation would induce action potential firing and bursting.

As demonstrated in chapter 4, an electrotonically coupled network can act as a current shunt influencing input resistance and timecourse of membrane potentials in individual neurons. Furthermore the coupled network modulated the properties of synaptic potentials. The membrane potential within the network affects the rise times of the fast EPSPs; when SPN are isopotential the rise times are faster than if a potential difference exists. This may partly be due to an increase in input resistance and less current shunt at isopotentiality. The initial fast rising phase of the action potential transmitted from the coupled SPN may also contribute to the increased fast EPSP rise time calculated here.

5.5 Summary

AD-SPN receive descending fast synaptic input from both sides of the spinal cord. Synaptic input can be excitatory, mediated by both NMDA and non-NMDA receptors, inhibitory, mediated by $GABA_A$ receptors utilising a chloride conductance, or biphasic. The biphasic component is evoked in electrotonically coupled AD-SPN and is composed of depolarising notch followed by a hyperpolarising component superimposed on and thus shunting the underlying fast excitatory postsynaptic potential. This biphasic component is a result of synaptically driven action potential firing in an electrotonically coupled SPN, which is subject to the low pass filtering properties of the electrotonic junctions. Thus the depolarising notch and hyperpolarising phase correspond to the action potential and afterhyperpolarising potential respectively. Furthermore the properties of the fast EPSPs are subject to the emergent properties of an electrotonically coupled neuronal network.

Figure 5.1 Fast EPSPs evoked in AD-SPN by stimulation in the ipsilateral and contralateral funiculus

A, Superimposed voltage responses to graded intensities of stimulation (5-11V, 5ms, 0.05Hz) applied in the ipsilateral (Ai) and contralateral (Aii) funiculi. Note the constant latencies and rise times in graded EPSPs (Ai, Aii) that could reach threshold for action potential generation. Aiii, Superimposed averaged (5 traces) EPSPs illustrate differences in latencies between ipsilateral and contralateral evoked responses. B, Fast EPSPs evoked by ipsilateral (Bi) and contralateral (Bii) lateral funiculi electrical stimulation show partial voltage dependence revealed by injection of constant negative current. C, Fast EPSPs evoked from the ipsilateral (Ci) and contralateral (Cii) lateral funiculi showed no failures in response to high frequency stimulation (4x10Hz).

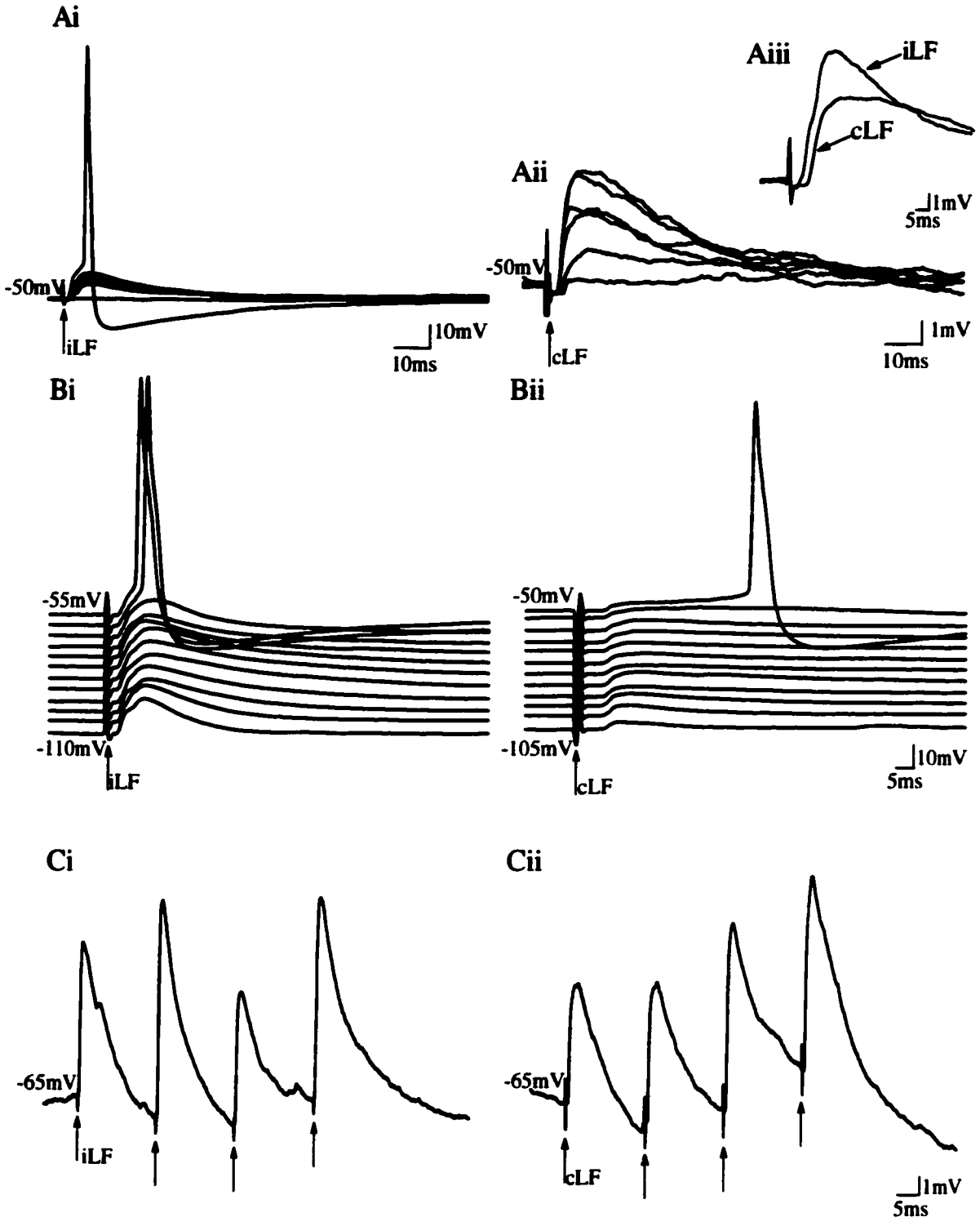
Ai
-50mV
iLF
10mV
10ms
Aiii
iLF
cLF
1mV
5ms
Aii
-50mV
cLF
1mV
10ms
Bi
-55mV
-110mV
iLF
Bii
-50mV
-105mV
cLF
10mV
5ms
Ci
-65mV
iLF
Cii
-65mV
cLF
1mV
5ms

Figure 5.1

Figure 5.3 Properties of the AMPA receptor mediated component of the fast EPSP

A, Fast EPSPs (1) evoked by electrical stimulation (11V, 5ms, 0.05Hz) of the ipsilateral (Ai) and contralateral (Aii) funiculi were recorded the presence of bicuculline (10μM) and strychnine (2μM) and subsequently averaged (n=8). Fast EPSPs were reduced in the presence of 10μM D-AP5 (2). The remaining fast rising and decaying component was blocked by 10μM CNQX (3). Fast EPSPs B, fast EPSPs evoked by ipsilateral and contralateral funiculi stimulation (6V, 5ms, 0.05Hz) were progressively reduced by increasing concentrations of GYKI 52466 (10-100μM). Membrane responses were obtained in the presence of D-AP5 (10μM), bicuculline (10μM) and strychnine (2μM) and reflect single superimposed traces. Ci, in the presence of D-AP5 (10μM), bicuculline (10μM) and strychnine (2μM)The peak amplitude of the fast EPSPs evoked by ipsilateral funiculi electrical stimulation increased with membrane hyperpolarisation. Fast EPSPs were obtained. Cii, The voltage dependence of the AMPA receptor mediated component plotted graphically extrapolates to a reversal potential of –22mV.

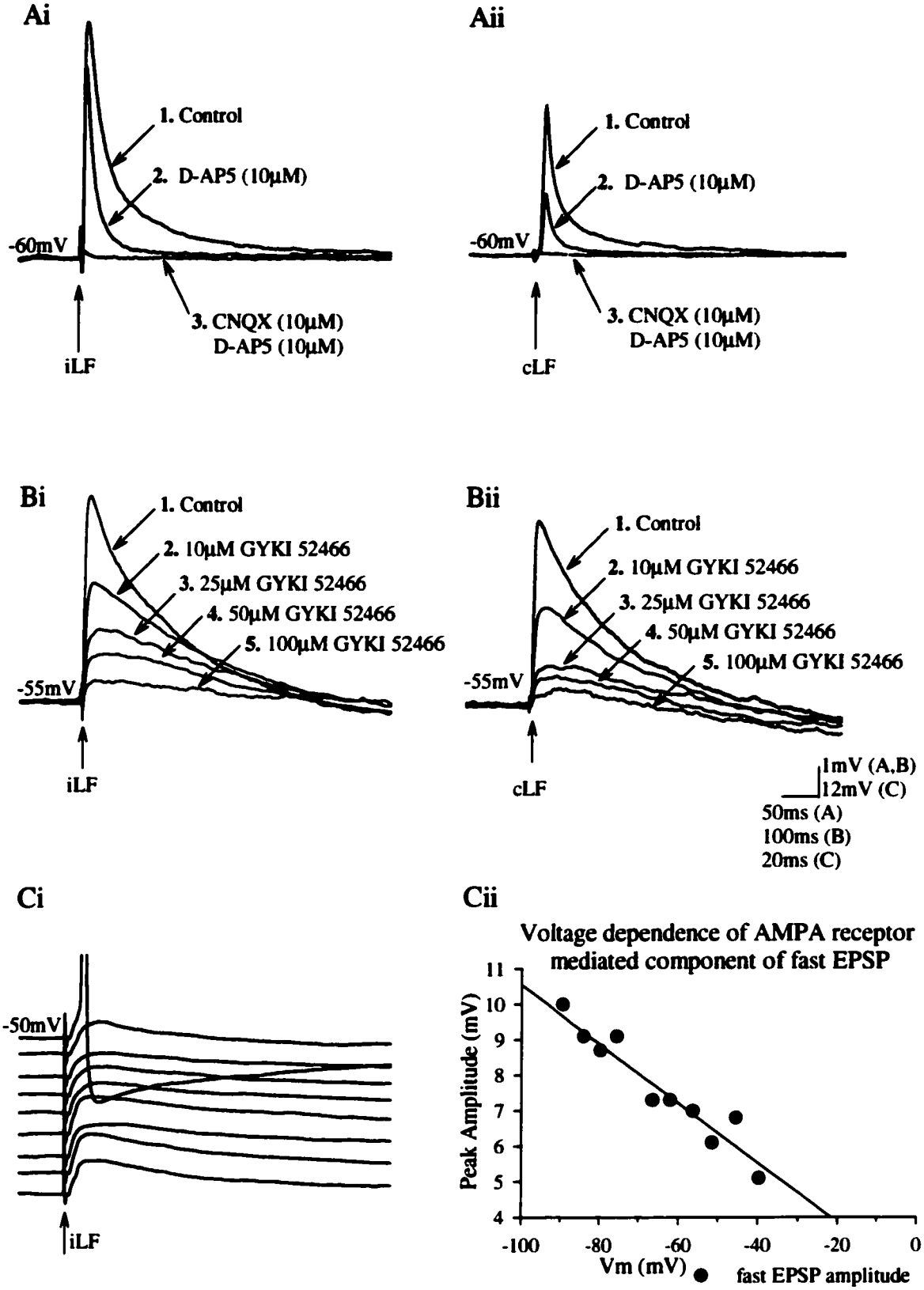
Ai
1. Control
2. D-AP5 (10μM)
-60mV
3. CNQX (10μM)
D-AP5 (10μM)
iLF
Aii
1. Control
2. D-AP5 (10μM)
-60mV
3. CNQX (10μM)
D-AP5 (10μM)
cLF
Bi
1. Control
2. 10μM GYKI 52466
3. 25μM GYKI 52466
4. 50μM GYKI 52466
5. 100μM GYKI 52466
-55mV
iLF
Bii
1. Control
2. 10μM GYKI 52466
3. 25μM GYKI 52466
4. 50μM GYKI 52466
5. 100μM GYKI 52466
-55mV
cLF
1mV (A,B)
12mV (C)
50ms (A)
100ms (B)
20ms (C)
Ci
-50mV
iLF
Cii
Voltage dependence of AMPA receptor mediated component of fast EPSP
Peak Amplitude (mV)
11
10
9
8
7
6
5
4
-100
-80
-60
-40
-20
0
Vm (mV)
fast EPSP amplitude

Figure 5.3

Figure 5.4 Properties of the NMDA receptor mediated component of the fast EPSP

A, Membrane responses show superimposed single fast EPSPs (1) evoked by electrical stimulation (8V, 5ms, 0.05Hz) of the ipsilateral (Ai) and contralateral (Aii) funiculi that increased in peak amplitude and duration upon removal of magnesium ions from the aCSF (2). Note action potential firing upon initial phase of fast EPSP from iLF (Ai) is truncated for clarity. Addition of 20μM D-AP5 blocked the fast EPSP (3). B, Single EPSPs evoked from ipsilateral (Bi, Bii, 5V) and contralateral (Biii, 8V) funiculi stimulation in the absence of magnesium show 3 patterns of firing: Bi, single action potential firing off the initial peak of the fast EPSP, Bii a burst of 8 action potentials, Biii, a burst of 4 action potentials on the plateau of the EPSP. C, Fast EPSPs evoked in the absence of magnesium show summation upon high frequency stimulation (4x10Hz) of the ipsilateral (5V, Ci) and contralateral (8V, Cii) funiculi. Hyperpolarisation of the membrane by injection of constant negative current revealed fast EPSPs underlying action potential firing at resting potentials (-60mV). All membrane responses showing fast EPSPs and action potential firing were evoked in the presence of NBQX (5μM), bicuculline (10μM) and strychnine (2μM).

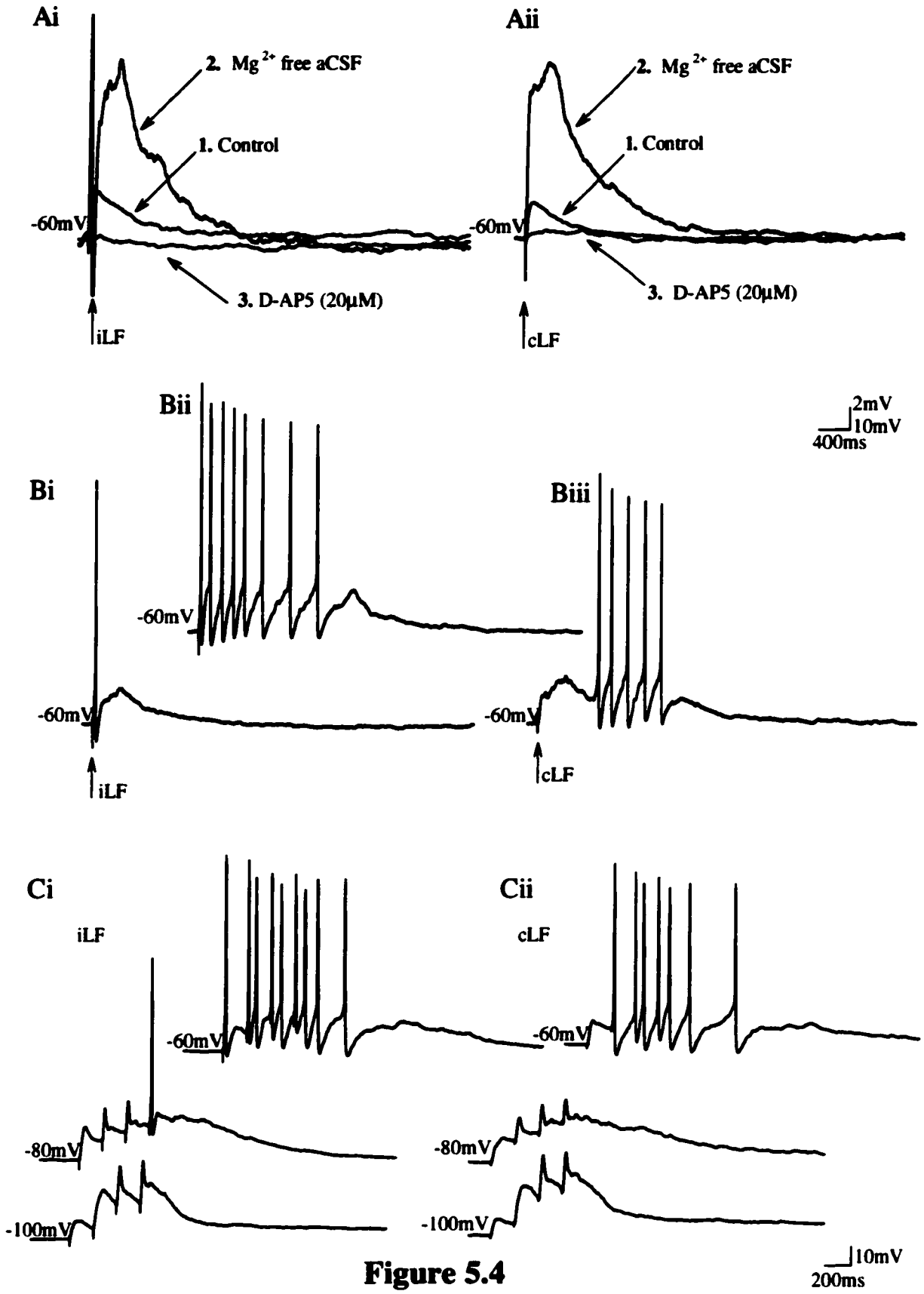
Ai
2. Mg 2+ free aCSF
1. Control
-60mV
3. D-AP5 (20µM)
iLF
Aii
2. Mg 2+ free aCSF
1. Control
-60mV
3. D-AP5 (20µM)
cLF
Bii
2mV
10mV
400ms
Bi
Biii
-60mV
-60mV
iLF
-60mV
cLF
Ci
iLF
Cii
cLF
-60mV
-60mV
-80mV
-80mV
-100mV
-100mV
10mV
200ms

Figure 5.4

Figure 5.5 Voltage dependence of the NMDA receptor mediated component of the fast EPSP

A, In the presence of 3.1mM external magnesium membrane responses show fast EPSPs evoked from the ipsilateral (Ai, 8V) and contralateral (Aii, 10V) funiculi that decreased in amplitude upon hyperpolarisation of the membrane by injection of constant negative current. B, In the absence of magnesium ions, membrane responses show fast EPSPs evoked from the ipsilateral (Ai, 8V) and contralateral (Aii, 10V) funiculi. Note the large peak amplitude and rapid rise times. Hyperpolarisation of the membrane the decreased the peak amplitude of the EPSP. All fast EPSPs were recorded in the presence of NBQX (5μM), bicuculline (10μM) and strychnine (2μM). C, The peak amplitude of the EPSP was normalised against the peak amplitude obtained at –50mV and plotted against membrane voltage. In the presence of external meagnesium (i) and in the absence of external magnesium (ii) the peak amplitude decreased with successive membrane hyperpolarisation (n=7).

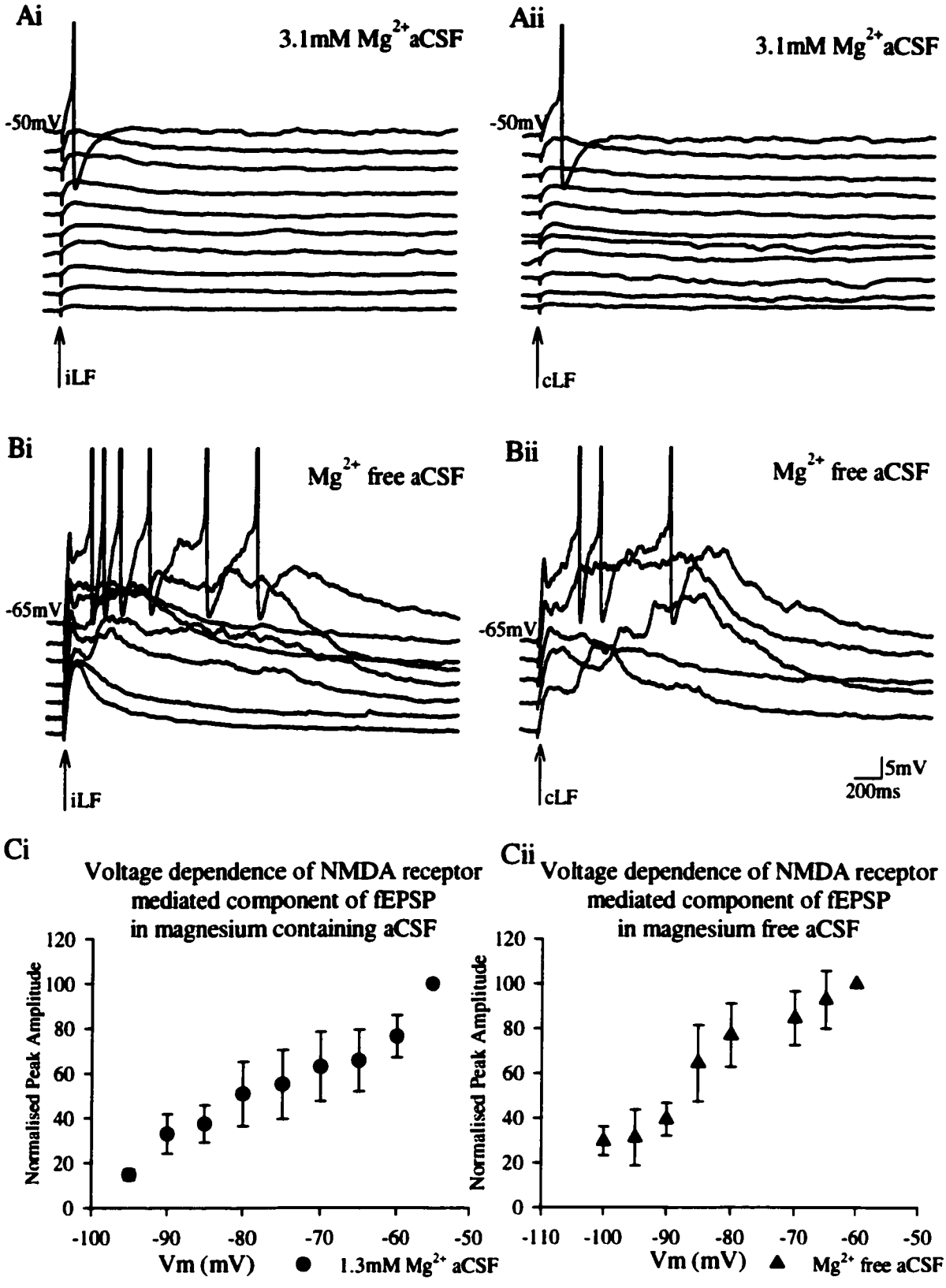
Ai
3.1mM Mg2+aCSF
-50mV
iLF
Aii
3.1mM Mg2+aCSF
-50mV
cLF
Bi
Mg2+ free aCSF
-65mV
iLF
Bii
Mg2+ free aCSF
-65mV
cLF
5mV
200ms
Ci
Voltage dependence of NMDA receptor mediated component of fEPSP in magnesium containing aCSF
Normalised Peak Amplitude
120
100
80
60
40
20
0
-100
-90
-80
-70
-60
-50
Vm (mV)
1.3mM Mg2+ aCSF
Cii
Voltage dependence of NMDA receptor mediated component of fEPSP in magnesium free aCSF
Normalised Peak Amplitude
120
100
80
60
40
20
0
-110
-100
-90
-80
-70
-60
-50
Vm (mV)
Mg2+ free aCSF

Figure 5.5

Figure 5.6 Properties of the fast IPSP

Superimposed voltage traces recorded in aCSF containing D-AP5 (10μM) and NBQX (5μM) show fast IPSPs evoked in response to electrical stimulation (5-11V, 5ms, 0.05Hz) of the ipsilateral (Ai, D) and contralateral (Aii, B) lateral funiculi. A, Bilateral fast IPSPs show constant latencies, similar rise times and a graded response to increasing stimulus intensities (5-11V). B, Fast IPSPs evoked from the ipsilateral funiculi showed no failures in response to high frequency stimulation (4x10Hz). Note action potential firing at the end of the fast IPSP. C, The graph depicts the change in peak amplitude of the fast IPSP evoked from the ipsilateral funiculi subsequent to hyperpolarisation of the membrane. The fast IPSP reversed polarity at a membrane potential of –58mV(n=3). D, Fast IPSPs evoked by stimulation in the ipsilateral funiculi (6V) were blocked by the addition of bicuculline (10μM) to the perfusate.

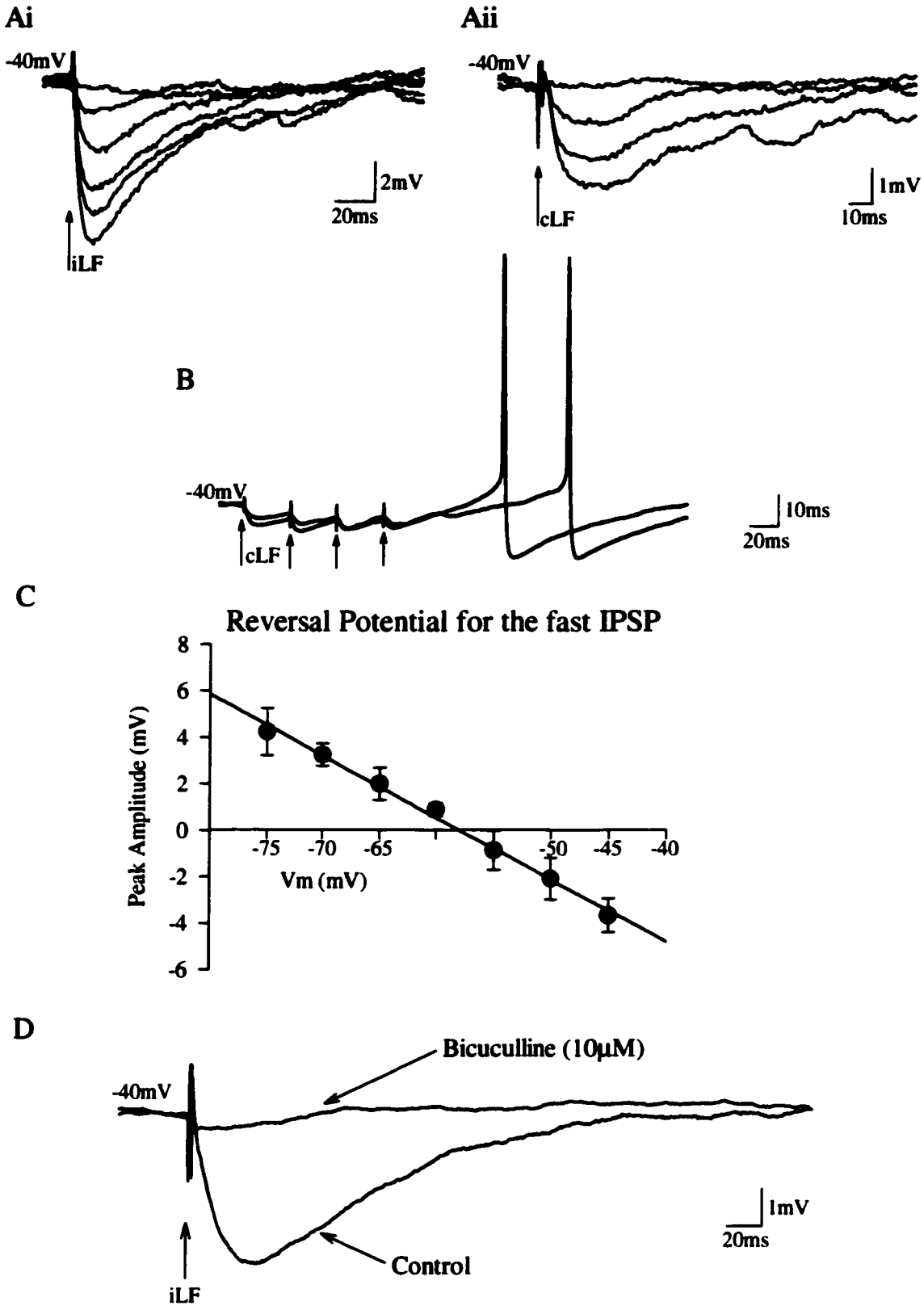
Ai
-40mV
2mV
20ms
iLF
Aii
-40mV
1mV
10ms
cLF
B
-40mV
cLF
10ms
20ms
C
Reversal Potential for the fast IPSP
Peak Amplitude (mV)
8
6
4
2
0
-2
-4
-6
-75
-70
-65
-50
-45
-40
Vm (mV)
D
Bicuculline (10μM)
-40mV
1mV
20ms
Control
iLF

Figure 5.6

Figure 5.7 Characteristics of the biphasic PSP.

A, The components of a biphasic PSP evoked in response to contralateral funicului stimulation (9V, 5ms, 0.05Hz) consist of an initial fast rising EPSP (star) followed by a superimposed depolarising transient (closed square) and subsequent afterhyperpolarisation (cross). Bi, Superimposed traces recorded in the presence of 5μM NBQX, 10μM bicuculline and 1μM strychnine display a NMDA receptor mediated EPSP evoked by low intensity ipsilateral funiculi stimulation (3V), a biphasic PSP evoked by higher stimulus intensities (5V) and action potentials evoked at high stimulus intensities (7V). Bii, On a longer time scale note the differences in decay times of the EPSP, biphasic PSP and afterhyperpolarising potential following the action potential. C, Simultaneous recordings from a pair of electrotonically coupled SPN reveal EPSPs evoked by low intensity (7V) ipsilateral funiculi stimulation (Ci, ii). Increasing the stimulus intensity 11V evokes an action potential in SPN 1 and a biphasic PSP in SPN 2. Note the electrotonic component of the biphasic PSP attenuates the chemically-mediated EPSP.

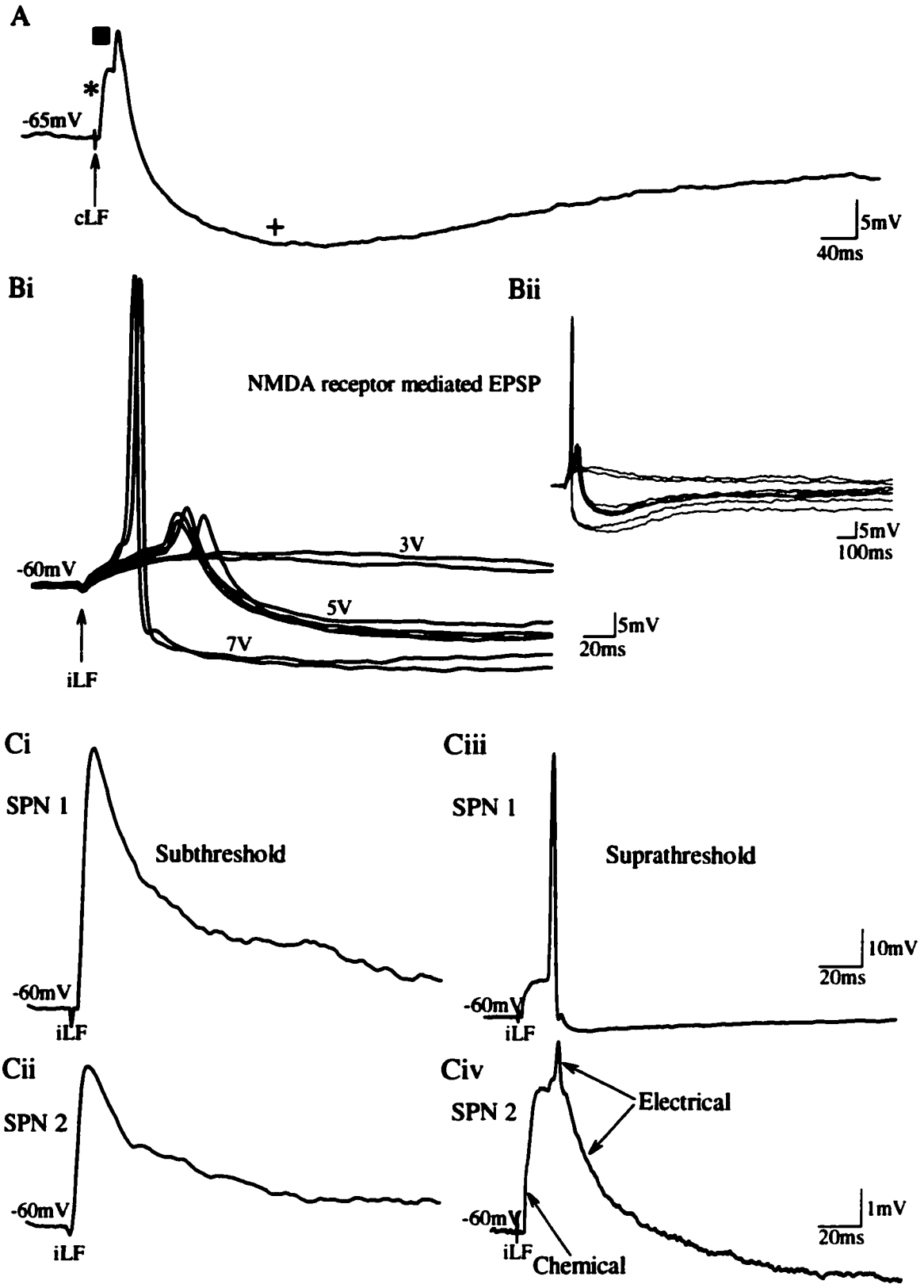
A
-65mV
cLF
5mV
40ms
Bi
Bii
NMDA receptor mediated EPSP
3V
5V
7V
-60mV
iLF
5mV
20ms
5mV
100ms
Ci
SPN 1
Subthreshold
-60mV
iLF
Ciii
SPN 1
Suprathreshold
10mV
20ms
-60mV
iLF
Cii
SPN 2
-60mV
iLF
Civ
SPN 2
Electrical
-60mV
iLF
Chemical
1mV
20ms

Figure 5.7

CHAPTER 6

THE SLOW INHIBITORY POSTSYNAPTIC POTENTIAL IN ADRENOMEDULLARY SYMPATHETIC PREGANGLIONIC NEURONS

6.1 Introduction

Catecholamines have long been recognised for contributing to the regulation of sympathetic outflow. Among the first indications were anatomical studies that revealed fluorescence for noradrenaline in the intermediate zone of the spinal cord of rat (Carlsson, 1964). Subsequent studies revealed the presence of tyrosine hydroxylase in nerve fibres surrounding retrogradely labeled SPN, including AD-SPN, both in rat (Anderson *et al.*, 1989) and cat (McLachlan and Oldfield, 1981). In both species, the noradrenergic fibres can be shown to form a ladder-like network, mimicking the topography of the dendrites of SPN, with longitudinal fibres forming smooth ladder supports and varicose transverse fibres forming the rungs. Some noradrenergic fibres appear to cross the midline and terminate contralaterally at the level of descussation (Carlsson *et al.*, 1964; McLachlan and Oldfield, 1981; Anderson *et al.*, 1989). Ultrastructural observations confirm direct contact with SPN, revealing contacts that are both symmetrical and asymmetrical in appearance (Chiba and Masuko, 1986; Milner *et al.*, 1988). Adrenergic agonists and antagonists have also been shown to bind to SPN membrane (Cabot *et al.*, 1984; Seybold and Elde, 1984).

The absence of tyrosine hydroxylase and PNMT immunoreactivity caudal to a spinal cord transection confirms that the majority of these fibers have a supraspinal origin. Indeed, neurons in the A5 region can be labeled with retrograde viral tracers into

the adrenal medulla (Strack *et al.*, 1989a). In addition, electrical and chemical stimulation of the locus coeruleus (A6) can evoke a release of catecholamines (Goadsby, 1985).

Various *in vivo* investigations imply that noradrenaline is a regulator of sympathetic outflow. For example, activation of catecholaminergic brainstem neurons has yielded both both pressor (Loewy *et al.*, 1979) and depressor (Coote and Macleod, 1974) cardiovascular responses. Conversely, central adrenergic receptor blockade can be seen to depress the baroreceptor inhibition of a somatosympathetic reflex (Coote *et al.*, 1981a) and the tonic brainstem inhibition of the spinal somatosympathetic reflex (Coote and Macleod, 1975). Injections of noradrenaline into the intermediolateral cell column are reported to both increase and depress heart rate, blood pressure and renal sympathetic nerve activity (Coote, 1985, Shi *et al.*, 1988). A role for catecholamines in mediating *both* sympathoinhibition and sympathoexcitation is supported by observations that both responses can be evoked by stimulation in the region of the A5 cell group, and both can be blocked after injection of the catecholamine neurotoxin 6-hydroxydopamine (Loewy *et al.*, 1979; Neil and Loewy, 1982; Woodruff *et al.*, 1986).

Subsequent *in vitro* studies on SPN have sought to clarify the actions of noradrenaline. In adult cat spinal cord slices, superfusion of noradrenaline produced depolarisation in 43.5%, hyperpolarisation in 23% and a biphasic response in 15.5 % of SPN located in T_2-T_3 (Yoshimura *et al.*, 1987b; Inokuchi *et al.*, 1992a). Noradrenaline's depolarisation was demonstrated to be mediated via α_1-adrenergic receptors, hyperpolarisation by α_2-adrenergic receptors. As the depolarisation, but not the hyperpolarisation, was sensitive to cobalt, low calcium aCSF and intracellular EGTA, it was proposed that α_1-adrenergic receptors activate a calcium-sensitive potassium

conductance (Inokuchi *et al.*, 1992a). In some neurons, a 'biphasic' response suggested that a subpopulation of SPN had both α_1- and α_2- adrenergic receptors. Evidence for synaptic release of catecholamines has been demonstrated after electrical stimulation of the lateral funiculi in adult cat, with depolarisation or hyperpolarisation blockable by α_1- and/or α_2- adrenergic receptors (Yoshimura *et al.*, 1987c). Thus sympathoexcitatory and sympathoinhibitory effects noted to follow supraspinal catecholamine cell group activation may well be the result of differential activation of α- adrenergic receptor subtypes at spinal levels.

In the rat, however, some similarities and discrepancies exist. Microiontophoresis of noradrenaline induced an increase in firing frequency in 71.5% and a decrease in firing frequency in 24% in SPN located in T_2 of the adult rat *in vivo* (Lewis and Coote, 1990a). In the neonatal spinal cord slice, superfusion of noradrenaline induced depolarisation via α_1-adrenergic receptors, but no hyperpolarising responses were reported (Ma and Dun, 1985). Superfusion of adrenaline also induced a depolarisation in 42% and a hyperpolarisation in 14% of SPN tested in neonatal spinal cord slices (Miyazaki *et al.*, 1989). The adrenergic induced depolarisation was also mediated by an α_1-adrenergic receptor-mediated closure of potassium channels, while the hyperpolarisation was mediated by an α_2-adrenergic receptor-mediated opening of potassium channels (Miyazaki *et al.*, 1989).

The investigations reported in this chapter further evaluated the role of noradrenergic receptors in mediating synaptic transmission to AD-SPN.

6.2 Results

6.21 Properties of the slow inhibitory postsynaptic potential

Inhibitory postsynaptic potentials were defined as slow when their duration exceeded that of the fast IPSPs (90-10% decay time >3s). Slow IPSPs were evoked in 13 of 19 AD-SPN tested by electrical stimulation of the ipsilateral and contralateral funiculi and in 26 SPN unidentified as to their target in T_7-T_{10}. Because the slow IPSP was preceeded by fast EPSPs that could reach threshold for action potential generation (see Chapter 5), NBQX (5μM) and D-AP5 (10μM) were routinely included in the perfusate (Figure 6.1). In addition, to minimise contamination by simultaneously activated fast IPSPs, strychnine (5μM) and bicuculline (10μM) were also included in the aCSF. A single stimuli pulse (5-11V, 0.5ms, 0.02Hz) could evoke the slow IPSP. However the response was larger and more prolonged following a repetitive stimulus of 4 pulses at 10Hz (5-11V, 0.5ms, 0.01-0.02Hz, Figure 6.2B) and thus this stimulus protocol was utilised throughout these experiments.

In AD-SPN slow IPSPs evoked from both lateral funiculi displayed constant latencies and a graded peak amplitude in response to increasing intensity of stimulation (Figure 6.2A). These features are consistent with a monosynaptic innervation. The slow IPSPs evoked by stimulation of the iLF had significantly shorter latencies than that evoked by cLF stimulation (38.1 ± 10.5ms compared to 124.4 ± 11.3ms, $P<0.001$, n=7). From membrane potentials close to rest (-60 to -70mV) 4 stimuli at 10Hz evoked a slow IPSP from the iLF and cLF with 10-90% rise times of 1.08 ± 0.20s and 1.08 ± 0.37s, a peak amplitude of 5.6 ± 3.4mV and 5.0 ± 2.3mV, and 90-10% decay times of 7.15 ± 4.10s and 9.16 ± 4.36s respectively (n=7, Table 6.3).

	iLF	cLF	n
Latency (ms)	38.10 ± 10.47	124.40 ± 11.26	7
Rise Time (s)	1.08 ± 0.20	1.08 ± 0.37	7
Peak Amplitude (mV)	5.55 ± 3.44	5.02 ± 2.30	7
Decay Time (s)	7.15 ± 4.83	9.16 ± 4.36	7

Table 6.3 Summary of the properties of slow IPSPs evoked in AD-SPN
Slow IPSPs were evoked in AD-SPN by electrical stimulation (4x10Hz, 5ms) of the ipsilateral and contralateral funiculi (iLF and cLF respectively). Latency was calculated from the end of the stimulus artifact to the start of the rise of the slow IPSP. Rise time represents the 10-90% time to reach peak amplitude. The decay time represents the 90-10% decay time of the slow IPSP.

The similarity of the rise times of the slow IPSP evoked from both lateral funiculi suggest that the presynaptic fibres innervate AD-SPN at an equidistant point from the recording electrode, which is presumably located at the soma. The amplitude of the slow IPSP was varied with both the number of stimuli and the stimulus intensity in a linearly increasing manner (1 stimuli evoked slow IPSPs with peak amplitudes of 4.2 ± 0.8mV and 90-10% decay times of 4.1 ± 2.4s, n=4, compared to 4x10Hz that evoked slow IPSPs with peak amplitudes of 5.6 ± 3.4mV and 90-10% decay times of 7.15 ± 4.10s). Increasing the frequency of stimulation decreased the amplitude and duration of the slow IPSP (4 stimuli at 100Hz evoked slow IPSPs with peak amplitudes of 1.8 ± 0.7mV and 90-10% decay times of 1.3 ± 0.9s compared to peak amplitudes of 5.2 ± 1.5 mV and 90-10% decay times of 2.3 ± 1.0s evoked by 4x 10Hz).

6.22 The slow IPSP is mediated by a potassium conductance

The slow IPSP is associated with a decrease in input resistance (from 724 ± 231.8MΩ , to 395.7 ± 86.9MΩ at peak of slow IPSP, a 39.8 ± 11.7% decrease, from iLF, n=4), observed upon injection of hyperpolarising current pulses from resting or holding membrane potentials during the slow IPSP (100pA, 800ms, 0.2Hz), indicative of channels opening. In aCSF containing 3.1mM potassium, hyperpolarisation of the membrane from –50mV to –100mV by injection of constant current resulted in a decrease in the amplitude of the slow IPSP from 8.5 ± 2.6mV at –50mV to 0.4 ± 0.2mV at –100mV (n=4, Figure 6.4A). After normalising slow IPSP amplitudes against the slow IPSP amplitude at rest (-50mV), the plot of the mean amplitude permitted extrapolation of a reversal potential at –99.1 mV (n=4, Figure 6.4C), approximating the equilibrium potential for potassium ions under our recording conditions (-98mV). In aCSF with nominally zero potassium, the amplitude of the slow IPSP at resting potentials was similar to that of control (at –50mV, peak amplitude of 4.8 ± 2.9mV compared to 5.3 ± 2.8 mV in control). Successive hyperpolarisation of the membrane to –100mV reduced the peak amplitude of the slow IPSP to 3.9 ± 2.7 mV (n=3, Figure 6.4Aii, B). No reversal was obtained upon hyperpolarisation to –120mV. The extrapolated value of the reversal potential in nominally potassium free aCSF was shifted in the negative direction (n=3 Figure 6.4C), in agreement with that predicted by the Nernst equation for potassium ions.

6.23 Pharmacology/receptor subtype mediating the slow IPSP

The receptor subtype and neurotransmitter mediating the slow IPSP was investigated by bath application of two noradrenergic uptake inhibitors. Xylamine

(10μM) extended the duration, measured as the 90-10% decay time, of the slow IPSP from 7.3 ± 2.3s to 12.6 ± 3.9s, (by 194.2 ±31.1% of control) and reduced the peak amplitude from 5.7 ± 2.8 to 3.2 ± 2.3mV (by 57.7 ± 11.4% of control, n=3). The noradrenergic uptake inhibition by xylamine may be offset by its uptake into the presynaptic terminal where it is believed to induce depletion of amines from the presynaptic terminals (Howard-Butcher *et al.*, 1985; Dudley, 1988). Therefore nisoxetine, a high affinity, bicyclic inhibitor of noradrenaline uptake (Wong and Bymaster, 1976; Leedham *et al.*, 1985; Tejani-Butt *et al.*, 1990) was tested. At a concentration of 100nM, nisoxetine extended the duration of the slow IPSP from 13.6 ± 3.2 to 24.9 ± 3.3s (to 198.3 ± 9.4% of control) but had minimal effect on peak amplitude (8.1 ± 2.2 in control to 8.1 ± 0.1mV in nisoxetine (to 74.5±8.8% of control, n=2, Figure 6.4A). The slow IPSP was unaffected either by prasozin (100-500nM, n=5), a prototypic α_1-adrenoceptor antagonist with low affinity for α_{2B} and α_{2C} adrenergic receptors, (see Bylund, 1992), or the β-adrenoceptor antagonist propanolol (10μM, n= 3 each, Figure 6.4C). The nonselective α-adrenoceptor antagonist, phentolamine (10μM) attenuated the peak amplitude of the slow IPSP (from 3.5 ± 0.4 to 0.3 ± 0.1mV, n=2) as did the high affinity α_2-adrenergic receptor antagonist, idazoxan (200nM to 1μM). In the presence of idazoxan the peak amplitude was reduced from 5.1 ± 2.6 to 1.8 ± 1.2 mV (to 44.4 ± 10.8 % of control) and decay time was reduced from 6.6 ± 4.9s to 0.8 ± 0.5s (to 21.8 ±17.7% of control) in the 5 of 6 neurons tested. Idazoxan completely blocked the slow IPSP in the remaining 1 neuron. The α_2-receptor antagonist yohimbine (0.5-1μM) blocked the slow IPSP in all 4 neurons tested.

6.24 Electrotonic coupling and slow IPSPs

The majority (n=21 of 26) of SPN that responded to electrical stimulation of the iLF and cLF with a slow IPSP were characterised by spontaneous oscillations in membrane potential, indicative of the presence of electrotonic coupling (see Chapter 4, Logan *et al.*, 1996; Nolan *et al.*, 1999). The effects of the slow IPSP on the oscillations in membrane potential were examined. An increase in intensity of electrical stimulation increased the peak amplitude and duration of the slow IPSP and appeared to delay the onset of the oscillations (n=10). The addition of xylamine to the aCSF enhanced the duration of the slow IPSP and the onset of oscillations was prolonged (Figure 6.6, n=3). Upon blockade of the slow IPSP with yohimbine 1μM, the oscillations in membrane potential were similar to control (Figure 6.7, n=3).

6.3 Discussion

These observations indicate that AD-SPN receive monosynaptic slow inhibitory synaptic inputs from fibres in both the ipsilateral and contralateral lateral funiculi. Slow IPSPs were interpreted to be monosynaptic in origin by their constant latencies and rise times. The similarity of rise times of the slow IPSP from the iLF and cLF suggest that the presynaptic fibres innervate AD-SPN at an equidistant point from the recording electrode.

6.31 Noradrenaline as a neurotransmitter in AD-SPN

This is the first report of a noradrenaline-mediated inhibition in AD- SPN in rat. The involvement of noradrenaline is indicated by the extended duration of the slow IPSP upon blockade of the noradrenaline uptake transporters on the presynaptic membrane. Nisoxetine exhibits a high affinity for the neuronal noradrenaline uptake transporter. The

decrease in amplitude of the slow IPSP upon addition of the uptake blockers could either be a result of desensitisation of the postsynatpic receptors or a consequence of a reduction in the amount of noradrenaline released from the presynaptic terminal due to sufficient refilled and available vesicles. There is no evidence for uptake transporters of adrenaline, however enzymes like catechol-O-methyltransferase break down adrenaline in the synaptic cleft (Trendelenburg, 1991; Amara and Kuhar, 1993).

Previous studies in rat observed that noradrenaline was excitatory and that adrenaline induced both excitation and inhibition in SPN (Ma and Dun, 1985; Miyazaki *et al.*, 1989). Although the presence of adrenaline is indicated by the localisation of PNMT containing nerve terminals in the intermediolateral cell column (Ross *et al.*, 1981), there are reasons to indicate that adrenaline does not contribute to neurotransmission in SPN. Quantitative biochemical data indicate small amounts of adrenaline in the spinal cord (Reid *et al.*, 1975). In the intermediolateral cell column the level of adrenaline has been reported as less than 0.05% of those of noradrenaline (Sved, 1989), or undetectable (Van der Gugten *et al.*, 1976). The absence of adrenaline in the intermediolateral cell column is conserved across species, with similar results obtained in rat (above), cat and rabbit (Zivin *et al.*, 1975; Fleetwood-Walker and Coote, 1981). Nonetheless, the similar affinities of adrenergic receptors for noradrenaline and adrenaline could explain the comparable effects of adrenaline application to SPN in rat to noradrenaline application in cat (Yoshimura *et al.*, 1987b; Miyazaki *et al.*, 1989; Bylund, 1992). That noradrenaline can mediate both an inhibition (this study) and excitation (Ma and Dun, 1985) in rat is comparable with that observed in cat (Yoshimura *et al.*, 1987b; Inokuchi *et al.*, 1992a).

6.32 Nature of the noradrenergic receptor

Pharmacological data suggest the slow inhibitory synaptic transmission in AD-SPN is mediated by noradrenaline acting via postsynaptic α_2-adrenoreceptors. Postsynaptic receptors responsive to noradrenaline can be subtyped pharmacologically into two α_1, four α_2 and three β receptors subtypes. While further α subunits have been cloned, these are at present not identifiable pharmacologically (Jones and Palacios, 1991; Bylund *et al.*, 1992). In AD-SPN, the slow IPSP is insensitive to the α_1- and β-adrenergic receptor antagonists prazosin and propanolol respectively. Prazosin also displays low affinity for receptors of the α_{2B} and α_{2C} subtypes, but not α_{2A} (MacDonald and Scheinin, 1995). Since the slow IPSP was reduced by yohimbine and idazoxan, α_2- and specifically α_{2A}-adrenergic receptors are most likely involved in mediating the slow hyperpolarisation in rat. These data compare favourably to those obtained in cat (Yoshimura *et al.*, 1987b; Inokuchi *et al.*, 1992a). Selectivity profiles reveal idazoxan has over 6 fold higher selectivity for α_2 / α_1 adrenergic receptors than yohimbine (288 vs 45 respectively) (Doxey *et al.*, 1983; Dabire, 1986). Therefore, in AD-SPN the component of the slow IPSP that was sensitive to idazoxan and insensitive to prazosin, is likely to be mediated by α_2A-adrenergic receptors, while the remaining component is likely to be a result of activation of non-adrenergic receptors. Idazoxan is known to bind with high affinity to non-adrenergic sites, that are separate from the receptor, and have been designated imidazoline binding sites (Ernsberger *et al.*, 1987; Hussain *et al.*, 1993). Unless there is cross talk between the α_2- adrenergic receptor and the imidazoline binding sites, these pharmacological tools can accurately define the presence of an α_{2A}-adrenergic receptor. In rat spinal cord, mRNA for the receptor subtype α_{2A} is present in the

intermediolateral cell column (Nicholas *et al.*, 1993) and also in lamina I, II and V, while α_{2C} is weakly present throughout the dorsal horn and α_{2B} is only occasionally observed in lamina II (Zeng and Lynch, 1991). Thus the pharmacological identification of the receptors mediating the slow IPSP in AD-SPN corresponds well to the molecular identification of subunits synthesised.

6.33 Signalling beyond the α_2-adrenergic receptor

The α_2-adrenergic receptor is a G-protein coupled receptor comprising 7 transmembrane spanning domains. Noradrenaline binding induces the activation of the G-protein heterotrimeric complex (G_α and $G_{\beta\gamma}$) via exchange of guanine trisphosphate for guanine diphosphate. In α_2-adrenergic receptors, pertussis toxin sensitive G_α subunits are indicative of inclusion of $G_{\alpha i}$ or $G_{\alpha o}$ subtypes, which are classically negatively coupled to adenylyl cylase and hence cyclic 3',5'-adenosine monophosphate (AMP) production (Bylund and Ray-Prenger, 1989). Subsequent modulation of protein kinases are believed to effect ion channel function. However pertussis toxin insensitive G-proteins can also couple to α_2-adrenergic receptors (Hille, 1994), thus $G_{\alpha s}$ and subsequently the phospholipase C intracellular pathway may be recruited to mediated cellular effects. Further experiments would be required to deduce the signalling pathway utilised upon the activation of α_2-adrenergic receptors in AD-SPN.

In AD-SPN synaptic activation of the postsynaptic α_2-adrenergic receptor evoked a change in conductance consistent with opening of potassium channels. In adult cat SPN, the noradrenaline evoked hyperpolarisation was inhibited with high concentrations of barium ions, but not by TEA, 4-aminopyridine nor caesium ions (Inokuchi *et al.*,

1992a). It is interesting to note that the long duration component of the transient outward rectifier identified in Chapter 3 was also blocked by high concentrations of barium ions, raising the possibility that these channels contribute to the long duration of the slow IPSP in AD-SPN. Presumably the initial hyperpolarising phase of the slow IPSP is sufficient to release inactivation of these barium sensitive channels to allow potassium efflux. Subsequent modulation of these channels by $G_{\beta\gamma}$ may slow the inactivation kinetics thus extending open time from 4-8s to 9-15s in the slow IPSP.

6.34 Effects of the slow IPSP on oscillations

The majority of SPN that responded to lateral funiculi stimulation with a slow IPSP displayed oscillations in membrane potential i.e. were electrotonically coupled. The slow IPSP could temporarily "over-ride" the oscillatory patterns, the return of which was determined by the decay time of the slow IPSP. One might speculate on the mechanisms involved. A) If pertussis toxin insensitive G-proteins were coupled to the α_2-adrenergic receptor, activation of G_α subunit could act via the cGMP pathway to increase inositol trisphosphate and induce calcium release from intracellular stores. This could cause a transient reduction in junction conductance, preventing current transfer between neurons and thus a reduction in oscillations in membrane potential, similar to the caffeine effects seen in Chapter 4. B) The activation of multiple noradrenergic axon collaterals, would cause the whole electrotonically coupled network to be hyperpolarised thus no SPN would reach threshold for action potential generation, resulting in a transient silencing of oscillations. Isopotentiality thoughout the network during the slow IPSP would increase input resistance enhancing the amplitude and duration of the slow IPSP. In addition

suppression of the network during the hyperpolarised phase would prevent fast synaptic input from reaching threshold. It may be speculated that termination of the slow IPSP could induce synchronised activity within the network. Nonetheless the slow IPSP is a powerful regulator of SPN excitability. A similar action of noradrenaline acting via α_2-adrenergic receptors and reducing spontaneous oscillations in membrane potential in neonatal locus coeruleus neurons has been observed (Williams and Marshall, 1987), however a mechanism of action was not proposed.

6.35 The origin of a noradrenergic input to AD-SPN

A) The locus coeruleus cell groups

The noradrenergic system, originating from the locus coeruleus region in the dorsolateral pons, is perhaps unrivaled in its divergence of projections throughout the central nervous system. As the noradrenergic content of the spinal cord originates almost entirely from higher brain regions (Dahlstrom, 1965; Haggendal and Dahlstrom, 1973; Magnusson, 1973; Nygren and Olson, 1977), the descending fibres are likely to have a considerable role in determining sympathetic output. However, in comparison with the forward projections, the organisation and projections of the descending tracts is less resolved. Of the two main spinal projeceting noradrenergic tracts the lateral tegmental pathway, containing axons from the noradrenergic groups A1, A2, A5 and A7 projecting through the dorsolateral funiculi, is likely to be involved in autonomic function. Clear evidence from anatomical studies including retrograde viral tracers, and autoradiographical and immunohistochemical studies are indicative of a dominant innervation of the intermediolateral cell column by the A5 cell group (Loewy *et al.*, 1979; Byrum and Guyenet, 1987; Strack *et al.*, 1989b). Therefore the A5 cell group is likely to

be the source of noradrenergic input to AD-SPN. Interestingly axons from the A5 cell group in the spinal cord also innervate both dorsal and ventral horns (Clark and Proudfit, 1993), suggesting a role in nociception and motor control and well as modulating autonomic outflow. Some studies report that fibres from the A5 may innervate the ventral motorneurons (Grzanna *et al.*, 1987). However differences in species, uptake of dye by fibres of passage or the presence of subgroups within the A5 that posses separate projections sites may account for the disparate results (Clark *et al.*, 1991; Proudfit and Clark, 1991). Nonetheless, the majority of studies propose a role of the A5 in the control of autonomic function.

B) The C1 group of the rostral ventrolateral medulla

The bulbospinal A1/C1 neurons within the rostral ventrolateral medulla make monosynaptic contacts with SPN (Milner *et al.*, 1988; Zagon and Smith, 1993) providing an excitatory drive (Jansen *et al.*, 1995b; Sun, 1996; Guyenet *et al.*, 2001) to regulate the sympathetic component of the baroreceptor reflex (Dampney, 1994; Sun, 1995). These neurons are not phenotypically adrenergic (Guyenet *et al.*, 1989) but release glutamate (Morrison *et al.*, 1989b). However recently studies indicating that approximately two thirds of the A1/C1 neurons contain tyrosine hydroxylase, dopamine-β-hydroxylase or PNMT (Guyenet *et al.*, 2001), raises the possibility of release of a catecholamine. The prevalent notion that the A1/ C1 area provides a sympathoexcitatory drive through the spinal cord is inconsistent with the strong inhibition of excitability in AD-SPN that stimulation of descending fibres produces, and therefore the A1/C1 region of the rostral ventrolateral medulla is unlikely to be the origin of this input to AD-SPN.

6.36 Noradrenergic pathways to AD-SPN are bilateral

In this study, AD-SPN received a noradrenergic input from both sides of the spinal cord. Bilaterality of catecholaminergic descending inputs has been described from the first classifications of catecholamines in the spinal cord where the level of decussation was observed at the same level as termination of nerve fibres (Carlsson, 1964; Dahlstrom, 1965). More recent studies have re-iterated this finding by utilising selective lesions of the locus coeruleus (Karoum *et al.*, 1980; Commissiong, 1981) and anterograde and retrograde tracing studies from the locus coeruleus and spinal cord respectively (Fritschy *et al.*, 1987; Fritschy and Grzanna, 1990). In addition *in vivo* studies indicate bilateral modulation of sympathetic outflow (catecholamine release and vasoconstriction) upon unilateral stimulation of the locus coeruleus. Recognition of a bilateral influence of the slow IPSP on AD-SPN excitability would imply a powerful mechanism for the co-ordination of central sympathetic function in relation to specific output i.e. the adrenal medulla, and in situations where activation and co-ordination of sympathetic subsystems is required i.e. co-activation of cardiac, vascular and adrenal systems. This issue is discussed in more detail in Chapter 7.

6.37 A physiological role for the slow IPSP

Little is known about the role of descending noradrenergic projections from the A5 cell group in autonomic function. In anaesthetised rats, injection of L-glutamate to the A5 cell group induced a decrease in arterial blood pressure and a redistribution of blood flow. This dilation of skeletal muscle and constriction of gastrointestinal tract blood supplies was absent in 6-hydroxydopamine treated rats (Stanek *et al.*, 1984). Therefore distinct excitation and inhibition of central sympathetic pathways by noradrenaline acting

via α_1- and α_2-adrenergic receptors could provide the mechanism for controlling blood distribution. However in un-anaesthetised rats, lesions of the A5 cell group by injections of 6-hydroxydopamine had no effect on arterial blood pressure and had small effects on sympathetic baroreceptor control of heart rate (Stornetta, 1986).

A subpopulation of noradrenergic brainstem neurons that project to the spinal cord send axon collaterals to simultaneously innervate the cerebral and cerebellar cortices, thalamus, hippocampus (Nagai *et al.*, 1981; Room *et al.*, 1981; Jones and Yang, 1985; Lucchi *et al.*, 1998). Thus noradrenergic neurons diverge both within spatial (e.g. ascending forebrain and descending spinal cord) and functional (e.g. autonomic, somatosensory, somatomotor, higher cortical functions ie awareness, sleep) modalities, providing potential pathways to integrate the autonomic nervous system with higher brain functions. Although defining a physiological role for the descending, bilateral noradrenergic input is difficult at present, the fact that it considerably depresses both individual AD-SPN and network activity on a long time scale, indicates a dominant role in the regulation of catecholamine secretion and autonomic function.

6.4 Summary

AD-SPN receive descending slow inhibitory synaptic input from both sides of the spinal cord, mediated by α_{2A}-adrenergic receptors coupled to a potassium conductance. The neurotransmitter is likely to be noradrenaline, originating from the A5 region of the brainstem. The majority of SPN receiving this innervation were electrotonically coupled, and the slow inhibitory input could be seen to regulate oscillations in membrane potential.

Figure 6.1 Activation of fast EPSPs and slow IPSPs in AD-SPN

Traces show single postsynaptic membrane responses to stimulation (4x10Hz, 9V) of ipsilateral (A) and contralateral (B) funiculi. Stimuli evoked slow IPSPs and fast EPSPs (inset Ai, Bi) that reached threshold for action potential generation. The fast EPSPs were blocked with the glutamatergic antagonists NBQX (5μM) and D-AP5 (10μM) (inset Aii, Bii).

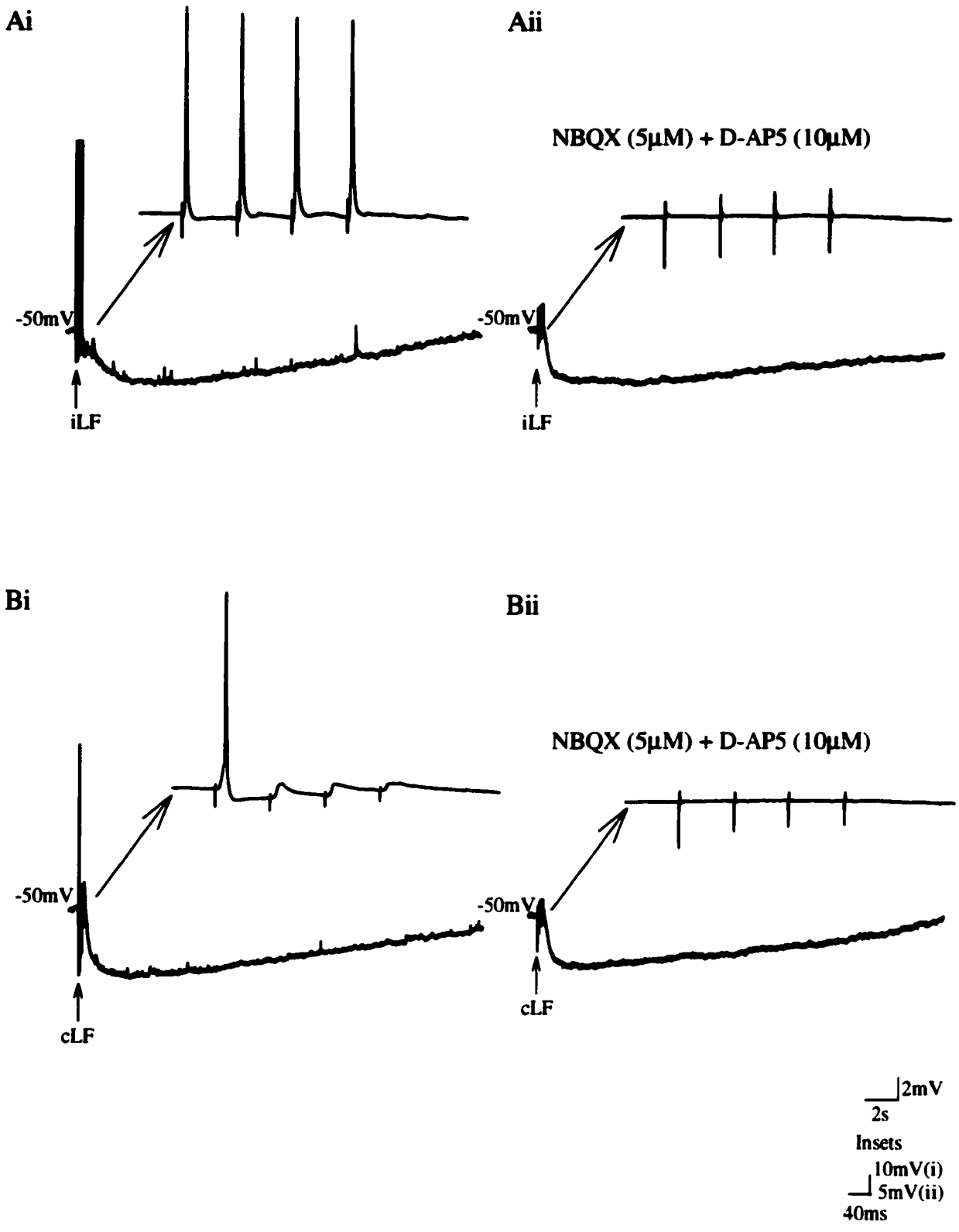
Ai
Aii
NBQX (5μM) + D-AP5 (10μM)
-50mV
iLF
-50mV
iLF
Bi
Bii
NBQX (5μM) + D-AP5 (10μM)
-50mV
cLF
-50mV
cLF
2mV
2s
Insets
10mV(i)
5mV(ii)
40ms

Figure 6.1

Figure 6.2 Characteristics of the slow IPSP in AD-SPN evoked from both sides of the spinal cord.

Superimposed averaged (n=3) postsynaptic membrane responses from the same neuron show IPSPs evoked by lateral funiculi stimulation at membrane potentials close to rest (-60mV). A, The amplitude of the slow IPSP increased as stimulus intensity was increased (8V, 10V, 12V). B, The amplitude and duration increased upon increasing the number of stimuli (1, 2 and 4 pulses at 10Hz).

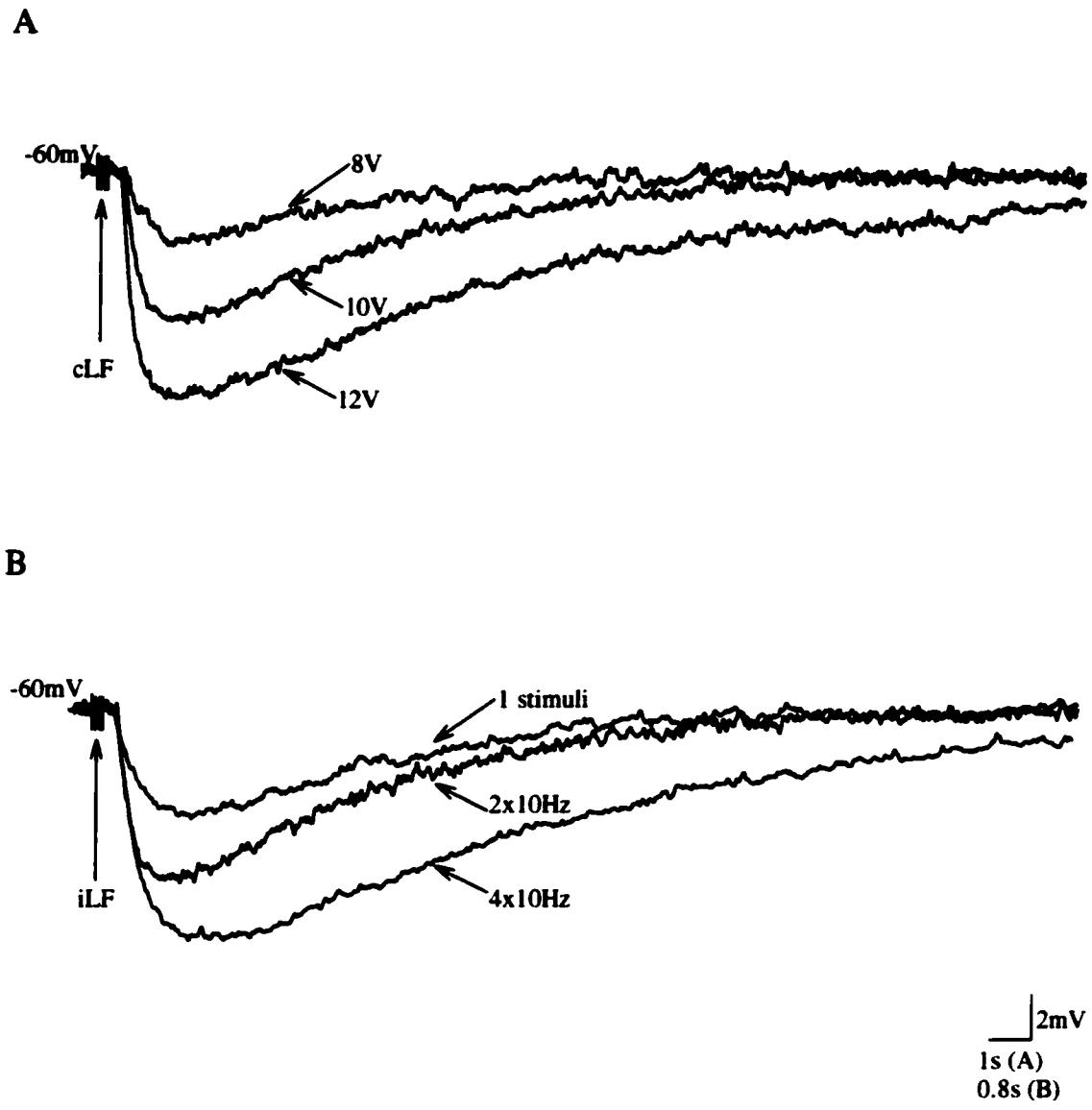
A
-60mV
8V
10V
12V
cLF
B
-60mV
1 stimuli
2x10Hz
4x10Hz
iLF
2mV
1s (A)
0.8s (B)

Figure 6.2

Figure 6.4 The slow IPSP is mediated by a potassium conductance

A, Membrane responses show slow IPSPs evoked in standard extracellular potassium concentrations (3.1mM) by electrical stimulation (4x10Hz) of the ipsilateral funiculi. The slow IPSP decreased upon hyperpolarisation of the membrane by injection of constant negative current and reached a null point at ≈ -100mV. Aii, Slow IPSP evoked in nominally 0mM extracellular potassium shows less voltage dependence upon hyperpolarisation of the membrane. B, Superimposed membrane responses showing the slow IPSP evoked by stimulation of the contralateral funiculi. Note the increase in amplitude under minimal potassium extracellular conditions. C, Plots show the peak amplitude of the slow IPSP normalised against that at resting or holding potentials of –50mV under control (circles) and minimal (triangles) extracellular potasssium concentrations (n= 4). Note the shift of reversal potential to more negative potential under nominally potassium free conditions.

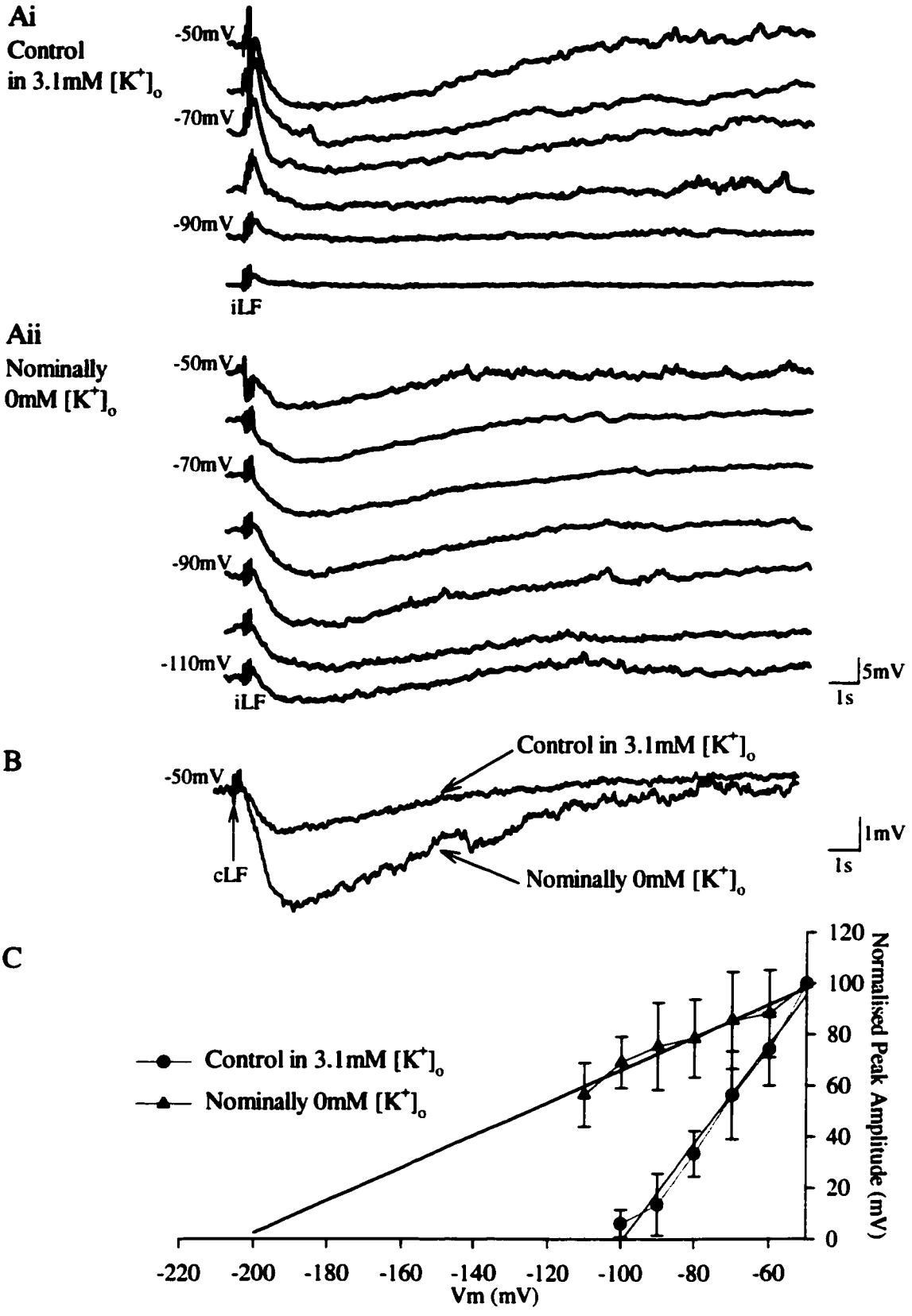
Ai
Control
in 3.1mM [K+]o
-50mV
-70mV
-90mV
iLF
Aii
Nominally
0mM [K+]o
-50mV
-70mV
-90mV
-110mV
iLF
5mV
1s
B
Control in 3.1mM [K+]o
-50mV
cLF
Nominally 0mM [K+]o
1mV
1s
C
Control in 3.1mM [K+]o
Nominally 0mM [K+]o
120
100
80
60
40
20
0
Normalised Peak Amplitude (mV)
-220
-200
-180
-160
-140
-120
-100
-80
-60
Vm (mV)

Figure 6.4

Figure 6.5 The slow IPSP is mediated by noradrenaline acting via α_2-adrenergic receptors

A, Superimposed averaged (n=3) postsynaptic membrane responses to ipsilateral funiculi stimulation (4x10Hz) show a slow IPSP that is enhanced in duration and reduced in peak amplitude upon increasing concentrations of the noradrenergic uptake inhibitor nisoxetine (100-200nM). B, The enhanced slow IPSP shown in A was reduced in peak amplitude and duration in the presence of the high affinity α_2-adrenergic receptor antagonist idazoxan (1μM).

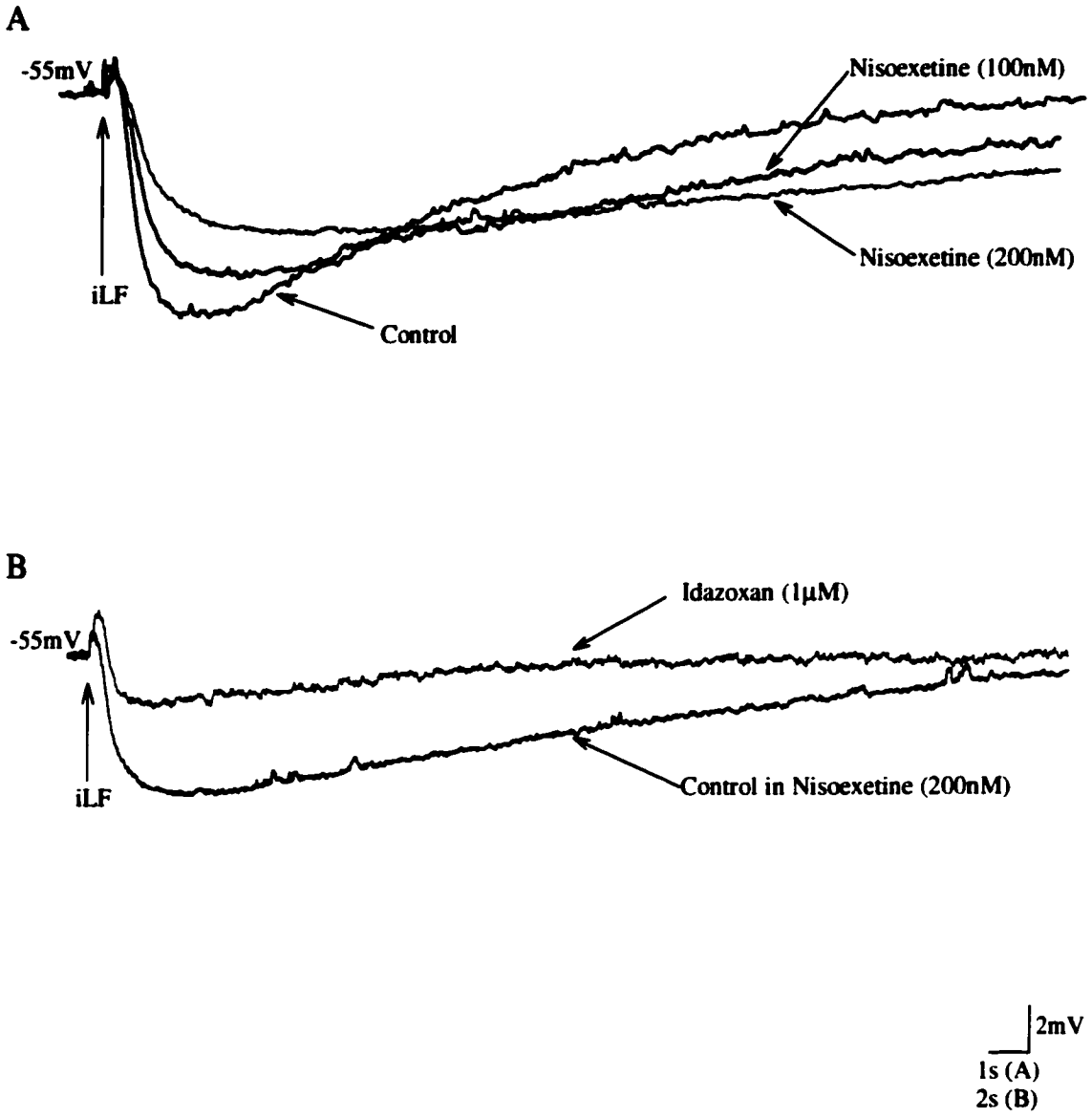
A
-55mV
Nisoexetine (100nM)
Nisoexetine (200nM)
iLF
Control
B
Idazoxan (1μM)
-55mV
iLF
Control in Nisoexetine (200nM)
2mV
1s (A)
2s (B)

Figure 6.5

Figure 6.6 The slow IPSP in electrotonic coupled SPN

A, Superimposed spontaneous membrane activity from a continuous trace showing oscillations in membrane potential that reach threshold for action potential generation. B, Superimposed single postsynaptic membrane responses to contralateral funiculi stimulation (4x10Hz) show the slow IPSP increased in amplitude and duration upon increasing stimulus intensity (6V-12V). Note the delay in onset of oscillations in membrane potential or action potential firing as stimulus intensity was increased. Ci, Superimposed single postsynaptic membrane responses to ipsilateral funiculi stimulation (4x10Hz, 10V) show the slow IPSP terminates with action potential firing at the peak of an oscillation in membrane potential. Subsequent addition of the noradrenergic uptake inhibitor xylamine (10μM) delayed the onset of oscillations in membrane potential (Cii). All traces are from the same neuron.

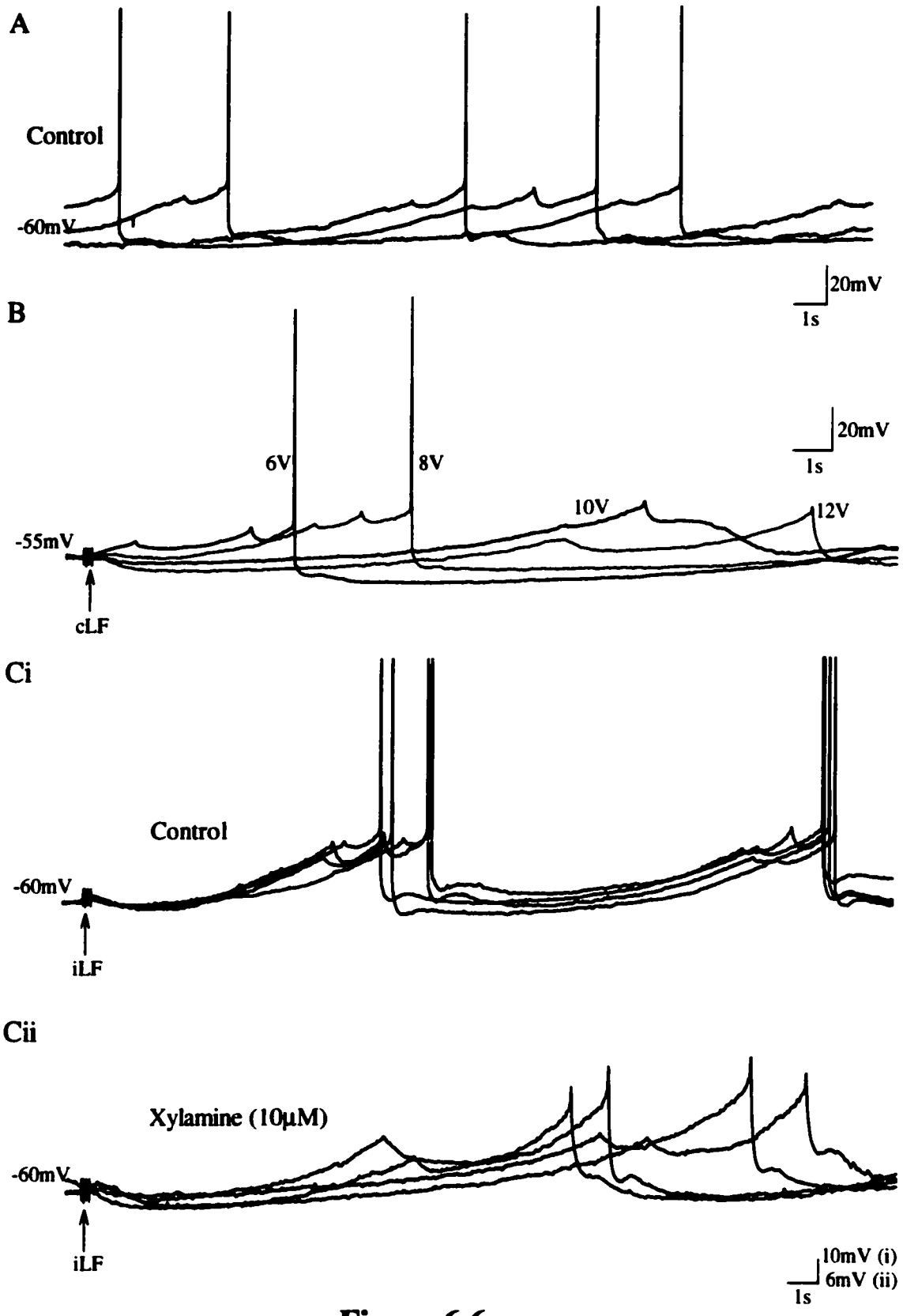
A
Control
-60mV
20mV
1s
B
6V
8V
10V
12V
20mV
1s
-55mV
cLF
Ci
Control
-60mV
iLF
Cii
Xylamine (10μM)
-60mV
iLF
10mV (i)
6mV (ii)
1s

Figure 6.6

Figure 6.7 Manipulations of the slow IPSP in electrotonically coupled SPN.

Ai, Superimposed single postsynaptic membrane responses to ipsilateral funiculi stimulation (4x10Hz, 7V) show the slow IPSP prevents the occurance of oscillations in membrane. Subsequent addition of the broad spectrum α-adrenergic receptor antagonist phentolamine (10μM) reduced the amplitude and duration of the slow IPSP, allowing the return of the oscillation rhythm (Aii). Bi, Superimposed single postsynaptic membrane responses to contralateral funiculi stimulation (4x10Hz, 12V) show the slow IPSP interrupts the patterns ofoscillation in membrane potential. Subsequent addition of the α_2-adrenergic receptor antagonist yohimbine (1μM) allows the return of the natural pattern of oscillations in membrane potential (Bii).

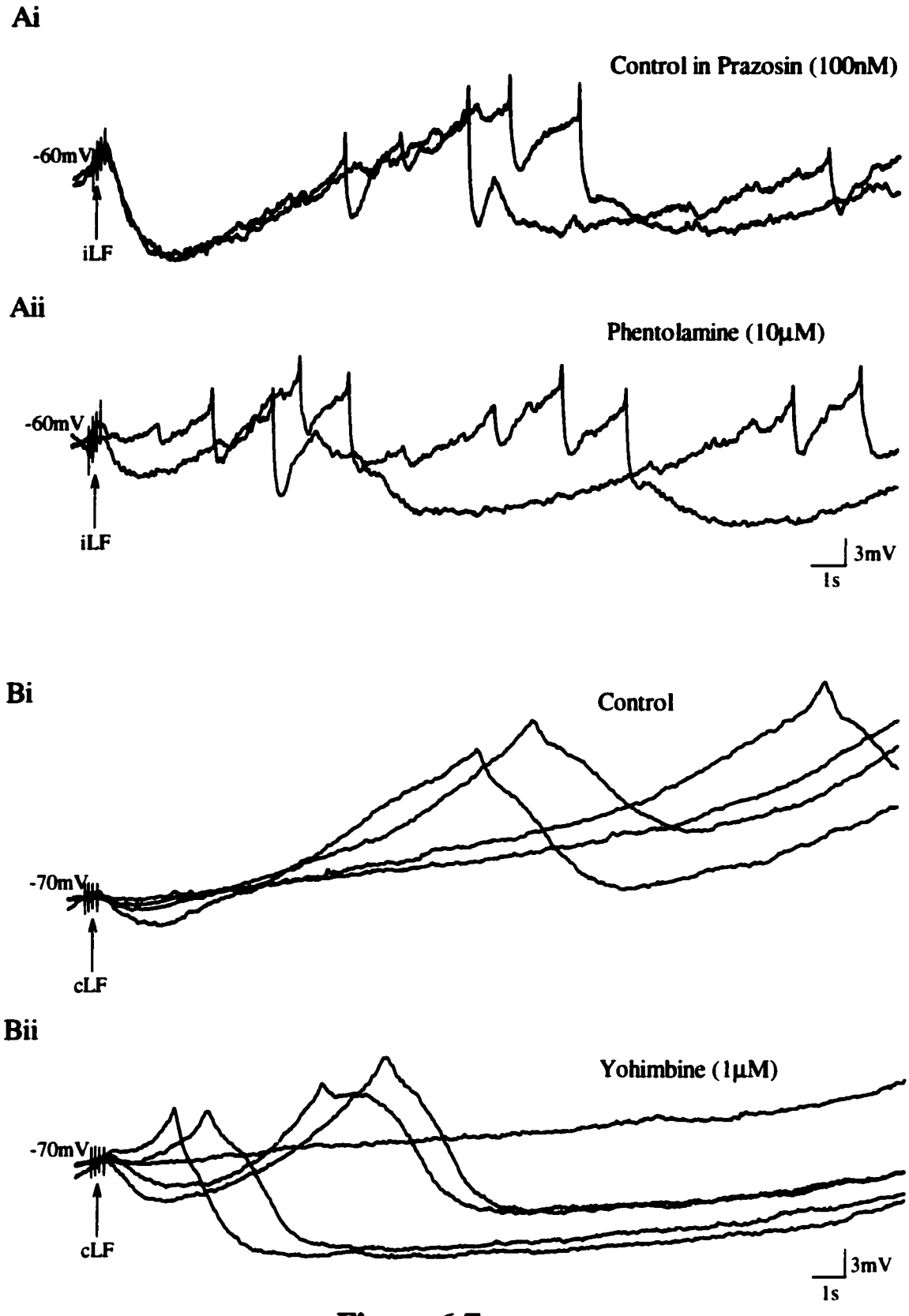
Ai
Control in Prazosin (100nM)
-60mV
iLF
Aii
Phentolamine (10μM)
-60mV
iLF
3mV
1s
Bi
Control
-70mV
cLF
Bii
Yohimbine (1μM)
-70mV
cLF
3mV
1s

Figure 6.7

CHAPTER 7

GENERAL DISCUSSION

7.1 Introduction

The sympathetic nervous system is responsible for a dynamic regulation of noradrenaline and adrenaline release from the adrenal medulla, varying from moment to moment homeostasis to immediate release during a stressful response. Despite the fundamental and familiar nature of the flight and fight behaviour, the spinal and central mechanisms controlling or mediating the range seen in these effects are for the most part still poorly understood. This study was undertaken to elucidate some mechanisms, both intrinsic and synaptic, that may contribute to the regulation of neuronal excitability in AD-SPN, the neurons that specifically control the release of catecholamines from the adrenal medulla.

The data presented here indicate that AD-SPN are a relatively homogeneous population with regard to their intrinsic membrane properties. These include 3 outward rectifying potassium conductances that contribute to the repolarisation phase of the action potential, an inward rectifying potassium conductance and 2 calcium conductances that can separately induce burst firing and prolong the action potential (Figure 7.1). Supraspinal sources are also known to regulate spinal sympathetic functions. In this study bilateral fast excitatory and inhibitory synaptic input to AD-SPN was demonstrated and shown to be mediated by the amino acids glutamate and GABA respectively. Bilateral slow synaptic inhibition could also be evoked by lateral funiculus stimulation, mediated by noradrenaline acting via postsynaptic α_2-adrenergic receptors coupled to a potassium conductance (Figure 7.2).

A striking feature of AD-SPN was that the majority exhibited evidence of electrotonic coupling. Synchronous and reciprocal activity, in conjunction with the intrinsic properties can be seen to promote rhythmical and burst firing patterns within this coupled network. The neuronal activity arising from interactions within the network and the strength of the electrotonic connections can be dynamically regulated by calcium. The neuronal activity intrinsic to the network provides a backdrop upon which incoming synaptic input is imposed. That the slow synaptic inhibitory input may depress the entire network is suggested by the absence of oscillations during the PSP. On the other hand the properties of fast synaptic input are subject to activity within the network. The rise time and peak amplitude may be affected by isopotentiality within the network and time course of the EPSP may be truncated by action potential firing in a neighbouring coupled SPN. Furthermore the oscillations may act as a temporal filter whereby only fast synaptic input that coincides with the peak of an oscillation reaches threshold for action potential generation. The intention for this chapter is to integrate the above into a model that gives insight into the central regulation of catecholamine secretion.

7.2 Technical Considerations

Data included in this study were obtained using the blind approach of the patch clamp technique. AD-SPN possess a comparable morphology, of oval somata and long dendritic arbours, and location in the ipsilateral intermediolateral cell columns of the T_4-T_{12} region, to that revealed by previous studies (Strack *et al.*, 1988; Cabot, 1990; Vera *et al.*, 1990). Since clusters of AD-SPN were observed in T_8-T_{11}, these slices were chosen for recording, a procedure that improved the probability of recording from a prelabeled SPN, but recognisably created a bias in the data obtained. Therefore caution should be

applied in extrapolating the results presented here to all AD-SPN. Previous anatomical retrograde labeling studies indicate that as many as 800 AD-SPN are present in the intermediolateral cell columns throughout the thoracic cord, with over 100 SPN present in T_9 (Holets and Elde, 1982; Strack *et al.*, 1988). Therefore the labeling achieved in this study represented a subset of all AD-SPN.

Unilateral adrenalectomy has been observed to decrease contralateral labeling of SPN in the neonatal rat (Ross, 1981), suggesting the possibility of bilateral innervation of the adrenal medulla during development. Retrogradely labeled SPN in rats from 9-16 days were not observed in the contralateral intermediolateral cell column in this study, in accordance with previous studies utilising a variety of retrogradely tracing dyes (e.g. Holets and Elde, 1982; Jensen *et al.*, 1992; Hong and Weaver, 1993).

7.3 A hierarchical and differential control of adrenal catecholamine release

An increasingly differentiated autonomic nervous system is becoming recognised as the structural basis for distinct peripheral organ control (Janig and McLachlan, 1992a; Morrison, 2001 See Chapter 1; Introduction sections 1.1, 1.22, 1.4). In cat, 3 types of SPN located at the T_3 level were discerned based on expression (or absence) of the shoulder on the repolarising phase of the action potential, resting membrane potential, input resistance and the A-conductance (Dembowsky *et al.*, 1986). SPN that project to the superior cervical ganglion possess differences in their intrinsic membrane properties (Spanswick *et al.*, 1998). Approximately one third of these SPN possess a time-dependent inward rectifer I_h, without time-independent rectification. Another third exhibit prolonged transient outward rectification and the remaining third possess time-independent inward rectification and prolonged transient outward rectification. The

absence of a shoulder on the repolarisation phase was noted as was the absence of oscillations in membrane potential (D.Spanswick, personal communications). Other studies report heterogeneity within the SPN population (Yoshimura *et al.*, 1986b; Pickering *et al.*, 1991; Inokuchi *et al.*, 1993c; Miyazaki *et al.*, 1996). In this study, all AD-SPN were relatively homogeneous regarding the expression of active membrane properties. Therefore a component of the differential control of peripheral targets could reside in the homogeneity of intrinsic properties of functional groups of SPN.

Differential release of noradrenaline and adrenaline from the adrenal medulla has long been known (Folkow, 1954; Feuerstein and Gutman, 1971; Marley and Livett, 1987; Edwards *et al.*, 1996). Since physiological stimuli like baroreceptor activation and hypoglycemia can selectively promote noradrenaline or adrenaline release respectively (Feuerstein and Gutman, 1971; Gagner *et al.*, 1985; Khalil *et al.*, 1986; Vollmer *et al.*, 1992) separate neuronal pathways have been proposed as the anatomical substrate to mediate this differential control (Matsui, 1965, 1979; Robinson *et al.*, 1983; Matsui, 1984, 1987). Differences within the AD-SPN population may be a component, for example in cat, where a subpopulation of AD-SPN contain the calcium binding protein, calretinin and predominantly innervate noradrenergic chromaffin cells (Edwards *et al.*, 1996). While such differences have yet to be described in rat, *in vivo* electrophysiological data indicate subtypes of SPN may be categorised according to the relation of their firing patterns to cardiac cycle and their response to electrical stimulation of the rostral ventrolateral medulla (Morrison and Reis, 1991). One group of SPN exhibit a short latency excitation in response to stimulation of the rostral ventrolateral medulla and are inhibited by increased arterial blood pressure (which modulates noradrenaline release) but unaffected by hypoglycemia (which induces adrenaline release). This group are

proposed to innervate noradrenaline secreting chromaffin cells. A second group exhibit long latency, early inhibition and late excitation in response to stimulation of the rostral ventrolateral medulla and are sensitive to glucopenia but relatively insensitive to changes in arterial blood pressure. These SPN are proposed to innervate adrenaline secreting chromaffin cells (Morrison and Cao, 2000) (Figure 7.3). All AD-SPN are inhibited by the Bezold-Jarish reflex (Cao and Morrison, 2000). Thus the features of differential and common regulatory control seem to exist in rat AD-SPN.

One possible source for the fast synaptic input to AD-SPN seen in this study may be cardiac baroreceptors. The primary recipients of baroreceptor afferents, the neurons of the nucleus tractus solitarius, project to numerous brainstem regions including the rostral ventrolateral medulla. The latter is a known source of both glutamatergic and GABAergic input to upper thoracic SPN (Deuchars *et al.*, 1995; Deuchars *et al.*, 1997), and therefore may also project to AD-SPN to modulate the release of noradrenaline. In this study no differences were noted regarding the presence of fast glutamatergic input in the AD-SPN population that could putatively account for noradrenaline versus adrenaline innervating AD-SPN. However it is probable that more than one functional pathway utilises glutamate as a neurotransmitter.

Immunohistochemical studies indicate that selective vasomotor responses engage discrete subsets of neurons in the brainstem region. For example, increases and decreases in arterial blood pressure produced *Fos*-like immunoreactivity in seperate areas of the nucleus tractus solitarius, rostral and caudal ventrolateral medulla, A5 and locus coeruleus, Kölliker-Fuse and parabrachial nucleus (Murphy *et al.*, 1994). Furthermore over 50% of catecholamine positive neurons in A1, A5 and A7 were *Fos*-positive (Murphy *et al.*, 1994). Since baroreceptor activation excites sympathoinhibitory neurons

in order to decrease blood pressure and noradrenaline release, it could be postulated that noradrenergic neurons in brainstem catecholamine cell groups are excited by input from the nucleus tractus solitarius. In turn these fibres project to AD-SPN to inhibit their activity, in a manner similar to the evoked slow IPSP. Such an input would ensure suppression of all the activity in the electrotonically coupled network thus preventing the secretion of noradrenaline.

Adrenal splanchnic sympathetic nerve activity is altered during hypoglycemia to increase adrenaline, but not noradrenaline, release (Vollmer *et al.*, 1992; Morrison and Cao, 2000). Aside from segmental visceral afferents from the liver and pancreas, AD-SPN may receive "information" from glucoresponsive neurons in the ventromedial hypothalamic nuclei or from glucose-sensitive neurons in the lateral hypothalamic area (Oomura *et al.*, 1969; Oomura *et al.*, 1974; Ashford *et al.*, 1990; Silver and Erecinska, 1998). Glucoresponsive neurons translate a low glucose stimuli into a decreased firing rate while glucose-sensitive neurons increase their firing frequency. Both the lateral hypothalamic area and the ventromedial hypothalamus, when electrically stimulated, can promote a selective increase in adrenaline secretion from the adrenal medulla (Brucke, 1952; Katsuki, 1955; Kumon *et al.*, 1977; Sumi and Umeda, 1979; Stoddard-Apter *et al.*, 1983). Therefore AD-SPN that project to adrenaline secreting chromaffin cells may receive excitatory input from glucoresponsive neurons in the ventromedial hypothalamus. On the other hand, AD-SPN may be under tonic inhibition by glucoresponsive neurons in the lateral hypothalamic area which may be relieved during hypoglycemia. Several neurotransmitter/hormonal system may involved in the control of blood glucose via descending pathways from the lateral and ventromedial hypothalamus to AD-SPN. Most noteworthy is orexin; a molecule that has been implicated in controlling food intake and

energy metabolism and that is present in lateral hypothalamic neurons that project to the intermediolateral cell column of the spinal cord (Sakurai *et al.*, 1998; Sakurai, 1999; van den Pol, 1999).

Integrative Mechanisms of AD-SPN

7.41 Intrinsic mechanisms controlling neuronal excitability

The decision of the AD-SPN "to fire or not to fire" is fundamental to adrenal catecholamine release. Action potential generation and repolarisation involves several conductances. The probability of AD-SPN reaching threshold for action potential firing is determined in part by resting membrane potential that is set by conductances that include the inward and the sustained outward potassium-mediated rectifying channels. At least six voltage-dependent conductances contribute to the action potential waveform: the classic Hodgkin-Huxley fast inactivating sodium and delayed rectifying potassium conductances (Miyazaki *et al.*, 1996); two outward rectifying potassium conductances (transient and sustained) and a calcium conductance, mediated by P- and N-type channels (Figure 7.4A). The contribution of at least two additional potassium conductances to the repolarisation of the action potential may highlight the importance of the concentration of calcium influx during spiking.

Mathematical analysis has estimated the local calcium influx during an action potential to be 3-4nM (the rest being bound) that increases to micromolar levels upon subsequent high frequency firing (Gamble and Koch, 1987). Experimental data from cortical pyramidal cells and bullfrog sympathetic ganglion cells have substantiated this hypothetical build up (Hernandez-Cruz *et al.*, 1990; Helmchen *et al.*, 1996). The increase of internal calcium can act as a record of neuronal activity and may be translated to a

process i.e. activation of enzyme or protein that is sensitive to calcium or contribute towards priming the endoplasmic reticular stores for calcium release (Berridge, 1998). The neuron, therefore possesses an index of previous activity and could regulate subsequent activity accordingly. This mechanism has been termed the "calcium set point" hypothesis (Johnson *et al.*, 1992; LeMasson *et al.*, 1993; Turrigiano *et al.*, 1994).

7.42 Sympathetic outflow and AD-SPN bursting

Sympathetic nerve activity is characterised by rhythmical bursts. The prominence of this feature suggests that it can provide both efficiency and flexibility in the regulation of catecholamine release and tone in peripheral structures of the autonomic nervous system (see Chapter 1.23). In the past, the search for loci for sympathetic rhythm generation focussed on autonomic areas in the brainstem (Zhong *et al.*, 1993; Gebber *et al.*, 1999). The present study adds to earlier evidence that bursting activity can also occur at the level of the SPN.

This study presents evidence that AD-SPN in particular possess at least two intrinsic mechanisms that can generate bursts of action potentials, a low threshold calcium spike and oscillations arising from electrotonic coupling, thus permitting the classification of these neurons as endogenous pacemakers (Selverston and Moulins, 1985). Both pacemaker potentials may be crowned with action potentials and subject to dynamic modulation by both intrinsic membrane properties and synaptic input.

A) Intrinsic membrane properties generate burst firing

Burst firing activity can arise out of combinations of intrinsic membrane properties. For example, in the inferior olivary neurons, repetitive calcium spikes arise

from a low threshold calcium conductance and calcium activated potassium conductance; the rate of bursting is determined by the activation of I_h (Bal and McCormick, 1997; Luthi and McCormick, 1998). Interactions between the potassium conductances I_h and I_D can also induce bursting activity (Adams and Levitan, 1985).

The membrane potential at the location of the T-channels determines activation of the low threshold conductance. Hyperpolarisation to approximately –70mV is required to release inactivation, upon which depolarisation, possibly via EPSPs, provides enough excitation to trigger activation of the low threshold spike. Alternatively if membrane potential is in the range or even slightly above that for activation of T-type channels, incoming IPSPs can relieve inactivation to trigger T-type activation on the rebound of the IPSP. The amplitude of the low threshold spike along with slow inactivation kinetics of the T-type channels may be sufficient to generate depolarisation at the soma to evoke an action potential.

The prolongation of firing in a burst that follows the initial sodium spike upon invasion of the soma by the low threshold spike could be the result of 2 mechanisms. Firstly, the plateau of depolarisation of the low threshold spike is sufficiently broad to permit a series of fast sodium spikes (Jahnsen and Llinas, 1984). The burst is terminated by the inactivation of the low threshold spike. Secondly, in cortical neurons, burst firing is facilitated by an afterdepolarising potential (White *et al.*, 1989). Back-propagation of somatic sodium spikes through the dendritic tree induces local depolarisation. The ensuing potential difference between the dendrites and soma induces ohmic currents that invade the soma as an afterdepolarising potential. In AD-SPN, it is likely that both mechanisms contribute to the sustained firing superimposed on the low threshold spike.

In both scenarios, firing may be terminated by the decaying phase of the low threshold spike.

The T-type calcium channels that mediate neuronal burst firing are commonly located on distal dendrites (Christie *et al.*, 1995; Huguenard, 1996; Destexhe *et al.*, 1998). Consequently, the low threshold spike will be modified by active membrane conductances and integrated with incoming synaptic potentials as it is transmitted to the soma. The interplay of the transient outward rectifier and the low threshold calcium spike is interesting because of their "similar" voltage dependencies. Both are inactive at rest and require hyperpolarisation to release inactivation so that they can be activated by depolarisation. Similar to thalamic relay neurons (Pape *et al.*, 1994), the voltage of activation is offset by ≈15mV. Therefore, from hyperpolarised membrane potentials, dendritic depolarisation will activate the low threshold spike before the transient outward rectification and a low threshold spike (or full action potential) will inactivate the channels responsible for the transient outward rectifier. A reduction in the voltage of activation of the transient outward rectifiers could set up a situation in which the activation of the low threshold spike also activates the potassium conductance thus slowing the development of the low threshold spike, and perhaps preventing it from reaching threshold for action potential generation (Figure 7.4B). Recent modeling studies based on experimental data suggest that neuronal activity is preferentially sensitive to small modulations of certain combinations of intrinsic conductances over distinct (large) modulation of one conductance (Goldman *et al.*, 2001). Small changes in the kinetics of the channels that mediate low threshold spike and the transient outward recifiers may have substantial consequences for the firing pattern of AD-SPN.

B) Electrotonic coupling generates burst firing

Electrotonic transmission differs from chemically mediated transmission in its speed and reciprocity. Since electrotonic junctions act as low pass filters, the size of the afterhyperpolarising potential determines burst firing properties. Blockade of the potassium conductances contributing to the afterhyperpolarising potential reduces the number of action potentials per burst to doublet or triplet firing patterns (Spanswick and Logan, 1990b). On the other hand, activation of the transient outward rectifiers prolong the interspike interval promoting low frequency firing and facilitating faithful transmission of the potential through the electrotonic junctions. In addition progressively depolarising stimuli will prevent activation of the transient outward rectifiers thus encoded in an increased firing frequency (Rogawski, 1985).

The impact of electrotonic coupling on neuronal output depends on its prevalence, properties and spatial organisation and also on the manner in which intrinsic and external influences are interpreted. During paired recordings it could be deduced that at least one additional SPN was included in the immediate network. Therefore AD-SPN may be arranged in small groups of oscillators, that could perhaps be entrained or synchronised by a strong input (i.e. the slow synaptic potentials). Indeed the arrangement of multiple central oscillators with free run frequencies that can be synchronised by central drive has been suggested as a means of synchronising pairs of sympathetic nerves involved in thermoregulation (Chang *et al.*, 1999a; Chang *et al.*, 2000a; Gilbey, 2001), although the central oscillators were not identified. Successive activation and synchronisation of AD-SPN units, in addition to the regulation of firing frequency may tailor the release of catecholamines. This could be analogous with the motor system, where successive

recruitment of motor units increases the force of muscle contraction in conjunction with an increased firing frequency (rate-coding) of the active motor units.

Coupled pairs of SPN exhibited differences in their input resistances, resulting in preferential current transfer. This arrangement could give cells dominance of activity over their neighbours, and can have implications for the effects of synaptic input. On the one hand, a single input to the "dominant" SPN could strongly influence the network. On the other hand, synaptic input to a "subservient" SPN could permit its selective activation (or inhibition). Such an arrangement might be described as a distributed parallel network.

Interestingly, both mechanisms that generate burst firing patterns i.e. the low threshold spike and electrotonic coupling, are critically determined by calcium ions: the low threshold spike requires calcium influx through the T-type channels once the membrane is hyperpolarised, while burst firing arising from the electrotonically coupled network is determined by the junctional conductance that is regulated by calcium released from internal stores. Furthermore calcium influx through high voltage activated calcium channels may either directly activate the calcium dependent potassium channels that contribute to the afterhyperpolarising potential or it may evoke calcium release from internal stores which may activate the slow afterhyperpolarising potential. Indeed this mechanism is active in sympathetic postganglionic neurons (Jobling *et al.*, 1993). The dependence on internal calcium of the number of action potentials comprising a burst, interburst amplitude and duration and bursting frequency suggests a central role in the control of neuronal excitability in AD-SPN (see Figure 7.5).

7.43 Integration of electrotonic network activity and synaptic input

Catecholamine release from the adrenal medulla is intimately controlled by the information encoded in the firing pattern and frequency of its preganglionic input. Under resting conditions the ratio of adrenaline to noradrenaline release from the adrenal medulla is 3:1, implying mass release of adrenaline compared to noradrenaline. Furthermore, stimulation of the splanchnic nerve in a burst pattern doubles the ratio of noradrenaline to adrenaline release and induces met-enkephalin release from the chromaffin cells in the adrenal medulla (Marley and Paton, 1961; Klevans, 1970; Bloom *et al.*, 1988). In this study, the regulation of electrotonic junctions by calcium facilitated 3 patterns of activity; high frequency synchronous firing, burst firing and, under high internal calcium conditions, all spontaneous activity ceased (Chapter 4). During these different neuronal activity patterns the junctional conductance, a measure of strength of current transfer and therefore "openness" of the channels, ranged from high to low respectively. Therefore the degree of "openness" of the junctions within the network determines the firing pattern. Subsequently, it could be proposed that the ratio of adrenaline to noradrenaline release is determined by the degree of "openness" of the electrotonic junctions between AD-SPN. At one end of the spectrum (A, below), high junctional conductances facilitate fast synchronous firing that would promote extensive adrenaline release. Subsequent closing (B) of the junctions facilitates a burst-like pattern of activity in the network favouring noradrenaline release. At the other end of the spectrum (C), further closure of the electrotonic junctions silences activity in the network preventing release of either adrenaline or noradrenaline.

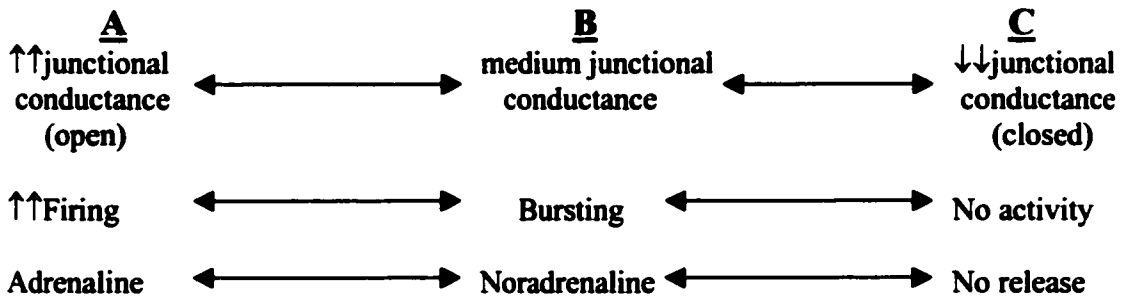

The question then arises "what is capable of regulating the electrotonic junctions so that firing patterns and subsequent adrenaline : noradrenaline ratios are altered?" Demonstrated in Chapter 4 is the ability of calcium released from internal stores to regulate junctional conductance and firing patterns in SPN. As indicated in Figure 7.5, calcium influx may occur through high voltage activated calcium channels, the NMDA sensitive glutamatergic receptor and though the electrotonic junctions themselves. In this scenario, calcium is likely to be acting as an intracellular messenger (Baux *et al.*, 1978). It could be speculated the presence of calretinin, or a similar type of molecule, in noradrenaline AD-SPN may prevent closure of the junctions by high intracellular calcium and thus drive the SPN towards a burst firing pattern of activity.

At the membrane level, mixed chemical and electrotonic synapses have been reported on both somatic and proximal dendritic membranes (Rash *et al.*, 1996). Gap junction plaques have been demonstrated at the centre of the contact zone between pre- and post-synaptic terminals and are surrounded by chemical synapses located at the periphery of the contact zone (Tuttle *et al.*, 1986). These anatomical data support a role for the integration of chemical and electrotonic signalling. Indeed, data presented by Pereda and Faber (1996) indicated that electrotonic coupling can be transiently (≈3mins) modulated by chemical activity. They suggest that calcium influx through NMDA

sensitive glutamatergic receptors activated a calcium-dependent regulatory protein that may phosphorylate the gap junction proteins in the postsynaptic terminal (Pereda and Faber, 1996). Both serine/threonine and tyrosine kinases, that include protein kinase C, mitogen-activated protein kinase (MAPK), v-Src, are able to phosphorylate artificially expressed gap junction channels (Yahuaca *et al.*, 2000, Cooper *et al.*, 2000). However, it is not presently known which protein kinases SPN possess and if they are able to modulate electrotonic junctions.

Neurotransmitters can modulate the degree of electrotonic and dye coupling in adult vertebrate neurons. Dopamine regulation of dye coupling has been reported in the retina (Lasater and Dowling, 1985), medulla, striatum (Cepeda, 1989), nucleus accumbens and in the invertebrate stomatogastric ganglion (Johnson, 1993). Serotonin reduced dye coupling in pyramidal neurons of the somatosensory cortex (Rorig and Sutor, 1996b). Long periods of exposure to noradrenaline decreased dye coupling in astrocytes through α_1-adrenergic receptors coupled to phospholipase C and protein kinase C activation (Giaume *et al.*, 1991). The effect of neurotransmitter modulation of electrotonic junctions in SPN would depend on the initial degree of "openness" of the electrotonic junctions. A decrease in junctional conductance may also act to segregate the network into individual neurons thereby permitting selective activation by synaptic input.

Previous studies indicate selective release of adrenaline or noradrenaline may be mediated by separate central pathways. If regulating the junctional conductance were a prime mechanism for determining the ratio of adrenaline to noradrenaline release the following could be proposed; Firstly, a hypoglycemic stimuli would activate neurons that utilise a neurotransmitter that facilitates a high degree of junction opening to induce high frequency and synchronous firing which would promote adrenaline release.

Secondly, baroreceptor activation excites neurons that utilise a neurotransmitter that favours the point of electrotonic junction "openness" that facilitates bursting and thus noradrenaline release.

Adrenal medulla activation has been reported to exhibit a higher threshold to particular stressors (cold exposure, haemorrage, hypoxia) compared to the rest of the sympathetic nervous system. Other forms of stress (severe hypoglycemia, acute hypoxia, acute ischaemic injury) can preferentially induce the release of catecholamines while suppressing the rest of the sympathetic nervous activity (Young *et al.*, 1984; Edwards, 1990). This may be due to the filtering properties of the electrotonic network present in AD-SPN. Fast synaptic input to AD-SPN is subject to modulation by the activity within the network and thus their influence is likely to be determined by the level of excitability within the network. For example, in the trough of the hyperpolarising phase of the oscillation in membrane potential a fast EPSP is likely to have little effect, while a fast EPSP occurring at the peak of an oscillation may drive the SPN to threshold. In this manner the activity in the network acts as a low pass temporal filter, with the emphasis on the timing of incoming synaptic activity. Such a preferential response of the network to inputs of specific frequencies is known as resonance, a property also observed during sleep in the corticothalamic loop by connections between inhibitory neurons and neurons containing T-type channels (McCormick and Bal, 1997). On the other hand, a slow IPSP, if sufficiently distributed, could have a substantial depressing effect on the oscillatory activity within the network. Therefore the filtering properties of the electrotonically coupled network may account for the high threshold that is required to be passed in order to activate the adrenal medulla.

Synaptic input may also be modified by the intrinsic conductances. Depending on the resting membrane potential, an IPSP may release the inactivation of the transient outward rectifiers and prolong the return to rest. Alternatively EPSPs from hyperpolarised potentials could activate the transient outward rectifiers or the low threshold spike, to modify their decay phase, thus prolonging the window for temporal summation. Furthermore, at positive and negative membrane potentials, synaptic potentials may be subject to shunting through the channels that mediate the sustained outward rectifier and the inward rectifier respectively.

7.5 Disorders implicating AD-SPN

7.51 Sustained outward rectification and seizures

Identification of mutated gene sequences that give rise to benign familial neonatal convulsions (Leppert *et al.*, 1989) led to the cloning of two voltage activated potassium channels (KCNQ2/3) (Biervert *et al.*, 1998) that mediate the pharmacologically identified M-current (Wang *et al.*, 1998). Mutations of the KCNQ2/3 channels leading to reduced current flow by as little as 25%, are sufficient to produce the hyperexcitable state characterising benign familial neonatal convulsions (Schroeder *et al.*, 1998). Similarly pharmacological suppression of the M-conductance induces depolarisation, an increased probability of action potential firing, and central muscarinic agonists are strong convulsants (Turski *et al.*, 1989; Marrion, 1997). The sustained outward rectifier identified in AD-SPN has similar kinetics (low-threshold, non-inactivating, voltage-dependent) and function (suppression of resting membrane potential, contribution to repolarisation of action potential, potential involvement in spike frequency adaptation) to the M-conductance mediated by KCNQ2/3 channels (see Chapter 3). In the same light

therefore, point mutations in the channel subunits or physiological modulation by neurotransmitters of the sustained outward rectifier will have substantial effects on the excitability of AD-SPN. At the very least, a non-action potential evoking stimuli could be turned into one that triggers firing and contributes to subsequent catecholamine release. At the other end of the spectrum, modulation of the sustained outward rectifier could evoke substantial and sustained action potential firing promoting excessive catecholamine release. In addition increased influx of calcium to the SPN would initiate a chain of events that may include calcium release from internal stores, closure of junctions and activation of nitric oxide synthase.

7.52 Hypertension

Hypertension is a sustained increase in systemic arterial pressure, as a consequence of increased peripheral resistance. The resulting increase in blood pressure can lead to stroke and cardiac arrest. That an overactive autonomic nervous system may be the cause of essential hypertension is indicated by enhanced pressor responses to cold and excitement and the slowing of progress of hypertension with drugs that block sympathetic outflow. Furthermore, the number and frequency of bursts in sympathetic nerve discharge increases with the development of hypertension in human subjects (Mancia *et al.*, 1997, 2000) and in animal models (McAllen and Malpas, 1997). Indeed excessive release of catecholamines has been associated with hypertension.

A role for nitric oxide in hypertension is suggested by studies showing inhibition of the synthesis of nitric oxide results in both acute and chronic hypertension, both in animals (Johnson and Freeman, 1992; Manning *et al.*, 1993; Ward and Angus, 1993) and in humans (Sander *et al.*, 1999). A sympathetic neuronal component to hypertension is

indicated by the observation that sympathectomy reduces the hypertensive action of nitric oxide inhibitors (Sander *et al.*, 1995). A subpopulation of SPN, including AD-SPN, contain nitric oxide synthase (Blottner and Baumgarten, 1992; Anderson *et al.*, 1993; Dun *et al.*, 1993; Saito *et al.*, 1994; Chiba and Tanaka, 1998). A reduction in nitric oxide synthase is observed in SPN in spontaneously hypertensive rats (Tang *et al.*, 1995). Interestingly, a high correlation exists between the presence of nitric oxide synthase and mRNA for connexin 32 (Matsumoto *et al.*, 1991). Nitric oxide can regulate coupling in the neocortex (Rorig and Sutor, 1996a), retina (DeVries and Schwartz, 1989) and striatum (O'Donnell and Grace, 1997). Therefore the regulation of SPN excitability by nitric oxide could be a potential mechanism for mediating a hyper autonomic state that may contribute to hypertension.

7.53 Hypercapnia and Hypoxia

The contribution of catecholamine secretion into the bloodstream in response to acute asphyxia (including hypoxia and hypercapnia / acidosis) is a well established emergency homeostatic mechanism, (see Biesold *et al.*, 1989 for references). In hypoxia, splanchnic nerve activity and catecholamine secretion are dependent on activation of the chemoreceptors in the bilateral carotid sinus nerve. In hypercapnia, the response is independent of carotid sinus nerve activation (Biesold *et al.*, 1989; Fukuda *et al.*, 1989). Hypoxia detected by carotid body chemoreceptors has been reported to induce an equal increase in both noradrenaline and adrenaline secretion from the adrenal medulla (Biesold *et al.*, 1989) and a selective activation of SPN whose axons project to adrenaline producing chromaffin cells (Cao and Morrison, 2001). The independence of catecholamine secretion to carotid sinus nerve activation in hypercapnia and high

reduction (but not absence) upon splanchnic nerve severance is suggestive of an additive mechanism involving both a direct effect on the chromaffin cells (Johnson *et al.*, 1981) and central chemoreceptors. As shown in Chapter 3, AD-SPN respond to physiologically low pH with a rapid decrease in resting membrane potential putatively facilitating action potential firing that is mediated by a distinct shift in the positive direction of the voltage of activation of the sustained outward rectifier. This mechanism could directly account for the increase in splanchnic nerve activity and catecholamine secretion observed in response to hypercapnia. SPN have extensive dendritic arbours that form a plexus like arrangement around the central canal area (Forehand, 1990; Vera *et al.*, 1990; Pyner and Coote, 1995) that may function as a detection system for changes in the cerebral spinal fluid composition. Alternatively, rich innervation of the spinal gray matter by small blood vessels emanating from the anterior spinal arteries could provide a local indicator of altered pH.

7.54 Spinal cord injury and autonomic hyperreflexia

Immediately upon spinal cord transection the autonomic nervous system plunges into a state of depression characterised by hypotension and bradycardia. These symptoms in part reflect the lack of supraspinal input to SPN. Within 2-4 weeks tone returns but with a higher end level of activity that, upon visceral or somatic stimulation, can result in hyperreflexic episodes. These life threatening episodes, characterised by dangerously high increases in arterial blood pressure, bradycardia and severe headaches, are mediated by mass discharge of the sympathetic nerves and secretion of catecholamines from the adrenal gland. Much evidence has accumulated to suggest that in the weeks following spinal cord transection, a rewiring of spinal sympathetic circuits takes place, resulting in

a less differentiated autonomic nervous system (Claus-Walker and Halstead, 1982; Wallin and Stjernberg, 1984; Krassioukov and Weaver, 1996; Llewellyn-Smith *et al.*, 1997a; Weaver *et al.*, 1997; Krenz and Weaver, 1998a; Llewellyn-Smith and Weaver, 2001).

Two properties of AD-SPN identified in this study may contribute to the undifferentiated sympathetic nervous system that facilitates autonomic hyperreflexic episodes. Firstly the absence of the substantial inhibition mediated by the noradrenergic slow IPSP is likely to tend AD-SPN towards a hyperexcitable state. Secondly mass activation and synchronisation of SPN across functional boundaries could be mediated by a proliferation of electrotonic coupling. Indeed dye coupling and the upregulation of gap junction connexin proteins has been reported upon deafferentation and axotomy of neurons within the central nervous system (Chang *et al.*, 2000b). These possibilities require further investigation.

7.6 Conclusion

The data presented in this study begin to elucidate the mechanisms by which AD-SPN excitability is regulated and hence by which catecholamine secretion from the adrenal medulla is controlled. If the homogeneity of intrinsic membrane properties in AD-SPN is typical of populations of SPN with a common target organ innervation, this may allow for the differential interpretation of supraspinal synaptic input and provide a base for differential end organ control. The presence of electrotonic coupling in a substantial proportion of AD-SPN provides a cellular mechanism for both the well known sympathetic rhythms observed in sympathetic nerves and for the mass coordination and synchronisation of activity across a population of neurons. Dynamic modulation of

electrotonic coupling strength by calcium modulates firing frequency and imparts directionality to the network. It is possible that other molecules i.e. nitric oxide, cyclic guanylate monophosphate and inositol trisphosphate, and neurotransmitters i.e. noradrenaline, dopamine and serotonin, may have a role in regulating the level of excitability within the electrotonically coupled network and thus contributing to catecholamine release.

Figure 7.1 A schematic diagram to illustrate the intrinsic membrane properties of AD-SPN

Featured are; the voltage dependent sodium conductance (V-dep Na^{+}), the transient outward rectifiers consisting of an A-conductance (I_{TOR}- I_A) and the long duration barium sensitive component (I_{TOR} –Ba^{2+}), the high voltage activated calcium conductance (HVA Ca^{2+}), the low threshold calcium conductance (LTS Ca^{2+}), the anomalous inward rectifying conductance (I_{AR}) and the sustained outward rectifying conductance (I_{SOR}).

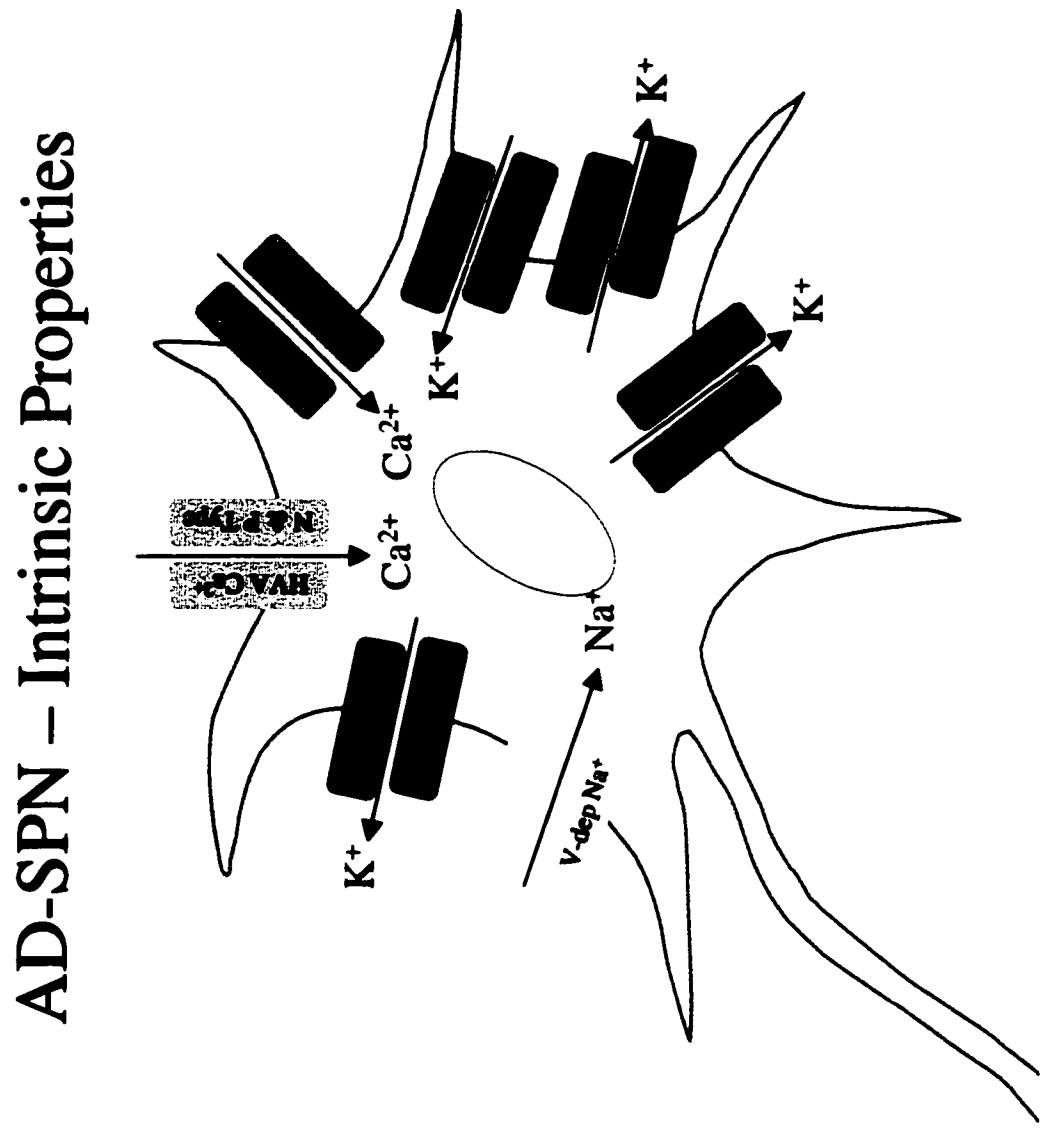

Figure 7.1

Figure 7.2 A schematic diagram to illustrate putative descending bilateral synaptic inputs to AD-SPN

Stimulation of both lateral funiculii evoked; fast EPSPs that were mediated by NMDA and AMPA sensitive glutamatergic receptors, fast IPSPs that were mediated by GABA A receptors, slow IPSPs that were mediated by noradrenaline acting via α_2-adrenergic receptors that were coupled to a potassium conductance.

AD-SPN – Synaptic Properties

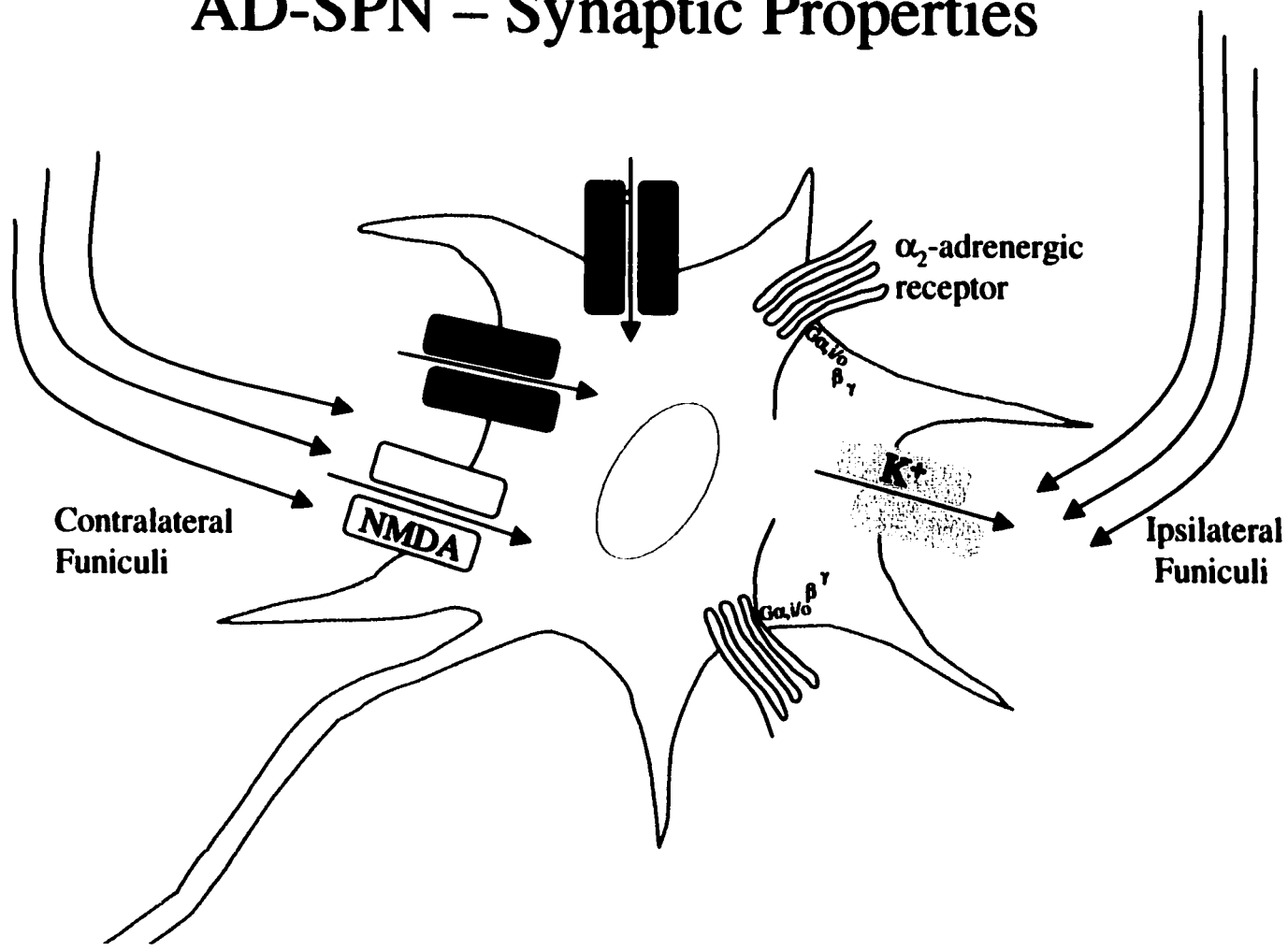

Figure 7.2

Figure 7.3 A schematic diagram depicting pathways that may contribute to a differential control of noradrenaline versus adrenaline secretion from the adrenal medulla

AD-SPN innervating noradrenaline and adrenaline secreting chromaffin cells may be differentiated by their selective activation by baroreceptor activation and hypoglycemia, respectively. 1) Input from the cardiac baroreceptors is relayed to neurons in the nucleus tractus solitarius which impinge on neurons in the rostral ventrolateral medulla that project to AD-SPN. Noradrenergic AD-SPN respond to stimulation of the rostral ventrolateral medulla with a short latency excitation, while adrenergic AD-SPN respond with a long latency, early inhibition and late excitation. Fast amino acid mediated synaptic transmission mediates pathways from the rostral ventrolateral medulla to SPN and may input to AD-SPN. 2) A hypoglycemic stimuli may modulate glucoresponsive or glucose-sensitive neurons in the lateral and / or ventromedial hypothalamus which project to adrenergic AD-SPN to induce a release of adrenaline. 3) Higher brain centres (i.e. the A5) may provide slow (inhibitory) synaptic input to AD-SPN. 4) Further distinctions can be made by the presence of the calretinin in noradrenergic AD-SPN. 5) Noradrenaline is preferentially released from the adrenal medulla by burst stimuli applied to the splanchnic nerve. Adrenaline release is promoted by regular firing patterns (see text for references).

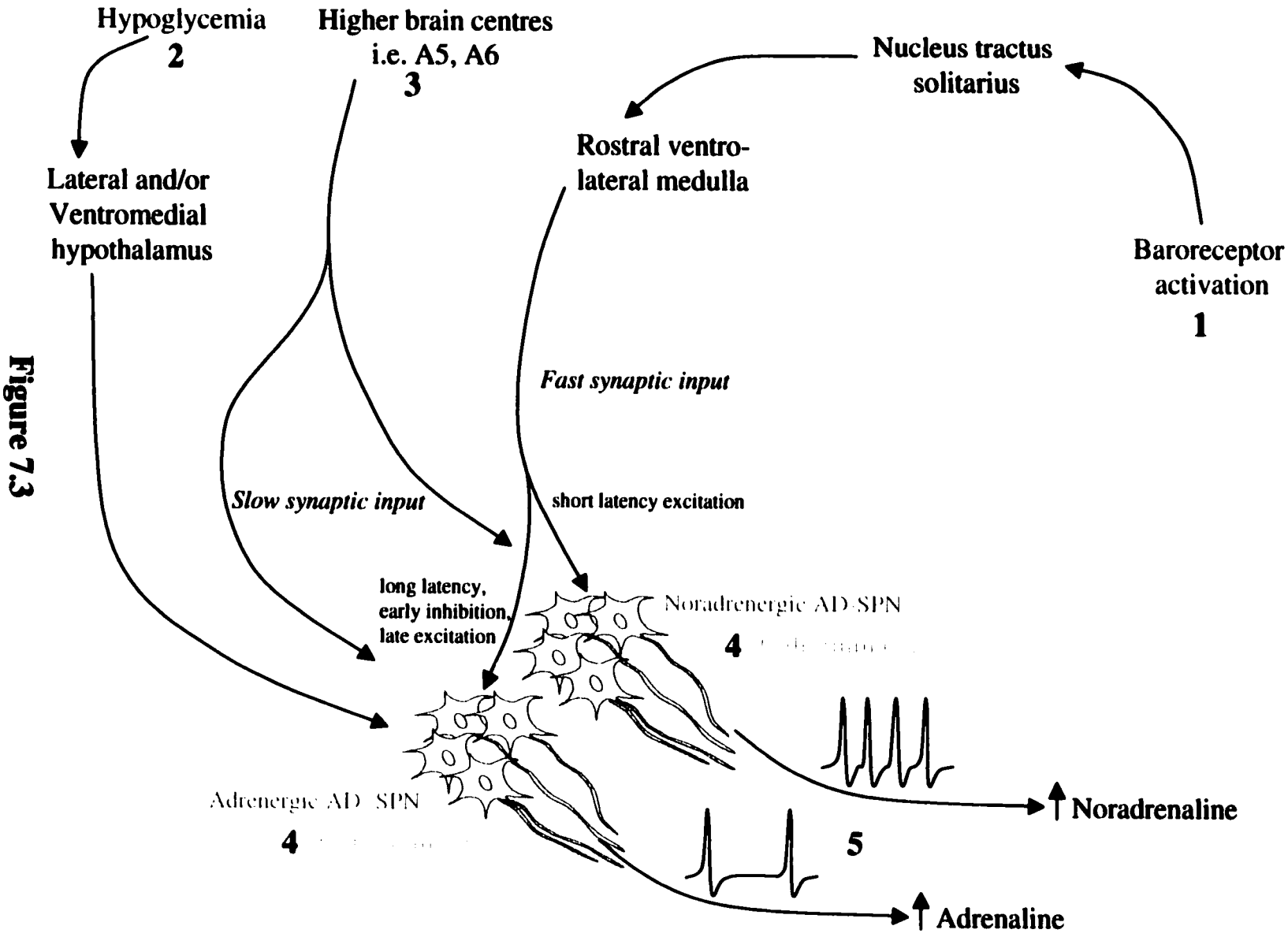
Hypoglycemia
2
Higher brain centres
i.e. A5, A6
3
Nucleus tractus
solitarius
Rostral ventro-
lateral medulla
Lateral and/or
Ventromedial
hypothalamus
Baroreceptor
activation
1
Fast synaptic input
Slow synaptic input
short latency excitation
long latency,
early inhibition,
late excitation
Noradrenergic AD SPN
4
Adrenergic AD SPN
4
5
Noradrenaline
Adrenaline

Figure 7.3

Figure 7.4 A schematic diagram to illustrate the contribution of intrinsic membrane conductances to the action potential waveform and to the generation of burst firing

A, The action potential is generated by the fast-activating voltage-dependent sodium conductance (gNa^+) and is repolarised by the activation of the transient outward rectifier (TOR), in particular the 4-aminopyridine sensitive A-conductance, and by the sustained outward rectifier (SOR) that is sensitive to quinine. Simultaneous activation of the high voltage activated calcium conductance that is mediated by N- and P-type calcium channels produced a shoulder on the repolarisation phase of the action potential. The afterhyperpolarising potential may be extended by the activation of TOR. B, The low threshold spike generated in the dendrites may be subject to modulation by the activation of outwardly rectifying potassium conductances whose channels are placed proximally. Bi, The low threshold spike mediates burst firing at the soma in the absence of TOR. A decrease in voltage of activation of the TOR may delay the onset of burst firing activity (second panel). Bii, the presence of the SOR may prevent threshold for successive action potential firing. The SOR contributes to the repolarising phase of the action potential, therefore the absence of the SOR may broaden the action potential (second panel). The SOR is characterised by a decrease in input resistance. Therefore the absence of the SOR may facilitate action potential firing (third panel).

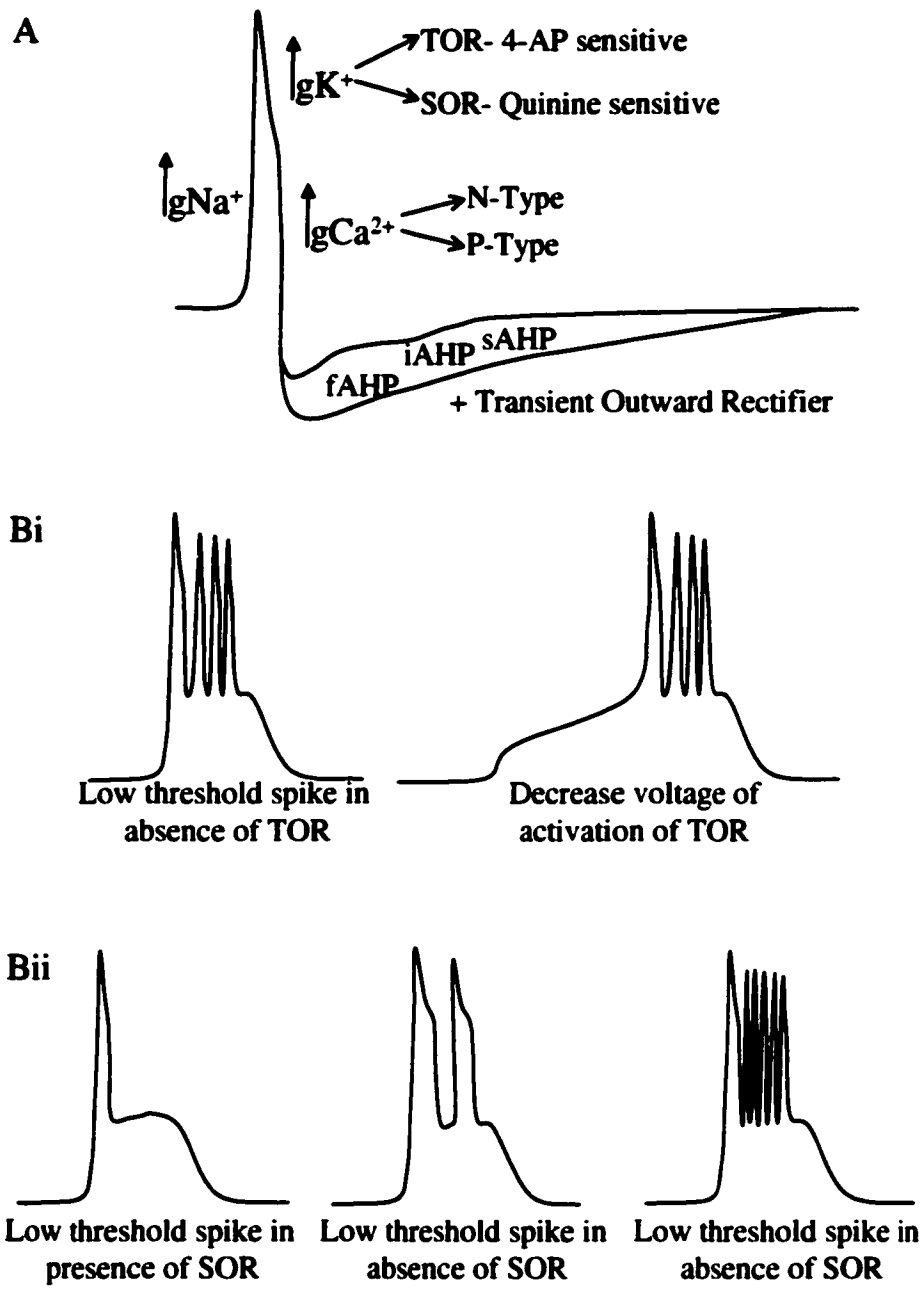
A
gK+
TOR- 4-AP sensitive
SOR- Quinine sensitive
gNa+
gCa2+
N-Type
P-Type
iAHP
sAHP
fAHP
+ Transient Outward Rectifier
Bi
Low threshold spike in absence of TOR
Decrease voltage of activation of TOR
Bii
Low threshold spike in presence of SOR
Low threshold spike in absence of SOR
Low threshold spike in absence of SOR

Figure 7.4

Figure 7.5 Schematic diagram to illustrate possible routes of calcium entry to AD-SPN and potential intracellular targets

Calcium may enter AD-SPN through 1. high and low voltage activated calcium channels 2. NMDA sensitive glutamatergic receptors 3. electrotonic junctions. Internal calcium may 4. permit the opening of calcium-dependent potassium channels, 5. activate calcium dependent protein kinases, 6. activate neuronal nitric oxide synthase to produce nitric oxide 7. prime intracellular stores to induce calcium release, 8. regulate the strength of electrotonic coupling between AD-SPN.

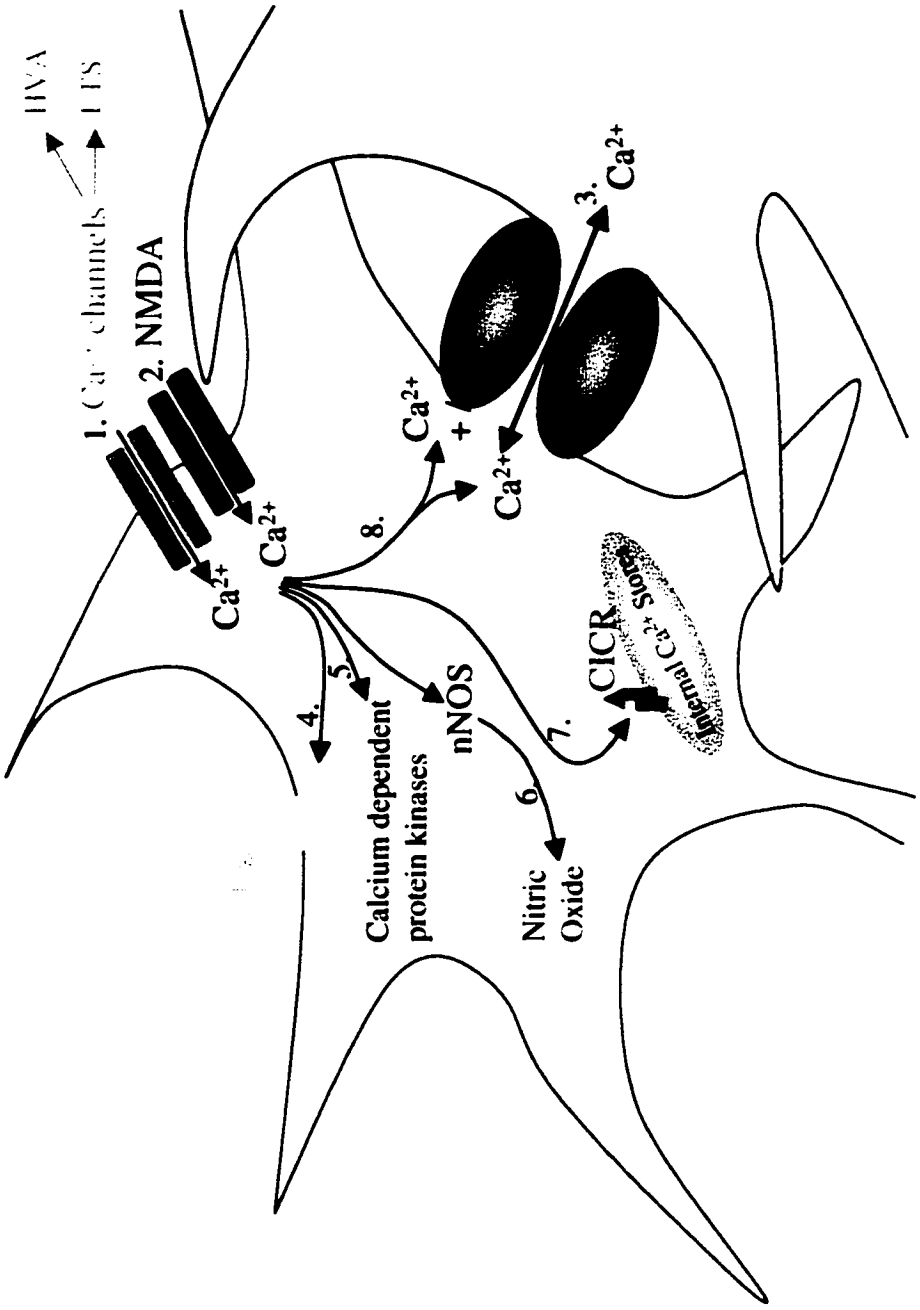
HVA
LVS
1. Ca2+ channels
2. NMDA
Ca2+
Ca2+
Ca2+
8.
Ca2+
+
Ca2+
3.
Ca2+
4.
5
nNOS
7.
CICR
Internal Ca2+ Store
6
Calcium dependent
protein kinases
Nitric
Oxide

Figure 7.5

REFERENCES

Adams WB, Levitan IB (1985) Voltage and ion dependences of the slow currents which mediate bursting in Aplysia neurone R15. *J Physiol* **360**:69-93.

Adrian ED, Bronk DW, Phillips G (1932) Discharges in mammalian sympathetic nerves. *J Physiol* **74**:115-133.

Akeyson EW, Schramm LP (1994) Splanchnic and somatic afferent convergence on cervical spinal neurons of the rat. *Am J Physiol* **266**:R268-276.

Allen AM, Adams JM, Guyenet PG (1993) Role of the spinal cord in generating the 2- to 6-Hz rhythm in rat sympathetic outflow. *Am J Physiol* **264**:R938-945.

Allen JM, Bloom SR, Edwards AV (1984) Release of neuropeptide Y in response to splanchnic nerve stimulation in the conscious calf. *Journal of Physiology* **357**:401-408.

Amara SG, Kuhar MJ (1993) Neurotransmitter transporters: recent progress. *Annu Rev Neurosci* **16**:73-93.

An WF, Bowlby MR, Betty M, Cao J, Ling HP, Mendoza G, Hinson JW, Mattsson KI, Strassle BW, Trimmer JS, Rhodes KJ (2000) Modulation of A-type potassium channels by a family of calcium sensors. *Nature* **403**:553-556.

Anderova M, Duchene AD, Barbara JG, Takeda K (1998) Vasoactive intestinal peptide potentiates and directly stimulates catecholamine secretion from rat adrenal chromaffin cells. *Brain Res* **809**:97-106.

Anderson CR, McLachlan EM, Srb-Christie O (1989) Distribution of sympathetic preganglionic neurons and monoaminergic nerve terminals in the spinal cord of the rat. *J Comp Neurol* **283**:269-284.

Anderson CR, Edwards SL, Furness JB, Bredt DS, Snyder SH (1993) The distribution of nitric oxide synthase-containing autonomic preganglionic terminals in the rat. *Brain Res* **614**:78-85.

Antal M, Polgar E, Chalmers J, Minson JB, Llewellyn-Smith I, Heizmann CW, Somogyi P (1991) Different populations of parvalbumin- and calbindin-D28k-immunoreactive neurons contain GABA and accumulate 3H-D-aspartate in the dorsal horn of the rat spinal cord. *J Comp Neurol* **314**:114-124.

Appel NM, Wessendorf MW, Elde RP (1986) Coexistence of serotonin- and substance P-like immunoreactivity in nerve fibers apposing identified sympathoadrenal preganglionic neurons in rat intermediolateral cell column. *Neurosci Lett* **65**:241-246.

Appel NM, Wessendorf MW, Elde RP (1987) Thyrotropin-releasing hormone in spinal cord: coexistence with serotonin and with substance P in fibers and terminals apposing identified preganglionic sympathetic neurons. *Brain Res* **415**:137-143.

Ascher P, Nowak L (1988) The role of divalent cations in the N-methyl-D-aspartate responses of mouse central neurones in culture. *J Physiol* **399**:247-266.

Ashford ML, Boden PR, Treherne JM (1990) Glucose-induced excitation of hypothalamic neurones is mediated by ATP- sensitive K+ channels. *Pflugers Arch* **415**:479-483.

Auerbach AA, Bennett MV (1969) A rectifying electrotonic synapse in the central nervous system of a vertebrate. *J Gen Physiol* **53**:211-237.

Backman SB, Henry JL (1983a) Effects of GABA and glycine on sympathetic preganglionic neurons in the upper thoracic intermediolateral nucleus of the cat. *Brain Res* **277**:365-369.

Backman SB, Henry JL (1983b) Effects of glutamate and aspartate on sympathetic preganglionic neurons in the upper thoracic intermediolateral nucleus of the cat. *Brain Res* **277**:370-374.

Backman SB, Sequeira-Martinho H, Henry JL (1990) Adrenal versus nonadrenal sympathetic preganglionic neurones in the lower thoracic intermediolateral nucleus of the cat: effects of serotonin, substance P, and thyrotropin-releasing hormone. *Can J Physiol Pharmacol* **68**:1108-1118.

Bacon SJ, Smith AD (1988) Preganglionic sympathetic neurones innervating the rat adrenal medulla: immunocytochemical evidence of synaptic input from nerve terminals containing substance P, GABA or 5-hydroxytryptamine. *J Auton Nerv Syst* **24**:97-122.

Bahring R, Dannenberg J, Peters HC, Leicher T, Pongs O, Isbrandt D (2001) Conserved Kv4 N-terminal domain critical for effects of Kv channel- interacting protein 2.2 on channel expression and gating. *J Biol Chem* **276**:23888-23894.

Bal T, McCormick DA (1997) Synchronized oscillations in the inferior olive are controlled by the hyperpolarization-activated cation current I(h). *J Neurophysiol* **77**:3145-3156.

Barnard EA, Skolnick P, Olsen RW, Mohler H, Sieghart W, Biggio G, Braestrup C, Bateson AN, Langer SZ (1998) International Union of Pharmacology. XV. Subtypes of gamma-aminobutyric acidA receptors: classification on the basis of subunit structure and receptor function. *Pharmacol Rev* **50**:291-313.

Baux G, Simonneau M, Tauc L, Segundo JP (1978) Uncoupling of electrotonic synapses by calcium. *Proc Natl Acad Sci U S A* **75**:4577-4581.

Beaudet MM, Braas KM, May V (1998) Pituitary adenylate cyclase activating polypeptide (PACAP) expression in sympathetic preganglionic projection neurons to the superior cervical ganglion. *J Neurobiol* **36**:325-336.

Beluli DJ, Weaver LC (1991) Areas of rostral medulla providing tonic control of renal and splenic nerves. *Am J Physiol* **261**:H1687-1692.

Bennett MV (1966) Physiology of electrotonic junctions. *Ann N Y Acad Sci* **137**:509-539.

Bennett MV (1977) Electrical transmission: a functional analysis and comparison to chemical transmission. In: Handbook of Physiology, The Nervous System (Kandel ER, ed), pp 357-416. Baltimore: Williams and Wilkins.

Bennett MV (2000) Electrical synapses, a personal perspective (or history). *Brain Res Brain Res Rev* **32**:16-28.

Bennett MV, Nakajima Y, Pappas GD (1967) Physiology and ultrastructure of electrotonic junctions. I. Supramedullary neurons. *J Neurophysiol* **30**:161-179.

Berridge MJ (1998) Neuronal calcium signaling. *Neuron* **21**:13-26.

Biervert C, Schroeder BC, Kubisch C, Berkovic SF, Propping P, Jentsch TJ, Steinlein OK (1998) A potassium channel mutation in neonatal human epilepsy. *Science* **279**:403-406.

Biesold D, Kurosawa M, Sato A, Trzebski A (1989) Hypoxia and hypercapnia increase the sympathoadrenal medullary functions in anesthetized, artificially ventilated rats. *Jpn J Physiol* **39**:511-522.

Bjorklund A, and Skagerberg, G (1982) Descending monoaminergic projections to the spinal cord. In: Brain stem control of spinal mechanisms (Bjorklund A, and Skagerberg, G, ed), pp 55-88. Amsterdam: Elsevier biomedical press.

Blaine JT, Ribera AB (1998) Heteromultimeric potassium channels formed by members of the Kv2 subfamily. *J Neurosci* **18**:9585-9593.

Block BM, Jones SW (1997) Delayed rectifier current of bullfrog sympathetic neurons: ion-ion competition, asymmetrical block and effects of ions on gating. *J Physiol* **499**:403-416.

Bloom SR, Edwards AV, Jones CT (1988) The adrenal contribution to the neuroendocrine responses to splanchnic nerve stimulation in conscious calves. *J Physiol* **397**:513-526.

Bloom SR, Edwards AV, Jones CT (1989) Neuroendocrine responses to stimulation of the splanchnic nerves in bursts in conscious, adrenalectomized, weaned lambs. *J Physiol* **417**:79-89.

Blottner D, Baumgarten HG (1992) Nitric oxide synthetase (NOS)-containing sympathoadrenal cholinergic neurons of the rat IML-cell column: evidence from histochemistry, immunohistochemistry, and retrograde labeling. *J Comp Neurol* **316**:45-55.

Bochefontaine L (1876) Etude experimentale de l'influence exercee par la faradiation de l'ecorce grise du cerveau sur quelques fonctions de la vie organique. *Arch Physiol Norm Pathol Ser* **2**:140-172.

Bogan N, Mennone A, Cabot JB (1989) Light microscopic and ultrastructural localization of GABA-like immunoreactive input to retrogradely labeled sympathetic preganglionic neurons. *Brain Res* **505**:257-270.

Boksa P, Livett BG (1984) Substance P protects against desensitization of the nicotinic response in isolated adrenal chromaffin cells. *J Neurochem* **42**:618-627.

Bolanos JP, Medina JM (1996) Induction of nitric oxide synthase inhibits gap junction permeability in cultured rat astrocytes. *J Neurochem* **66**:2091-2099.

Bredt DS, Wang TL, Cohen NA, Guggino WB, Snyder SH (1995) Cloning and expression of two brain-specific inwardly rectifying potassium channels. *Proc Natl Acad Sci U S A* **92**:6753-6757.

Brew HM, Forsythe ID (1995) Two voltage-dependent K+ conductances with complementary functions in postsynaptic integration at a central auditory synapse. *J Neurosci* **15**:8011-8022.

Bronk DW, Ferguson, L.K., Margaria, R., Solant D.Y., (1936) The activity of the cardiac sympathetic centres. *Am J Physiol* **117**:237-249.

Brown H, Difrancesco D (1980) Voltage-clamp investigations of membrane currents underlying pace-maker activity in rabbit sino-atrial node. *J Physiol* **308**:331-351.

Brucke F, Kaindl F, Mayer H (1952) Uber die veranderung in der zusammemsetzung des nebennierenmarkinkretes bei elektrish reizung des hypothalamus. *Arch Int Pharmacodyn* **88**:497.

Bruzzone R, White TW, Paul DL (1996) Connections with connexins: the molecular basis of direct intercellular signaling. *Eur J Biochem* **238**:1-27.

Bylund DB (1992) Subtypes of alpha 1- and alpha 2-adrenergic receptors. *Faseb J* **6**:832-839.

Bylund DB, Ray-Prenger C (1989) Alpha-2A and alpha-2B adrenergic receptor subtypes: attenuation of cyclic AMP production in cell lines containing only one receptor subtype. *J Pharmacol Exp Ther* **251**:640-644.

Bylund DB, Blaxall HS, Iversen LJ, Caron MG, Lefkowitz RJ, Lomasney JW (1992) Pharmacological characteristics of alpha 2-adrenergic receptors: comparison of pharmacologically defined subtypes with subtypes identified by molecular cloning. *Mol Pharmacol* **42**:1-5.

Byrum CE, Guyenet PG (1987) Afferent and efferent connections of the A5 noradrenergic cell group in the rat. *J Comp Neurol* **261**:529-542.

Byrum CE, Stornetta R, Guyenet PG (1984) Electrophysiological properties of spinally-projecting A5 noradrenergic neurons. *Brain Res* **303**:15-29.

Cabot JB (1990) Sympathetic Preganglionic Neurons: Cytoarchitecture, Ultrastructure and Biophysical Properties. In: Central Regulation of Autonomic Functions (Loewy AD, Spyer, K.M., ed), pp 44-67. New York: Oxford University Press.

Cabot JB, Bogan N (1987) Light microscopic observations on the morphology of sympathetic preganglionic neurons in the pigeon, Columba livia. *Neuroscience* **20**:467-486.

Cabot JB, Alessi V, Bushnell A (1992) Glycine-like immunoreactive input to sympathetic preganglionic neurons. *Brain Res* **571**:1-18.

Cabot JB, Edwards E, Bogan N, Schechter N (1984) Alpha-2-adrenergic receptors in avian spinal cord: increases in apparent density associated with the sympathetic preganglionic cell column. *J Auton Nerv Syst* **11**:77-89.

Cabot JB, Alessi V, Carroll J, Ligorio M (1994) Spinal cord lamina V and lamina VII interneuronal projections to sympathetic preganglionic neurons. *J Comp Neurol* **347**:515-530.

Cabot JB, Bushnell A, Alessi V, Mendell NR (1995) Postsynaptic gephyrin immunoreactivity exhibits a nearly one-to-one correspondence with gamma-aminobutyric acid-like immunogold-labeled synaptic inputs to sympathetic preganglionic neurons. *J Comp Neurol* **356**:418-432.

Cammack C, Logan SD (1996) Excitation of rat sympathetic preganglionic neurones by selective activation of the NK1 receptor. *J Auton Nerv Syst* **57**:87-92.

Cannon WB (1939) The wisdom of the body: New York.

Cannon WB, Newton NF, Bright EM, MenkinV, Moore RM (1929) Some aspects of the physiology of animals susriving complete exclusion of sympathetic nerve impulses. *Am J Physiol* **89**:84-107.

Cao WH, Morrison SF (2000) Responses of adrenal sympathetic preganglionic neurons to stimulation of cardiopulmonary receptors. *Brain Res* **887**:46-52.

Cao WH, Morrison SF (2001) Differential chemoreceptor reflex responses of adrenal preganglionic neurons. *Am J Physiol Regul Integr Comp Physiol* **281**:R1825-1832.

Carbone E, Lux HD (1984) A low voltage-activated, fully inactivating Ca channel in vertebrate sensory neurones. *Nature* **310**:501-502.

Carlen PL, Skinner F, Zhang L, Naus C, Kushnir M, Perez Velazquez JL (2000) The role of gap junctions in seizures. *Brain Res Brain Res Rev* **32**:235-241.

Carlsson A, Falck, B, Fuxe K, Hillarp N, (1964) Cellular localisation of monoamines in the spinal cord. *Acta physiologica scandanavica* **60**:112-119.

Cechetto DF, Saper CB (1988) Neurochemical organization of the hypothalamic projection to the spinal cord in the rat. *J Comp Neurol* **272**:579-604.

Cepeda C (1989) dye-coupling in the neostriatum of the rat. I. Modulation by dopamine depleting lesions. *Synapse* **2**:229-237.

Chang HS, Staras K, Gilbey MP (2000a) Multiple oscillators provide metastability in rhythm generation. *J Neurosci* **20**:5135-5143.

Chang HS, Staras K, Smith JE, Gilbey MP (1999a) Sympathetic neuronal oscillators are capable of dynamic synchronization. *J Neurosci* **19**:3183-3197.

Chang Q, Gonzalez M, Pinter MJ, Balice-Gordon RJ (1999b) Gap junctional coupling and patterns of connexin expression among neonatal rat lumbar spinal motor neurons. *J Neurosci* **19**:10813-10828.

Chang Q, Pereda A, Pinter MJ, Balice-Gordon RJ (2000b) Nerve injury induces gap junctional coupling among axotomized adult motor neurons. *J Neurosci* **20**:674-684.

Charlton CG, Helke CJ (1987) Substance P-containing medullary projections to the intermediolateral cell column: identification with retrogradely transported rhodamine- labeled latex microspheres and immunohistochemistry. *Brain Res* **418**:245-254.

Chiba T, Masuko S (1986) Direct synaptic contacts of catecholamine axons on the preganglionic sympathetic neurons in the rat thoracic spinal cord. *Brain Res* **380**:405-408.

Chiba T, Kaneko T (1993) Phosphate-activated glutaminase immunoreactive synapses in the intermediolateral nucleus of rat thoracic spinal cord. *Neuroscience* **57**:823-831.

Chiba T, Tanaka K (1998) A target specific pathway from nitric oxide synthase immunoreactive preganglionic sympathetic to superior cervical ganglion neurons innervating the submandibular salivary gland. *J Auton Nerv Syst* **71**:139-147.

Christie BR, Eliot LS, Ito K, Miyakawa H, Johnston D (1995) Different Ca2+ channels in soma and dendrites of hippocampal pyramidal neurons mediate spike-induced Ca^{2+} influx. *J Neurophysiol* **73**:2553-2557.

Christie MJ, Williams JT, North RA (1989) Electrical coupling synchronizes subthreshold activity in locus coeruleus neurons in vitro from neonatal rats. *J Neurosci* **9**:3584-3589.

Church J, Baimbridge KG (1991) Exposure to high-pH medium increases the incidence and extent of dye coupling between rat hippocampal CA1 pyramidal neurons in vitro. *J Neurosci* **11**:3289-3295.

Clark FM, Proudfit HK (1991) The projection of noradrenergic neurons in the A7 catecholamine cell group to the spinal cord in the rat demonstrated by anterograde tracing combined with immunocytochemistry. *Brain Res* **547**:279-288.

Clark FM, Proudfit HK (1993) The projections of noradrenergic neurons in the A5 catecholamine cell group to the spinal cord in the rat: anatomical evidence that A5 neurons modulate nociception. *Brain Res* **616**:200-210.

Clark FM, Yeomans DC, Proudfit HK (1991) The noradrenergic innervation of the spinal cord: differences between two substrains of Sprague-Dawley rats determined using retrograde tracers combined with immunocytochemistry. *Neurosci Lett* **125**:155-158.

Claus-Walker J, Halstead LS (1982) Metabolic and endocrine changes in spinal cord injury: II (section 1). Consequences of partial decentralization of the autonomic nervous system. *Arch Phys Med Rehabil* **63**:569-575.

Clement ME, McCall RB (1995) Effects of inhibitory amino acids on the frequency components in sympathetic nerve discharge. *Brain Res* **696**:258-261.

Clements JD, Lester RA, Tong G, Jahr CE, Westbrook GL (1992) The time course of glutamate in the synaptic cleft. *Science* **258**:1498-1501.

Cobbett P, Legendre P, Mason WT (1989) Characterization of three types of potassium current in cultured neurones of rat supraoptic nucleus area. *J Physiol* **410**:443-462.

Cohen AS, Moore KA, Bangalore R, Jafri MS, Weinreich D, Kao JP (1997) Ca(2+)-induced Ca2+ release mediates Ca2+ transients evoked by single action potentials in rabbit vagal afferent neurones. *J Physiol* **499**:315-328.

Cohen MI, Gootman PM (1970) Periodicities in efferent discharge of splanchnic nerve of the cat. *Am J Physiol* **218**:1092-1101.

Collingridge GL, Lester RA (1989) Excitatory amino acid receptors in the vertebrate central nervous system. *Pharmacol Rev* **41**:143-210.

Colquhoun D, Jonas P, Sakmann B (1992) Action of brief pulses of glutamate on AMPA/kainate receptors in patches from different neurones of rat hippocampal slices. *J Physiol* **458**:261-287.

Comer AM, Gibbons HM, Qi J, Kawai Y, Win J, Lipski J (1999) Detection of mRNA species in bulbospinal neurons isolated from the rostral ventrolateral medulla using single-cell RT-PCR. *Brain Res Brain Res Protoc* **4**:367-377.

Commissiong JW (1981) Evidence that the noradrenergic coerulospinal projection decussates at the spinal level. *Brain Res* **212**:145-151.

Connor HE, Drew GM (1987) Do adrenaline-containing neurones from the rostral ventrolateral medulla excite preganglionic sympathetic cell bodies? *J Auton Pharmacol* **7**:87-96.

Constanti A, Galvan M (1983) Fast inward-rectifying current accounts for anomalous rectification in olfactory cortex neurones. *J Physiol* **335**:153-178.

Cooper CD, Solan JL, Dolejsi MK, Lampe PD (2000) Analysis of connexin phosphorylation sites. *Methods* **20**: 196-204

Coote JH (1988) The organisation of cardiovascular neurons in the spinal cord. *Rev Physiol Biochem Pharmacol* **110**:147-285.

Coote JH (1985) Noradrenergic projections to the spinal cord and their role in cardiovascular control. *J Auton Nerv Syst* **14**:255-262.

Coote JH, Macleod VH (1974) The influence of bulbospinal monoaminergic pathways on sympathetic nerve activity. *J Physiol* **241**:453-475.

Coote JH, Macleod VH (1975) The spinal route of sympatho-inhibitory pathways descending from the medulla oblongata. *Pflugers Arch* **359**:335-347.

Coote JH, Westbury DR (1979) Intracellular recordings from sympathetic preganglionic neurones. *Neurosci Lett* **15**:171-175.

Coote JH, Macleod VH, Fleetwood-Walker SM, Gilbey MP (1981a) Baroreceptor inhibition of sympathetic activity at a spinal site. *Brain Res* **220**:81-93.

Coote JH, Macleod VH, Fleetwood-Walker S, Gilbey MP (1981b) The response of individual sympathetic preganglionic neurones to microelectrophoretically applied endogenous monoamines. *Brain Res* **215**:135-145.

Coupland RE (1965) The Natural History of the Chromaffin Cell. London: Longmans.

Coyle JT (1997) The nagging question of the function of N-acetylaspartylglutamate. *Neurobiol Dis* **4**:231-238.

Cribbs LL, Lee JH, Yang J, Satin J, Zhang Y, Daud A, Barclay J, Williamson MP, Fox M, Rees M, Perez-Reyes E (1998) Cloning and characterization of alpha1H from human heart, a member of the T-type Ca2+ channel gene family. *Circ Res* **83**:103-109.

Dabire H (1986) Idazoxan: a novel pharmacological tool for the study of alpha 2-adrenoceptors. *J Pharmacol* **17**:113-118.

Dahlstrom A, Fuxe K, (1965) Evidence for the existance of monoamine groups in the central nervous system. II. Experimentally induced changes in the intraneuronal amine levels of bulbospinal neuron systems. *Acta Physiol Scand Suppl* **247**:1-36.

Daly JW, Butts-Lamb P, Padgett W (1983) Subclasses of adenosine receptors in the central nervous system: interaction with caffeine and related methylxanthines. *Cell Mol Neurobiol* **3**:69-80.

Dampney RA (1994) Functional organization of central pathways regulating the cardiovascular system. *Physiol Rev* **74**:323-364.

Dampney RA, McAllen RM (1988) Differential control of sympathetic fibres supplying hindlimb skin and muscle by subretrofacial neurones in the cat. *J Physiol* **395**:41-56.

Dampney RA, Goodchild AK, Tan E (1985) Vasopressor neurons in the rostral ventrolateral medulla of the rabbit. *J Auton Nerv Syst* **14**:239-254.

Decher N, Maier M, Dittrich W, Gassenhuber J, Bruggemann A, Busch AE, Steinmeyer K (2001) Characterization of TASK-4, a novel member of the pH-sensitive, two-pore domain potassium channel family. *FEBS Lett* **492**:84-89.

Delius W, Hagbarth KE, Hongell A, Wallin BG (1972) Manoeuvres affecting sympathetic outflow in human skin nerves. *Acta Physiol Scand* **84**:177-186.

Dembowsky K, Czachurski J, Seller H (1985a) Morphology of sympathetic preganglionic neurons in the thoracic spinal cord of the cat: an intracellular horseradish peroxidase study. *J Comp Neurol* **238**:453-465.

Dembowsky K, Czachurski J, Seller H (1985b) An intracellular study of the synaptic input to sympathetic preganglionic neurones of the third thoracic segment of the cat. *J Auton Nerv Syst* **13**:201-244.

Dembowsky K, Czachurski J, Seller H (1986) Three types of sympathetic preganglionic neurones with different electrophysiological properties are identified by intracellular recordings in the cat. *Pflugers Arch* **406**:112-120.

Dermietzel R (1996) Molecular diversity and plasticity of gap junctions in the nervous system. In: Gap junctions in the nervous system (Spray DC, Dermietzel R, ed), pp 13-38. Heidelberg: Springer-Verlag.

Dermietzel R, Spray DC (1993) Gap junctions in the brain: where, what type, how many and why? *Trends Neurosci* **16**:186-192.

Destexhe A, Neubig M, Ulrich D, Huguenard J (1998) Dendritic low-threshold calcium currents in thalamic relay cells. *J Neurosci* **18**:3574-3588.

Deuchars SA, Morrison SF, Gilbey MP (1995) Medullary-evoked EPSPs in neonatal rat sympathetic preganglionic neurones in vitro. *J Physiol* **487**:453-463.

Deuchars SA, Spyer KM, Gilbey MP (1997) Stimulation within the rostral ventrolateral medulla can evoke monosynaptic GABAergic IPSPs in sympathetic preganglionic neurons in vitro. *J Neurophysiol* **77**:229-235.

DeVries SH, Schwartz EA (1989) Modulation of an electrical synapse between solitary pairs of catfish horizontal cells by dopamine and second messengers. *J Physiol* **414**:351-375.

Dittmar C (1873) Uber die lage sogenannten gefasscentrums in der Medulla oblongata. *Ber Verh Sachs Akad Wiss Leipzis Math Phys Kl* **25**:449-469.

Dolphin AC (1995) The G.L. Brown Prize Lecture. Voltage-dependent calcium channels and their modulation by neurotransmitters and G proteins. *Exp Physiol* **1**:1-36.

Donevan SD, Rogawski MA (1993) GYKI 52466, a 2,3-benzodiazepine, is a highly selective, noncompetitive antagonist of AMPA/kainate receptor responses. *Neuron* **10**:51-59.

Doupnik CA, Davidson N, Lester HA (1995) The inward rectifier potassium channel family. *Curr Opin Neurobiol* **5**:268-277.

Doxey JC, Roach AG, Smith CF (1983) Studies on RX 781094: a selective, potent and specific antagonist of alpha 2-adrenoceptors. *Br J Pharmacol* **78**:489-505.

Draguhn A, Traub RD, Schmitz D, Jefferys JG (1998) Electrical coupling underlies high-frequency oscillations in the hippocampus in vitro. *Nature* **394**:189-192.

Drolet G, Gauthier P (1985) Peripheral and central mechanisms of the pressor response elicited by stimulation of the locus coeruleus in the rat. *Can J Physiol Pharmacol* **63**:599-605.

Dudek F, Andrew RD, MacVicar BA, Snow RW, Taylor CP, (1983) Recent evidence for and possible significance of gap junctions and electrotonic synapses in the mammalian brain. In: Basic mechanisms of neuronal hyperexcitability, pp 31-73. New York: Alan R. Liss Inc.

Dudley MW (1988) The depletion of rat cortical norepinephrine and the inhibition of [3H]norepinephrine uptake by xylamine does not require monoamine oxidase activity. *Life Sci* **43**:1871-1877.

Dun NJ, Mo N (1988) In vitro effects of substance P on neonatal rat sympathetic preganglionic neurones. *J Physiol* **399**:321-333.

Dun NJ, Mo N (1989) Inhibitory postsynaptic potentials in neonatal rat sympathetic preganglionic neurones in vitro. *J Physiol* **410**:267-281.

Dun NJ, Dun SL, Wu SY, Forstermann U, Schmidt HH, Tseng LF (1993) Nitric oxide synthase immunoreactivity in the rat, mouse, cat and squirrel monkey spinal cord. *Neuroscience* **54**:845-857.

Edwards A (1990) Autonomic control of endocrine pancreatic and adrenal function. In: Central regulation of autonomic function (Loewy A, Spyer KM, ed), pp 286-309. New York, Oxford: Oxford University Press.

Edwards AV, Jones CT (1993) Autonomic control of adrenal function. *J Anat* **183**:291-307.

Edwards DH, Heitler WJ, Krasne FB (1999) Fifty years of a command neuron: the neurobiology of escape behavior in the crayfish. *Trends Neurosci* **22**:153-161.

Edwards SL, Anderson CR, Southwell BR, McAllen RM (1996) Distinct preganglionic neurons innervate noradrenaline and adrenaline cells in the cat adrenal medulla. *Neuroscience* **70**:825-832.

Egelhaaf M, Benjamin PR (1983) Coupled neuronal oscillators in the snail Lymnaea stagnalis: endogenous cellular properties and network interactions. *J Exp Biol* **102**:93-114.

Elias CF, Lee C, Kelly J, Aschkenasi C, Ahima RS, Couceyro PR, Kuhar MJ, Saper CB, Elmquist JK (1998) Leptin activates hypothalamic CART neurons projecting to the spinal cord. *Neuron* **21**:1375-1385.

Enoch DM, Kerr FW (1967a) Hypothalamic vasopressor and vesicopressor pathways. II. Anatomic study of their course and connections. *Arch Neurol* **16**:307-320.

Enoch DM, Kerr FW (1967b) Hypothalamic vasopressor and vesicopressor pathways. I. Functional studies. *Arch Neurol* **16**:290-306.

Ernsberger P, Meeley MP, Mann JJ, Reis DJ (1987) Clonidine binds to imidazole binding sites as well as alpha 2- adrenoceptors in the ventrolateral medulla. *Eur J Pharmacol* **134**:1-13.

Ertel SI, Ertel EA (1997) Low-voltage-activated T-type Ca2+ channels. *Trends Pharmacol Sci* **18**:37-42.

Farmer DH (1998) Rhythmicity, synchronisation and binding in human and primate motor systems. *J Physiol* **509.1**:3-14.

Fedida D, Maruoka ND, Lin S (1999) Modulation of slow inactivation in human cardiac Kv1.5 channels by extra- and intracellular permeant cations. *J Physiol* **515**:315-329.

Feuerstein G, Gutman Y (1971) Preferential secretion of adrenaline or noradrenaline by the cat adrenal in vivo in response to different stimuli. *Br J Pharmacol* **43**:764-775.

Fink M, Lesage F, Duprat F, Heurteaux C, Reyes R, Fosset M, Lazdunski M (1998) A neuronal two P domain K+ channel stimulated by arachidonic acid and polyunsaturated fatty acids. *Embo J* **17**:3297-3308.

Fleetwood-Walker SM, Coote JH (1981) The contribution of brain stem catecholamine cell groups to the innervation of the sympathetic lateral cell column. *Brain Res* **205**:141-155.

Folkow B (2000) Perspectives on the integrative functions of the 'sympatho-adrenomedullary system'. *Auton Neurosci* **83**:101-115.

Folkow B, von Euler US (1954) Selective activation of noradrenaline and adrenaline producing cells in the cat's adrenal gland by hypothalamic stimulation. *Circ Res* **11**:191-195.

Forehand CJ (1990) Morphology of sympathetic preganglionic neurons in the neonatal rat spinal cord: an intracellular horseradish peroxidase study. *J Comp Neurol* **298**:334-342.

Forehand CJ, Ezerman EB, Rubin E, Glover JC (1994) Segmental patterning of rat and chicken sympathetic preganglionic neurons: correlation between soma position and axon projection pathway. *J Neurosci* **14**:231-241.

Francke PF, Culberson JL, Carmichael SW, Robinson RL (1982) Bilateral secretory responses of the adrenal medulla during stimulation of hypothalamic or mesencephalic sites. *J Neurosci Res* **8**:1-6.

Fritschy JM, Grzanna R (1990) Demonstration of two separate descending noradrenergic pathways to the rat spinal cord: evidence for an intragriseal trajectory of locus coeruleus axons in the superficial layers of the dorsal horn. *J Comp Neurol* **291**:553-582.

Fritschy JM, Lyons WE, Mullen CA, Kosofsky BE, Molliver ME, Grzanna R (1987) Distribution of locus coeruleus axons in the rat spinal cord: a combined anterograde transport and immunohistochemical study. *Brain Res* **437**:176-180.

Fukuda T, Kosaka T (2000) Gap junctions linking the dendritic network of GABAergic interneurons in the hippocampus. *J Neurosci* **20**:1519-1528.

Fukuda Y, Sato A, Suzuki A, Trzebski A (1989) Autonomic nerve and cardiovascular responses to changing blood oxygen and carbon dioxide levels in the rat. *J Auton Nerv Syst* **28**:61-74.

Fulton BP, Miledi R, Takahashi T (1980) Electrical synapses between motoneurons in the spinal cord of the newborn rat. *Proc R Soc Lond B Biol Sci* **208**:115-120.

Furshpan E, Potter DD, (1959) Transmission at the giant motor synapses of the crayfish. *J Physiol* **145**:289-325.

Gagner JP, Gauthier S, Sourkes TL (1985) Descending spinal pathways mediating the responses of adrenal tyrosine hydroxylase and catecholamines to insulin and 2-deoxyglucose. *Brain Res* **325**:187-197.

Galarreta M, Hestrin S (1999) A network of fast-spiking cells in the neocortex connected by electrical synapses. *Nature* **402**:72-75.

Gamble E, Koch C (1987) The dynamics of free calcium in dendritic spines in response to repetitive synaptic input. *Science* **236**:1311-1315.

Gebber GL, Zhong S, Lewis C, Barman SM (1999) Differential patterns of spinal sympathetic outflow involving a 10-Hz rhythm. *J Neurophysiol* **82**:841-854.

Getting PA, Willows AO (1973) Burst formation in electrically coupled neurons. *Brain Res* **63**:424-429.

Getting PA, Willows AO (1974) Modification of neuron properties by electrotonic synapses. II. Burst formation by electrotonic synapses. *J Neurophysiol* **37**:858-868.

Giaume C, Marin P, Cordier J, Glowinski J, Premont J (1991) Adrenergic regulation of intercellular communications between cultured striatal astrocytes from the mouse. *Proc Natl Acad Sci U S A* **88**:5577-5581.

Gibson JR, Beierlein M, Connors BW (1999) Two networks of electrically coupled inhibitory neurons in neocortex. *Nature* **402**:75-79.

Gilbey MP (2001) Multiple oscillators, dynamic synchronization and sympathetic control. *Clin Exp Pharmacol Physiol* **28**:130-137.

Gilbey MP, Stein RD (1991) Characteristics of sympathetic preganglionic neurones in the lumbar spinal cord of the cat. *J Physiol* **432**:427-443.

Gilbey MP, Coote JH, Macleod VH, Peterson DF (1981) Inhibition of sympathetic activity by stimulating in the raphe nuclei and the role of 5-hydroxytryptamine in this effect. *Brain Res* **226**:131-142.

Goadsby PJ (1985) Brainstem activation of the adrenal medulla in the cat. *Brain Res* **327**:241-248.

Goldman MS, Golowasch J, Marder E, Abbott LF (2001) Global structure, robustness, and modulation of neuronal models. *J Neurosci* **21**:5229-5238.

Goldstein SA, Bockenhauer D, O'Kelly I, Zilberberg N (2001) Potassium leak channels and the KCNK family of two-P-domain subunits. *Nat Rev Neurosci* **2**:175-184.

Gordon FJ (1985) Spinal GABA receptors and central cardiovascular control. *Brain Res* **328**:165-169.

Grkovic I, Andersen, C.R., (1996) Distribution of immunoreactivity for the NK1 receptor on different subpopulations of sympathetic preganglionic neurons in the rat. *J Comp Neurol* **374**:376-386.

Grossman SD, Wolfe BB, Yasuda RP, Wrathall JR (1999) Alterations in AMPA receptor subunit expression after experimental spinal cord contusion injury. *J Neurosci* **19**:5711-5720.

Grossman SD, Wolfe BB, Yasuda RP, Wrathall JR (2000) Changes in NMDA receptor subunit expression in response to contusive spinal cord injury. *J Neurochem* **75**:174-184.

Grzanna R, Chee WK, Akeyson EW (1987) Noradrenergic projections to brainstem nuclei: evidence for differential projections from noradrenergic subgroups. *J Comp Neurol* **263**:76-91.

Guyenet P (1990) Role of the ventral medulla oblongata in blood pressure regulation. In: Central regulation of autonomic functions (Loewy A, Spyer, KM, ed), pp 145-167. Oxford: Oxford University Press.

Guyenet PG (1991) Central noradrenergic neurons: the autonomic connection. *Prog Brain Res* **88**:365-380.

Guyenet PG, Haselton JR, Sun MK (1989) Sympathoexcitatory neurons of the rostroventrolateral medulla and the origin of the sympathetic vasomotor tone. *Prog Brain Res* **81**:105-116.

Guyenet PG, Schreihofer AM, Stornetta RL (2001) Regulation of sympathetic tone and arterial pressure by the rostral ventrolateral medulla after depletion of C1 cells in rats. *Ann N Y Acad Sci* **940**:259-269.

Haas KF, Macdonald RL (1999) GABAA receptor subunit gamma2 and delta subtypes confer unique kinetic properties on recombinant GABAA receptor currents in mouse fibroblasts. *J Physiol* **514**:27-45.

Haggendal J, Dahlstrom A (1973) The time course of noradrenaline decrease in rat spinal cord following transection. *Neuropharmacology* **12**:349-354.

Hagiwara S, Miyazaki S, Moody W, Patlak J (1978) Blocking effects of barium and hydrogen ions on the potassium current during anomalous rectification in the starfish egg. *J Physiol* **279**:167-185.

Halliwell JV, Adams PR (1982) Voltage-clamp analysis of muscarinic excitation in hippocampal neurons. *Brain Res* **250**:71-92.

Harrison R, Wang SC, Berry C (1939) Decussations of the efferent pathways from the hypothalamus. *Am J Physiol* **125**:449-456.

Hayes K, Weaver LC (1990) Selective control of sympathetic pathways to the kidney, spleen and intestine by the ventrolateral medulla in rats. *J Physiol* **428**:371-385.

Helke CJ, Sayson SC, Keeler JR, Charlton CG (1986) Thyrotropin-releasing hormone-immunoreactive neurons project from the ventral medulla to the intermediolateral cell column: partial coexistence with serotonin. *Brain Res* **381**:1-7.

Helmchen F, Imoto K, Sakmann B (1996) Ca2+ buffering and action potential-evoked Ca2+ signaling in dendrites of pyramidal neurons. *Biophys J* **70**:1069-1081.

Hernandez-Cruz A, Sala F, Adams PR (1990) Subcellular calcium transients visualized by confocal microscopy in a voltage-clamped vertebrate neuron. *Science* **247**:858-862.

Hess W, Akert K (1955) Experimental data on the role of the hypothalamus in mechanism of emotional behaviour. *Arch Neurol Psychiat* **73**:127-129.

Hestrin S (1993) Different glutamate receptor channels mediate fast excitatory synaptic currents in inhibitory and excitatory cortical neurons. *Neuron* **11**:1083-1091.

Hestrin S, Sah P, Nicoll RA (1990a) Mechanisms generating the time course of dual component excitatory synaptic currents recorded in hippocampal slices. *Neuron* **5**:247-253.

Hestrin S, Nicoll RA, Perkel DJ, Sah P (1990b) Analysis of excitatory synaptic action in pyramidal cells using whole- cell recording from rat hippocampal slices. *J Physiol* **422**:203-225.

Hillarp N (1946) Functional organisation of the peripheral autonomic innervation. *Acta Anat [Suppl]* **4**:1-153.

Hille B (1994) Modulation of ion-channel function by G-protein-coupled receptors. *Trends Neurosci* **17**:531-536.

Hillyard DR, Monje VD, Mintz IM, Bean BP, Nadasdi L, Ramachandran J, Miljanich G, Azimi-Zoonooz A, McIntosh JM, Cruz LJ, et al. (1992) A new Conus peptide ligand for mammalian presynaptic Ca2+ channels. *Neuron* **9**:69-77.

Hirsch MD, Helke CJ (1988) Bulbospinal thyrotropin-releasing hormone projections to the intermediolateral cell column: a double fluorescence immunohistochemical-retrograde tracing study in the rat. *Neuroscience* **25**:625-637.

Hoh JH, John SA, Revel JP (1991) Molecular cloning and characterization of a new member of the gap junction gene family, connexin-31. *J Biol Chem* **266**:6524-6531.

Hoh JH, Sosinsky GE, Revel JP, Hansma PK (1993) Structure of the extracellular surface of the gap junction by atomic force microscopy. *Biophys J* **65**:149-163.

Holets V, Elde R (1982) The differential distribution and relationship of serotoninergic and peptidergic fibers to sympathoadrenal neurons in the intermediolateral cell column of the rat: a combined retrograde axonal transport and immunofluorescence study. *Neuroscience* **7**:1155-1174.

Holgert H, Holmberg K, Hannibal J, Fahrenkrug J, Brimijoin S, Hartman BK, Hokfelt T (1996) PACAP in the adrenal gland--relationship with choline acetyltransferase, enkephalin and chromaffin cells and effects of immunological sympathectomy. *Neuroreport* **8**:297-301.

Hollmann M, Heinemann S (1994) Cloned glutamate receptors. *Annu Rev Neurosci* **17**:31-108.

Holmqvist MH, Cao J, Knoppers MH, Jurman ME, Distefano PS, Rhodes KJ, Xie Y, An WF (2001) Kinetic modulation of Kv4-mediated A-current by arachidonic acid is dependent on potassium channel interacting proteins. *J Neurosci* **21**:4154-4161.

Holmqvist MH, Cao J, Hernandez-Pineda R, Jacobson MD, Carroll KI, Sung MA, Betty M, Ge P, Gilbride KJ, Brown ME, Jurman ME, Lawson D, Silos-Santiago I, Xie Y, Covarrubias M, Rhodes KJ, Distefano PS, An WF (2002) Elimination of fast inactivation in Kv4 A-type potassium channels by an auxiliary subunit domain. *Proc Natl Acad Sci U S A* **99**:1035-1040.

Hong Y, Weaver LC (1993) Distribution of immunoreactivity for enkephalin, substance P and vasoactive intestinal peptide in fibres surrounding splanchnic sympathetic preganglionic neurons in rats. *Neuroscience* **57**:1121-1133.

Hosoya Y (1980) The distribution of spinal projection neurons in the hypothalamus of the rat, studied with the HRP method. *Exp Brain Res* **40**:79-87.

Hosoya Y, Sugiura Y, Okado N, Loewy AD, Kohno K (1991) Descending input from the hypothalamic paraventricular nucleus to sympathetic preganglionic neurons in the rat. *Exp Brain Res* **85**:10-20.

Houssay B-A, Molinelli E-A (1925) Centre adrenalino-secreteur hypothalamique. *C r Seanc Soc Biol* **93**:1454-1455.

Howard-Butcher S, Blaha CD, Lane RF (1985) Differential effects of xylamine on extracellular concentrations of norepinephrine and dopamine in rat central nervous system: an in vivo electrochemical study. *J Pharmacol Exp Ther* **233**:58-63.

Huangfu D, Hwang LJ, Riley TA, Guyenet PG (1992) Splanchnic nerve response to A5 area stimulation in rats. *Am J Physiol* **263**:R437-446.

Huguenard JR (1996) Low-threshold calcium currents in central nervous system neurons. *Annu Rev Physiol* **58**:329-348.

Huguenard JR, Prince DA (1991) Slow inactivation of a TEA-sensitive K current in acutely isolated rat thalamic relay neurons. *J Neurophysiol* **66**:1316-1328.

Hussain JF, Kendall DA, Wilson VG (1993) Species-selective binding of [3H]-idazoxan to alpha 2-adrenoceptors and non-adrenoceptor, imidazoline binding sites in the central nervous system. *Br J Pharmacol* **109**:831-837.

Iijima T, Matsumoto G, Kidokoro Y (1992) Synaptic activation of rat adrenal medulla examined with a large photodiode array in combination with a voltage-sensitive dye. *Neuroscience* **51**:211-219.

Imai S, Suzuki T, Sato K, Tokimasa T (1999) Effects of quinine on three different types of potassium currents in bullfrog sympathetic neurons. *Neurosci Lett* **275**:121-124.

Inokuchi H, Yoshimura M, Polosa C, Nishi S (1992a) Adrenergic receptors (alpha 1 and alpha 2) modulate different potassium conductances in sympathetic preganglionic neurons. *Can J Physiol Pharmacol* **70**:S92-97.

Inokuchi H, Yoshimura M, Polosa C, Nishi S (1993a) Tachykinins depress a calcium-dependent potassium conductance in sympathetic preganglionic neurons. *Regul Pept* **46**:367-369.

Inokuchi H, Yoshimura M, Polosa C, Nishi S (1993b) Heterogeneity of the afterhyperpolarization of sympathetic preganglionic neurons. *Kurume Med J* **40**:177-181.

Inokuchi H, Yoshimura M, Trzebski A, Polosa C, Nishi S (1992b) Fast inhibitory postsynaptic potentials and responses to inhibitory amino acids of sympathetic preganglionic neurons in the adult cat. *J Auton Nerv Syst* **41**:53-59.

Inokuchi H, Yoshimura M, Yamada S, Polosa C, Nishi S (1992c) Fast excitatory postsynaptic potentials and the responses to excitant amino acids of sympathetic preganglionic neurons in the slice of the cat spinal cord. *Neuroscience* **46**:657-667.

Inokuchi H, Masuko S, Chiba T, Yoshimura M, Polosa C, Nishi S (1993c) Membrane properties and dendritic arborization of the intermediolateral nucleus neurons in the guinea-pig thoracic spinal cord in vitro. *J Auton Nerv Syst* **43**:97-106.

Inoue M, Fujishiro N, Ogawa K, Muroi M, Sakamoto Y, Imanaga I, Shioda S (2000) Pituitary adenylate cyclase-activating polypeptide may function as a neuromodulator in guinea-pig adrenal medulla. *J Physiol* **528**:473-487.

Isbrandt D, Leicher T, Waldschutz R, Zhu X, Luhmann U, Michel U, Sauter K, Pongs O (2000) Gene structures and expression profiles of three human KCND (Kv4) potassium channels mediating A-type currents I(TO) and I(SA). *Genomics* **64**:144-154.

Ishimatsu M, Williams JT (1996) Synchronous activity in locus coeruleus results from dendritic interactions in pericoerulear regions. *J Neurosci* **16**:5196-5204.

Jahnsen H, Llinas R (1984) Electrophysiological properties of guinea-pig thalamic neurones: an in vitro study. *J Physiol* **349**:205-226.

Jan LY, Jan YN (1997) Cloned potassium channels from eukaryotes and prokaryotes. *Annu Rev Neurosci* **20**:91-123.

Janig W, McLachlan EM (1987) Organization of lumbar spinal outflow to distal colon and pelvic organs. *Physiol Rev* **67**:1332-1404.

Janig W, McLachlan EM (1992a) Specialized functional pathways are the building blocks of the autonomic nervous system. *J Auton Nerv Syst* **41**:3-13.

Janig W, McLachlan EM (1992b) Characteristics of function-specific pathways in the sympathetic nervous system. *Trends Neurosci* **15**:475-481.

Jansen AS, Loewy AD (1997) Neurons lying in the white matter of the upper cervical spinal cord project to the intermediolateral cell column. *Neuroscience* **77**:889-898.

Jansen AS, Wessendorf MW, Loewy AD (1995a) Transneuronal labeling of CNS neuropeptide and monoamine neurons after pseudorabies virus injections into the stellate ganglion. *Brain Res* **683**:1-24.

Jansen AS, Nguyen XV, Karpitskiy V, Mettenleiter TC, Loewy AD (1995b) Central command neurons of the sympathetic nervous system: basis of the fight-or-flight response. *Science* **270**:644-646.

Jensen I, Pilowsky P, Llewellyn-Smith I, Minson J, Chalmers J (1992) Sympathetic preganglionic neurons projecting to the adrenal medulla and aorticorenal ganglion in the rabbit. *Brain Res* **586**:125-129.

Jia Z, Agopyan N, Miu P, Xiong Z, Henderson J, Gerlai R, Taverna FA, Velumian A, MacDonald J, Carlen P, Abramow-Newerly W, Roder J (1996) Enhanced LTP in mice deficient in the AMPA receptor GluR2. *Neuron* **17**:945-956.

Jobling P, McLachlan EM, Sah P (1993) Calcium induced calcium release is involved in the afterhyperpolarization in one class of guinea pig sympathetic neurone. *J Auton Nerv Syst* **42**:251-257.

Johnson B (1993) Amine modulation of electrical coupling in the pyloric network of the lobster stomatogastric ganglion. *J Comp Physiol* **172**:715-732.

Johnson CD, Gilbey MP (1996) On the dominant rhythm in the discharges of single postganglionic sympathetic neurones innervating the rat tail artery. *J Physiol* **497**:241-259.

Johnson CD, Gilbey MP (1998) Focally recorded single sympathetic postganglionic neuronal activity supplying rat lateral tail vein. *J Physiol* **508**:575-585.

Johnson EM, Jr., Koike T, Franklin J (1992) A "calcium set-point hypothesis" of neuronal dependence on neurotrophic factor. *Exp Neurol* **115**:163-166.

Johnson JW, Ascher P (1990) Voltage-dependent block by intracellular Mg2+ of N-methyl-D-aspartate- activated channels. *Biophys J* **57**:1085-1090.

Johnson RA, Freeman RH (1992) Sustained hypertension in the rat induced by chronic blockade of nitric oxide production. *Am J Hypertens* **5**:919-922.

Johnson RG, Carty S, Scarpa A (1981) The electrochemical proton gradient drives catecholamine uptake in isolated chromaffin granules and ghosts. In: Advances in the biosciences: Synthesis and storage of adrenal catecholamines, pp 179-185. Oxford, New York: Pergamon Press.

Jonas P, Racca C, Sakmann B, Seeburg PH, Monyer H (1994) Differences in Ca2+ permeability of AMPA-type glutamate receptor channels in neocortical neurons caused by differential GluR-B subunit expression. *Neuron* **12**:1281-1289.

Jones BE (1991) Noradrenergic locus coeruleus neurons: their distant connections and their relationship to neighboring (including cholinergic and GABAergic) neurons of the central gray and reticular formation. *Prog Brain Res* **88**:15-30.

Jones BE, Yang TZ (1985) The efferent projections from the reticular formation and the locus coeruleus studied by anterograde and retrograde axonal transport in the rat. *J Comp Neurol* **242**:56-92.

Jones CR, Palacios JM (1991) Autoradiography of adrenoceptors in rat and human brain: alpha- adrenoceptor and idazoxan binding sites. *Prog Brain Res* **88**:271-291.

Jones KA, Baughman RW (1988) NMDA- and non-NMDA-receptor components of excitatory synaptic potentials recorded from cells in layer V of rat visual cortex. *J Neurosci* **8**:3522-3534.

Jones KA, Baughman RW (1991) Both NMDA and non-NMDA subtypes of glutamate receptors are concentrated at synapses on cerebral cortical neurons in culture. *Neuron* **7**:593-603.

Jorgensen NR, Geist ST, Civitelli R, Steinberg TH (1997) ATP- and gap junction-dependent intercellular calcium signaling in osteoblastic cells. *J Cell Biol* **139**:497-506.

Joshi S, Levatte MA, Dekaban GA, Weaver LC (1995) Identification of spinal interneurons antecedent to adrenal sympathetic preganglionic neurons using trans-synaptic transport of herpes simplex virus type 1. *Neuroscience* **65**:893-903.

Kachi T, Suzuki T, Takahashi G, Quay WB (1993) Differences between adrenomedullary adrenaline and noradrenaline cells: quantitative electron-microscopic evaluation of their differential cellular association with supporting cells. *Cell Tissue Res* **271**:257-261.

Kadzielawa K (1983) Inhibition of the activity of sympathetic preganglionic neurones and neurones activated by visceral afferents, by alpha-methylnoradrenaline and endogenous catecholamines. *Neuropharmacology* **22**:3-17.

Kandler K, Katz LC (1995) Neuronal coupling and uncoupling in the developing nervous system. *Curr Opin Neurobiol* **5**:98-105.

Kandler K, Katz LC (1998) Coordination of neuronal activity in developing visual cortex by gap junction-mediated biochemical communication. *J Neurosci* **18**:1419-1427.

Kannan H, Hayashida Y, Yamashita H (1989) Increase in sympathetic outflow by paraventricular nucleus stimulation in awake rats. *Am J Physiol* **256**:R1325-1330.

Kano M, Garaschuk O, Verkhratsky A, Konnerth A (1995) Ryanodine receptor-mediated intracellular calcium release in rat cerebellar Purkinje neurones. *J Physiol* **487**:1-16.

Karoum F, Commissiong JW, Neff NH, Wyatt RJ (1980) Biochemical evidence for uncrossed and crossed locus coeruleus projections to the spinal cord. *Brain Res* **196**:237-241.

Karschin C, Dissmann E, Stuhmer W, Karschin A (1996) IRK(1-3) and GIRK(1-4) inwardly rectifying K+ channel mRNAs are differentially expressed in the adult rat brain. *J Neurosci* **16**:3559-3570.

Katafuchi T, Yoshimatsu H, Oomura Y, Sato A (1986) Responses of adrenal catecholamine secretion to lateral hypothalamic stimulation and lesion in rats. *Brain Res* **363**:141-144.

Katsuki S, Ikemoto T, Shimada H, Hagiwara F, Kanai J, (1955) The functional relationship between the hypothalamus and the anterior pituitary-adrenal axis. *Endocrinology Japan* **2**:303-312.

Katz B (1949) Les constantes electriques de la membrane du muscle. *Arch Sci Physiol* **3**:285-299.

Keast JR (1991) Patterns of co-existence of peptides and differences of nerve fibre types associated with noradrenergic and non-noradrenergic (putative cholinergic) neurons in the major pelvic ganglion of the male rat. *Cell Tissue Res* **266**:405-415.

Keinanen K, Wisden W, Sommer B, Werner P, Herb A, Verdoorn TA, Sakmann B, Seeburg PH (1990) A family of AMPA-selective glutamate receptors. *Science* **249**:556-560.

Keller BU, Konnerth A, Yaari Y (1991) Patch clamp analysis of excitatory synaptic currents in granule cells of rat hippocampus. *J Physiol* **435**:275-293.

Kesse WK, Parker TL, Coupland RE (1988) The innervation of the adrenal gland. I. The source of pre- and postganglionic nerve fibres to the rat adrenal gland. *J Anat* **157**:33-41.

Khalil Z, Livett BG, Marley PD (1986) The role of sensory fibres in the rat splanchnic nerve in the regulation of adrenal medullary secretion during stress. *J Physiol* **370**:201-215.

Kiehn O, Tresch MC (2002) Gap junctions and motor behavior. *Trends Neurosci* **25**:108-115.

Klevans L, Gebber GL (1970) Comparison of differential secretion of adrenal catecholamines by splanchnic nerve stimulation and cholinergic agents. *Journal of Pharmacology and Experimental Therapeutics* **172**:69-76.

Klugbauer N, Marais E, Lacinova L, Hofmann F (1999) A T-type calcium channel from mouse brain. *Pflugers Arch* **437**:710-715.

Korn H, Sotelo C, Crepel F (1973) Electronic coupling between neurons in the rat lateral vestibular nucleus. *Exp Brain Res* **16**:255-275.

Koval M, Geist ST, Westphale EM, Kemendy AE, Civitelli R, Beyer EC, Steinberg TH (1995) Transfected connexin45 alters gap junction permeability in cells expressing endogenous connexin43. *J Cell Biol* **130**:987-995.

Krassioukov AV, Weaver LC (1996) Morphological changes in sympathetic preganglionic neurons after spinal cord injury in rats. *Neuroscience* **70**:211-225.

Krenz NR, Weaver LC (1998a) Changes in the morphology of sympathetic preganglionic neurons parallel the development of autonomic dysreflexia after spinal cord injury in rats. *Neurosci Lett* **243**:61-64.

Krenz NR, Weaver LC (1998b) Sprouting of primary afferent fibers after spinal cord transection in the rat. *Neuroscience* **85**:443-458.

Krukoff TL (1986) Segmental distribution of corticotropin-releasing factor-like and vasoactive intestinal peptide-like immunoreactivities in presumptive sympathetic preganglionic neurons of the cat. *Brain Res* **382**:153-157.

Krukoff TL, Ciriello J, Calaresu FR (1985) Segmental distribution of peptide-like immunoreactivity in cell bodies of the thoracolumbar sympathetic nuclei of the cat. *J Comp Neurol* **240**:90-102.

Krupp J, Feltz P (1993) Synaptic- and agonist-induced chloride currents in neonatal rat sympathetic preganglionic neurones in vitro. *J Physiol* **471**:729-748.

Krupp J, Feltz P (1995) Excitatory postsynaptic currents and glutamate receptors in neonatal rat sympathetic preganglionic neurons in vitro. *J Neurophysiol* **73**:1503-1512.

Krupp J, Bordey A, Feltz P (1997) Electrophysiological evidence for multiple glycinergic inputs to neonatal rat sympathetic preganglionic neurons in vitro. *Eur J Neurosci* **9**:1711-1719.

Krupp JJ, Vissel B, Heinemann SF, Westbrook GL (1998) N-terminal domains in the NR2 subunit control desensitization of NMDA receptors. *Neuron* **20**:317-327.

Kubota A, Ootsuka Y, Xu T, Terui N (1995) The 10-Hz rhythm in the sympathetic nerve activity of cats, rats and rabbits. *Neurosci Lett* **196**:173-176.

Kumar NM, Gilula NB (1996) The gap junction communication channel. *Cell* **84**:381-388.

Kumon A, Takahashi A, Kori-Hara T (1977) Epinephrine: a mediator of plasma glycerol elevation by hypothalamic stimulation. *Am J Physiol* **233**:E369-373.

Kuramoto H, Kondo H, Fujita T (1986) Neuropeptide tyrosine (NPY)-like immunoreactivity in adrenal chromaffin cells and intraadrenal nerve fibers of rats. *Anat Rec* **214**:321-328.

Kutsuwada T, Kashiwabuchi N, Mori H, Sakimura K, Kushiya E, Araki K, Meguro H, Masaki H, Kumanishi T, Arakawa M, et al. (1992) Molecular diversity of the NMDA receptor channel. *Nature* **358**:36-41.

Lai CC, Wu SY, Lin HH, Dun NJ (1997) Excitatory action of pituitary adenylate cyclase activating polypeptide on rat sympathetic preganglionic neurons in vivo and in vitro. *Brain Res* **748**:189-194.

Landisman CE, Long MA, Beierlein M, Deans MR, Paul DL, Connors BW (2002) Electrical synapses in the thalamic reticular nucleus. *J Neurosci* **22**:1002-1009.

Langley JN (1903) Das sympathische und verwandte nervose systeme der wirbeltiere (autonomes nervoses system). *ergen physiol* **27**:818-872.

Langley JN (1921) The Autonomic nervous System: Cambridge.

Lasater EM, Dowling JE (1985) Dopamine decreases conductance of the electrical junctions between cultured retinal horizontal cells. *Proc Natl Acad Sci U S A* **82**:3025-3029.

Laskey W, Polosa C (1988) Characteristics of the sympathetic preganglionic neuron and its synaptic input. *Prog Neurobiol* **31**:47-84.

Lee JH, Gomora JC, Cribbs LL, Perez-Reyes E (1999a) Nickel block of three cloned T-type calcium channels: low concentrations selectively block alpha1H. *Biophys J* **77**:3034-3042.

Lee JH, Daud AN, Cribbs LL, Lacerda AE, Pereverzev A, Klockner U, Schneider T, Perez-Reyes E (1999b) Cloning and expression of a novel member of the low voltage-activated T- type calcium channel family. *J Neurosci* **19**:1912-1921.

Leedham JA, Foley AJ, Pennefather JN (1985) Some pharmacological actions of nisoxetine, a bicyclic inhibitor of noradrenaline uptake. *Arch Int Pharmacodyn Ther* **277**:39-55.

LeMasson G, Marder E, Abbott LF (1993) Activity-dependent regulation of conductances in model neurons. *Science* **259**:1915-1917.

Leppert M, Anderson VE, Quattlebaum T, Stauffer D, O'Connell P, Nakamura Y, Lalouel JM, White R (1989) Benign familial neonatal convulsions linked to genetic markers on chromosome 20. *Nature* **337**:647-648.

Lesage F, Lazdunski M (2000) Molecular and functional properties of two-pore-domain potassium channels. *Am J Physiol Renal Physiol* **279**:F793-801.

Leslie J, Nolan MF, Logan SD, Spanswick D, (2000) Electrotonic coupling between sympathetic preganglionic neurons in neonatal and adult rat, in vitro. *J Physiol Proceedings* **528P**:108P.

Lester RA, Jahr CE (1992) NMDA channel behavior depends on agonist affinity. *J Neurosci* **12**:635-643.

Lester RA, Clements JD, Westbrook GL, Jahr CE (1990) Channel kinetics determine the time course of NMDA receptor-mediated synaptic currents. *Nature* **346**:565-567.

Levitan H, Tauc L, Segundo JP (1970) Electrical transmission among neurons in the buccal ganglion of a mollusc, Navanax inermis. *J Gen Physiol* **55**:484-496.

Lewis DI, Coote JH (1990a) Excitation and inhibition of rat sympathetic preganglionic neurones by catecholamines. *Brain Res* **530**:229-234.

Lewis DI, Coote JH (1990b) The influence of 5-hydroxytryptamine agonists and antagonists on identified sympathetic preganglionic neurones in the rat, in vivo. *Br J Pharmacol* **99**:667-672.

Lewis DI, Coote JH (1996) Baroreceptor-induced inhibition of sympathetic neurons by GABA acting at a spinal site. *Am J Physiol* **270**:H1885-1892.

Lewis DI, Sermasi E, Coote JH (1993) Excitatory and indirect inhibitory actions of 5-hydroxytryptamine on sympathetic preganglionic neurones in the neonate rat spinal cord in vitro. *Brain Res* **610**:267-275.

Li P, Wilding TJ, Kim SJ, Calejesan AA, Huettner JE, Zhuo M (1999) Kainate-receptor-mediated sensory synaptic transmission in mammalian spinal cord. *Nature* **397**:161-164.

Li Z, Ferguson AV (1996) Electrophysiological properties of paraventricular magnocellular neurons in rat brain slices: modulation of IA by angiotensin II. *Neuroscience* **71**:133-145.

Li-Smerin Y, Aizenman E, Johnson JW (2000) Inhibition by intracellular Mg(2+) of recombinant N-methyl-D-aspartate receptors expressed in Chinese hamster ovary cells. *J Pharmacol Exp Ther* **292**:1104-1110.

Liss B, Franz O, Sewing S, Bruns R, Neuhoff H, Roeper J (2001) Tuning pacemaker frequency of individual dopaminergic neurons by Kv4.3L and KChip3.1 transcription. *Embo J* **20**:5715-5724.

Liu H, Llewellyn-Smith IJ, Pilowsky P, Basbaum AI (1992) Ultrastructural evidence for GABA-mediated disinhibitory circuits in the spinal cord of the cat. *Neurosci Lett* **138**:183-187.

Livett B, Marley PD, (1993) Noncholinergic control of adrenal catecholamine secretion. [Review]. *Journal of Anatomy* **183**:277-289.

Livett BG, Mizobe F, Dean DM. (1979) Substance P inhibits nicotinic activation of chromaffin cells. *Nature* **278**:256-257.

Llewellyn-Smith IJ, Weaver LC (2001) Changes in synaptic inputs to sympathetic preganglionic neurons after spinal cord injury. *J Comp Neurol* **435**:226-240.

Llewellyn-Smith IJ, Pilowsky P, Minson JB, Chalmers J (1995a) Synapses on axons of sympathetic preganglionic neurons in rat and rabbit thoracic spinal cord. *J Comp Neurol* **354**:193-208.

Llewellyn-Smith IJ, Phend KD, Minson JB, Pilowsky PM, Chalmers JP (1992) Glutamate-immunoreactive synapses on retrogradely-labelled sympathetic preganglionic neurons in rat thoracic spinal cord. *Brain Res* **581**:67-80.

Llewellyn-Smith IJ, Minson JB, Pilowsky PM, Arnolda LF, Chalmers JP (1995b) The one hundred percent hypothesis: glutamate or GABA in synapses on sympathetic preganglionic neurons. *Clin Exp Hypertens* **17**:323-333.

Llewellyn-Smith IJ, Cassam AK, Krenz NR, Krassioukov AV, Weaver LC (1997a) Glutamate- and GABA-immunoreactive synapses on sympathetic preganglionic neurons caudal to a spinal cord transection in rats. *Neuroscience* **80**:1225-1235.

Llewellyn-Smith IJ, Arnolda LF, Pilowsky PM, Chalmers JP, Minson JB (1998) GABA- and glutamate-immunoreactive synapses on sympathetic preganglionic neurons projecting to the superior cervical ganglion. *J Auton Nerv Syst* **71**:96-110.

Llewellyn-Smith IJ, Martin CL, Minson JB, Pilowsky PM, Arnolda LF, Basbaum AI, Chalmers JP (1997b) Neurokinin-1 receptor-immunoreactive sympathetic preganglionic neurons: target specificity and ultrastructure. *Neuroscience* **77**:1137-1149.

Llinas R, Yarom Y (1981) Electrophysiology of mammalian inferior olivary neurones in vitro. Different types of voltage-dependent ionic conductances. *J Physiol* **315**:549-567.

Llinas R, Baker R, Sotelo C (1974) Electrotonic coupling between neurons in cat inferior olive. *J Neurophysiol* **37**:560-571.

Loewy AD, Araujo JC, Kerr FW (1973) Pupillodilator pathways in the brain stem of the cat: anatomical and electrophysiological identification of a central autonomic pathway. *Brain Res* **60**:65-91.

Loewy AD, McKellar S, Saper CB (1979) Direct projections from the A5 catecholamine cell group to the intermediolateral cell column. *Brain Res* **174**:309-314.

Loewy AD, Marson L, Parkinson D, Perry MA, Sawyer WB (1986) Descending noradrenergic pathways involved in the A5 depressor response. *Brain Res* **386**:313-324.

Logan SD, Pickering AE, Gibson IC, Nolan MF, Spanswick D (1996) Electrotonic coupling between rat sympathetic preganglionic neurones in vitro. *J Physiol* **495**:491-502.

Lorenzon NM, Foehring RC (1995) Characterization of pharmacologically identified voltage-gated calcium channel currents in acutely isolated rat neocortical neurons. I. Adult neurons. *J Neurophysiol* **73**:1430-1442.

Lucchi ML, Callegari E, Barazzoni AM, Chiocchetti R, Clavenzani P, Bortolami R (1998) Cerebellar and spinal projections of the coeruleus complex in the duck: a fluorescent retrograde double-labeling study. *Anat Rec* **251**:392-397.

Lundberg JM, Hokfelt T, Nilsson G, Terenius L, Rehfeld J, Elde R, Said S (1978) Peptide neurons in the vagus, splanchnic and sciatic nerves. *Acta Physiol Scand* **104**:499-501.

Luthi A, McCormick DA (1998) H-current: properties of a neuronal and network pacemaker. *Neuron* **21**:9-12.

Ma RC, Dun NJ (1985) Norepinephrine depolarizes lateral horn cells of neonatal rat spinal cord in vitro. *Neurosci Lett* **60**:163-168.

Ma W, Saunders PA, Somogyi R, Poulter MO, Barker JL (1993) Ontogeny of GABAA receptor subunit mRNAs in rat spinal cord and dorsal root ganglia. *J Comp Neurol* **338**:337-359.

MacDonald E, Scheinin M (1995) Distribution and pharmacology of alpha 2-adrenoceptors in the central nervous system. *J Physiol Pharmacol* **46**:241-258.

MacDonald JF, Porietis AV, Wojtowicz JM (1982) L-Aspartic acid induces a region of negative slope conductance in the current-voltage relationship of cultured spinal cord neurons. *Brain Res* **237**:248-253.

Macdonald RL, Olsen RW (1994) $GABA_A$ receptor channels. *Annu Rev Neurosci* **17**:569-602.

MacVicar BA, Dudek FE (1981) Electrotonic coupling between pyramidal cells: a direct demonstration in rat hippocampal slices. *Science* **213**:782-785.

Madison DV, Malenka RC, Nicoll RA (1986) Phorbol esters block a voltage-sensitive chloride current in hippocampal pyramidal cells. *Nature* **321**:695-697.

Magistretti J, Mantegazza M, Guatteo E, Wanke E, (1996) Action potentials recorded with patch-clamp amplifiers: are they genuine? *Trends in Neurosciences.* **19(12)**:530-4

Magnusson T (1973) Effect of chronic transection on dopamine, noradrenaline and 5-hydroxytryptamine in the rat spinal cord. *Naunyn Schmiedebergs Arch Pharmacol* **278**:13-22.

Magoul R, Onteniente B, Geffard M, Calas A (1987) Anatomical distribution and ultrastructural organization of the GABAergic system in the rat spinal cord. An immunocytochemical study using anti-GABA antibodies. *Neuroscience* **20**:1001-1009.

Malpas SC (1998) The rhythmicity of sympathetic nerve activity. *Prog Neurobiol* **56**:65-96.

Mancia G, Grassi G, Parati G, Zanchetti A (1997) The sympathetic nervous system in human hypertension. *Acta Physiol Scand Suppl* **640**:117-121.

Mancia G, Grassi G, Parati G, Zanchetti A (2000) The sympathetic nervous system in human hypertension. *Rev Port Cardiol* **19 Suppl 2**:II15-19.

Mann-Metzer P, Yarom Y (1999) Electrotonic coupling interacts with intrinsic properties to generate synchronized activity in cerebellar networks of inhibitory interneurons. *J Neurosci* **19**:3298-3306.

Mannard A, Polosa C (1973) Analysis of background firing of single sympathetic preganglionic neurons of cat cervical nerve. *J Neurophysiol* **36**:398-408.

Manning RD, Jr., Hu L, Mizelle HL, Montani JP, Norton MW (1993) Cardiovascular responses to long-term blockade of nitric oxide synthesis. *Hypertension* **22**:40-48.

Marley E, Paton DM, (1961) The output of sympathetic amines from the cat's adrenal gland in response to splanchnic nerve activity. *Journal of Physiology* **155**:1-27.

Marley PD, Livett BG, (1987) Differences between the mechanisms of adrenaline and noradrenaline secretion from isolated, bovine, adrenal chromaffin cells. *Neuroscience Letters* **77**:81-86.

Marrion NV (1997) Control of M-current. *Annu Rev Physiol* **59**:483-504.

Marshall KC, Christie MJ, Finlayson PG, Williams JT (1991) Developmental aspects of the locus coeruleus-noradrenaline system. *Prog Brain Res* **88**:173-185.

Martin AO, Mathieu MN, Chevillard C, Guerineau NC (2001) Gap junctions mediate electrical signaling and ensuing cytosolic Ca2+ increases between chromaffin cells in adrenal slices: A role in catecholamine release. *J Neurosci* **21**:5397-5405.

Martin DS, Haywood JR (1992) Sympathetic nervous system activation by glutamate injections into the paraventricular nucleus. *Brain Res* **577**:261-267.

Martina M, Schultz JH, Ehmke H, Monyer H, Jonas P (1998) Functional and molecular differences between voltage-gated K+ channels of fast-spiking interneurons and pyramidal neurons of rat hippocampus. *J Neurosci* **18**:8111-8125.

Massa PT, Mugnaini E (1982) Cell junctions and intramembrane particles of astrocytes and oligodendrocytes: a freeze-fracture study. *Neuroscience* **7**:523-538.

Mathie A, Wooltorton JR, Watkins CS (1998) Voltage-activated potassium channels in mammalian neurons and their block by novel pharmacological agents. *Gen Pharmacol* **30**:13-24.

Matsui H (1965) Effect of myelencephalic stimulation on the secretion of noradrenaline and adrenaline of the adrenal gland in the cat. *Tohoku J Exp Med* **87**:332-337.

Matsui H (1979) Adrenal medullary secretory response to stimulation of the medulla oblongata in the rat. *Neuroendocrinology* **29**:385-390.

Matsui H (1984) Adrenal medullary secretion in response to diencephalic stimulation in the rat. *Neuroendocrinology* **38**:164-168.

Matsui H (1987) Effect of subthalamic stimulation of adrenal epinephrine and norepinephrine secretion in the rat. *Brain Res* **417**:158-160.

Matsumoto A, Arnold AP, Micevych PE (1989) Gap junctions between lateral spinal motoneurons in the rat. *Brain Res* **495**:362-366.

Matsumoto A, Arai Y, Urano A, Hyodo S (1991) Cellular localization of gap junction mRNA in the neonatal rat brain. *Neurosci Lett* **124**:225-228.

Matsumoto M, Takayama K, Miura M (1994) Distribution of glutamate- and GABA-immunoreactive neurons projecting to the vasomotor center of the intermediolateral nucleus of the lower thoracic cord of Wistar rats: a double-labeling study. *Neurosci Lett* **174**:165-168.

Mayer M, Partin KM, Patneau DK, Wong LA, Vyklicky LJ, Benveniste M, Bowie D (1995) *Desensitization at AMPA, Kainate and NMDA Receptors*. In: Excitatory amino acids and synaptic transmission (Wheal H. T, A., ed), pp 89-98. london: academic press.

Mayer ML, Westbrook GL (1987) Permeation and block of N-methyl-D-aspartic acid receptor channels by divalent cations in mouse cultured central neurones. *J Physiol* **394**:501-527.

McAllen RM (1986) Action and specificity of ventral medullary vasopressor neurones in the cat. *Neuroscience* **18**:51-59.

McAllen RM, Dampney RA (1990) Vasomotor neurons in the rostral ventrolateral medulla are organized topographically with respect to type of vascular bed but not body region. *Neurosci Lett* **110**:91-96.

McAllen RM, Malpas SC (1997) Sympathetic burst activity: characteristics and significance. *Clin Exp Pharmacol Physiol* **24**:791-799.

McAllen RM, Dampney, R.A.L. (1989) Central Neural Organisation of Cardiovascular Control. In: Central Neural Organisation of Cardiovascular Control. Progress in Brain Research (Ciriello J, Caverson, M.M., Polosa, C.,, ed), pp p233-242. Amsterdam: Elsevier.

McCall RB (1983) Serotonergic excitation of sympathetic preganglionic neurons: a microiontophoretic study. *Brain Res* **289**:121-127.

McCall RB, Clement ME (1994) Role of serotonin1A and serotonin2 receptors in the central regulation of the cardiovascular system. *Pharmacol Rev* **46**:231-243.

McCormick DA, Bal T (1997) Sleep and arousal: thalamocortical mechanisms. *Annu Rev Neurosci* **20**:185-215.

McLachlan EM, Hirst GD (1980) Some properties of preganglionic neurons in upper thoracic spinal cord of the cat. *J Neurophysiol* **43**:1251-1265.

McLachlan EM, Oldfield BJ (1981) Some observations on the catecholaminergic innervation of the intermediate zone of the thoracolumbar spinal cord of the cat. *J Comp Neurol* **200**:529-544.

McMahon DG (1994) Modulation of electrical synaptic transmission in zebrafish retinal horizontal cells. *J Neurosci* **14**:1722-1734.

McMahon DG, Mattson MP (1996) Horizontal cell electrical coupling in the giant danio: synaptic modulation by dopamine and synaptic maintenance by calcium. *Brain Res* **718**:89-96.

McNair CJ, Baxter GJ, Kerr R, Maxwell DJ (1998) Glutamate receptor subunits associated with rat sympathetic preganglionic neurons. *Neurosci Lett* **256**:29-32.

Meadows HJ, Randall AD (2001) Functional characterisation of human TASK-3, an acid-sensitive two-pore domain potassium channel. *Neuropharmacology* **40**:551-559.

Milner TA, Morrison SF, Abate C, Reis DJ (1988) Phenylethanolamine N-methyltransferase-containing terminals synapse directly on sympathetic preganglionic neurons in the rat. *Brain Res* **448**:205-222.

Minson J, Pilowsky, P., Llewellyn-Smith, I., Kaneko, T., Kapoor, V., Chalmers, J. (1991) Glutamate in spinally projecting neurons of the rostral ventral medulla. *Brain Res* **555**:326-331.

Miyazaki T, Coote JH, Dun NJ (1989) Excitatory and inhibitory effects of epinephrine on neonatal rat sympathetic preganglionic neurons in vitro. *Brain Res* **497**:108-116.

Miyazaki T, Dun NJ, Kobayashi H, Tosaka T (1996) Voltage-dependent potassium currents of sympathetic preganglionic neurons in neonatal rat spinal cord thin slices. *Brain Res* **743**:1-10.

Montano N, Porta A, Malliani A (2001) Evidence for central organization of cardiovascular rhythms. *Ann N Y Acad Sci* **940**:299-306.

Montano N, Cogliati C, da Silva VJ, Gnecchi-Ruscone T, Massimini M, Porta A, Malliani A (2000) Effects of spinal section and of positive-feedback excitatory reflex on sympathetic and heart rate variability. *Hypertension* **36**:1029-1034.

Monyer H, Seeburg PH, Wisden W (1991) Glutamate-operated channels: developmentally early and mature forms arise by alternative splicing. *Neuron* **6**:799-810.

Monyer H, Sprengel R, Schoepfer R, Herb A, Higuchi M, Lomeli H, Burnashev N, Sakmann B, Seeburg PH (1992) Heteromeric NMDA receptors: molecular and functional distinction of subtypes. *Science* **256**:1217-1221.

Moortgat KT, Bullock TH, Sejnowski TJ (2000) Gap junction effects on precision and frequency of a model pacemaker network. *J Neurophysiol* **83**:984-997.

Moreno AP, Rook MB, Fishman GI, Spray DC (1994) Gap junction channels: distinct voltage-sensitive and -insensitive conductance states. *Biophys J* **67**:113-119.

Morrison SF (1993) Raphe pallidus excites a unique class of sympathetic preganglionic neurons. *Am J Physiol* **265**:R82-89.

Morrison SF (2001) Differential control of sympathetic outflow. *Am J Physiol Regul Integr Comp Physiol* **281**:R683-698.

Morrison SF, Gebber GL (1982) Classification of raphe neurons with cardiac-related activity. *Am J Physiol* **243**:R49-59.

Morrison SF, Reis DJ (1991) Responses of sympathetic preganglionic neurons to rostral ventrolateral medullary stimulation. *Am J Physiol* **261**:R1247-1256.

Morrison SF, Cao WH (2000) Different adrenal sympathetic preganglionic neurons regulate epinephrine and norepinephrine secretion. *Am J Physiol Regul Integr Comp Physiol* **279**:R1763-1775.

Morrison SF, Callaway J, Milner TA, Reis DJ (1989a) Glutamate in the spinal sympathetic intermediolateral nucleus: localization by light and electron microscopy. *Brain Res* **503**:5-15.

Morrison SF, Ernsberger P, Milner TA, Callaway J, Gong A, Reis DJ (1989b) A glutamate mechanism in the intermediolateral nucleus mediates sympathoexcitatory responses to stimulation of the rostral ventrolateral medulla. *Prog Brain Res* **81**:159-169.

Mosbacher J, Schoepfer R, Monyer H, Burnashev N, Seeburg PH, Ruppersberg JP (1994) A molecular determinant for submillisecond desensitization in glutamate receptors. *Science* **266**:1059-1062.

Motawei K, Pyner S, Ranson RN, Kamel M, Coote JH (1999) Terminals of paraventricular spinal neurones are closely associated with adrenal medullary sympathetic preganglionic neurones: immunocytochemical evidence for vasopressin as a possible neurotransmitter in this pathway. *Exp Brain Res* **126**:68-76.

Munsch T, Budde T, Pape HC (1997) Voltage-activated intracellular calcium transients in thalamic relay cells and interneurons. *Neuroreport* **8**:2411-2418.

Murphy AZ, Ennis M, Shipley MT, Behbehani MM (1994) Directionally specific changes in arterial pressure induce differential patterns of fos expression in discrete areas of the rat brainstem: a double-labeling study for Fos and catecholamines. *J Comp Neurol* **349**:36-50.

Nagai T, Satoh K, Imamoto K, Maeda T (1981) Divergent projections of catecholamine neurons of the locus coeruleus as revealed by fluorescent retrograde double labeling technique. *Neurosci Lett* **23**:117-123.

Nathan T, Jensen MS, Lambert JD (1990) The slow inhibitory postsynaptic potential in rat hippocampal CA1 neurones is blocked by intracellular injection of QX-314. *Neurosci Lett* **110(3)**:309-13

Neil JJ, Loewy AD (1982) Decreases in blood pressure in response to L-glutamate microinjections into the A5 catecholamine cell group. *Brain Res* **241**:271-278.

Nicholas AP, Pieribone V, Hokfelt T (1993) Distributions of mRNAs for alpha-2 adrenergic receptor subtypes in rat brain: an in situ hybridization study. *J Comp Neurol* **328**:575-594.

Nicholson BJ, Weber PA, Cao F, Chang H, Lampe P, Goldberg G (2000) The molecular basis of selective permeability of connexins is complex and includes both size and charge. *Braz J Med Biol Res* **33**:369-378.

Nielsen HS, Hannibal J, Fahrenkrug J (1998) Embryonic expression of pituitary adenylate cyclase-activating polypeptide in sensory and autonomic ganglia and in spinal cord of the rat. *J Comp Neurol* **394**:403-415.

Niesen C, Charlton MP, Carlen PL (1991) Postsynaptic and presynaptic effects of the calcium chelator BAPTA on synaptic transmission in rat hippocampal dentate granule neurons. *Brain Res.***555**:319-325

Nolan MF, Logan SD, Spanswick D (1999) Electrophysiological properties of electrical synapses between rat sympathetic preganglionic neurones in vitro. *J Physiol* **519 Pt 3**:753-764.

Nowak L, Bregestovski P, Ascher P, Herbet A, Prochiantz A (1984) Magnesium gates glutamate-activated channels in mouse central neurones. *Nature* **307**:462-465.

Nygren LG, Olson L (1977) A new major projection from locus coeruleus: the main source of noradrenergic nerve terminals in the ventral and dorsal columns of the spinal cord. *Brain Res* **132**:85-93.

O'Donnell P, Grace AA (1997) Cortical afferents modulate striatal gap junction permeability via nitric oxide. *Neuroscience* **76**:1-5.

Ohya S, Morohashi Y, Muraki K, Tomita T, Watanabe M, Iwatsubo T, Imaizumi Y (2001) Molecular cloning and expression of the novel splice variants of K(+) channel-interacting protein 2. *Biochem Biophys Res Commun* **282**:96-102.

Okada Y, Ninomiya I (1983) Different cardiac and renal inhibitory and excitatory areas in rabbit hypothalamus. *Am J Physiol* **244**:H832-838.

Oomura Y, Ono T, Ooyama H, Wayner MJ (1969) Glucose and osmosensitive neurones of the rat hypothalamus. *Nature* **222**:282-284.

Oomura Y, Ooyama H, Sugimori M, Nakamura T, Yamada Y (1974) Glucose inhibition of the glucose-sensitive neurone in the rat lateral hypothalamus. *Nature* **247**:284-286.

Ootsuka Y, Xu T, Terui N (1995) The spinally mediated 10-Hz rhythm in the sympathetic nerve activity of cats. *J Auton Nerv Syst* **54**:89-103.

Orer HS, Clement ME, Barman SM, Zhong S, Gebber GL, McCall RB (1996) Role of serotonergic neurons in the maintenance of the 10-Hz rhythm in sympathetic nerve discharge. *Am J Physiol* **270**:R174-181.

Ozawa S, Kamiya H, Tsuzuki K (1998) Glutamate receptors in the mammalian central nervous system. *Prog Neurobiol* **54**:581-618.

Pape HC, Budde T, Mager R, Kisvarday ZF (1994) Prevention of Ca(2+)-mediated action potentials in GABAergic local circuit neurones of rat thalamus by a transient K+ current. *J Physiol* **478 Pt 3**:403-422.

Parker TL, Kesse WK, Mohamed AA, Afework M (1993) The innervation of the mammalian adrenal gland. *J Anat* **183**:265-276.

Parker TL, Kesse, W.K., Tomlinson, A., Coupland, R.E., (1988) Ontogenesis of preganglionic sympathetic innervation of rat adrenal chromaffin cells. In: Progress in Catecholamine Research; Basic Aspects and Peripheral Mechanisms (Dahlstrom A, Belmaker, R.H., Sandler, M.,, ed), pp 227-232. new york: Alan R Liss.

Patneau DK, Mayer ML (1990) Structure-activity relationships for amino acid transmitter candidates acting at N-methyl-D-aspartate and quisqualate receptors. *J Neurosci* **10**:2385-2399.

Pellegrini-Giampietro DE, Gorter JA, Bennett MV, Zukin RS (1997) The GluR2 (GluR-B) hypothesis: Ca(2+)-permeable AMPA receptors in neurological disorders. *Trends Neurosci* **20**:464-470.

Pereda AE, Faber DS (1996) Activity-dependent short-term enhancement of intercellular coupling. *J Neurosci* **16**:983-992.

Perez-Reyes E (1999) Three for T: molecular analysis of the low voltage-activated calcium channel family. *Cell Mol Life Sci* **56**:660-669.

Perez-Reyes E, Cribbs LL, Daud A, Lacerda AE, Barclay J, Williamson MP, Fox M, Rees M, Lee JH (1998) Molecular characterization of a neuronal low-voltage-activated T-type calcium channel. *Nature* **391**:896-900.

Petras JM, Cummings JF (1972) Autonomic neurons in the spinal cord of the Rhesus monkey: a correlation of the findings of cytoarchitectonics and sympathectomy with fiber degeneration following dorsal rhizotomy. *J Comp Neurol* **146**:189-218.

Pickering AE, Spanswick D, Logan SD (1991) Whole-cell recordings from sympathetic preganglionic neurons in rat spinal cord slices. *Neurosci Lett* **130**:237-242.

Pickering AE, Spanswick D, Logan SD (1994) 5-Hydoxytryptamine evokes depolarizations and membrane potential oscillations in rat sympathetic preganglionic neurones. *J Physiol* **480**:109-121.

Pilowsky P, Llewellyn-Smith IJ, Minson J, Chalmers J (1992) Sympathetic preganglionic neurons in rabbit spinal cord that project to the stellate or the superior cervical ganglion. *Brain Res* **577**:181-188.

Polosa C, Yoshimura M, Nishi S (1988) Electrophysiological properties of sympathetic preganglionic neurons. *Annu Rev Physiol* **50**:541-551.

Pongracz F, Firestein S, Shepherd GM (1991) Electrotonic structure of olfactory sensory neurons analyzed by intracellular and whole cell patch techniques. *J Neurophysiol* **65**:747-758.

Proudfit HK, Clark FM (1991) The projections of locus coeruleus neurons to the spinal cord. *Prog Brain Res* **88**:123-141.

Pyner S, Coote JH (1994a) A comparison between the adult rat and neonate rat of the architecture of sympathetic preganglionic neurones projecting to the superior cervical ganglion, stellate ganglion and adrenal medulla. *J Auton Nerv Syst* **48**:153-166.

Pyner S, Coote JH (1994b) Evidence that sympathetic preganglionic neurones are arranged in target- specific columns in the thoracic spinal cord of the rat. *J Comp Neurol* **342**:15-22.

Pyner S, Coote JH (1995) Arrangement of dendrites and morphological characteristics of sympathetic preganglionic neurones projecting to the superior cervical ganglion and adrenal medulla in adult cat. *J Auton Nerv Syst* **52**:35-41.

Rajan S, Wischmeyer E, Xin Liu G, Preisig-Muller R, Daut J, Karschin A, Derst C (2000) TASK-3, a novel tandem pore domain acid-sensitive K+ channel. An extracellular histiding as pH sensor. *J Biol Chem* **275**:16650-16657.

Rall W (1969) Time constants and electrotonic length of membrane cylinders and neurons. *Biophys J* **9**:1483-1508.

Randall A, Tsien RW (1995) Pharmacological dissection of multiple types of Ca2+ channel currents in rat cerebellar granule neurons. *J Neurosci* **15**:2995-3012.

Ranson RN, Motawei K, Pyner S, Coote JH (1998) The paraventricular nucleus of the hypothalamus sends efferents to the spinal cord of the rat that closely appose sympathetic preganglionic neurones projecting to the stellate ganglion. *Exp Brain Res* **120**:164-172.

Rash JE, Dillman RK, Bilhartz BL, Duffy HS, Whalen LR, Yasumura T (1996) Mixed synapses discovered and mapped throughout mammalian spinal cord. *Proc Natl Acad Sci U S A* **93**:4235-4239.

Rash JE, Staines WA, Yasumura T, Patel D, Furman CS, Stelmack GL, Nagy JI (2000) Immunogold evidence that neuronal gap junctions in adult rat brain and spinal cord contain connexin-36 but not connexin-32 or connexin-43. *Proc Natl Acad Sci U S A* **97**:7573-7578.

Rathouz M, Trussell L (1998) Characterization of outward currents in neurons of the avian nucleus magnocellularis. *J Neurophysiol* **80**:2824-2835.

Reid JL, Zivin JA, Foppen FH, Kopin IJ (1975) Catecholamine neurotransmitters and synthetic enzymes in the spinal cord of the rat. *Life Sci* **16**:975-984.

Revel JP, Hoh JH, John SA, Laird DW, Puranam K, Yancey SB (1992) Aspects of gap junction structure and assembly. *Semin Cell Biol* **3**:21-28.

Riphagen CL, Bauce, L., Veale, W.L., Pittman Q.J., (1986) The effects of intrathecal administration of arginine-vasopressin and substance P on blood pressure and adrenal secretion of epinephrine. *J Auton Nerv Syst* **16**:91-99.

Robinson RL, Culberson JL, Carmichael SW (1983) Influence of hypothalamic stimulation on the secretion of adrenal medullary catecholamines. *J Auton Nerv Syst* **8**:89-96.

Roerig B, Feller MB (2000) Neurotransmitters and gap junctions in developing neural circuits. *Brain Res Brain Res Rev* **32**:86-114.

Rogawski M (1985) The A-current. how ubiquitous a feature of excitable cells is it? *Trends Neurosci* **83**:214-219.

Room P, Postema F, Korf J (1981) Divergent axon collaterals of rat locus coeruleus neurons: demonstration by a fluorescent double labeling technique. *Brain Res* **221**:219-230.

Rorig B, Sutor B (1996a) Nitric oxide-stimulated increase in intracellular cGMP modulates gap junction coupling in rat neocortex. *Neuroreport* **7**:569-572.

Rorig B, Sutor B (1996b) Serotonin regulates gap junction coupling in the developing rat somatosensory cortex. *Eur J Neurosci* **8**:1685-1695.

Rose B, Loewenstein WR (1975) Permeability of cell junction depends on local cytoplasmic calcium activity. *Nature* **254**:250-252.

Ross CA, Armstrong DM, Ruggiero DA, Pickel VM, Joh TH, Reis DJ (1981) Adrenaline neurons in the rostral ventrolateral medulla innervate thoracic spinal cord: a combined immunocytochemical and retrograde transport demonstration. *Neurosci Lett* **25**:257-262.

Ross L, Smollen A, Cherry J. (1981) Neonatal unilateral adrenalectomy affects the normal pattern and density of the remaining adrenal medulla. *Society for Neuroscience abstracts* **7**:70.

Rousseau E, Meissner G (1989) Single cardiac sarcoplasmic reticulum Ca2+-release channel: activation by caffeine. *Am J Physiol* **256**:H328-333.

Rubin E, Purves D (1980) Segmental organization of sympathetic preganglionic neurons in the mammalian spinal cord. *J Comp Neurol* **192**:163-174.

Rudy B (1988) Diversity and ubiquity of K channels. *Neuroscience* **25**:729-749.

Sah P, McLachlan EM (1991) Ca(2+)-activated K+ currents underlying the afterhyperpolarization in guinea pig vagal neurons: a role for Ca(2+)-activated Ca2+ release. *Neuron* **7**:257-264.

Sah P, McLachlan EM (1992) Potassium currents contributing to action potential repolarization and the afterhyperpolarization in rat vagal motoneurons. *J Neurophysiol* **68**:1834-1841.

Sah P, McLachlan EM (1995) Membrane properties and synaptic potentials in rat sympathetic preganglionic neurons studied in horizontal spinal cord slices in vitro. *J Auton Nerv Syst* **53**:1-15.

Saint-Amant L, Drapeau P (2001) Synchronization of an embryonic network of identified spinal interneurons solely by electrical coupling. *Neuron* **31**:1035-1046.

Saito S, Kidd GJ, Trapp BD, Dawson TM, Bredt DS, Wilson DA, Traystman RJ, Snyder SH, Hanley DF (1994) Rat spinal cord neurons contain nitric oxide synthase. *Neuroscience* **59**:447-456.

Sakurai T (1999) Orexins and orexin receptors: implication in feeding behavior. *Regul Pept* **85**:25-30.

Sakurai T, Amemiya A, Ishii M, Matsuzaki I, Chemelli RM, Tanaka H, Williams SC, Richardson JA, Kozlowski GP, Wilson S, Arch JR, Buckingham RE, Haynes AC, Carr SA, Annan RS, McNulty DE, Liu WS, Terrett JA, Elshourbagy NA, Bergsma DJ, Yanagisawa M (1998) Orexins and orexin receptors: a family of hypothalamic neuropeptides and G protein-coupled receptors that regulate feeding behavior. *Cell* **92**:573-585.

Sander M, Hansen PG, Victor RG (1995) Sympathetically mediated hypertension caused by chronic inhibition of nitric oxide. *Hypertension* **26**:691-695.

Sander M, Chavoshan B, Victor RG (1999) A large blood pressure-raising effect of nitric oxide synthase inhibition in humans. *Hypertension* **33**:937-942.

Sandler VM, Barbara JG (1999) Calcium-induced calcium release contributes to action potential-evoked calcium transients in hippocampal CA1 pyramidal neurons. *J Neurosci* **19**:4325-4336.

Sasek CA, Helke CJ (1989) Enkephalin-immunoreactive neuronal projections from the medulla oblongata to the intermediolateral cell column: relationship to substance P-immunoreactive neurons. *J Comp Neurol* **287**:484-494.

Sawchenko PE, Swanson LW (1982) Immunohistochemical identification of neurons in the paraventricular nucleus of the hypothalamus that project to the medulla or to the spinal cord in the rat. *J Comp Neurol* **205**:260-272.

Sawynok J, Yaksh TL (1993) Caffeine as an analgesic adjuvant: a review of pharmacology and mechanisms of action. *Pharmacol Rev* **45**:43-85.

Schramm LP, Strack, A.M., Platt, K.B., Loewy, A.D. (1993) Peripheral and central pathways regulating the kidney: a study using pseudorabies virus. *Brain Res* **616**.

Schroeder BC, Kubisch C, Stein V, Jentsch TJ (1998) Moderate loss of function of cyclic-AMP-modulated KCNQ2/KCNQ3 K+ channels causes epilepsy. *Nature* **396**:687-690.

Schwanzel-Fukuda M, Morrell JI, Pfaff DW (1984) Localization of forebrain neurons which project directly to the medulla and spinal cord of the rat by retrograde tracing with wheat germ agglutinin. *J Comp Neurol* **226**:1-20.

Schwartzkroin PA, Prince DA (1979) Recordings from presumed glial cells in the hippocampal slice. *Brain Res* **161**:533-538.

Selverston AI, Moulins M (1985) Oscillatory neural networks. *Annu Rev Physiol* **47**:29-48.

Serodio P, Rudy B (1998) Differential expression of Kv4 K+ channel subunits mediating subthreshold transient K+ (A-type) currents in rat brain. *J Neurophysiol* **79**:1081-1091.

Serodio P, Vega-Saenz de Miera E, Rudy B (1996) Cloning of a novel component of A-type K+ channels operating at subthreshold potentials with unique expression in heart and brain. *J Neurophysiol* **75**:2174-2179.

Seutin V, Mkahli F, Massotte L, Dresse A (2000) Calcium release from internal stores is required for the generation of spontaneous hyperpolarizations in dopaminergic neurons of neonatal rats. *J Neurophysiol* **83**:192-197.

Seybold VS, Elde RP (1984) Receptor autoradiography in thoracic spinal cord: correlation of neurotransmitter binding sites with sympathoadrenal neurons. *J Neurosci* **4**:2533-2542.

Sheardown MJ, Nielsen EO, Hansen AJ, Jacobsen P, Honore T (1990) 2,3-Dihydroxy-6-nitro-7-sulfamoyl-benzo(F)quinoxaline: a neuroprotectant for cerebral ischemia. *Science* **247**:571-574.

Shen E, Dun NJ (1990) Neonate rat sympathetic preganglionic neurons intracellularly labelled with lucifer yellow in thin spinal cord slices. *J Auton Nerv Syst* **29**:247-254.

Shen E, Mo N, Dun NJ (1990) APV-sensitive dorsal root afferent transmission to neonate rat sympathetic preganglionic neurons in vitro. *J Neurophysiol* **64**:991-999.

Shen E, Wu SY, Dun NJ (1994) Spontaneous and transmitter-induced rhythmic activity in neonatal rat sympathetic preganglionic neurons in vitro. *J Neurophysiol* **71**:1197-1205.

Shi H, Lewis DI, Coote JH (1988) Effects of activating spinal alpha-adrenoreceptors on sympathetic nerve activity in the rat. *J Auton Nerv Syst* **23**:69-78.

Shmigol A, Verkhratsky A, Isenberg G (1995) Calcium-induced calcium release in rat sensory neurons. *J Physiol* **489**:627-636.

Sillar KT, Simmers AJ (1994) Electrical coupling and intrinsic neuronal oscillations in Rana temporaria spinal cord. *Eur J Morphol* **32**:293-298.

Silver IA, Erecinska M (1998) Glucose-induced intracellular ion changes in sugar-sensitive hypothalamic neurons. *J Neurophysiol* **79**:1733-1745.

Simon AM, Goodenough DA (1998) Diverse functions of vertebrate gap junctions. *Trends Cell Biol* **8**:477-483.

Sloper JJ, Powell TP (1978) Dendro-dendritic and reciprocal synapses in the primate motor cortex. *Proc R Soc Lond B Biol Sci* **203**:23-38.

Slotkin TA, (1986) Development of the sympathoadrenal axis. In *Developmental Neurobiology of the Autonomic Nervous System* (Gootman PM, ed) pp 69-96

Slotkin TA, Chantry, C.J., Bartolome, J., (1986) Development of central control of adrenal catecholamine biosynthesis and release. *Advances in Bioscience* **36**:95-102.

Sohl G, Degen J, Teubner B, Willecke K (1998) The murine gap junction gene connexin36 is highly expressed in mouse retina and regulated during brain development. *FEBS Lett* **428**:27-31.

Spanswick D, Logan SD (1990a) Sympathetic preganglionic neurones in neonatal rat spinal cord in vitro: electrophysiological characteristics and the effects of selective excitatory amino acid receptor agonists. *Brain Res* **525**:181-188.

Spanswick D, Logan SD (1990b) Spontaneous rhythmic activity in the intermediolateral cell nucleus of the neonate rat thoracolumbar spinal cord in vitro. *Neuroscience* **39**:395-403.

Spanswick D, Renaud LP, Logan SD (1998) Bilaterally evoked monosynaptic EPSPs, NMDA receptors and potentiation in rat sympathetic preganglionic neurones in vitro. *J Physiol* **509**:195-209.

Spanswick D, Pickering AE, Gibson IC, Logan SD (1994) Inhibition of sympathetic preganglionic neurons by spinal glycinergic interneurons. *Neuroscience* **62**:205-216.

Spanswick D, Pickering AE, Gibson IC, Logan SD (1995) Excitation of sympathetic preganglionic neurons via metabotropic excitatory amino acid receptors. *Neuroscience* **68**:1247-1261.

Spray DC, Harris AL, Bennett MV (1981) Gap junctional conductance is a simple and sensitive function of intracellular pH. *Science* **211**:712-715.

Spyer K (1990) The central nervous organisation of reflex circulatory control. In: *Central Regulation of Autonomic Functions* (Loewy AD, Spyer, K.M., ed), pp 168-188. New York: Oxford University Press.

Staley KJ, Otis TS, Mody I (1992) Membrane properties of dentate gyrus granule cells: comparison of sharp microelectrode and whole-cell recordings. *J Neurophysiol* **67**:1346-1358.

Stanek KA, Neil JJ, Sawyer WB, Loewy AD (1984) Changes in regional blood flow and cardiac output after L-glutamate stimulation of A5 cell group. *Am J Physiol* **246**:H44-51.

Staras K, Chang HS, Gilbey MP (2001) Resetting of sympathetic rhythm by somatic afferents causes post-reflex coordination of sympathetic activity in rat. *J Physiol* **533**:537-545.

Stegenga SL, Kalb RG (2001) Developmental regulation of N-methyl-D-aspartate- and kainate-type glutamate receptor expression in the rat spinal cord. *Neuroscience* **105**:499-507.

Steinberg TH, Civitelli R, Geist ST, Robertson AJ, Hick E, Veenstra RD, Wang HZ, Warlow PM, Westphale EM, Laing JG, et al. (1994) Connexin43 and connexin45 form gap junctions with different molecular permeabilities in osteoblastic cells. *Embo J* **13**:744-750.

Stern JE, Armstrong WE (1997) Sustained outward rectification of oxytocinergic neurones in the rat supraoptic nucleus: ionic dependence and pharmacology. *J Physiol* **500**:497-508.

Stern P, Behe P, Schoepfer R, Colquhoun D (1992) Single-channel conductances of NMDA receptors expressed from cloned cDNAs: comparison with native receptors. *Proc R Soc Lond B Biol Sci* **250**:271-277.

Stoddard SL, Bergdall VK, Townsend DW, Levin BE (1986a) Plasma catecholamines associated with hypothalamically-elicited flight behavior. *Physiol Behav* **37**:709-715.

Stoddard SL, Bergdall VK, Townsend DW, Levin BE (1986b) Plasma catecholamines associated with hypothalamically-elicited defense behavior. *Physiol Behav* **36**:867-873.

Stoddard-Apter SL, Siegel A, Levin BE (1983) Plasma catecholamine and cardiovascular responses following hypothalamic stimulation in the awake cat. *J Auton Nerv Syst* **8**:343-360.

Storm JF (1990) Potassium currents in hippocampal pyramidal cells. *Prog Brain Res* **83**:161-187.

Stornetta RL, Guyenet PG (1999) Distribution of glutamic acid decarboxylase mRNA-containing neurons in rat medulla projecting to thoracic spinal cord in relation to monoaminergic brainstem neurons. *J Comp Neurol* **407**:367-380.

Stornetta RL, Guyenet, PG, MaCarthy, R (1986) Modulation of autonomic outflow by pontine A5 noradrenergic neurons. In: Brain and blood pressure control (Nakamura K, ed), pp 23-28. Amsterdam: Elsevier Science Publishers.

Strack AM, Sawyer WB, Marubio LM, Loewy AD (1988) Spinal origin of sympathetic preganglionic neurons in the rat. *Brain Res* **455**:187-191.

Strack AM, Sawyer WB, Platt KB, Loewy AD (1989a) CNS cell groups regulating the sympathetic outflow to adrenal gland as revealed by transneuronal cell body labeling with pseudorabies virus. *Brain Res* **491**:274-296.

Strack AM, Sawyer WB, Hughes JH, Platt KB, Loewy AD (1989b) A general pattern of CNS innervation of the sympathetic outflow demonstrated by transneuronal pseudorabies viral infections. *Brain Res* **491**:156-162.

Sumi T, Umeda Y (1979) Adrenal epinephrine in hyperuricemia induced by hypothalamic stimulation of the rat. *Am J Physiol* **236**:E212-215.

Sun MK (1995) Central neural organisation and control of sympathetic nervous system in mammals. *Prog Neurobiol* **47**:157-233.

Sun MK (1996) Pharmacology of reticulospinal vasomotor neurons in cardiovascular regulation. *Pharmacol Rev* **48**:465-494.

Sved AF (1989) PNMT-containing catecholaminergic neurons are not necessarily adrenergic. *Brain Res* **481**:113-118.

Swanson LW, Kuypers HG (1980) The paraventricular nucleus of the hypothalamus: cytoarchitectonic subdivisions and organization of projections to the pituitary, dorsal vagal complex, and spinal cord as demonstrated by retrograde fluorescence double-labeling methods. *J Comp Neurol* **194**:555-570.

Tachibana M, Wenthold RJ, Morioka H, Petralia RS (1994) Light and electron microscopic immunocytochemical localization of AMPA- selective glutamate receptors in the rat spinal cord. *J Comp Neurol* **344**:431-454.

Takahashi T (1990) Membrane currents in visually identified motoneurones of neonatal rat spinal cord. *J Physiol* **423**:27-46.

Talbot MJ & Sayer RJ (1996) Intracellular QX-314 inhibits calcium currents in hippocampal CA1 pyramidal neurons. *J Neurophys* **76(3)**:2120-4

Talley EM, Cribbs LL, Lee JH, Daud A, Perez-Reyes E, Bayliss DA (1999) Differential distribution of three members of a gene family encoding low voltage-activated (T-type) calcium channels. *J Neurosci* **19**:1895-1911.

Tang FR, Tan CK, Ling EA (1995) A comparative study of NADPH-diaphorase in the sympathetic preganglionic neurons of the upper thoracic cord between spontaneously hypertensive rats and Wistar-Kyoto rats. *Brain Res* **691**:153-159.

Taylor RF, Schramm LP (1987) Differential effects of spinal transection on sympathetic nerve activities in rats. *Am J Physiol* **253**:R611-618.

Tejani-Butt SM, Brunswick DJ, Frazer A (1990) [3H]nisoxetine: a new radioligand for norepinephrine uptake sites in brain. *Eur J Pharmacol* **191**:239-243.

Teubner B, Odermatt B, Guldenagel M, Sohl G, Degen J, Bukauskas F, Kronengold J, Verselis VK, Jung YT, Kozak CA, Schilling K, Willecke K (2001) Functional expression of the new gap junction gene connexin47 transcribed in mouse brain and spinal cord neurons. *J Neurosci* **21**:1117-1126.

Tkatch T, Baranauskas G, Surmeier DJ (2000) Kv4.2 mRNA abundance and A-type K(+) current amplitude are linearly related in basal ganglia and basal forebrain neurons. *J Neurosci* **20**:579-588.

Todd AJ, Sullivan AC (1990) Light microscope study of the coexistence of GABA-like and glycine-like immunoreactivities in the spinal cord of the rat. *J Comp Neurol* **296**:496-505.

Todd AJ, Watt C, Spike RC, Sieghart W (1996) Colocalization of GABA, glycine, and their receptors at synapses in the rat spinal cord. *J Neurosci* **16**:974-982.

Tolle TR, Berthele A, Zieglgansberger W, Seeburg PH, Wisden W (1993) The differential expression of 16 NMDA and non-NMDA receptor subunits in the rat spinal cord and in periaqueductal gray. *J Neurosci* **13**:5009-5028.

Tombaugh GC, Somjen GG (1996) Effects of extracellular pH on voltage-gated Na^+, K^+ and Ca^{2+} currents in isolated rat CA1 neurons. *J Physiol* **493**:719-732.

Tomlinson A, Coupland RE (1990) The innervation of the adrenal gland. IV. Innervation of the rat adrenal medulla from birth to old age. A descriptive and quantitative morphometric and biochemical study of the innervation of chromaffin cells and adrenal medullary neurons in Wistar rats. *J Anat* **169**:209-236.

Tomlinson A, Durbin J, Coupland RE (1987) A quantitative analysis of rat adrenal chromaffin tissue: morphometric analysis at tissue and cellular level correlated with catecholamine content. *Neuroscience* **20**:895-904.

Traub RD, Wong RK (1983) Synaptic mechanisms underlying interictal spike initiation in a hippocampal network. *Neurology* **33**:257-266.

Traub RD, Bibbig A (2000) A model of high-frequency ripples in the hippocampus based on synaptic coupling plus axon-axon gap junctions between pyramidal neurons. *J Neurosci* **20**:2086-2093.

Traub RD, Schmitz D, Jefferys JG, Draguhn A (1999) High-frequency population oscillations are predicted to occur in hippocampal pyramidal neuronal networks interconnected by axoaxonal gap junctions. *Neuroscience* **92**:407-426.

Trendelenburg U (1991) The TiPS lecture: functional aspects of the neuronal uptake of noradrenaline. *Trends Pharmacol Sci* **12**:334-337.

Trequattrini C, Petris A, Franciolini F (1996) Characterization of a neuronal delayed rectifier K current permeant to Cs and blocked by verapamil. *J Membr Biol* **154**:143-153.

Tresch MC, Kiehn O (2000) Motor coordination without action potentials in the mammalian spinal cord. *Nat Neurosci* **3**:593-599.

Tsien RW, Lipscombe D, Madison DV, Bley KR, Fox AP (1988) Multiple types of neuronal calcium channels and their selective modulation. *Trends Neurosci* **11**:431-438.

Tucker DC, Saper CB (1985) Specificity of spinal projections from hypothalamic and brainstem areas which innervate sympathetic preganglionic neurons. *Brain Res* **360**:159-164.

Turrigiano G, Abbott LF, Marder E (1994) Activity-dependent changes in the intrinsic properties of cultured neurons. *Science* **264**:974-977.

Turski L, Ikonomidou C, Turski WA, Bortolotto ZA, Cavalheiro EA (1989) Review: cholinergic mechanisms and epileptogenesis. The seizures induced by pilocarpine: a novel experimental model of intractable epilepsy. *Synapse* **3**:154-171.

Tuttle R, Masuko S, Nakajima Y (1986) Freeze-fracture study of the large myelinated club ending synapse on the goldfish Mauthner cell: special reference to the quantitative analysis of gap junctions. *J Comp Neurol* **246**:202-211.

Ungerstedt U (1971) Stereotaxic mapping of the monoamine pathways in the rat brain. *Acta Physiol Scand Suppl* **367**:1-48.

van den Pol AN (1999) Hypothalamic hypocretin (orexin): robust innervation of the spinal cord. *J Neurosci* **19**:3171-3182.

Van der Gugten J, Palkovits M, Wijnen HL, Versteeg DH (1976) Regional distribution of adrenaline in rat brain. *Brain Res* **107**:171-175.

van der Want JJ, Gramsbergen A, Ijkema-Paassen J, de Weerd H, Liem RS (1998) Dendro-dendritic connections between motoneurons in the rat spinal cord: an electron microscopic investigation. *Brain Res* **779**:342-345.

Veenstra RD (1996) Size and selectivity of gap junction channels formed from different connexins. *J Bioenerg Biomembr* **28**:327-337.

Velazquez JL, Han D, Carlen PL (1997) Neurotransmitter modulation of gap junctional communication in the rat hippocampus. *Eur J Neurosci* **9**:2522-2531.

Venance L, Rozov A, Blatow M, Burnashev N, Feldmeyer D, Monyer H (2000) Connexin expression in electrically coupled postnatal rat brain neurons. *Proc Natl Acad Sci U S A* **97**:10260-10265.

Vera PL, Hurwitz BE, Schneiderman N (1990) Sympathoadrenal preganglionic neurons in the adult rabbit send their dendrites into the contralateral hemicord. *J Auton Nerv Syst* **30**:193-198.

Vera PL, Ellenberger HH, Haselton JR, Haselton CL, Schneiderman N (1986) The intermediolateral nucleus: an 'open' or 'closed' nucleus? *Brain Res* **386**:84-92.

Verkhratsky A, Orkand RK, Kettenmann H (1998) Glial calcium: homeostasis and signaling function. *Physiol Rev* **78**:99-141.

Viana F, Gibbs L, Berger AJ (1990) Double- and triple-labeling of functionally characterized central neurons projecting to peripheral targets studied in vitro. *Neuroscience* **38**:829-841.

Viana F, Bayliss DA, Berger AJ (1993) Calcium conductances and their role in the firing behavior of neonatal rat hypoglossal motoneurons. *J Neurophysiol* **69**:2137-2149.

Vignes M, Collingridge GL (1997) The synaptic activation of kainate receptors. *Nature* **388**:179-182.

Vollmer RR, Baruchin A, Kolibal-Pegher SS, Corey SP, Stricker EM, Kaplan BB (1992) Selective activation of norepinephrine- and epinephrine-secreting chromaffin cells in rat adrenal medulla. *Am J Physiol* **263**:R716-721.

von Dalnok GK, Menssen HD (1986) A quantitative electron microscopic study of the effect of glucocorticoids in vivo on the early postnatal differentiation of paraneuronal cells in the carotid body and the adrenal medulla of the rat. *Anat Embryol* **174**:307-319.

von Euler U, Folkow B (1958) The effect of stimulation of autonomic areas in the cerebral cortex upon the adrenaline and noradrenaline secretion from the adrenal gland in cat. *Acta Physiol Scand* **42**:313-320.

Wallin BG, Stjernberg L (1984) Sympathetic activity in man after spinal cord injury. Outflow to skin below the lesion. *Brain* **107**:183-198.

Walton KD, Navarrete R (1991) Postnatal changes in motoneurone electrotonic coupling studied in the in vitro rat lumbar spinal cord. *J Physiol* **433**:283-305.

Wang HS, Pan Z, Shi W, Brown BS, Wymore RS, Cohen IS, Dixon JE, McKinnon D (1998) KCNQ2 and KCNQ3 potassium channel subunits: molecular correlates of the M-channel. *Science* **282**:1890-1893.

Ward JE, Angus JA (1993) Acute and chronic inhibition of nitric oxide synthase in conscious rabbits: role of nitric oxide in the control of vascular tone. *J Cardiovasc Pharmacol* **21**:804-814.

Wasman L, Flynn JP (1962) Direct attack elicited from hypothalamus. *Arch Neurol* **6**:220-227.

Watanabe A (1958) The interaction of electrical activity amoung neurones of lobster cardiac ganglion. *Japanese Journal of Physiology* **8**:305-318.

Watanabe M, Mishina M, Inoue Y (1994) Distinct spatiotemporal distributions of the N-methyl-D-aspartate receptor channel subunit mRNAs in the mouse cervical cord. *J Comp Neurol* **345**:314-319.

Watkins JC (2000) l-glutamate as a central neurotransmitter: looking back. *Biochem Soc Trans* **28**:297-309.

Weaver LC, Cassam AK, Krassioukov AV, Llewellyn-Smith IJ (1997) Changes in immunoreactivity for growth associated protein-43 suggest reorganization of synapses on spinal sympathetic neurons after cord transection. *Neuroscience* **81**:535-551.

Wessendorf MW, Elde R. (1987) The coexistance of serotonin- and substance P- like immunoreactivity in the spinal cord of the rat as shown by immunofluorescent double labeling. *J Neurosci* **7**:3252-3263.

Westerhaus MJ, Loewy AD (2001) Central representation of the sympathetic nervous system in the cerebral cortex. *Brain Res* **903**:117-127.

White G, Lovinger DM, Weight FF (1989) Transient low-threshold Ca^{2+} current triggers burst firing through an afterdepolarizing potential in an adult mammalian neuron. *Proc Natl Acad Sci U S A* **86**:6802-6806.

Wigmore MA, Lacey MG (2000) A Kv3-like persistent, outwardly rectifying, Cs^{+}-permeable, K^{+} current in rat subthalamic nucleus neurones. *J Physiol* **527 Pt 3**:493-506.

Willette RN, Punnen-Grandy S, Krieger AJ, Sapru HN (1987) Differential regulation of regional vascular resistance by the rostral and caudal ventrolateral medulla in the rat. *J Auton Nerv Syst* **18**:143-151.

Williams JT, Marshall KC (1987) Membrane properties and adrenergic responses in locus coeruleus neurons of young rats. *J Neurosci* **7**:3687-3694.

Williams ME, Washburn MS, Hans M, Urrutia A, Brust PF, Prodanovich P, Harpold MM, Stauderman KA (1999) Structure and functional characterization of a novel human low-voltage activated calcium channel. *J Neurochem* **72**:791-799.

Willows AO, Dorsett DA, Hoyle G (1973) The neuronal basis of behavior in Tritonia. 3. Neuronal mechanism of a fixed action pattern. *J Neurobiol* **4**:255-285.

Wong DT, Bymaster FP (1976) Effect of nisoxetine on uptake of catecholamines in synaptosomes isolated from discrete regions of rat brain. *Biochem Pharmacol* **25**:1979-1983.

Woodruff ML, Baisden RH, Whittington DL (1986) Effects of electrical stimulation of the pontine A5 cell group on blood pressure and heart rate in the rabbit. *Brain Res* **379**:10-23.

Yahuaca P, Ek-Vitorin JF, Rush P, Delmar M, Taffet SM (2000) Identification of a protein kinase activity that phosphorylates connexin43 in a pH-dependent manner. *Braz J Med Biol Res* **33**:399-406.

Yamashita H, Kannan H, Kasai M, Osaka T (1987) Decrease in blood pressure by stimulation of the rat hypothalamic paraventricular nucleus with L-glutamate or weak current. *J Auton Nerv Syst* **19**:229-234.

Yanagihara K, Irisawa H (1980) Inward current activated during hyperpolarization in the rabbit sinoatrial node cell. *Pflugers Arch* **385**:11-19.

Yang QZ, Hatton GI (1988) Direct evidence for electrical coupling among rat supraoptic nucleus neurons. *Brain Res* **463**:47-56.

Yardley CP, Stein RD, Weaver LC (1989) Tonic influences from the rostral medulla affect sympathetic nerves differentially. *Am J Physiol* **256**:R323-331.

Yoshimura M, Nishi S (1982) Intracellular recordings from lateral horn cells of the spinal cord in vitro. *J Auton Nerv Syst* **6**:5-11.

Yoshimura M, Polosa C, Nishi S (1986a) Afterhyperpolarization mechanisms in cat sympathetic preganglionic neuron in vitro. *J Neurophysiol* **55**:1234-1246.

Yoshimura M, Polosa C, Nishi S (1986b) Electrophysiological properties of sympathetic preganglionic neurons in the cat spinal cord in vitro. *Pflugers Arch* **406**:91-98.

Yoshimura M, Polosa C, Nishi S (1987a) Noradrenaline induces rhythmic bursting in sympathetic preganglionic neurons. *Brain Res* **420**:147-151.

Yoshimura M, Polosa C, Nishi S (1987b) Slow IPSP and the noradrenaline-induced inhibition of the cat sympathetic preganglionic neuron in vitro. *Brain Res* **419**:383-386.

Yoshimura M, Polosa C, Nishi S (1987c) Slow EPSP and the depolarizing action of noradrenaline on sympathetic preganglionic neurons. *Brain Res* **414**:138-142.

Yoshimura M, Polosa C, Nishi S (1987d) Afterdepolarization mechanism in the in vitro, cesium-loaded, sympathetic preganglionic neuron of the cat. *J Neurophysiol* **57**:1325-1337.

Yoshimura M, Polosa C, Nishi S (1987e) A transient outward rectification in the cat sympathetic preganglionic neuron. *Pflugers Arch* **408**:207-208.

Young J (1939) Partial degeneration of the nerve supply of the adrenal. A study in autonomic innervation. *J Anat* **73**:540-550.

Young JB, Rosa RM, Landsberg L (1984) Dissociation of sympathetic nervous system and adrenal medullary responses. *Am J Physiol* **247**:E35-40.

Zagon A, Smith AD (1993) Monosynaptic projections from the rostral ventrolateral medulla oblongata to identified sympathetic preganglionic neurons. *Neuroscience* **54**:729-743.

Zeng DW, Lynch KR (1991) Distribution of alpha 2-adrenergic receptor mRNAs in the rat CNS. *Brain Res Mol Brain Res* **10**:219-225.

Zhang DQ, McMahon DG (2001) Gating of retinal horizontal cell hemi gap junction channels by voltage, Ca2+, and retinoic acid. *Mol Vis* **7**:247-252.

Zhong S, Huang ZS, Gebber GL, Barman SM (1993) Role of the brain stem in generating the 2- to 6-Hz oscillation in sympathetic nerve discharge. *Am J Physiol* **265**:R1026-1035.

Zhou SY, Gilbey MP (1995) Sympathoexcitatory influence of a fast conducting raphe-spinal pathway in the rat. *Am J Physiol* **268**:R1230-1235.

Zhou XF, Livett BG (1990a) Substance P has biphasic effects on catecholamine secretion evoked by electrical stimulation of perfused rat adrenal glands in vitro. *J Auton Nerv Syst* **31**:31-39.

Zhou XF, Livett BG (1990b) Substance P increases catecholamine secretion from perfused rat adrenal glands evoked by prolonged field stimulation. *J Physiol* **425**:321-334.

Zivin JA, Reid JL, Saavedra JM, Kopin IJ (1975) Quantitative localization of biogenic amines in the spinal cord. *Brain Res* **99**:293-301.